# COMPARATIVE PROTEOMIC STUDY ON PARALYTIC SHELLFISH TOXINS (PSTS) PRODUCING DINOFLAGELLATES

**MAK YUN LAM**

**M.Phil**

**The Hong Kong Polytechnic University**

**2013**

**The Hong Kong Polytechnic University**

**Department of Applied Biology and Chemical Technology**

# COMPARATIVE PROTEOMIC STUDY ON PARALYTIC SHELLFISH TOXINS (PSTS) PRODUCING DINOFLAGELLATES

**By**

**MAK YUN LAM**

**A thesis submitted in partial fulfillment of the requirements for the degree of Master of Philosophy**

**December 2012**

## CERTIFICATE OF ORIGINALITY

**I hereby declare that this thesis is my own work and that, to the best of my knowledge and belief, it reproduces no material previously published or written, nor material that has been accepted for the award of any other degree or diploma, except where due acknowledgement has been made in the text.**

Mak Yun Lam

## Abstract

Paralytic shellfish poisoning (PSP) is caused by paralytic shellfish toxins (PST) and it is very harmful as it has a high mortality rate as well as rapid onset. The understanding of the PST production mechanism in dinoflagellates was hindered by lack of genomic information due to its large genome size. In this study, proteomic as well as transcriptomic approaches were attempted to study the PST-biosynthetic process in order to find proteins related to PSTs production. Background information was gathered for two toxic PST-producing *Alexandrium catenella* (AC-T) and *Gymnodinium catenatum* (GC-T) and two non-toxic (non-PST-producing *A. catenella* (AC-N) and *A. tamarense* (AT-N)) dinoflagellates in my laboratory. rDNA sequences in the internal transcribed (ITS) region, growth curves, cell volume, protein expression profiles (PEPs), toxin profiles and endogenous free arginine levels were gathered for these 4 dinoflagellates. AC-T and AC-N were found to have a high homology (97%) in their ITS sequences. They also have very similar exponential growth, cell volume and PEPs. Endogenous free arginine levels in AC-T and GC-T showed no direct relationship to their cellular toxin contents. Nitrate-enrichment/limitation and phosphate limitation did not induce GC-T to show any significant changes in cellular toxin contents in the exponential growth phase. Similarly, nitrate-enrichment/limitation did not cause any significant changes of cellular toxin contents in AC-T. However, phosphate limitation in AC-T culture is significantly increased the toxin contents of AC-T to around 4 folds. Supplements of exogenous arginine to the culture of both GC-T and AC-T did not cause any significant increase of toxin contents. Hence it was decided to perform comparative proteomic experiments (a) between AC-T and AC-N as well as (b) AC-T with and without phosphate-limitation.

With the support of a newly established transcriptome database built with a standard strain of *A. catenella* and available in-house, classical 2-dimensional gel electrophoresis (2-DE) followed with matrix-assisted laser desorption/ionization time-of-flight tandem mass spectrometry (MALDI-TOF-TOF MS), liquid chromatography electrospray ionization ion-trap tandem mass spectrometry (LC ESI-ion-trap MS/MS) with and without sulfonation for protein identification were performed. 65 proteins were found to be differentially expressed between AC-T and AC-N in the exponential phase and 7 of them were identified and upregulated. These

proteins included photosynthetic proteins ribulose 1,5-bisphosphate carboxylase/oxygenase (Rubisco II), glyceraldehyde-3 phosphate dehydrogenase (G3PD), peridinin-chlorophyll a protein (PCP) and light harvesting protein (LHP). Others are methionine adenosyltransferase (MAT), transcriptional regulator and either heat shock protein 70 (HSP70) or peridinin chlorophyll-a binding protein apoprotein precursor. On the other hand, 22 proteins of AC-T were found to be differentially expressed under phosphate limitation. 3 of them were identified and down-regulated. They are G3PD, plastid oxygen-evolving enhancer 1-2 precursor (OEE) and LHP. These 2 sets of results are apparently contradictory to each other as increased G3PD and LHP were seen upregulated in AC-T (in comparison with AC-N) but they were down-regulated when AC-T was subjected to phosphate limiting growth condition. Nonetheless, the results could be summarized into two predications. Firstly, in toxic AC-T, the ability to produce PST is related to photosynthetic activities of the dinoflagellates. There may be a particular set of genes in AC-T that is lacking in AC-N, which enable PST production and this set of gene function may have some linkage with photosynthesis. Secondly, in the epigenetic level, phosphate limitation induce/inhibit another set of genes functions which may introduce additional control of PST amount in AC-T. Therefore, the total amount of PST produced was increased in AC-T under phosphate-stress.

## List of publications and presentations arise as a direct result of this study:

**Publications** (Appendix C)

Lee FWF, Ho KC, Mak DYL and Lo SCL (2011) Authentication of the proteins expression profiles (PEPs) identification methodology in a bloom of *Karenia digitata*, the most damaging harmful algal bloom causative agent in the history of Hong Kong. Harmful Algae. **12**, pp.1-10

Mak DYL, Lee FWF, Ho KC Ho and Lo SCL. Comparative study between a toxic and non-toxic strain of *Alexandrium catenella. "*New Era in HAB Research" - Proceedings of the 5th International Conference on Prevention and Management of Harmful Algal Blooms in South China Sea, 29th March to 1st April, 2012 in Macau, pp.49-58

**Conference Presentations**

***Oral Presentation*** (Appendix D)

Mak DYL, Comparative study between toxic and non-toxic strain of *Alexandrium catenella*. In "New Era in HAB Research – 5th International Conference on the Prevention and Management of Harmful Algal Blooms in South China Sea (HABSCS -2012)" held in Macau on 29th March to 1st April, 2012.

***Poster*** (Appendix E)

Mak DYL, Lee FWF and Lo SCL. Toxin production and endogenous arginine level of *Gymnodinium catenatum*, a marine dinoflagellate. 5th International Functional Food Symposium held in Hong Kong, 10th to 11th March, 2011.

## Acknowledgements

What a challenging time in these years! After finishing this project, I feel that my IQ, EQ and AQ are also “upregulated”. Of course, I am not the only one who pays effort in this project and I would like to take this opportunity to express my sincere gratitude to all who always stands by me during this hard time.

Foremost, I would like to express my sincere gratitude to my supervisor Professor Samuel Lo, for his fatherly guidance, encouragement, patience, advice and support. Under his intensive training, I have learnt how to be a “good scientist”. And he is the key factor that leads to the fulfillment of my study.

I would also like to express my deep appreciation to my co-supervisor Doctor Fred Lee. As a talented researcher, he usually provides me new insights into my project and helping me search for solutions when problems come. His enthusiasm in researches makes me realize the happiness and satisfaction of research work.

Besides my supervisors, I would like to thank my senior Doctor Hang-Kin Kong, for his technical assistance of the proteomic works. In addition to direct contribution to my project, he always set a fine example of how a scientist should be. His creativeness brings me a lot of inspiration and fun in researches.

I would like to thank my fellow lab-mates, Katie, Jacky, Sirius, Thomas, Him, Oliver, CY and Waiting, for their continuous support throughout the project. I am also extremely grateful to Steve for his technical help of arginine assay in the project. He is really a very nice guy.

And I would like to express my sincere thanks to my family for their love and cares. I am always thankful to them.

## Table of Contents

## List of Figures

## List of Tables

## Abbreviations

| | |
|---|---|
| AC-T | Toxic *Alexandrium catenella* |
| AC-N | Non-toxic *Alexandrium catenella* |
| AT-N | Non-toxic *Alexandrium tamarense* |
| GC-T | Toxic *Gymnodinium catenatum* |

| | |
|---|---|
| 1,3-BPG | 1,3-diphosphoglycerate |
| 2-DE | Two dimensional gel electrophoresis |
| Acetyl-CoA | Acetyl coenzyme A |
| ANACC | Australian National Algae Culture Collection |
| Arg | Arginine |
| ASP | amnesic shellfish poisoning |
| ATP | Adenosine triphosphate |
| BALST | Basic Local Alignment Search Tool |
| CCMP | Provasoli-Guillard National Center for Culture of Marine Phytoplankton |
| CWC | Chemical Weapons Convention |
| DCMU | 3-(3,4-dichlorophenyl)-1,1-dimethylurea |
| DD | differential display |
| DFAAs | dissolved amino acids |
| DLA | Direct Linear Analysis |
| DSP | diarrheic shellfish poisoning |
| DTT | dithiothreitol |
| EBI | European Bioinformatics Institute |
| EMBOSS | European Molecular Biology Open Software Suite |
| EST | expressed sequence tag |
| FDA | Food and Drug Administration |
| G3P | glyceraldehyde-3-phosphate |
| G3PD | glyceraldehyde-3 phosphate dehydrogenase |
| HABs | harmful algal blooms |
| HSP70 | heat shock protein 70 |
| IAA | iodoacetamine |
| ICAT | Isotope-coded affinity tag |
| IEF | isoelectric focusing |
| IOC | Intergovernmental Oceanographic Commission |
| IPG | Immobilized pH gradient |

| | |
|---|---|
| ITS | Internal Transcribed Spacer |
| LC ESI-iontrap MS/MS | liquid chromatography electrospray ionization iontrap tandem mass spectrometry |
| LC-MALDI | liquid chromatography-matrix assisted laser desorption/ionization |
| LHC | light-harvesting complex |
| LHP | light-harvesting protein |
| LSU | large subunit |
| MALDI-TOF | matrix assisted laser desorption/ionization-time of flight |
| MALDI-TOF/MS | matrix assisted laser desorption/ionization-time of flight tandem mass spectrometry |
| MAT | methionine adenosyltransferase |
| MW | molecular weight |
| NADPH | Reduced nicotinamide adenine dinucleotide phosphate |
| NAP50 | Nitrogen-associated protein-50 |
| NCBI | National Centre for Biotechnology Information |
| NSP | neurotoxic shellfish poisoning |
| OEE | oxygen-evolving enhancer |
| PCP | peridinin-chlorophyll a protein |
| PEPs | proteins expression profiles |
| PFMs | peptide mass fingerprints |
| pI | isoelectric point |
| PSP | Paralytic Shellfish Poisoning |
| PSTs | Paralytic shellfish toxins |
| PTFE | Polytetrafluoroethylene |
| RAPD | random amplification of polymorphic DNA |
| Rubisco II | ribulose 1,5-bisphosphate carboxylase/oxygenase II |
| SAH | S-adenosylhomocysteine |
| SAM | S-adenosylmethionine |
| SDS-PAGE | sodium dodecyl sulfate polyacrylamide gel electrophoresis |
| SPITC | 4-sulfophenyl isothiocyanate |
| STX | saxitoxin |
| TFA | trifluoroacetic acid |
| UPLC | Ultra Performance Liquid Chromatography |

# Chapter 1 Introduction: Literature Review of Paralytic Shellfish Toxins (PSTs)

## 1.1 Paralytic Shellfish Poisoning (PSP)

Globally, more than 60,000 incidences of marine algal toxins poisoning are reported annually (Gill et al., 2003). Primarily, poisoning events caused by algal toxins as contaminants are called shellfish poisoning. Shellfish poisonings have been problematic to human health and the environment for many decades. It is of public concern for a long time. According to different intoxicating symptoms, poisoning caused by algal toxins can be classified into four types: amnesic shellfish poisoning (ASP), diarrhetic shellfish poisoning (DSP), neurotoxic shellfish poisoning (NSP) and paralytic shellfish poisoning (PSP). These causative alkaloid toxins are so potent that even a very small quantity (about 500 μg), which can be easily accumulated in just one 100 g serving of shellfish, could be fatal to human. On a global scale, nearly 2000 cases of human poisoning with nearly 15% mortality through fishes or shellfishes consumption are reported each year (Hallegraeff, 1993). Among these four types of poisoning, PSP-toxins (or paralytic shellfish toxins, PSTs) are the most studied algal toxin (see later sections). PSP has a high mortality rate as it has a rapid onset. The time of onset to the complete development of the poisoning effects usually required thirty minutes to several hours post-exposure (García et al., 2004; Sobel and Painter, 2005). The high mortality rate is a big threat to public health.

Outbreaks of PSP mostly occurred in the coastal areas (Figure 1.1). One of the most serious PSP incidence occurred in Champerico (on the Pacific coast of Guatemala), from July to August in 1987. In this incidence, more than 187 people were affected (70% were hospitalized and 14% died) (Rodrigue et al., 1990). PSP has long been a problem of Alaska, North America. Between 1973 and 1994, with 66 PSP outbreaks, 143 people were reported sick and 2 died (Gessner and Middaugh, 1995). In Asia, from the year 1987 to 1999, there were 1716 cases of PSP related cases with 94 deaths in the Philippines alone (Azanza and MaxTaylor, 2001). Most PSP cases were due to the consumption of contaminated shellfish. The toxins causing PSP are mainly produced by microscopic algae called dinoflagellates. These dinoflagellates are primary producers of the food web and also one of the causative agents of harmful algal blooms (HABs). Filter feeders, such as bivalve mollusks, accumulate these toxins when they feed on these

dinoflagellates. Because mollusks and filter feeders have high tolerance to these toxins, these toxins can reside and be concentrated within tissues of these organisms for weeks and months. These toxins can remain bioactive, i.e. toxic. As a result, higher level consumers, including marine mammals and humans, are exposed to larger doses of toxins (Llewellyn, 2006). In the unfortunate incidence of PSP, the initial symptom includes an initial burning and tingling sensation on the lips, tongue and face; which gradually intensify to include facial and perioral paresthesias. Some individuals may also have headache, dizziness, stomach cramps, nausea and vomiting. Ataxia and dysmetria may occur when the harmful effects spread to the other parts of the body. In serious cases of intoxication, the symptoms can include respiratory failure with diaphragmatic and chest wall muscle paralysis, leading to death (Clark et al., 1999; Llewellyn, 2006; Sobel and Painter, 2005).

**Figure 1.1.** Global Distribution of PSP in 2006. Orange spots/shaded areas represented affected areas.

The negative impacts of PSP are not limited to that of health only; PSP also greatly affect the environment and aquaculture-related economy. Due to the increased consumption of seafood and so the increased establishment of related business, the economic impacts of PSP become much more severe than in the past. PSP may lead to early and prolonged closure of the aquaculture-harvesting areas and fishing grounds which concomitantly bring great loss to fishermen, processors, and related industries. An example of this type of huge damaging effect is a single PSP outbreak that occurred in Maine, USA. It inflicted an estimate of US $6-million loss in total (Shumway et al., 1988). During and shortly after the PSP incidence, because of fear of possible contaminated seafood, consumers demand for these seafood items were depressed. International trade of molluscan shellfishes was affected as well. However, preventative measures including the introduction of extensive surveillance and enforcement activities, such as shellfish-monitoring programs, are costly (Halstead and Schantz, 1984; Shumway et al., 1988). Therefore, there is a need to understand why autotrophs such as the dinoflagellates have to produce PSTs. Further, there is also needs to understand what factors promote production of these toxins and in what circumstances would HAB occur.

### 1.2 Paralytic Shellfish Toxins (PSTs)

Saxitoxin (STX) is the most prominent etiological agents of PSP. It is non-proteinaceous in nature. The name “saxitoxin” comes after its first recognition, which is extracted from the giant Alaskan butter clam, *Saxidomus giganteus* (Hughes and Merson, 1976; Moustafa et al., 2009; Wang, 2008). STX is the parent compound of various PSTs. It is a trialkyl tetrahydropurine consisted of a fused five-membered ring at an angular position, a ketone hydrate and two stabilizing electron-withdrawing guanidinium groups (Dell’Aversano et al., 2008). With different side chains, analogues of PSTs are classified into 3 main groups: Carbamoyl compounds (saxitoxins and gonyautoxins), N-sulfocarbamoyl compounds (B toxins and C toxins) and Decarbamoyl compounds (Oshima, 1995b) (Figure 1.2). Having two guanidinium groups, STX and its 30 naturally occurring analogues are readily soluble in water and possesses 2 $pK_a$’s (Llewellyn, 2006). It should be stressed that different PST analogues have different toxicities and that are dependent on their side chains (Table 1.1).

**Figure 1.2.** Chemical structure of PSTs.

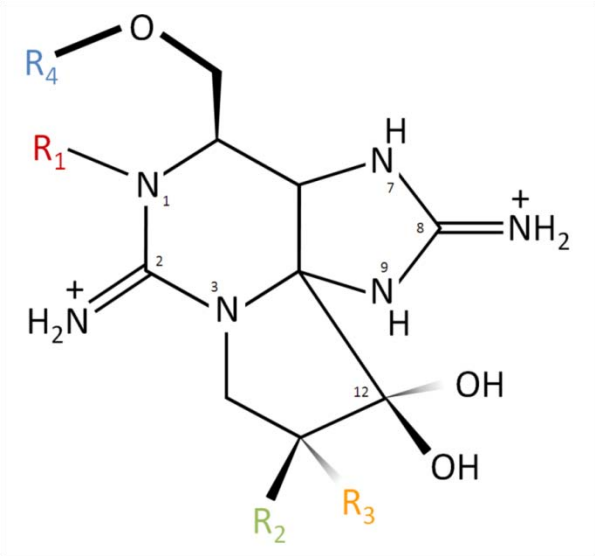


**Table 1.1.** Classification of PSP toxins. *Data adopted from Oshima* (Oshima, 1995b)

| Category | Toxin | $R_1$ | $R_2$ | $R_3$ | $R_4$ | Molecular weight | Relative Toxicity (STX=1) |
|---|---|---|---|---|---|---|---|
| Carbamoyl Compounds | STX | H | H | H | $H_2NCO$- | 301 | 1 |
| | NeoSTX | OH | H | H | | 317 | 0.92 |
| | GTX1 | OH | H | $OSO_3^-$ | | 412 | 0.99 |
| | GTX2 | H | H | $OSO_3^-$ | | 396 | 0.36 |
| | GTX3 | H | $OSO_3^-$ | H | | 396 | 0.64 |
| | GTX4 | OH | $OSO_3^-$ | H | | 412 | 0.73 |
| N-sulfocarbamoyl Compounds | B1 | H | H | H | $^-O_3SNHCOO$- | 380 | 0.06 |
| | B2 | OH | H | H | | 396 | No data |
| | C1 | H | H | $OSO_3^-$ | | 476 | <0.01 |
| | C2 | H | $OSO_3^-$ | H | | 476 | <0.01 |
| | C3 | OH | H | $OSO_3^-$ | | 0.01 | 0.1 |
| | C4 | OH | $OSO_3^-$ | H | | 0.06 | 0.06 |
| Decarbamoyl compounds | dcSTX | H | H | H | H | 258 | 0.51 |
| | dcNeoSTX | OH | H | H | | 274 | No data |
| | dcGTX1 | OH | H | $OSO_3^-$ | | 369 | No data |
| | dcGTX2 | H | H | $OSO_3^-$ | | 353 | 0.65 |
| | dcGTX3 | H | $OSO_3^-$ | H | | 353 | 0.75 |
| | dcGTX4 | OH | $OSO_3^-$ | H | | 369 | No data |

As a group, STX is a potent toxin with heat- and acid-stable characteristics. It remains toxic and cannot be destroyed even after exposure to high temperature, such as that by autoclaving (121$^{o}$C for 15 minutes) and there is still no specific antidote available (RaLonde, 1996). The strong lethality within a short period after exposure further emphasizes its danger as a poison. The poisonous activity comes from the dihydroxy group on the five-membered ring, targeting the sodium channels in nerve and muscle cell membranes (Halstead and Schantz, 1984). Compared to cyanide, PSP toxins have a 100 times greater toxicity. $LD_{50}$ in mice varied among different routes of administration with about 10 μg/kg intraperitoneally; 8.5 μg/kg intravenously; 13 μg/kg subcutaneously and 263 μg/kg orally (Davio, 1985; Wiberg and Stephenson, 1960). Together with mustard gases and sarin, saxitoxin is listed in Schedule 1 of the Chemical Weapons Convention (CWC).

Mechanistically, PSTs and their analogues are neurotoxins. The presence of PSTs blocks the sodium channels of nerve cells, preventing sodium ions from entering the cytoplasm through these channel proteins. Hence, signal transmission is interfered. As no impulse could be generated and/or stimulations transmitted, symptoms including numbness and paralysis are seen. Similar blocking of nervous signal transmission also occurred at the neuromuscular junctions. It was found that the charged 7,8,9 guanidinium groups and the dihydroxy group, which could be hydrated into keto form, are critically involving in forming bonds with the sodium channels. The complex formed blocks the external orifice of the channels (Strichartz, 1984). Other studies also found that STX, the most potent PSTs, can bind to the calcium and potassium channels in other animals (Su et al., 2004; Wang et al., 2003).

Amounts of PSTs present in biological materials can be measured with various methods. However, the mouse bioassay remains the standard assay which is approved by the Food and Drug Administration (FDA) of the United States for detecting PSTs. The time required for the toxin to kill the tested mice is recorded and it is converted into mouse unit (MU) by a standardized conversion method. One MU, equivalent to 0.18 g of active poison, is said to be the amount of toxin that kill a 20-gram mouse in 15 minutes through intraperitoneal injection. This method gives an estimation of the amounts of active toxins present (Horwitz, 1980;

RaLonde, 1996). However, because of animal ethics issues and the inability of this method to access toxin composition in the sample, use of the mouse bioassay has decreased and more scientists have shifted to other technologies such as high performance liquid-chromatography and neuroblastoma cell-line assay for detecting PSTs.

### 1.3 Sources of PSTs

PSTs are synthesized mainly by microalgae. STX and its derivatives, the most common PSTs, are synthesized by several genera of marine dinoflagellates and freshwater cyanobacteria (Hallegraeff et al., 1991; Lagos et al., 1999; McBarron et al., 1975; Oshima et al., 1990). It should be stressed that most outbreaks of PSP events were associated with marine dinoflagellates. In the Taxonomic Reference List of Toxic Plankton Algae of Intergovernmental Oceanographic Commission (IOC), of the 90 PSTs producing microalgae, 70 species are dinoflagellates (Camacho et al., 2007; Gallacher and Smith, 1999).

#### 1.3.1 Dinoflagellates

Dinoflagellates are a large group of planktons, with over 2000 species, and more than half of them are photosynthetic in nature. They are one of the major primary producers which are usually found in coastal waters around the world. Some of them can be found in freshwater system. They can exist in both pelagic and benthic habitats. They are mostly unicellular but chains could be found in some species when single cells connected with each other. Sizes of the cells usually ranged from 5 to 2000 microns in diameter and can vary for different species as well as for different stages of their life cycles (Lee, 2007). Dinoflagellates exhibit some unique features, including the presence of pusule (series of vesicles near the base of flagella for osmoregulation, macromolecule uptake and secretion), plastids surrounded by three membranes and the presence of single- or dual-gene mini-circles (Barbrook and Howe, 2000; Gibbs, 1981; Sze, 1998; Zhang et al., 1999).

It was estimated that the DNA content of dinoflagellates could be as high as 200 Gbp and hence about 80 times that of human (Lin, 2006). Reproduction of dinoflagellates is usually performed by mitosis. Sexual reproduction may also occur by the formation and fusion of the

gametes, resulting in a diploid (planozygote) (Graham and Lee, 2000). When the surrounding environment becomes unfavorable, vegetative dinoflagellates will form cysts. Cysts are the resting cells with the following 4 characteristics: 1) their thecal plates are separated from the cell surface; 2) the flagella are shed off; 3) a cyst wall is formed and 4) non-motile. The world-wide spread of PSP may be explained by the transportation of the various species of toxic dinoflagellates in the form of cysts to new habitat by means of water current and ballast water of ships (Hallegraeff, 1998). It should be noted that cysts of the toxic strain of dinoflagellates are also toxic and could pass on its PSTs to the upper level consumers (Oshima et al., 1992).

### 1.4 PSTs Producing Dinoflagellates

Not all dinoflagellates are toxic in nature. Among them, three genera of dinoflagellates were found to be able to produce PSTs including *Alexandrium*, *Gymnodinium* and *Pyrodinium* (Figure 1.3).

**Figure 1.3.** Distribution of PSTs producing dinoflagellates.

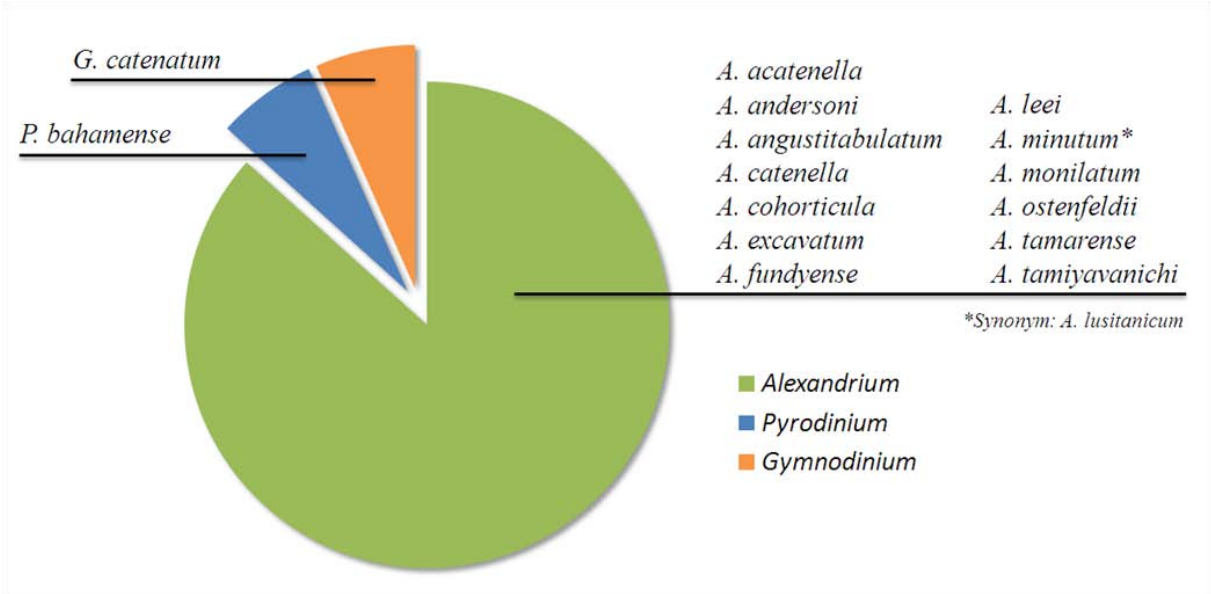

### 1.4.1 *Alexandrium spp.*

As shown in Figure 1.3, a sizable portion of PST-producing dinoflagellates belongs to the *Alexandrium* genus. They exist widely in different regions all over the world. Generally, the blooming of *Alexandrium* species takes place in estuarine coastal regions and the frequency of occurrence have significantly increased over the past few decades (Anderson et al., 1994). Within the genus, there is a range of morphological variations. Such variations may due to natural variations, sexual reproduction (which increases the generic diversities) and different environmental conditions. *Alexandrium spp.* has the typical structures of dinoflagellates without any spines or horns, but with a characteristic apical pore plate and thin cell wall. Ends of the central grooves displaced about one girdle width and the margins have very shallow ridges (Figure 1.4).

**Figure 1.4.** General structure of *Alexandrium*.

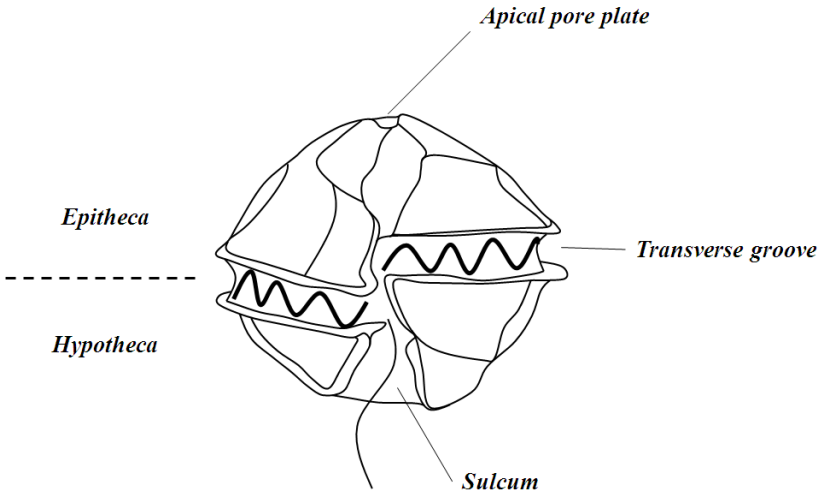


*Alexandrium* cells are round or oval and their sizes ranged from 20 to 50 µm in diameter. In addition to single cells, they may also form pairs or in chains. Two kinds of cysts could be formed by *Alexandrium*: the pellicle- and the resting-cysts. Pellicle cysts are produced from vegetative cells when the environmental conditions are not favorable. These cysts require a dormancy period and only have a limited durability, not overwintering. Compared to the

pellicle cysts, resting cyst are more resistant to environmental extremes (Balech, 1985a; RaLonde, 1996).

As not all *Alexandrium* species are toxic, it is important to know the identity, behavior and toxicity of the causative agents during a HAB so as to devise prompt and suitable measures to combat its negative impacts. Identification of the *Alexandrium* species has long been accomplished using their morphological characteristics. For example, the proportion of epitheca to the hypotheca could be used to distinguish *A. acatenella* from *A. catenella*. It is because *A. catenella* have equal lengths of epitheca and hypotheca while *A. acatenella* have a longer epitheca. Sizes, shapes, porulation of the surfaces, characteristically arrangement of the thecal plates, chain lengths, etc. are essential for morphological identification. However, morphological identification methods required a significant degree of observation and personal judgment. Hence, there is frequent disagreement on the classification and/or identification of *Alexandrium* when morphological features were used for identification. Subsequently, gene-sequence based methods, i.e. sequence of ribosomal-RNA genes, has been used more often for identification purposes (Agriculture Fisheries and Conservative Department, 2008; Balech, 1985a; Litaker et al., 2007; Taylor et al., 2003). Unfortunately, these methods required prior knowledge of genes of the dinoflagellates being identified. In the protein level, Lee and his coworkers had adopted a matrix-assisted laser desorption/ionization time-of-flight (MALDI-TOF) mass spectrometry based protein profiling method for fast identification of dinoflagellates down to species level. This method required no prior knowledge of the causative agent(s) of a HAB (Lee et al., 2008).

Not all species of *Alexandrium* produce PSTs. Some species in the genus are non-toxic, e.g. *A. affine* (Band-Schmidt et al., 2003; Wang et al., 2006). Many studies have been carried out focusing on *Alexandrium* as this genus could be found globally and relatively easy to culture. Nonetheless, the linkage of toxic *Alexandrium* to PSP was discovered as early as 1937 (Sommer et al., 1937). Within the genus, the toxin profiles are different among different species. Variations included the amounts of PSTs synthesized and the toxin compositions, leading to the great differences in toxicities. Further, different strains of the same species isolated from

different regions were reported to have different toxin profiles. This deviations could be a result of variations sequel to variations in availability of nutrients and environmental conditions (Wang et al., 2006). Some species, like *A. catenella* in Baja California, could generate high toxin content with low cell numbers (Hernández-Becerril et al., 2007). It should be stressed that morphological identification methodologies sometimes could not accurately identify dinoflagellates of the *tamarense*/*catenella*/*fundyense* complex because of their small morphological difference. That reaffirms the need for fast and accurate species identification methodologies.

Different *Alexandrium* species were known to produce different amounts and profiles of toxins. Lim and Ogata reported that under identical culturing conditions, 4 species of *Alexandrium* have similar but not identical toxin contents and composition (Lim and Ogata, 2005). Although all of them produce chiefly gonyautoxins (GTX) 1 and 4, B1 toxin was specifically present *in A. tamiyavanichii* while B2 toxin was only found in *A. peruvianum*. Further, it was found that only *A. minutum* processed a little amount of GTX2, GTX3, STX and NeoSTX. Different species of *Alexandrium* in the study produced different amounts of the same toxin, either in terms of molar percentage (highest % of GTX1 and GTX4 in *A. minutum*) or toxin content (highest amount per cell by *A. tamiyavanichii*). Moreover, *A. andersoni* was reported to produce mainly STX and NeoSTX (Ciminiello *et al.* 1999; Ciminiello *et al.* 2000).

Differences in toxigenicity were also reported in different strains of the same species. Ichimi and his team had isolated 20 strains of *A. tamarense* from Sendai Bay and Nagatsura-ura (Ichimi et al., 2002). For both locations, the toxin compositions of the isolates at the same site have a large variation already. One isolate from Nagatsura-ura produced nearly 80% of GTXs while another had only about 20% of GTXs. Ichimi and coworkers tried to explain the observations with the hypothesis that there was an introduction of DNA from other strains (in the form of cysts) from other geographical areas into the region before subsequent re-combination of different toxin genomes within the population. Likewise, two different strains of *A. tamarense* isolated from the South China Sea demonstrated different toxin profiles (Wang and Hesieh, 2005; Wang and Hsieh, 2002b). *A. tamarense* CI01 produce chiefly C2 toxins while

*A. tamarense* HK9301 produce other C toxins and also GTX1, GTX4 as well as GTX5. Similar findings were reported in other *Alexandrium* species (Lim et al., 2006; Wang et al., 2006).

The variation in toxicity of the same species of *Alexandrium* could range from highly toxic to non-toxic. In 2007, Touzet and coworkers reported that both toxic and non-toxic strains of A*. minutum* were found after extensive monitoring of the Irish coastal regions (Touzet et al., 2007a). Blooming of the species sometimes did not result in shellfish toxin accumulation. Besides natural occurrence, toxic and non-toxic pairs of the same species of *Alexandrium* were also found in the laboratory grown cultures (Cho et al., 2008). After several years of sub-culturing, a non-toxic subclone isolate was unpredictably found from the original toxic *A. tamarense* culture when it was used for another experiment. Such information implies that the toxigenic characteristic of *Alexandrium sp.* is not always present in all strains of the species.

### 1.4.2 *Gymnodinium spp.*

Within the genus of *Gymnodinium*, *Gymnodinium catenatum* (Figure 1.5) is the only PST-producing toxic species known. Among the known PST-producing dinoflagellates, *G. catenatum* is the only unarmored dinoflagellate which is able to produce PSTs. Morphologically, it has the distinctive feature of having a transverse groove line in the middle of the cell and a left-handed displacement with 20% of the cell length (Kofoid and Swezy, 1921). Further, both the cingulum and sulcum are deep. The sulcum extends to and surrounds the apex in the region of apical horse-shoe groove. The shape of the cells will change from elongate-ovoid to squarish-ovoid when the cells changed from single-celled (or pair) stage to the chain-forming stage. The apex is conical; the antapex is rounded and bilobed when the cells are not in chains. In contrast, chain-forming cells have slightly apico-antapical compressions. Its nucleus is at the centre of the cell. Plenty of yellow-brown chloroplasts, noticeable pyrenoids for $CO_2$ fixation and lipid globules are also present in the cells (Blackburn et al., 1989; Fukuyo et al., 1990; Graham, 1943; Larsen and Moestrup, 1989; Steidinger and Tangen, 1996; Taylor et al., 2003). *G. catenatum* can have both asexual and sexual reproduction. Cysts would form after nutrient deficiency. The cysts are rounded shape with unique micro-reticulation coverings.

**Figure 1.5.** General feature of *Gymnodinium catenatum*.

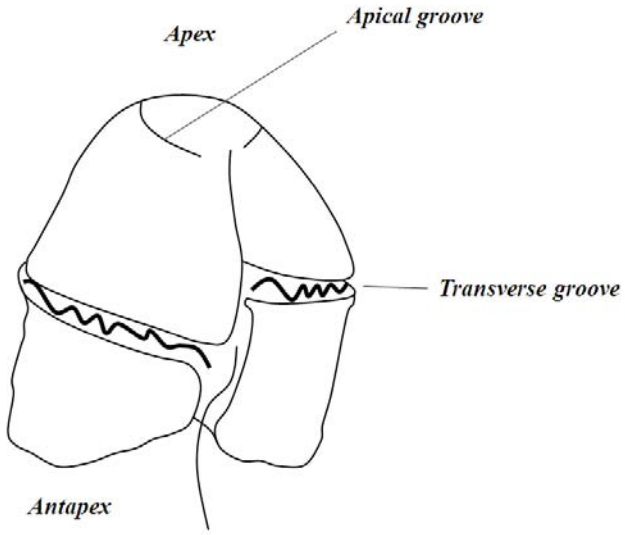


Similar to that of the *Alexandrium* species, toxins profiles of *G. catenatum* in different countries differs. The research group of Oshima reported that the toxin composition profiles of different strains of *G. catenatum* isolated from Australia, Spain and Japan were different from each other (Oshima et al., 1993). C1 and C2 toxins constituted the largest proportion (over 75 %) of the total toxins produced in the Australian and Japanese strains; while the Spanish strain produce only 30% of C1 + C2 toxins, similar to the amount of B2 toxins. C3 and C4 toxins were found in the Australian and Spanish strains but not in the Japanese strains. Variation in toxin composition profiles of *G. catenatum* could further be found among strains from different sampling locations of the same geographical region (Gárate-Lizárraga et al., 2005); and also among different strain isolates of a single blooming event (Ordas et al., 2004).

### 1.4.3 *Pyrodinium spp.*

The Greek word "Pyr" means fire. *Pyrodinium* species are bioluminescent dinoflagellates which are able to produce light by themselves. So far, only the species *bahamense* is found to be toxigenic for PSTs production (MacLean, 1977). It is named as such as the species was found in Bahamas (Plate, 1906). *P. bahamense* has similar structure to *Alexandrium* species, but their

thecae are much heavier and covered with dense fine spinulae (Figure 1.6). Left-handed girdle displacement is present. Further, the surface has large prominent pores and the edges of most sutures are marked with strong low flanges. The apex is shaped as a low horn and includes a large triangular apical pore complex. The attachment pore at the posterior end is silt-like. Moreover, there is a distinct ventral pore in the forth apical plate and clear lists of the girdles. The lists of sulcum are large and in contact with each other, making a tunnel at the antapical side. Single cells process spines on the apical and antapical surface. Their cysts are spiny (Morquecho, 2008; Steidinger and Tester, 1980).

**Figure 1.6.** General feature of *Pyrodinium bahamense*.

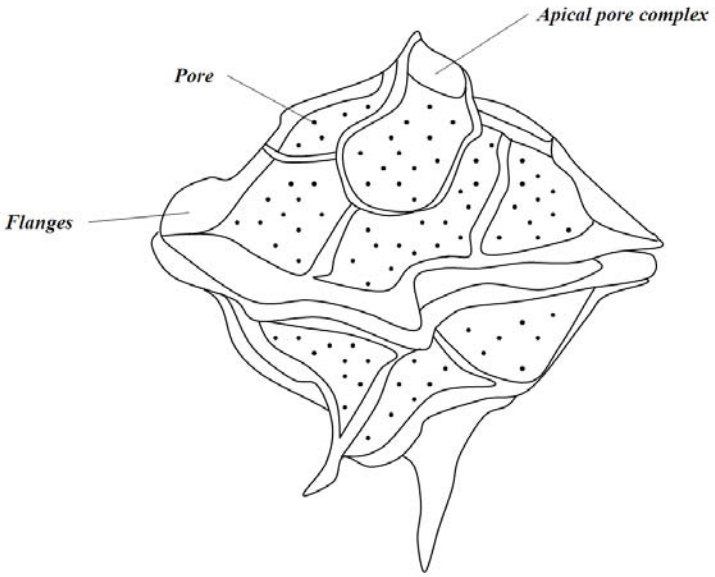


Two varieties of *P. bahamense*, with dissimilar morphologies, were identified from different geographic regions (Table 1.2). *P. bahamense var. compressum* is found principally in South-east Asian to Indo-Pacific waters, while *var. bahamense* were discovered in the tropical West Atlantic (Steidinger and Tester, 1980). As shown in Table 1.2, the two variants have several differences. *P. bahamense var. compressum* are capable to form chains while *var. bahamense* are single-celled or maximal in pairs. The chain forming cells are a little flattened anterior-posteriorly, compared to the round shaped single individual. Spines are only present

on the apical side of the first cell (most anterior) and on the antapical side of the last cell (most posterior). *P. bahamense var. bahamense* have a more pronounced apical horn, larger spines, but less prominent pores (Badylak et al., 2004). Another characteristic difference between the two variants is the PSTs producing abilities. *P. bahamense var. bahamense* is nontoxic, which differentiates them from the toxic *var. compressum* (Steidinger and Tester, 1980). However, Balech opined that the differences between the two variants may be a result of ecological factors and not genetically based (Balech, 1985b). However, in 2006, Landsberg reported that a clone of *P. bahamense var. bahamense* isolated from the Indian River Lagoon in Florida is also toxic (Landsberg et al., 2006).

**Table 1.2.** Comparsion between *P. bahamense var. compressum* and *var. bahamense* (Badylak et al., 2004; Morquecho, 2008; Steidinger and Tester, 1980).

| | ***P. bahamense* varieties** | |
|---|---|---|
| | ***var. compressrum*** | ***var. bahamense*** |
| **luminescence** | Luminescent | Luminescent |
| **Ventral pore** | On the 4th apical plate | On the 4th apical plate |
| **Shape** | Flattened longitudinally | Rounded |
| **Girdles** | Clear list, left-handed displacement | Clear list, left-handed displacement |
| **Apical horn** | Less pronounced | More pronounced |
| **Surface pores** | More prominent | Less prominent |
| **Association** | Chain-forming | Single / paired |
| **Surface spines** | Limited on the anterior and the posterior surfaces of the first and the last cells in the chain respectively | On both anterior and posterior surfaces |
| **First reported** | Bahamas (Plate, 1906) | Florida (Steidinger and Tester, 1980) |
| **Principal occurrence** | South-east Asian and Indo-Pacific waters | Tropical West Atlantic |
| **Reports of toxigenicity** | PSP toxic (MacLean, 1977) | Non-toxic (Steidinger and Tester, 1980)<br>PSP Toxic (Landsberg et al., 2006) |

Regional differences in toxin production can also be found in *Pyrodinium bahamense*. As early as 1987, toxin profile of *P. bahamense* isolate from Palau composed of GTX4, B1, STX and NeoSTX with a minute amount of dcSTX (Oshima et al., 1987). Later in Malaysia, another isolate

(*P. bahamense var. compressum*) was found to have a different pattern that B2 toxin was detected with no GTX4 formed (Usup et al., 1994). The NeoSTX and B1 toxins of that isolate were found to comprise around 80% of the total toxin content. Presence of GTX2, GTX3 and the absence of dcSTX were found in the Guatemala strain (Rosales-Loessener et al., 1989). In a recent study, however, Gedaria and coworkers showed that the Bamban Bay's strain (*var. compressum*) in Philippines are capable of producing chiefly STX (90%) and a little of dcSTX and B1 toxins (Gedaria et al., 2007). On the other hand, it was found that *P. bahamense var. bahamense* had a simple profile with only three toxins (73% of B1 toxins, 26% of STX and the rest was dcSTX). The reason for their variations in toxicities is still inconclusive.

### 1.5 PSTs Producing Bacteria

It is known that live dinoflagellates populations, including those cultures in laboratories, coexist with free-living and/or harbored bacteria (Bold and Wynn, 1978; Hold et al., 2001b). These bacteria could exhibit either beneficial or harmful impact on the biology of algae (Doucette et al., 1998; Gallacher and Smith, 1999). It was found that some bacteria could have a direct effect on the production of toxins in dinoflagellates. There was even some suggestion that the harbored bacteria are the real sources of PSP toxins produced. There are two lines of evidence: 1) It was found that a non-toxic dinoflagellate clone could be transformed to become a toxic dinoflagellate clone after being inoculated with a *Pseudomonas* bacterium isolated from the corresponding toxic strain (Silva and Sousa, 1981). 2) The discovery that some bacteria produce STX themselves (Kodama et al., 1990). Many debates exist on such issue. However, subsequent experiments showed that elimination of bacteria from some toxic dinoflagellates do not eliminate the toxin synthesizing abilities of the algae (Hold et al., 2001a; Uribe and Espejo, 2003). Nevertheless, it was shown that the amount of the toxins produced were down-regulated after its co-existing bacteria were eliminated. Overall, the bacterial-algal relationship on PSTs production is complicated and lots of questions remain unanswered.

### 1.6 PST Toxicity and Arginine

Arginine was postulated to be a precursor for saxitoxin synthesis. Its relationship to the PSTs content had been examined (Shimizu et al., 1984). When one plotted the toxicity against arginine concentration in a culture, a positive correlation was reported (John and Flynn, 2000). Research group of Flynn also reported similar results (Flynn et al., 1994). However, in both studies, arginine alone was not the only controlling factor in cellular toxicity. Experiments showed that the positive correlation seen with arginine increase was dependent on the nutrient status, i.e. N and phosphate. Flynn suggested a toxin-taurine relationship in addition to the toxin-arginine relationship (Flynn et al., 1994). On the other hand, Flynn and coworkers compared several *Alexandrium spp.* and found that the intracellular arginine levels were the highest in the most toxic species (Flynn et al., 1996). Direct effect of arginine on the toxin content has been studied by John and Flynn (John and Flynn, 1999). Exogenous arginine was added to the culture and the toxicity was found to be increased. However, an unnatural concentration of arginine was needed to cause the effect. In contrast, in most batch-cultured experiments of *Alexandrium spp.* performed by Anderson's group, variations of concave patterns of arginine with time were found to mirror the convex patterns of toxin content (Anderson et al., 1990b). The inconsistent findings illustrate the complexity of the actual role of arginine in PSTs production. Further, the arginine-toxin relationship in *Gymnodinium sp.* has not been reported.

### 1.7 Toxigenic Variation

It is known that the toxicities of dinoflagellates varied at different phases of its cycle. A toxic dinoflagellate does not produce toxins in the same extent at all time over its various life stages. Many studies reported that the rate of toxins production is highest during the mid-exponential stage of growth and decrease as it approach the stationary phase (Anderson et al., 1990a; Boyer et al., 1987; Hamasaki et al., 2001; Hwang DF and Lu YH, 2000; Ogata et al., 1987; Wang et al., 2006). Anderson's group proposed that the cells tend to maintain a certain constitutive amount of toxins intracellularly after dividing from the parent cells (Anderson et al., 1990b). As cell division is active and the nutrients levels are abundant during the exponential phase, the

rate of toxin production is increased (Chan et al., 2005). When the dinoflagellates develop into the stationary phase, cell division rate drops to a low level. Further, the essential nutrients for toxin production (e.g. nitrate) may become limiting, then the toxin producing rate may decrease concomitantly. Another possible explanation for the decline is the shortage of $CO_2$ and shift of pH which decreased the amount of raw material and enzymatic activities for toxin production (Anderson et al., 1990a). It should be stressed that contradictory observations on the increase/decrease of toxin levels do exist in the literature with some reports claiming that the toxins levels reach the maximum at stationary phase. The higher amounts of toxin content were presumed to be the results of decreased cell division rate and the surplus of arginine for toxin production (Oshima and Yasumoto, 1979; Wang and Hesieh, 2005; White, 1978). Such discrepancy on the toxin profiles observed was sometimes attributed to the differences in the species (or strains) of dinoflagellates used for individual studies, the experimental setup, the toxin extraction method and difference in methods used for maintaining the dinoflagellates cultures.

Besides reports on variations in toxin levels at different growth stages, toxin biosynthesis was also examined at the cell-cycle level. Anderson and coworkers reported that there is a direct proportional relationship between specific growth rates and specific toxin production rates (Anderson et al., 1990b). Research team of Taroncher-Oldenburg followed Anderson's implication that toxin synthesis might be linked to cell cycle events. They synchronized the growth of these dinoflagellates with a long dark incubation period to arrest the population at a particular point of their cell cycle. After restoring the normal light-dark cycle, individual cells started at the same phase in terms of their cell cycle. Samples were collected at 2-hour intervals for toxin measurements. Their results showed that toxin production was induced by light and preceded over a discrete period in the $G_1$ phase, for about 8–10 hour (Taroncher-Oldenburg et al., 1997). On the other hand, Siu's research group followed with similar synchronization methodology but for a shorter period, and they found that the toxin contents were increased about 1-hour after entering the S phase. The toxin content remains at a high level until the end of $G_2$/M phase (Siu et al., 1997). They then suggested that PSTs biosynthesis occurred in parallel with DNA synthesis. Implications from those two studies are

inconclusive as there were many differences in the experimental setup between them. For example, Taroncher-Oldenburg and coworkers worked on *A. fundyense* while Siu and coworkers worked on *A. catenella*. However, both studies did show that toxins production is not continuous throughout the whole cell cycle.

Lastly, the notion that toxin composition could be used as a "genetic fingerprint" for differentiation of different dinoflagellates had been contemplated by many groups as the individual profiles changed very little with different growth stages (Cembella et al., 1987; Gedaria et al., 2007; Ogata et al., 1987; Parkhill and Cembella, 1999; Usup et al., 1994). However, contradictory results were also reported by some groups who stated that the compositions of toxins did change with different growth stages induced by different growth conditions (Anderson et al., 1990b; Boczar et al., 1988; Wang and Hesieh, 2005). Therefore, the notion needs to be further substantiated and more investigations are needed to focus on the biosynthesis and the compositional relationships of the PSP toxins within an isolate of dinoflagellates.

## 1.8 Physical and Environmental Factors that Affects Toxin Production

PSTs producing dinoflagellates around the world were reported to have a wide range of toxigenicity. Parts of such variations could be attributed to different genetic traits. Variations in toxigenicity can be caused by other external factors. Many studies aimed to elucidate the relationship among these factors with toxins production were performed. The following is a summary of the external factors that may affect PSTs production. Unless specifically annotated, the experiments reported were performed in batch-cultures.

### 1.8.1 Availability of Nitrates

PSP toxins are nitrogen-rich compounds with 32.6% of molecular weight of STX are nitrogen and hence the availability of nitrogen is expected to have significant effect on toxin production. A positive relationship between nitrogen supply and PST production has been documented by many studies (Anderson et al., 1990a; Flynn et al., 1994; John and Flynn, 2000; McIntyre et al., 1997; Strichartz, 1984; Wang and Hsieh, 2002b). Increased nitrate content in the culture

medium as the principal source of N is known to increase PSTs production. This $NO_3$-dependent variation was found in *Gymnodinium catenatum* and several *Alexandrium* species. When these cultures were subjected to $NO_3$-limiting conditions, toxin productivity decreased (Touzet et al., 2007b). Anderson's research group suggested that, when $NO_3$ is limiting, competition of N sources between PSTs production mechanisms and other important metabolic pathways become significant and eventually toxins production was decreased (Anderson et al., 1990a). On the other hand, if $NO_3$ is in excess of the requirement needed for cell growth, surplus $NO_3$ will be used for biosynthesis of PSTs and it was suggested as the N storage for some dinoflagellates (Chan et al., 2005; Loeblich, 1984; Siu et al., 1997). However, the exact mechanism of how $NO_3$ availability translate into different PST production rate is still unknown (Leong et al., 2004; Oshima et al., 1993).

### 1.8.2 Availability of Phosphates

Several studies reported that toxin content dramatically increases under $PO_4$-limiting condition (Anderson et al., 1990a; Boyer et al., 1987; Lippemeier et al., 2003; Siu et al., 1997). Data from Siu and coworkers showed that toxin accumulation inside the cells could happen even at $PO_4$-omitted medium, which is not the case in other studies (Siu et al., 1997). Regardless of this difference, increases in toxin content in $PO_4$-limited but normal $NO_3$ culture could be explained with a widely accepted reason. It was proposed that phosphorus is essential for DNA (nucleotide) synthesis. When the supply of P is inadequate, DNA synthesis and cell division ceased. Less amount of arginine (precursor of PSTs) produced continuously will be used for metabolic activities in cell division and so become available for PSTs production (Anderson et al., 1990b). The relationship could also be viewed as a higher toxin content resulting from usual rate of PST synthesis in a growing but undivided cell (due to lack of $PO_4$ for DNA synthesis). Phosphate limitation usually does not change the toxin composition. In addition, the claim that $PO_4$-limited condition which has no DNA synthesis, may give support to the findings by Taroncher-Oldenburg et al. who reported that the toxin was synthesized in $G_1$ phase, before the production of daughter chromatins (Taroncher-Oldenburg et al., 1997). It should be reiterated

that the exact mechanism of how PST is produced is not known in dinoflagellates. How increased arginine with decreased phosphate increase PST production is currently unknown.

### 1.8.3 N:P Ratio

As a sequel of the low-phosphate high toxin observations, it should be noted that some investigators did not explain fully that the enhancement of toxin production with "phosphate limitation" was coupled to a normal amount of nitrate. That is, enhanced toxin production was associated with "high nitrogen/phosphate ratio". Touzet and coworkers reported that the N:P ratio needed to be high for the toxin quota to be increased. These authors suggested that individual decrease of either $NO_3$ or $PO_4$ would impair the normal functioning, including growth and toxin synthesis of the cells (Touzet et al., 2007b).

### 1.8.4 Availability of Other Nitrogen Sources

Other than nitrates, the effects of toxin synthesis by other forms of N sources had also been studied. Effects of nitrate (oxidized form of nitrogen) and ammonium (reduced form) as the N source on toxins production rate were compared. It was found that $NH_4$-grown culture increased the synthesis of toxins more than that of $NO_3$-grown culture (John and Flynn, 2000; Lim et al., 2009; Wood and Flynn, 1995). Experiments performed by Leong' group showed that increases in cellular toxin levels co-occurred with increases in concentrations of both N sources (Leong et al., 2004). However, the toxin contents were 5-6 times higher when cells were grown under $NH_4$ as the N source than that of $NO_3$. Wood and Flynn suggested that $NO_3$ imposed some kind of N-stress to the metabolic activity of the cells which somehow hampered the availability of N for toxin synthesis (Wood and Flynn, 1995). As a result, $NO_3$ induced production of fewer toxins. Besides, toxin compositions were found to be relatively stable under cultivation conditions with both N sources. However, some experiments produced somewhat different results. Wang and Hesieh reported that the toxin content in cells decreases a lot when $NH_4$ was used to replace $NO_3$ as the N source (Wang and Hesieh, 2005). Flynn and coworkers also found that when N was added to the stationary N-starved *G. catenatum* culture, $NO_3$ fed cells gave more toxins than $NH_4$ did (Flynn et al., 1996). The different results were again attributed to the

different species or strain studied. Leong's group reported that urea concentration and toxin levels had a negative relationship, implying that dinoflagellates cells may utilize urea in a different mechanism other than those used by $NO_3$ and $NH_4$ (Leong et al., 2004).

### 1.8.5 Arginine

As elaborated earlier, arginine was found as the precursor for saxitoxin synthesis in cyanobacteria (Shimizu et al., 1984). In the presence of ammonium as the nitrogen source, addition of exogenous arginine caused an increase in toxin production in *A. fundyense* (John and Flynn, 1999). It is currently taken that exogenous arginine increase toxin production in all species of toxic dinoflagellates.

### 1.8.6 Light Intensity

Effects of light intensity on toxins production in dinoflagellates which are autotrophs are complicated to access as light is also an important factor for photosynthesis. On this note, some scientists believe that toxin production is affected indirectly by light which is associated with growth rate (Ogata et al., 1989; Parkhill and Cembella, 1999). The research group of Ogata found an inverse relationship between toxin content and light-dependent growth rate in *A. tamarense* (Ogata et al., 1987). Hamasaki's group also documented a coincidence of high cellular toxicity under low light intensity with reduced growth rate (Hamasaki et al., 2001). On the contrary, Lim and coworkers showed that difference in growth in two discrete temperatures did not resulted in difference in cellular toxin contents (Lim et al., 2006). The authors implied that variation to toxins biosynthesis was a response to light, instead of a function of growth response. Moreover, various other groups also reported contradicting results from their studies on light-toxin production (Usup et al., 1994; Wang and Hesieh, 2005). It may be due to the fact that different organisms were used in their studies and also the ranges of light intensities being tested were different. Despite of these factors, maximum cellular toxins productivity seems to occur generally at intermediate light intensity, which is for sub-optimal growth. Certainly, more studies are required to understand the mechanisms involved.

### 1.8.7 Temperature

The observations that PSTs contents in the algal blooming regions were higher in some seasons were taken as a sign that temperature is a factor that may affect PSTs production (Anderson et al., 1990b; Gedaria et al., 2007; Navarro et al., 2006). Similar to light intensity, growth-related inverse relationships were commonly found in toxin contents against culturing temperatures. Cellular toxicities were highest under sub-optimal (lower) temperature. These patterns of relationship were seen in *Alexandrium sp.* and *Pyrodinium sp.*, which accumulate most toxins with several degrees (5–7$^{o}$C) lower than that required for their optimal growth (Siu et al., 1997; Usup et al., 1994). Great compositional change in toxin profile was not found by changing the culturing temperature (Oshima et al., 1993). Specific growth rate was reduced concomitantly. Could such co-occurrence be explained by a simple relationship that slower cell division contribute to the toxin accumulation inside the cells? Results obtained with the Malaysian *P. bahamense* strain seems to imply the contrary (Usup et al., 1994). With the same temperature range, it is shown that the rate of toxins content enhancement is greater than the decrease in growth rate. Other factors such as turnover rates of cellular components were also implicated to be involved. Enzymatic metabolism might be retarded and so more arginine is available for toxin synthesis. These hypotheses need to be verified by more biochemical researches in the future (Wang et al., 2006).

### 1.8.8 Salinity

Salinity probably is the most uncertain factor that may affect PSTs biosynthesis. White and others studied the effects of salinity on toxin production and reported positive relationship between them (White, 1978). On the other hand, Usup's group and Hamasaki's group reported a negative relationship (Usup et al., 1994). Some others claimed that the effect is neutral (Anderson et al., 1990b; Flynn et al., 1996). These contradictory findings could be a result of the use of different species of dinoflagellates. Lim and Ogata had performed a comparative study on the effects of salinity on four tropical *Alexandrium spp.* Under the same experimental setup, the four species showed different response to the effects of variation in salinities. They concluded that the salinity effects are both regional- and species-dependent (Lim and Ogata,

2005). Additionally, the difference observed in different studies might be a consequence of the difference in experimental setups, including the acclimation time and the range of salinity gradients being tested (Wang et al., 2006). Hence, whether the salinity effect is direct or growth-related is still an open question (Parkhill and Cembella, 1999; Wang et al., 2006). Nonetheless, comparatively, compositional changes of these toxins by salinity are somehow more apparent than that of light and temperature (Lim and Ogata, 2005; Oshima et al., 1993).

### 1.8.9 Others

Besides factors elaborated above, effects of other factors such as pH, $Fe^{3+}$, $Cu^{2+}$, amount of dissolved amino acids (DFAAs) and nutritional supplements such as $HCO_3^-$ etc. on toxin production had also been investigated (Hwang and Lu, 2001; John and Flynn, 1999; Wang and Hsieh, 2002a). Hwang and Lu reported that toxins production in a strain of *A. minutum* was highest at optimal pH and optimal concentration of $Fe^{3+}$ and $Cu^{2+}$ (Hwang and Lu, 2001). John and Flynn found that the use of DFAAs did not enhance the toxin content in *A. fundyense* (John and Flynn, 1999). Wang and Hsieh reported that supplementation of $HCO_3^-$ could increase the yield of C2 toxins in *A. tamarense* ATCI01 (Wang and Hsieh, 2002a). Nonetheless, their findings needed to be confirmed by others and with more dinoflagellates species to be tested. Summing up, it is felt that PSTs biosynthesis in dinoflagellates is a combination of variation in genetic traits and effects of environmental factors. All these factors had a complex interplay and hence the story of toxigenicities of these organisms is very complicated!

## 1.9 Genomic and Proteomic Studies on PSTs Producing Dinoflagellates

Because of the extremely large genome sizes of most PSTs producing dinoflagellates, whole genome sequencing of any regular dinoflagellate is finally inhibitory. Consequently, development of molecular biology related technologies in the research field of dinoflagellate is non-existence. The mechanism of toxin production in dinoflagellates on the molecular biology level is poorly understood. Nevertheless, after crossing two different strains of the toxic dinoflagellates *A. catenella*, Sako and coworkers reported that toxin profiles in the F1 progeny followed that as predicted by the Mendelian inheritance fashion (Sako et al., 1992). This clearly

shows the chromosomal localization of genes involved in PSTs biosynthesis in these dinoflagellates. Some other attempts were made subsequently to find out the genes involved in the biosynthesis of PSTs. However, as elaborated earlier, this task is difficult as the genome size is huge. Nonetheless, a few studies had made some progress in this front.

A study using differential display (DD) by Taroncher-Oldenburg's group had successfully identified and characterized three differentially expressed genes in *A. fundyense* (Taroncher-Oldenburg and Anderson, 2000). Based on the previous findings of their group, toxins syntheses were postulated to be restricted in the $G_1$ phase. DD of mRNA produced in different cell stages when toxin production was turned on and off was studied. The results were verified by RNA dot blot analysis. The results revealed one down-regulated and two up-regulated genes when toxin production was "turned on". However, it seems that only the down-regulated gene, coding for S-Adenosylhomocysteine hydrolase, might have some correlation to STX biosynthesis. Further, this enzyme is not specific to STX production. It also regulates the S-adenosylmethionine (SAM) pathway, which is involved in many metabolic processes in dinoflagellates. In the results section later, I am going to show that SAM pathway is involved in the STX biosynthesis.

The research group of Touzet compared the toxic strain and the non-toxic strain of *A. minutum* isolated from southern and western coastal waters of Ireland (Touzet et al., 2007a). Without the distinction from LSU rDNA (ITS1-5.8S-ITS2) sequence alignment, random amplification of polymorphic DNA analysis (RAPD) of these strains leads to genetic linkage classification of these strains into two clusters. The clusters are apparently developed from their respective geographical regions, as the "toxic" cluster contains a non-toxic *A. tamarense* clone isolated from the same area as the toxic *A. minutum*. Nonetheless, the segregation of toxic and non-toxic characters coincided with their respective clusters. These results showed the possibility that the toxic and non-toxic strains of PSTs producing dinoflagellates can be developed from a common ancestor.

Genetic and toxigenic differences at the strain level induced after sexual reproduction posed additional complications for comparative genomic analysis in dinoflagellates. Studies in clones with high genetically consistence could minimize the problem. Cho and coworkers

reported the development of a non-toxic subclone from the parental toxic *A. tamarense* clone (Cho et al., 2008). Phylogenic analysis using 28S and ITS1-5.8S-ITS2 sequences found no difference, suggesting that both clones were arisen from the same cell, not contamination. This pair of axenic subclone which differ in their toxigenicities were then used for comparison. Differences in gene expression were found using subtractive hybridization methodologies. Two and four predominant bands were produced by the toxic and non-toxic subclones respectively. The differing sequences were in the homologous fragments of cytochrome c oxidase III and the 5'-flanking region of cytochrome b. Although the experiment could not explain the variation in these two regions between the toxic and the non-toxic subclones, the results implied that the difference in the toxigenicities was not due to translational regulation, but to the dissimilarity of mRNA sequence and hence differential expression of gene products. In 2009, genomic information associated with PST production was reported from a study on cyanobacteria, another source of PSTs production (Moustafa et al., 2009). Using comparative phylogenomic analyses between toxic strain of *Cylindrospermopsis raciborskii T3* and its non-toxic sister, 9 genes which were believed to be specific to STX production were found. Among these genes, N-terminal end of the *sxtA* gene was found to be homologous to the EST from the toxic strain of *Alexandrium catenella*. The study by Stüken's group is probably the most meaningful as they showed that genes required for STX synthesis are encoded in the nuclear genomes of dinoflagellates, such as *A. fundyense*. They sequenced > 1.2 x $10^6$ mRNA transcripts from 2 STX producing *A. fundyense* and *A. minutum*. They reported that many STX-producing dinoflagellates contain the *sxtA* gene. They postulated that *sxtA* is related to STX synthesis. However, 3 strains of the non-toxic *Alexandrium spp.* have the *sxt* gene but they did not produce STX (Stuken et al., 2011). No data on *sxtA* expression level in various conditions was presented then or afterwards by others (see below).

Nevertheless, genomic studies such as the above do not provide conclusive information on the biosynthetic mechanism of PSTs. On the other hand, proteomic studies which investigate the difference in protein expression levels may serve as the stepping-stone to achieve this aim. Several toxic and non-toxic strains of *A. minutum* were analyzed by 2-dimensional electrophoresis (2-DE). The 2-DE analysis revealed that 2 proteins (named T1 and

T2) and 4 others (NT1, NT2, NT3 and NT4) were differentially expressed in the toxic and non-toxic strains respectively (Chan et al., 2005). Further, T1 was also found to be expressed in toxic *A. tamarense* irrespective to the toxin composition and geographical region (Chan et al., 2006). Protein identification by a combination of MALDI-TOF MS and N-terminal amino acid sequencing revealed the sequences of these proteins, showing that T1, NT1, NT2 and NT3 had very similar sequences and protein mass fingerprints (PMFs). These proteins only have several amino acids difference in the backbones of these proteins. Whether expression of these proteins is regulated by pre-translational or post-translational mechanisms are still inconclusive. Further, it should also be stressed that some subsequent studies on the non-toxic *A. minutum* questioned that this non-toxic strain of *Alexandrium* species is in fact not an *A. minutum* strain.

### 1.10 Limitations on the Studies of PSTs Biosynthetic Mechanism

Despite much effort, how PSTs are biosynthesized and regulated remains unknown. There are several reasons for the difficulty. Firstly, the most fundamental one is the large genome size of dinoflagellates. Cultured dinoflagellates have DNA content ranges from 5-200 pg DNA/cell (Lin, 2006), while that of human is only about 3 pg DNA/cell. Sequencing of the whole dinoflagellate genome is currently too demanding financially. Secondly, there is currently no appropriate tools for genetic manipulations. Therefore, genetic manipulations, knock-down and/or knock-out of specific genes in dinoflagellates are not feasible. Thirdly, even if the cloning process is possible by targeting only to PSTs synthesizing genes, there is difficulty in finding an appropriate host which can produce PSTs. Fourthly, expression of the cloned genes would be another problem since abundant gene products (potent toxins in this case) would probably be toxic or even lethal to the host (Nagai and Thøgersen, 1987; Sharma, 1986; Weising et al., 1988). Fifthly, another difficulty is the lack of understanding of the order in which the precursors of toxins are assembled to the final toxic products. No intermediates and specific enzymes have been identified which would give clues to the mechanism. For example, saxitoxin N-sulfotransferase had been found in toxic *G. catenatum*, but non-toxic strain of the species and even shellfish also exhibits its activity (Oshima, 1995a). Our current understanding of the identities of the precursors (arginine, $\alpha$-ketoglutarate, ornithine and acetate) (Shimizu et al., 1984) are not

sufficient for finding the toxin biosynthetic pathway. Sixthly, the variation in the toxin contents and also the toxin compositions within a population or between species posted another level of complication to the toxin production pathway. Although many dinoflagellates produce same kinds of toxins, their genes could vary largely because they could be products of different assortments of genes from their parents. This genetic diversity of the PSTs producing organisms further increases the difficulty of pinpointing the toxin synthesizing genes.

To circumvent some of the problems listed above, some researchers suggested that artificial mutation aimed to produce non-toxin producing dinoflagellates from toxin-producing dinoflagellates could be performed. Comparisons of these mutants with the wild type aiming to find PSTs biosynthetic genes would be easier. For example, toxic dinoflagellates will be allowed to grow under chemical or UV treatment to promote their mutagenesis aiming to produce non-toxic mutants (Claudia et al., 2004; Omura et al., 2003). In this approach, problems relied on how to screen the toxic or non-toxic cells. Due to the randomness of mutations and also the large genome of dinoflagellates, a very high through-put method for screening the presence of intracellular PSTs is needed. Unfortunately, this technology is currently lacking.

Besides sifting through genetic mutational methodologies, transcriptomic and proteomic approaches were also used to find the PST biosynthetic genes. However, without the support of dinoflagellate genomic database, the mRNA as well as differentially expressed proteins found could not be accurately annotated. The contribution of these results in finding the PST biosynthetic pathway is not direct. On the other hand, mRNA found from comparative transcriptomics may undergo translationally regulation and thus not truly reflecting the final toxin-related product (Morse et al., 1989). Additionally, many proteins in dinoflagellates are unique, e.g. dinoflagellates form of Ribulose 1,5-bisphosphate carboxylase/oxygenase II (RuBisCO II) (Rowan et al., 1996b) and Nitrogen-associated protein-50 (NAP50) (Lee et al., 2009). Taken overall, study of dinoflagellates in the molecular biology level is at its infancy stage and much needed to be done.

### 1.11 Potential Studying Approaches of PSTs Biosynthesis in the Future

Although the studies of dinoflagellates, particularly their toxigenicities, are limited in many ways, there are potential approaches for researches with newer enabling technologies. One of these new enabling technologies is the provision of second-generation high-throughput sequencing technique. The classical Sanger's chain-termination method only generate comparatively small amount of DNA sequences. Although such method could now be improved to give 1-2 million base pairs (bp) sequences in one day, modern sequencing platforms with much greater output were introduced. 454 FLX system (Roche), SOLiD system (ABI) and SBS system (Illumina/Solexa) could attain a throughput with about 200 million bp per day (Strausberg et al., 2008); while Direct Linear Analysis (DLA) and Nanopore sequencing could even generate a human genome within 24 hours (Chan, 2005). With these platforms, generation of transcriptomes, if not genomes, of dinoflagellates will become feasible and possible. Recently, the expressed sequence tag (EST) of *Symbiodinium*, a species of dinoflagellate, has been completely sequenced by the University of California Merced (DOE Joint Genome Institute, 2009). Last year, with the aid of a 454 FLX system and prior knowledge of *sxt1* gene cluster in cyanobacteria, Stüken and his team discovered several homologues of *sxtA* gene in the transcriptomes of two toxic species, *Alexandrium fundyense* and *Alexandrium minutum* (Stuken et al., 2011). Followed-up experiments using PCR techniques showed good agreement of the association of PSP toxigenicity and the presence of *sxtA1* and *A4* genes. However, both *sxtA1* and *A4* fragments were also found in the non-toxic strain of *A. tamarense*. Hence, the two gene fragments could not serve as clear-cut toxicity markers. Since the publication in 2011 by Stüken and his team about the sxtA1-4 genes, neither information on the corresponding proteins nor mRNA information is known. Successful verification of the functions of these genes is yet to be reported. Taken overall, despite the fact that there are different sources of PSTs production, including that from different genera of dinoflagellates and also certain types of cyanobacteria, it is reported that toxic cyanobacteria and dinoflagellates assembled a largely different set of enzymes for STX production (Hackett et al., 2012). Nonetheless, even if the *sxtA* gene is truly related to PST-production, only one gene discovery could not fully explain the whole PST-biosynthetic mechanism. Other types of enabling

technologies, e.g. the use of Isotope-coded affinity tag (ICAT) and isotope-coded-protein-labeling (ICPL) coupled to liquid chromatography-matrix assisted laser desorption/ionization time-of-flight mass spectrometry (LC-MALDI-TOF-MS) could also provide a useful platform for comparative studies between (1) protein expressions in toxic and non-toxic strains of PSTs producing dinoflagellates and (2) protein expressions of the same strain of dinoflagellates but in different PST-production conditions. Results of these studies may be used as biomarkers of toxicity and/or provide clues for the enzymes involved in the PST-production process. In this study, transcriptomic as well as proteomic approaches were used to study the PST-biosynthetic process.

## Chapter 2 Aim and Objectives

As elaborated in Chapter 1, the mechanism of PST biosynthetic pathway is not clear. It is envisioned that modern day proteomic technologies, with the support of transcriptomic data, could be used to find some of proteins involved in the PST biosynthetic pathway. Elucidation of some of these proteins will provide clues for further studies into the PST-biosynthetic pathway.

### 2.1 Aim of the Study

The primary aim of this study is to find proteins related to PSTs production in a model toxin-producing dinoflagellate.

### 2.2 Objectives

a) Compare the toxin profiles in *Alexandrium catenella* and *Gymnodinium catenatum* (two species of PST-producing dinoflagellates) with respect to different growth phases.

b) Study the effects of nitrate enrichment, nitrate reduction, phosphate reduction and exogenous arginine on toxin production in the 2 species of PST-producing dinoflagellates.

c) (i) Between the 2 species of PSTs-producing dinoflagellates, select a strain in which an environmental condition that could induce the largest difference in amount of PST produced.

(ii) Comparison of differentially expressed proteins between (1) the toxic strain of dinoflagellate selected and a non-toxic strain; (2) high and low PST producing conditions.

d) Verification experiments to confirm or otherwise that some of the proteins found are related to PST production.

## Chapter 3 General Materials and Methods

### 3.1 Selection of Dinoflagellates in this Study

It is known that three species of dinoflagellates are capable of producing PSTs. They belong to 3 genera: *Alexandrium*, *Gymnodinium* and *Pyrodinium*. *Pyrodinium* is a dinoflagellate that occurs specifically in the Philippines and we have no access to it. On the other hand, *Gymnodinium sp.* and *Alexandrium spp.* were found both locally and available from an algal research institute. In our hands, we have more than 10 strains of *Alexandrium spp.* Among these *Alexandrium*, *A. catenella* was known to be a fast-growing strong PSTs producer and cause high toxicity worldwide (Hernández-Becerril et al., 2007; Kim et al., 1993; Nagai et al., 2006; Siu et al., 1997). In this study, the most toxic and fast-growing *A. catenella* was selected. In addition, non-toxic strain of *A. catenella* was also available from an algal research institute. Together with a selected toxic strain of *A. catenella* in our procession, these 2 strains served as the toxic and non-toxic pair for comparison and hence were chosen to be the subjects of this study. Other selected strains included a toxic *Gymnodinium* species and a non-toxic *Alexandrium tamarense.*

### 3.2 Origin of the Dinoflagellates Used in this Study

A toxic *Alexandrium catenella* (AC-T in this thesis) which was isolated in March 2009 from the Silver Mine Bay, Hong Kong, was found to have high toxicity and growth rate (see Chapter 4). Hence, it was selected for further study. The non-toxic strain of *A. catenella* (CS-319; AC-N in this thesis) was obtained from Australian National Algae Culture Collection (ANACC) and was isolated from ballast water of a ship “Gloden Crux” in Singapore by C. Bolch. Another non-toxic strain called *Alexandrium tamarense* (CCMP116; non-toxic; AT-N in this thesis) and a toxic strain of *Gymnodinium catenatum* (CCMP1937; GC-T in this thesis) were obtained from The Provasoli-Guillard National Center for Culture of Marine Phytoplankton (CCMP), USA. The two dinoflagellates were collected from Ria de Vigo in Spain, by B. Jose Maria Navaz and R.V. Navaz respectively.

### 3.3 Growing Conditions of the Dinoflagellates

All cultures of dinoflagellates were grown in a Versatile Environmental Test Chamber, Model MLR-350 (SANYO, Japan). The temperature and light intensity of the chamber was kept at 22$^{o}$C and 7 µmole $m^{-2}s^{-1}$ respectively, under a 12:12 hours light:dark cycle. L1 medium prepared with Instant Ocean synthetic sea salts (Aquarium Systems, France) were used for growing all cultures. The ingredients are: 882 µM $NaNO_3$ (Riedel-de Haën, Germany), 36.2 µM $NaH_2PO_4$ (Riedel-de Haën, Germany), 10 nM $H_2SeO_3$, 11.7 µM $Na_2EDTA$ (usb, USA), 11.7 µM $FeCl_3$, 0.91 µM $MnCl_2$, 80 nM $ZnSO_4$, 50 nM $CoCl_2$, 10 nM $CuSO_4$, 82.2 nM $Na_2MoO_4$, 10 nM $NiSO_4$, 10 nM $Na_3VO_4$, 10 nM $K_2CrO_4$, 296 nM thiamine (vitamin $B_1$), 2.05 nM biotin (vitamin H) and 0.369 nM cyanocobalamin (vitamin $B_{12}$). Unless stated, all chemicals were obtained from Sigma (USA). Stock cultures were kept at exponential growth phase by transferring to new medium in a ratio of 1:4 v/v within 2 to 3 week intervals. Experimental cultures were inoculated with vegetative cells from stock cultures at mid- or late-exponential phases after centrifugation at 360 x g for 5 minutes. Concentrations of inoculums were examined and the experimental cultures were started with 1000 cells $mL^{-1}$ by concentration and 500 mL by volume on Day 0.

### 3.4 Cell Harvesting

Numbers of cells in these cultures are counted before harvesting the cells. Cultures of dinoflagellates were harvested by centrifugation at 2700 x g for 5 minutes using a centrifuge (BEOCO, Germany) and 50-mL centrifuge tubes. Cell pellets were finally collected into a 1.7 mL microcentrifuge tube before being stored in -80$^{o}$C for further use.

### 3.5 Cell Counts, Monitoring of Growth Phases and Calculation of Specific Growth Rates

Determination of algal density in the cultures was performed using the Sedgewick-Rafter counting chamber. 1 mL of algal culture, fixed with 10 µL of Lugol's solution, was filled into the chamber and examined under light microscope. Specific growth rates are calculated using the following formula where $N_2$ and $N_1$ are the cell density in form of cell numbers per ml at their corresponding time point, $t_2$ and $t_1$, respectively:

$$\text{Specific Growth Rate} = [\ln(N_2) - \ln(N_1)]/(t_2 - t_1)$$

### 3.6 Measurement of Cell Volume

Cell volumes were estimated by measuring the dimensions of the algae and calculated with a method developed by Hillebrand for estimating cell volume of dinoflagellates (Hillebrand et al., 1999). With bench-top light microscope (Leica, Germany) linked with external digital screen (Nikon, Japan), diameter (*d*) and height (*h*) of the cells were recorded and the cell volume (*V*) were calculated with the following formula:

$$V = \frac{\pi}{6} \times d^2 \times h$$

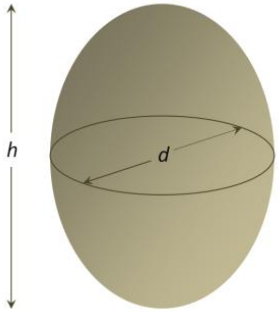


### 3.7 Extraction of DNA and PCR-based Identification

Identities of the dinoflagellates being studied were confirmed by sequencing the ribosomal genes. 200 mL of dinoflagellate culture in exponential phase was harvested. Prior to PCR-based identification, cells were disrupted by warming at 72$^{o}$C and DNA contents inside were extracted using a commercial kit called High Pure PCR Template Preparation Kit (Roche, Switzerland). PCR was performed with the genomic DNA obtained, targeting at the Internal Transcribed Spacer (ITS) region and the 5.8s ribosomal DNA. Primers used for amplifying the ITS region in *Alexandrium spp.* were ITSA and ITSB (Adachi et al., 1996). Primers used for the *Gymnodinium spp.* were self-designed by selecting the highly conserved nucleotide sequences outside the ITS region of different *Gymnodinium* species. Sequences of the oligonucleotides used were shown in Table 3.1. Amplification was performed by 35 cycles of 3 steps each cycle: denaturing (94$^{o}$C; 40s), annealing (50$^{o}$C; 40s) and elongation (72$^{o}$C; 60s), and ended with 72$^{o}$C for a further 10 minutes. Purified PCR products were cloned into pGEM-T easy vectors (Promega, USA). Cloned plasmids were extracted by a commercial kit called the QIAprep® Spin Miniprep Kit (QIAGEN, USA) and the DNA sequences obtained using Sanger method provided by commercial facilities.

**Table 3.1.** Primer sequences used for ribosomal gene identification

| Primers | Targeting species | Sequences |
|---|---|---|
| **Gym ITS f1** | *Gymnodinium spp.* | 5' GCAGCGGAAAGTTTAGTGAACC 3' |
| **Gym ITS r2** | | 5' CTKAGAACRYRTGCCGTRCACG 3' |
| **ITS A** | *Alexandrium spp.* | 5' CCGGATCCAAGCTTTCGTAACAAGGHTCCGTAGGT 3' |
| **ITS B** | | 5' CCGGATCCGTCGACAKATGCTTAARTTCAGCRGG 3' |

### 3.8 Performance of Protein Expression Profiles (PEPs)

Protein expression profiles of exponential culture were obtained with a MALDI-TOF mass spectrometer, Autoflex III (Bruker, Germany). Harvested cells (around 1 million cells) suspended in 0.1 % trifluoroacetic acid (TFA) (Aldrich, USA) were first sonicated for 3 minutes with 15s/15s pulse intervals before centrifugation. After removing the debris by centrifugation, protein samples were cleaned up with C-18/C-4 zip tips (Millipore, USA) with 0.1 % TFA and eluted with 0.1 % TFA with 50 % acetonitrile (Duksan, Korea). The samples were then mixed with matrix solution prepared by saturated sinapinic acid (SA) in elution buffer in the ratio of 1:1. The mixtures were then spotted onto MALDI-target plates called MTP AnchorChip$^{TM}$ (Bruker, Germany). Mass spectrometry was performed with linear mode at an accelerating voltage of 20 kV and a 300 ns delay time. Spectrum of a sample ranged from m/z accuracy of 0.2 to 2 kDa was generated by summation of spectra from 2000 to 3000 laser shots of each sample. External calibration was performed simultaneously with Protein Calibration Standard I (Bruker, Germany).

### 3.9 Neuroblastoma Toxicity Assay

Toxicities of dinoflagellates samples were measured by functional cellular assay with the Neuro-2A cell line (ATCC, USA). Cell toxicity was expressed as ρgSTXeq (saxitoxin equivalents) cell$^{-1}$. Neuro-2A cell line was cultured using Minimum Essential Medium (MEM) (Gibco, USA) with 10 % Fetal Bovine Serum (Gibco, USA) at 37 $^{o}$C and in a humidified 5 % $CO_2$ atmosphere. Toxicity assays were performed in a 96-well microtiter plate (Iwaki, Japan) with 2500 cells in each well. After cells were incubated overnight with a 5 % FBS MEM medium, extracted toxins and the STX

standards (NRC, Canada) were added. Followed by gently shaking, 10 mM ouabain (Sigma, USA) and 1 mM veratridine (Sigma, USA) were added. The two chemicals were used to induce influxing of $Na^+$ ions into the cells which caused swelling and cell death. After another overnight incubation, cellular viabilities were measured by MTT assay kit (Promega, USA). Since PSTs could block the $Na^+$ ion channel which cancel the effect of the drugs added, higher cell viability indicate more toxin was introduced into the cell. Toxicities of the dinoflagellate samples were then quantified with the aid of a standard curve constructed with different amounts of STX.

### 3.10 Extraction of Toxins from Samples and its Analysis

Toxin levels in the dinoflagellate samples were analyzed by a UPLC system (Waters, USA) coupled with pre-column oxidation method developed previously (Lawrence et al., 1996). Endogenous toxins in samples were first extracted with 1 mL portions of 0.05 M acetic acid (International Laboratory, USA) prior to sonication (3 minutes in total with 15s/15s pulse intervals). The samples were then centrifuged at 15000 x g for 5 minutes. Debris were removed and the supernatants were then stored under -20$^{o}$C before use. Separation and quantification of PSTs were achieved by performing reversed phase UPLC with a 2.1 X 100 mm HSS T3 column (Waters, USA). Prior to injection into the UPLC system for separation and quantification, the samples were divided into 2 portions and each portion oxidized with one of two different oxidation methods. Samples intended to measure its contents of STX, dcSTX, GTX2+3, GTX5 and C1+2 were analyzed with 2-minute oxidation by 10 % hydrogen peroxide solution in 1 M sodium hydroxide (Riedel-de Haën, Germany) before being stopped by 5 % acetic acid (VWR, USA). NEO and GTX1+4 were analyzed with 1-minute oxidation with periodate oxidant prepared with 0.1 M periodic acid (Aldrich, USA), 0.1 M ammonium formate (Sigma, USA) and 0.1 M sodium phosphate dibasic (Riedel-de Haën, Germany) before being stopped by 7 % acetic acid. After the reaction, the oxidized toxin solutions were filtered into sample vials with 0.2 µm PTFE syringe filters (Waters, USA). Two mobile phases were used for the UPLC analyses: 0.1 M ammonium formate (pH 6.0, buffer A) and 0.1M ammonium formate with 5 % acetonitrile (pH 6.0, buffer B). Flow rate was kept at 0.5 mL/minute and column temperature was kept at 35$^{o}$C. The gradient program was divided into 3 steps with different ratios of buffer A to buffer B: 95:5

from the 0 to 2.5 minutes, 70:30 from the 2.5 to 5 minutes and 100:0 from the 5 to 6 minutes. Separated toxins were detected by fluorometer with λex 340 nm and λem 395 nm. Peak areas in the UPLC chromatograms were measured and the amounts of cellular toxins were quantified with the standard curves.

### 3.11 Extraction of Free Cellular Arginine in the Dinoflagellates and Its Analysis

Harvested cells were disrupted by sonication with about 200 µL of water. After centrifugation at 15000 x g for 5 minutes, supernatants of the cell lysates were then mixed with 10 % sulfosalicylic acid (SSA).The solution was allowed to cool to $4^{o}$C. Followed by one-hour incubation, protein precipitates was removed after another centrifugation for 5 minutes at 15000 x g. The amino acid solution was then filtered with a 0.2 µm syringe filter (Iwaki, Japan) and the filtrate dropped into sample vials for amino acid quantification. Measurement of the amount of arginine present was performed by injection into an amino acid analyzer (Biochrom-30 from Biochrom , UK). On occasions that proteolysis of the intracellular proteins should be avoided, protease inhibitors cocktails (Sigma, USA) were added to the samples before sonication to prevent proteases degradation.

### 3.12 Extraction of Proteins

Proteins were extracted from the harvested cells with the use of Trizol (Roche, Switzerland). Protocol of the extraction procedure was optimized for sample preparation of dinoflagellates for 2-dimensional gel electrophoresis. Briefly, about 1X $10^{6}$ cells in one single microcentrifuge tube was added with 300 µL Trizol reagent. Cell breakage was performed by totally 3 minutes of sonication with brief 15 seconds pulses on ice. After making up the volume to 1 mL by Trizol reagent, the cell lysate was further added with 200 µL of chloroform (International Laboratory, USA). The mixture was then subjected to vigorous shaking for 15 seconds. Afterwards, the mixture was allowed to stand for several minutes before being centrifuged at 12000 x g for 15 minutes. Subsequently, the upper pale-yellow layer and the inter-layer pellets were discarded before mixing with 300 µL of 96 % ethanol (International Laboratory, USA) to the lower layer. After standing in room temperature for several minutes, another centrifugation at 3000 x g for

6 minutes was performed. 1.2 mL of isopropanol (International Laboratory, USA) was mixed with the supernatant in a new 2 mL microcentrifuge tube by inverting the tube up and down. Proteins in the mixture were precipitated after several hours in room temperature. Followed by centrifugation at 14000 x g for 10 minutes, the protein pellet was washed with 96 % ethanol and allowed to air dried. Depending on the amounts of the protein pellets, various amounts of lysis buffer were added to solubilize the pellets under room temperature and overnight. Finally, the protein solution was removed from the insoluble substances and stored in -20$^{o}$C until further studies.

### 3.13 Determination of Protein Concentration

The amounts of extracted proteins were quantified by a modified Bradford protein assay using a commercially available Bradford reagent from Bio-Rad (USA) (Ramagli and Rodriguez, 1985). The protein samples in 10 µL of lysis buffer were diluted into 800 µL of distilled water before mixing with 200 µL of Bradford reagent. After standing for 5 minutes in room temperature, absorbance of the mixture in 595 ηm was measured and the amount of proteins quantified by a standard curve constructed with known amounts of proteins. 10 µL of lysis buffer that contains light absorbing urea should be used as the control solution.

# Chapter 4 Background Examination and Toxigenicity Measurements on the PSTs-producing and non-PSTs-producing dinoflagellates

## 4.1 Introduction

In this thesis, as elaborated in Chapter 2, the ultimate aim is to understand the mechanism of PST-biosynthesis in dinoflagellates. Since we need to compare protein expression between the toxic and non-toxic strains in one set of experiment, it is important to ascertain identities of the *Alexandrium spp.* under investigation. Identification of dinoflagellates by morphological characteristics is not accurate as many morphospecies of the *Alexandrium catenella*/*fundyense*/*tamarense* complex have very similar morphological characteristics. Besides possible laboratory artifacts that may be generated during the various steps of sample preparation, a significant amount of technical expertise as well as subjective judgment are required for the morphology-based identification method. For the species that we have, the *Alexandrium catenella* and *Gymnodinium catenatum* are known to be toxic. However, it is uncommon that CS-319 (a dinoflagellate classified as *Alexandrium catenella* taxonomically by ANACC) is reported as non-toxic. DNA-based morphologies seem to be more dependable. Litaker (2007) reported that the Internal Transcribed Spacer (ITS) region of ribosomal-DNA (rDNA) is highly conserved at species level and could serve as the "DNA barcode" for identification of dinoflagellates. With the aid of universal primers and self-designed primers listed in Table 3.1, the ITS1-5.8S-ITS2 rDNA sequences had been amplified and sequenced. For ease of presentation, strain codes GC-T, AC-T, AC-N and AT-N were used to represent toxic *Gymnodinium catenatum* (CCMP1937), Hong Kong isolated toxic *Alexandrium catenella*, non-toxic *Alexandrium catenella* (CS-319) and non-toxic *Alexandrium tamarense* (CCMP116) respectively.

Further, other background information of the several strains under investigations was also studied in order to build a strong foundation for the eventual proteomic comparison at the end.

## 4.2 Materials and Methods

Unless specified, all the materials and methods were described in Chapter 3 already.

## 4.3 Results and Discussion

### 4.3.1 DNA-based Identification

Figure 4.1 showed the alignment results of the complete sequence of ITS1-5.8S-ITS2 region of the selected strain of *Gymnodinium catenatum* (GC-T) with other strains of *G. catenatum* in the GenBank database. Sequence of the selected strain of GC-T matches submitted for alignment matched exactly as that of CS-309/03 (FJ823541), CSIC744 (AM998536) and GC53AM (AY506591); and only with a difference of 4 nucleotides to the other strains (AF208247). Therefore, GC-T is confirmed as *Gymnodinium catenatum*.

Figure 4.2 showed alignment of the complete sequences of ITS1-5.8S-ITS2 region of the selected strains of *Alexandrium catenella* (AC-T and AC-N) with other strains of *A. catenella* in the GenBank database. Sequence of the selected strain matched with high homogeneity to other *A. catenella* sequences including that of A4 (GU477599), ACDH (EF030049), MI7 (AB006990) and ACATC2 (AJ580317). Therefore, the identities of AC-T and AC-N are confirmed.

Figure 4.3 showed alignment of the complete sequence of ITS1-5.8S-ITS2 region of the selected strain of *Alexandrium tamarense* (AT-N) with other strains of *A. tamarense* in the GenBank database. Sequence of the selected strain matched exactly as that of other stains of *A. tamarense*, including that of IEO-PE1V (AJ514908) and CCMP2022 (HM483849). There is only one nucleotide difference to WKS-1 (AB006991). Therefore AT-N in our collection is confirmed as *A. tamarense*.

**Figure 4.1.** Alignment of the complete sequence of ITS1-5.8S-ITS2 region of the selected strain of *Gymnodinium catenatum* (GC-T; highlighted in red boxes) with other strains of *G. catenatum* in the GenBank database. The sequence of GC-T submitted matched exactly that of the other *Gymnodinium catenatum* strains filed in the database, including that of CS-309/03 (FJ823541), CSIC744 (AM998536) and GC53AM (AY506591). There is only a difference of 4 to that of another strain (AF208247).

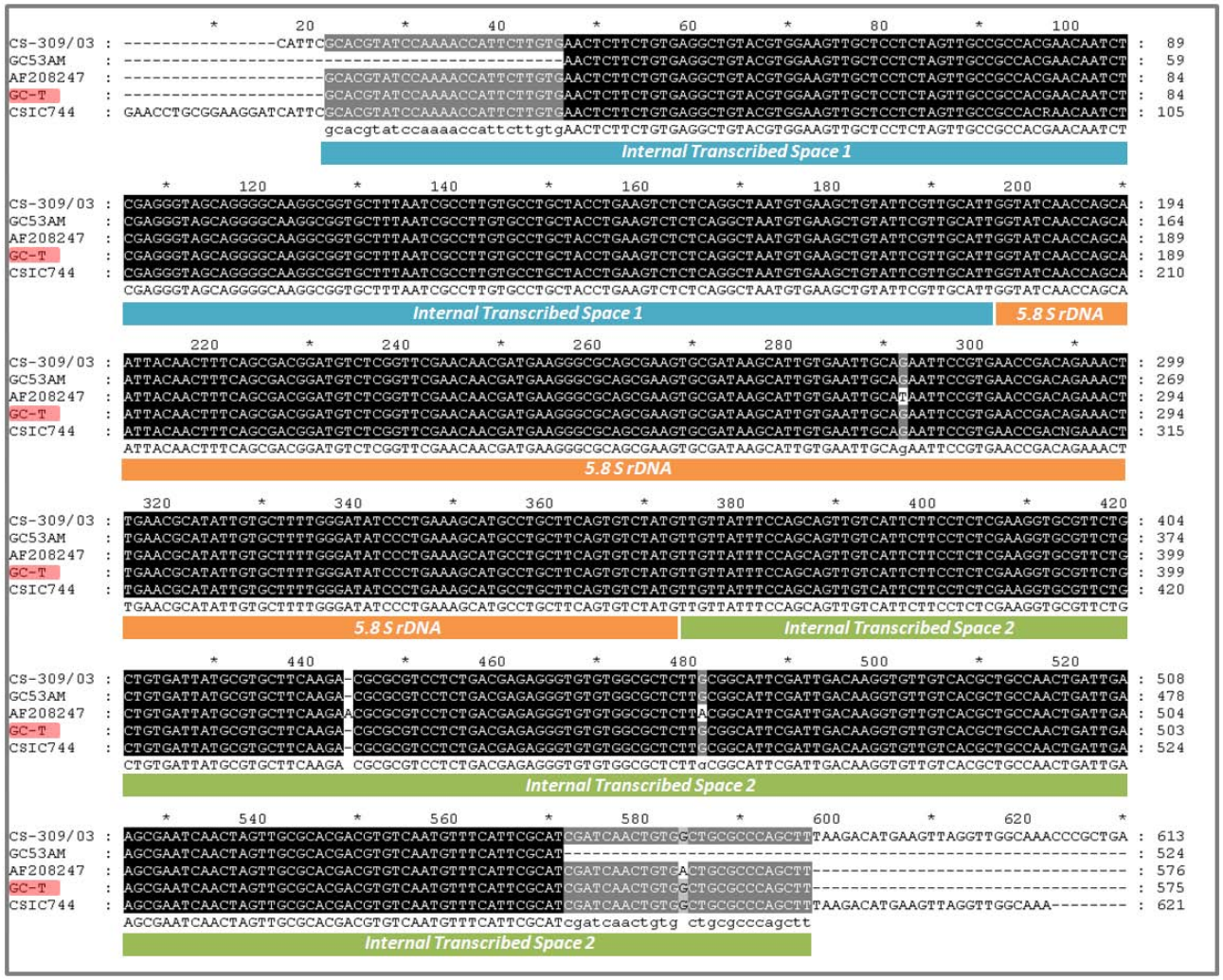

**Figure 4.2.** Alignment of the complete sequences of ITS1-5.8S-ITS2 region of the selected strains of *Alexandrium catenella* (AC-T and AC-N; highlighted in red and blue boxes respectively) with that of the other strains of *A. catenella* in the GenBank database. The sequence submitted matched with that of known *A. catenella* strains in the database with high homogeneity. The strains matched are A4 (GU477599), ACDH (EF030049), MI7 (AB006990) and ACATC2 (AJ580317).

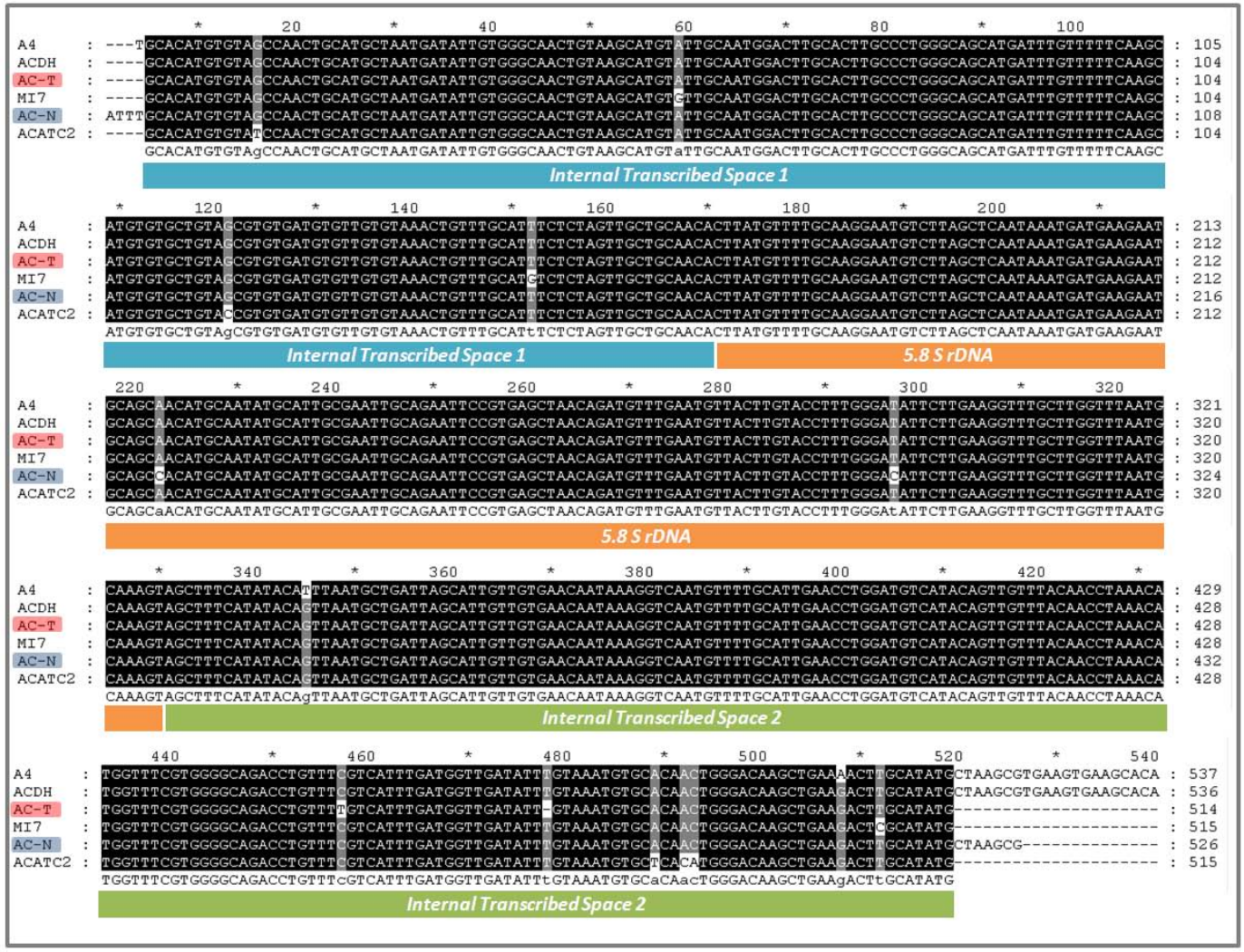

**Figure 4.3.** Alignment of the complete sequence of ITS1-5.8S-ITS2 region of the strain of *Alexandrium tamarense* (AT-N; highlighted in red boxes) in our hands with that of other strains of *A. tamarense* in the GenBank database. The sequence of the selected strain submitted by us matched exactly with those of *A. tamarense* in the database, including that of IEO-PE1V (AJ514908) and CCMP2022 (HM483849). There is only one nucleotide difference to WKS-1 (AB006991).

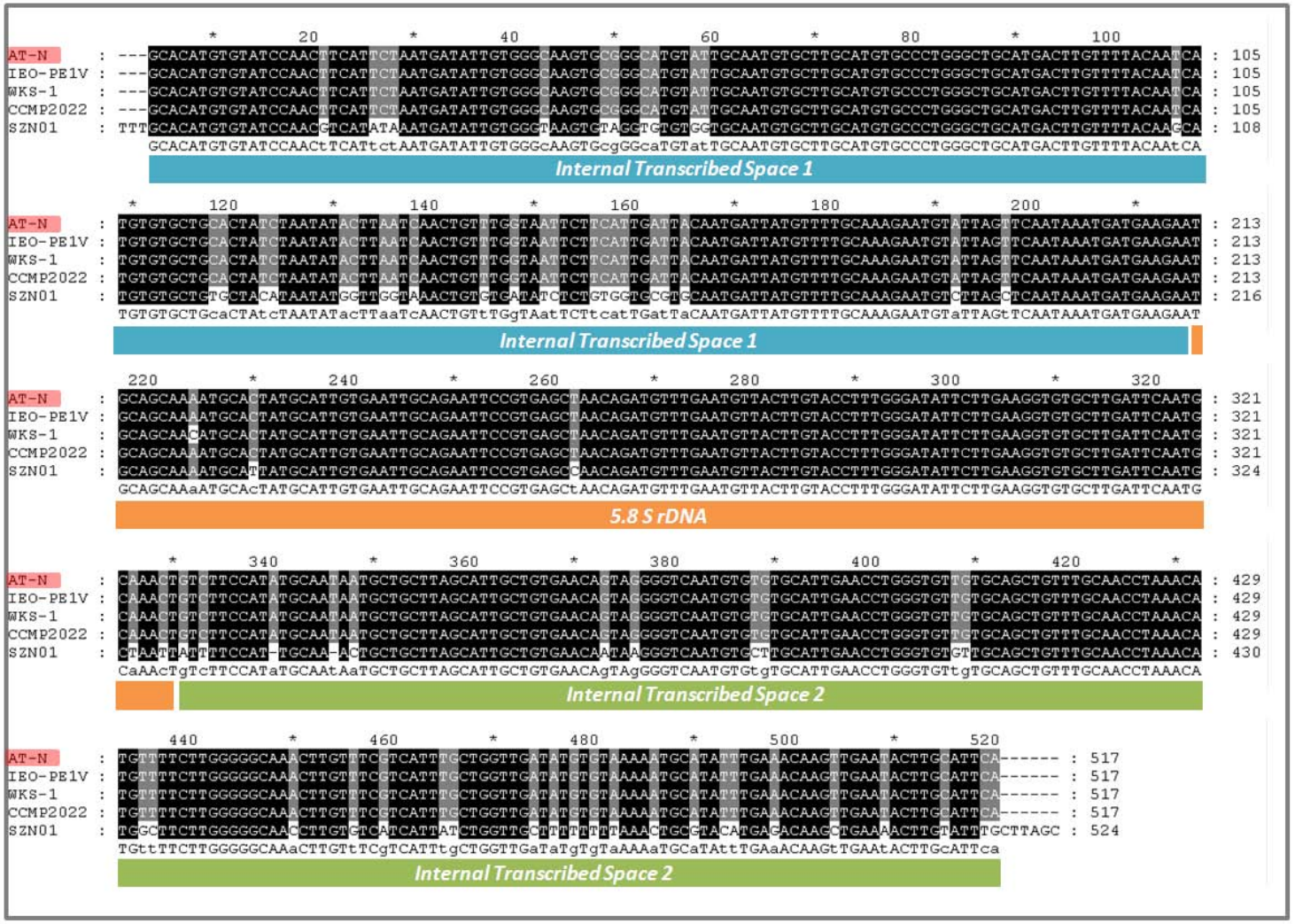

As it is easy to confuse the identity between *A. catenella* and *A. tamarense* when examining their morphological characteristics, DNA sequences in the ITS regions of the several species of dinoflagellates in the present study were compared to each other. Figure 4.4 showed the results of alignment of the ITS sequences. Homologies of the sequences are summarized in Figure 4.5 below. GC-T has the lowest similarity (around 45%) to the other species as it is in a different genus. AC-T and AC-N have 97% similarity, showing that their ITS sequences were quite similar. Being under the same genus level, the inter-species similarity of the ITS sequences of AT-N to AC-T and AC-N are down to 82% and 81% respectively (Figure 4.5).

**Figure 4.4.** Alignment of the complete DNA sequences of ITS1-5.8S-ITS2 regions of the 4 dinoflagellates in the present study.

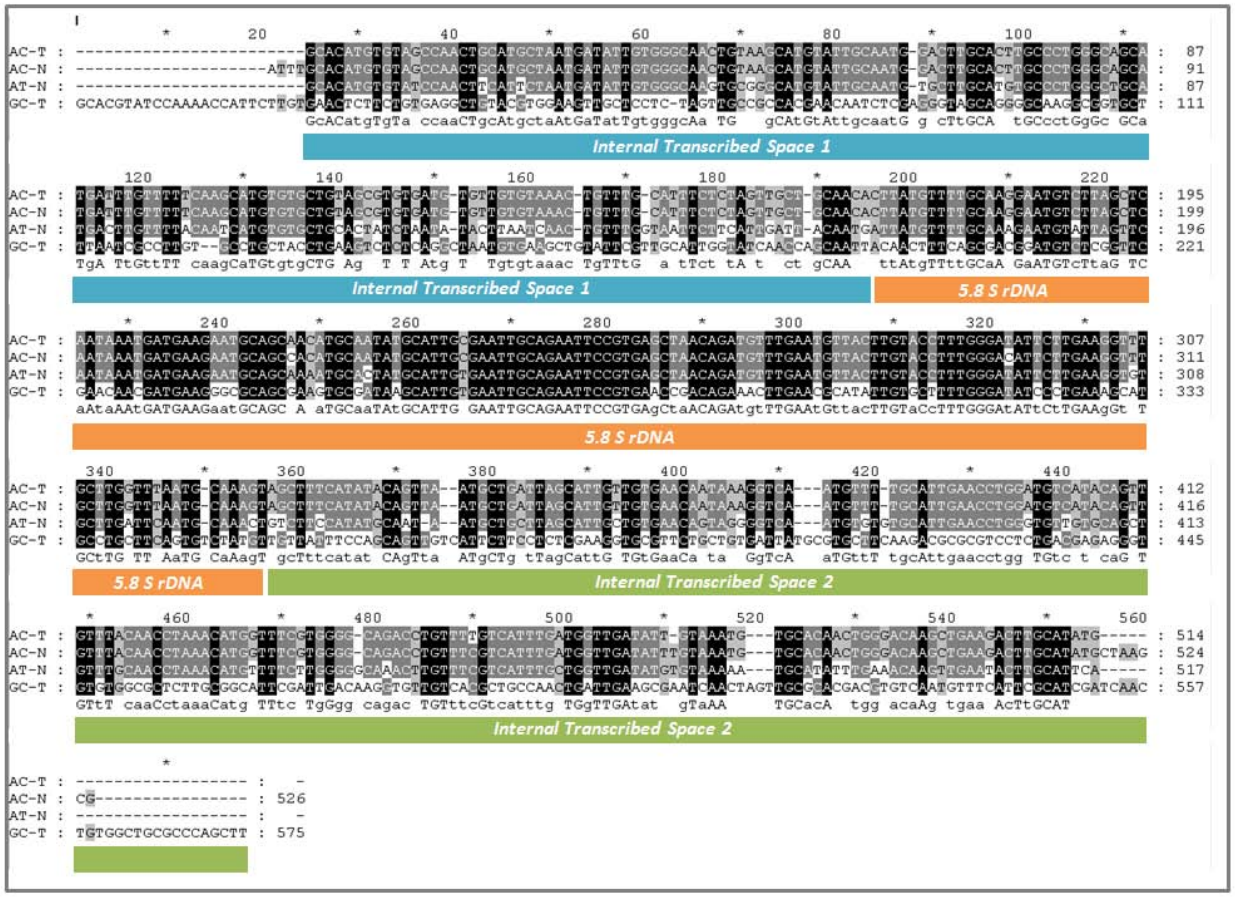

**Figure 4.5.** Percentage similarities of the complete DNA sequence of ITS1-5.8S-ITS2 regions among the 4 dinoflagellates in the present study. Inter-genus homology was about 44-45%. Inter-species homology was 81-82%. Intra-species homology was 97%.

| | GC-T | AT-N | AC-N |
|---|---|---|---|
| AC-T | 44 % | 82 % | 97 % |
| AC-N | 45 % | 81 % | |
| AT-N | 45 % | | |

### 4.3.2 Protein Expression Profiles (PEPs)

In addition to the molecular approach for identification of dinoflagellates, our group previously developed a fast identification method for dinoflagellates using the matrix-assisted laser desorption/ionization time-of-flight (MALDI-TOF) mass spectrometry down to species level (Lee et al., 2008). This methodology utilized the characteristics that each strain of dinoflagellates (and organisms in that respect) will have a unique set of proteins in its body and documentation of these proteins (in the form of protein-expression-profiles, PEPs) will serve as a mean of identification. In the previous work, we showed that dinoflagellates of different species can be distinguished from each other and sometimes the identification can be down to sub-species level (Lee et al., 2008). In this thesis, with the 3 *Alexandrium* species and *Gymnodinium* species, protein expression profiles (PEPs) of these species were documented. It is intended to show that PEPs of different species would be different while PEPs of same species would be similar but each with some unique peaks of their own. Figure 4.6 shows that PEPs of the exponential cultures of the 4 dinoflagellates under investigation. It was found that dinoflagellates of different species have different patterns of PEPs. PEP of GC-T, in particular, is very different from that of the other dinoflagellates. Difference in PEPs exists when AT-N is compared to that of either AC-T or AC-N. Hence, it can be taken that AT-N in our hands is a different species when

compared to AC-T and AC-N. On the other hand, the PEPs of AC-T and AC-N are similar to each other, sharing some major peaks (3048 m/z, 3236 m/z and 3763 m/z). The results provide further confirmation about the similarities and difference of abundant proteins of AC-T, AC-N and AT-N.

**Figure 4.6.** Protein expression profiles (PEPs) of AT-N, GC-T, AC-N and AC-T. The mass spectra were calibrated both externally and internally. Different patterns were shown by different species. There is high similarity between the two species of *A. catenella* (AC-T and AC-N).

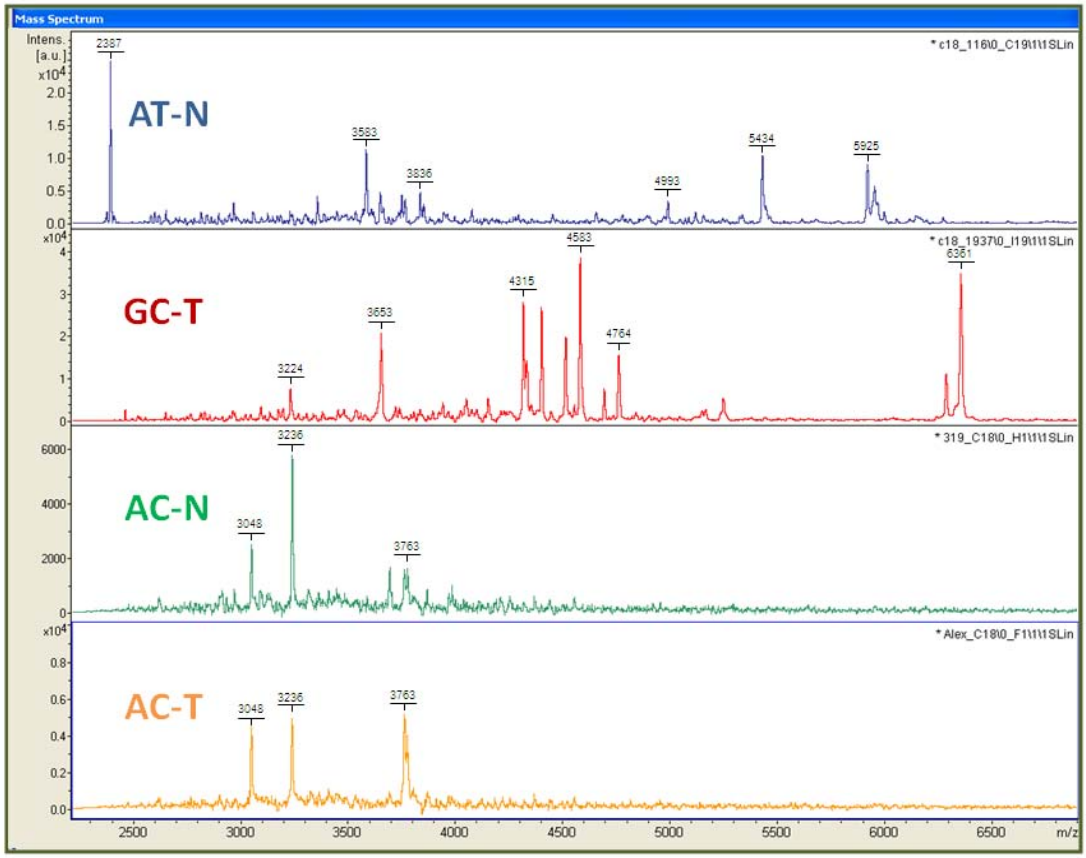


### 4.3.3 Growth Cycles

It was reported that toxin synthesis was at its highest rate during the more metabolically active phase (Anderson et al., 1990a; Boyer et al., 1987; Hamasaki et al., 2001). Therefore, it will be of interest to document the different stages of growth especially the exponential phases of the dinoflagellates being studied. Growth curves were constructed by documenting the cell densities at 2 to 3-days intervals. Figure 4.7 shows the growth curves of the studied

dinoflagellates in a single scale. (For individual curve, see Appendix A1-4.) All 4 curves have similar patterns of typical growth curve which have a general trend of 4 different growth phases.

Cultures were first started, there were a few days of lag phase for adaptation. *Alexandrium spp.* (AC-T, AC-N and AT-N) were found to have a shorter period (2 days) of lag phase when compared to *Gymnodinium* species. (GC-T) (5 days). Further, a little drop of cell density was found from GC-T in this phase. This may due to the fact that the algal cells were weakened by the centrifugal forces used for harvesting and before culturing as *Gymnodinium* species was not armored by strong theca and so it exhibited a longer adaptation period.

After days of adaptation, the cultures entered the exponential (log) phase. During this phase, the cells started to divide in high rates until they reached a stage of maximum cell density. Specific growth rates of exponential growth are listed in Table 4.1. The exponential growths of the 4 dinoflagellates were different. GC-T had the longest exponential phase but with a lowest growth rates (0.08 $day^{-1}$). AC-T and AC-N had a similar exponential growth from day 2-25. Both the specific growth rates were 0.12 $day^{-1}$. However, the toxic species (AC-T) has a further longer exponential growth for about 9 days. AT-N has the shortest exponential growth that stopped at day 10. Siu et al. (2007) reported that the mean growth rate of *A. catenella* under 25$^{o}$C was 0.28 $day^{-1}$ and another study reported the growth rate of *G. catenatum* at the same temperature ranged from 0.12–0.17 $day^{-1}$ in its exponential phase (Oh et al., 2002). In the present study, the specific growth rates were found to be less than that from the literature. Such deviation may be due to the different growth conditions employed, including light intensity, salinity and ingredients in the seawater used. For comparison purposes, experiments used cultures in the exponential phases were chosen as Day 18-20 for GC-T, AC-T and AC-N, and Day 8 for AT-N.

**Table 4.1.** Specific growth rates of exponential growth of the various dinoflagellates studied.

| Species | [$day^{-1}$] |
|---|---|
| GC-T | 0.08 |
| AC-T | 0.12 |
| AC-N | 0.12 |
| AT-N | 0.24 |

**Figure 4.7.** Growth curves of the 4 dinoflagellates being studied. Log phases of the species are indicated. GC-T had the longest log phase but the lowest log growth rate. AC-T had the highest maximum cell density among the species. Both the maximum cell density and the length of log phase are lowest and shortest for AT-N (Bars indicate + S.D. of triplicates).

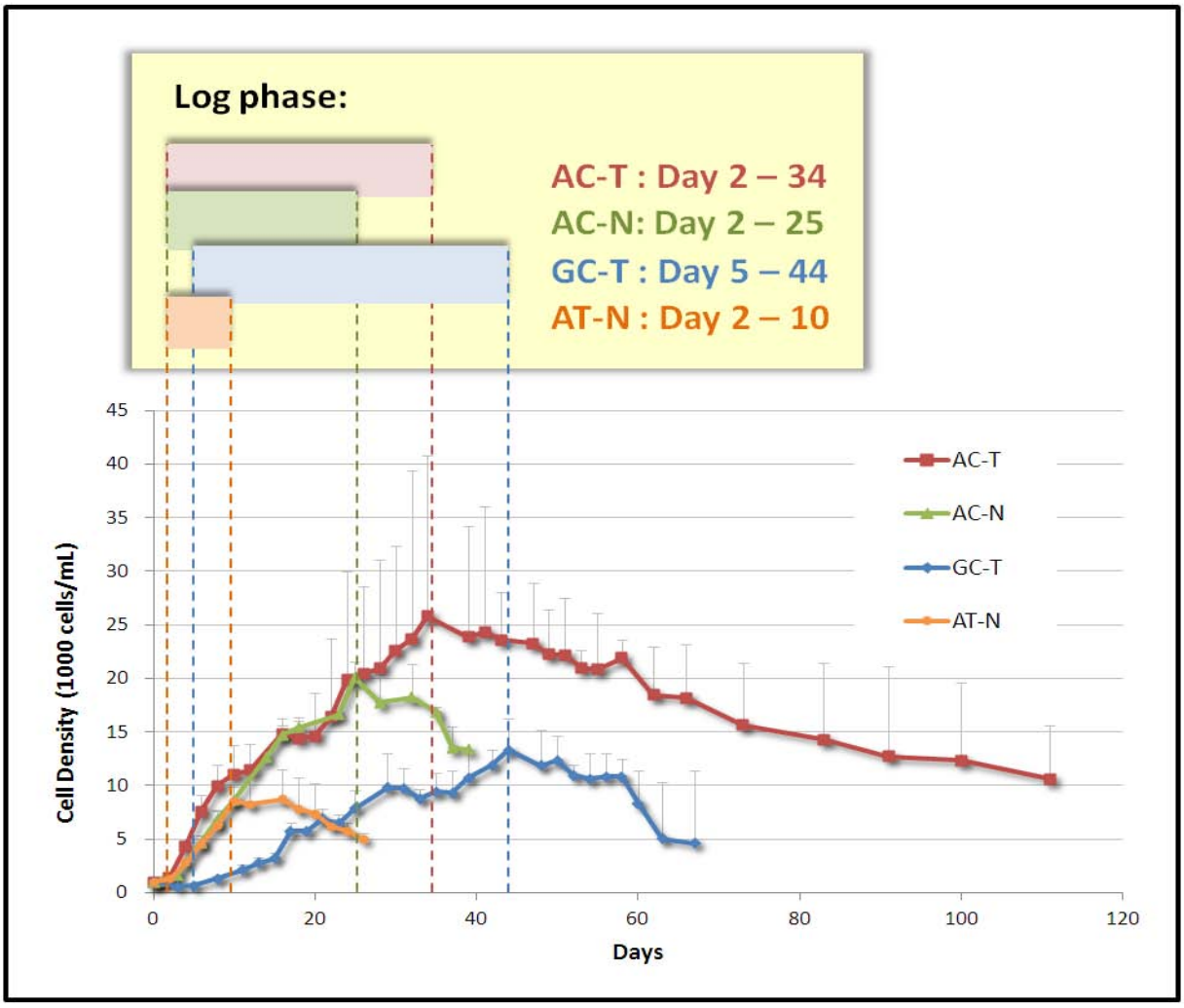


After reaching the maximum cell densities, the cultures began the stationary phases and eventually into the decline phases. AC-T has the highest maximum cell density (26000 cells/mL) among the 4 species, while the non-toxic strain (AC-N) has about 20000 cells/mL. GC-T and AT-N have a relatively low maximum cell density that are about 13300 cells/mL and 8500 cells/mL respectively. Many factors may be involved for affecting the maximum cell densities and the starting of stationary and decline phase. Limiting conditions of various essential nutrients and the presence of associated bacteria could also affect the rates of growth of dinoflagellates (Uribe and Espejo, 2003).

### 4.3.4 Neuroblastoma Toxicity Assay

Toxicity of dinoflagellates could simply be estimated through the summing up the STX equivalents of different PSTs with their contents in the samples. In the present study, toxicity of the two toxic dinoflagellates was analyzed with an established neuroblastoma assay. Such functional assay expressed the toxicity in terms of pgSTX equivalent per cell (pgSTXeq/cell) with the aid of standard curves (Appendix A5). Table 4.2 shows the results of toxicity assay of GC-T and AC-T at their exponential phases (Day 18). GC-T was shown to be highly toxic, which is about 35 folds of AC-T. However, for the non-toxic dinoflagellates, toxicity was almost zero in the neuroblastoma assay, as illustrated by AT-N. Nonetheless, it should be stressed that this neuroblastoma assay is a functional assay but the various components of the PSTs that make up the total toxicity is unknown. Therefore, a UPLC-based toxicity profile assay is established to document toxicity profiles of the toxic dinoflagellates studied in this thesis.

**Table 4.2.** Results of neuroblastoma toxicity assay (± S.D. of triplicates). GC-T was found to be highly toxic, compared to AC-T. Toxicity of AT-N was almost zero.

| Species | Toxigenicity | Cellular Toxicity (pgSTXeq/cell) |
|---|---|---|
| **GC-T** | Toxic | 57.1 ± 17.7 |
| **AC-T** | | 1.64 ± 0.58 |
| **AT-N** | Non-toxic | ≈ 0 ($7.2 \times 10^6$) |

### 4.3.5 Measurement of Cell Volume

UPLC-based toxin profile measurement is a measure of toxigenicity and it is generally expressed as a measured toxin amount against the cell number (Flynn et al., 1994; Leong et al., 2004; Lim et al., 2009; Wang et al., 2006). However, the reliance of cell number ignores the fact that different dinoflagellates could have different cell sizes. Cellular toxin content may not be enough to truly reflect the toxin production rate (see section 4.3.6 below). Further, cell volume could be affected by other environmental factors including temperature and light. Taking cell volume into account, toxin production of dinoflagellates in different sizes could be compared

on the same basis. Figure 4.8 shows the cell dimension measurements of the 4 dinoflagellates under light microscope. Using the formula mentioned in the previous chapter, cell volume were calculated and listed in Table 4.3. GC-T were found to have the largest cell size (24.3 X $10^3$ $\mu m^3$), which were about 3 folds of AC-T and AC-N. This may provide a possible reason for the low growth rate of GC-T. When compared to the *Alexandrium* species, GC-T needs more nutrients for building up the cell volume and hence less was available for cell division. There is no change of cell volume in different growth phases of any individual species.

**Figure 4.8.** Microscopic images and cell diameters of (a) GC-T; (b) AC-T; (c) AC-N and (d) AT-N.

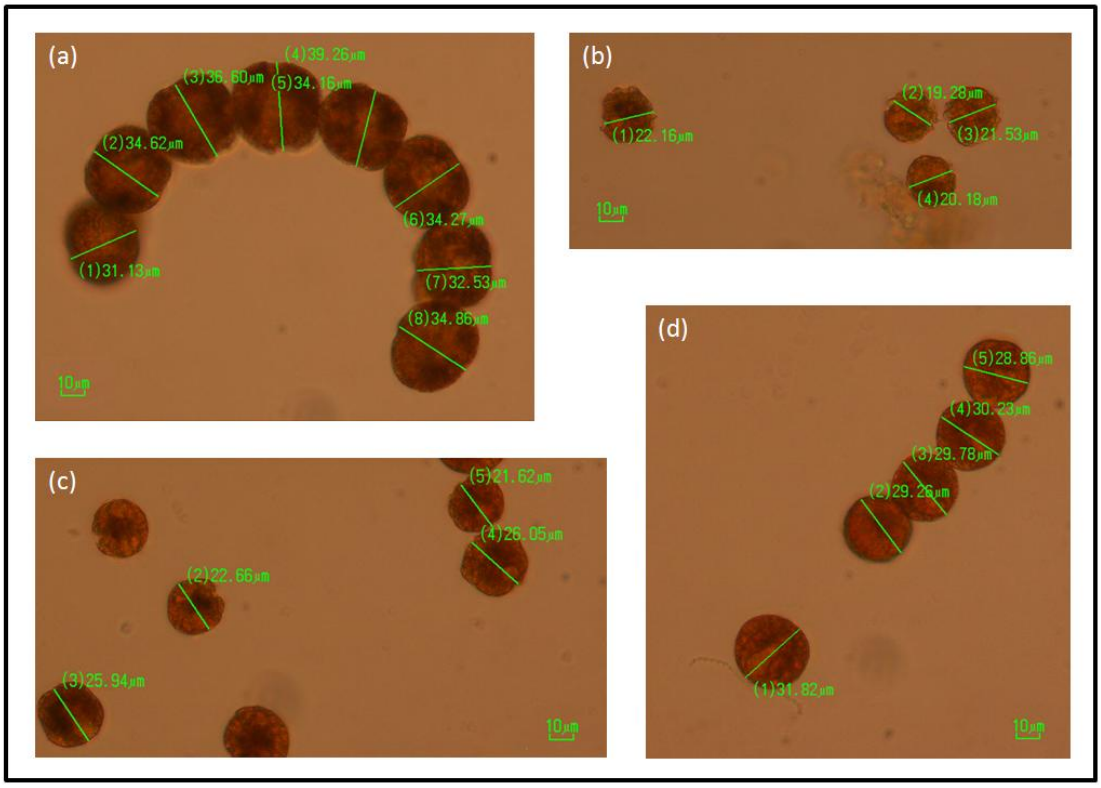


**Table 4.3.** Average cell volumes (in $10^3$ $\mu m^3$ ± S.D.; n=6) of the 4 dinoflagellates at their log phases.

| **Species** | **Cell volume (X $10^3$ $\mu m^3$)** |
|---|---|
| *Gymnodinium catenatum* (GC-T) | 24.3 ± 3.8 |
| Toxic *Alexandrium catenella* (AC-T) | 8.4 ± 1.6 |
| Non-toxic *Alexandrium catenella* (AC-N) | 7.8 ± 2.1 |
| *Alexandrium tamarense* (AT-N) | 15.5 ± 2.2 |

### 4.3.6 Toxin Profiles

Toxins contents were analyzed through the UPLC system with pre-column oxidation methods adopted by Lawrence (1996). As shown from the spectra in Figure 4.9-4.10, various paralytic shellfish toxins (PSTs) were identified with their corresponding retention time of the standards. And the toxin amounts of the dinoflagellates samples were quantified according to the standard curves (Appendix A6).

**Figure 4.9.** (a) Spectrum of standards of GTX1,4 and NEO, using the periodate oxidation method. (b) Spectrum of dinoflagellates samples (Day 18 sample of AC-T). PSTs peaks were identified according to the corresponding retention time in the standards.

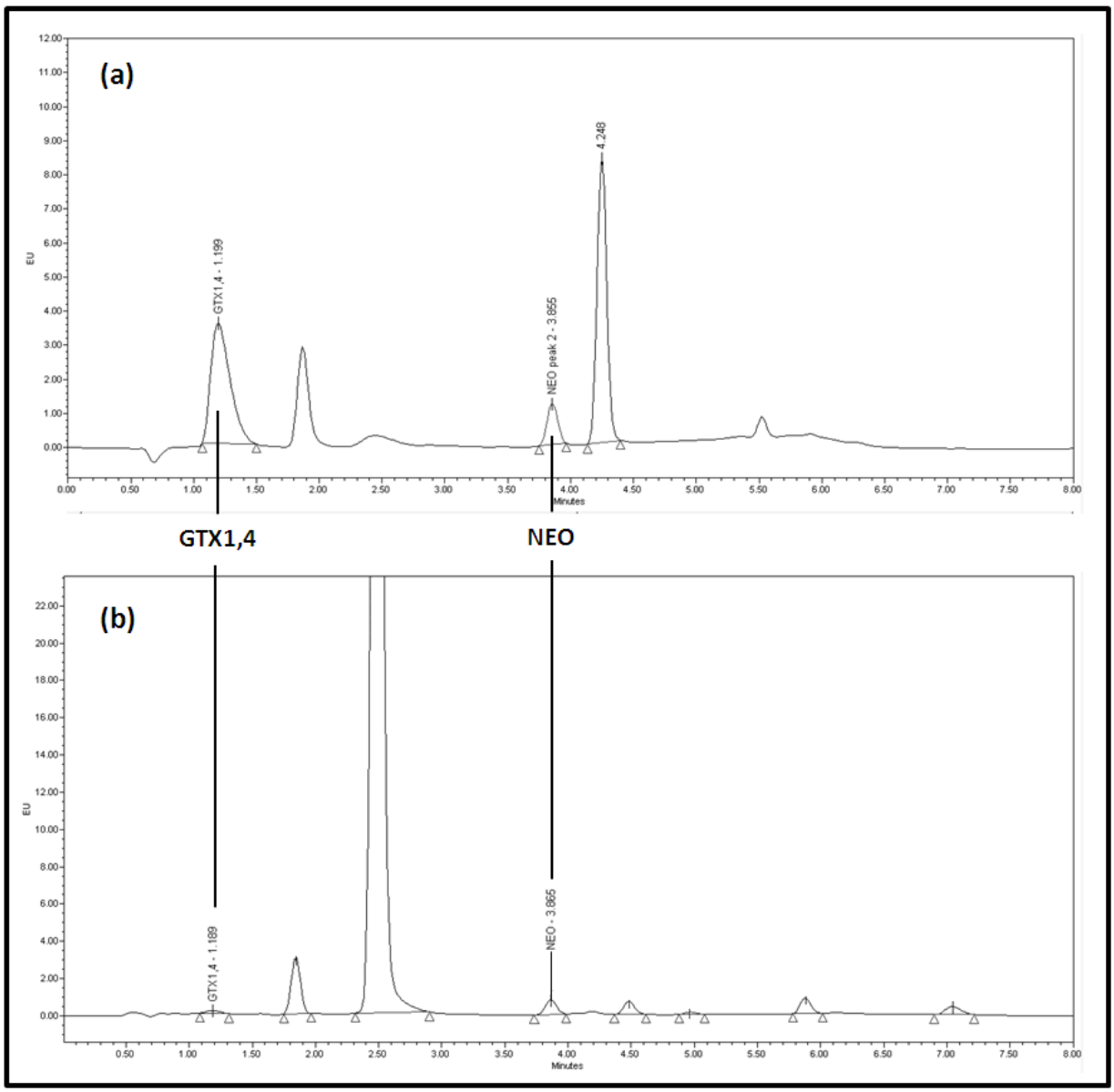

**Figure 4.10.** (a) Spectra of PST standards, including that of dcGTX2,3, C1,2, dcSTX, GTX2,3, GTX5 and STX, using the peroxide oxidation method. (b) Spectrum of a sample of Day 18 of AC-T. PSTs peaks were identified according to the corresponding retention times in the chromatograms of the standards.

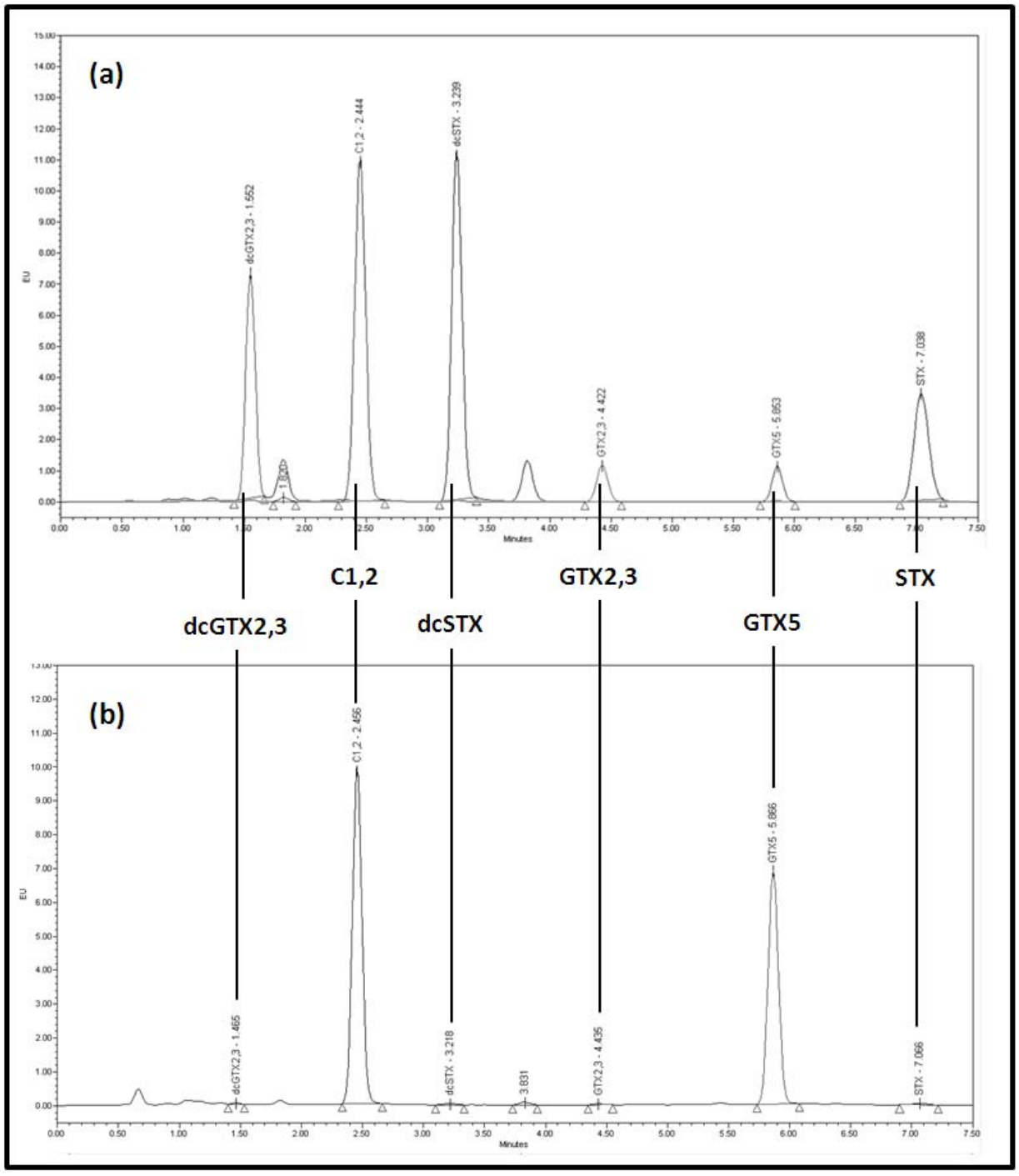

Several sampling time points were taken at different growth phases of the dinoflagellates studied. Figures 4.11-4.13 showed the toxin profiles of the 4 species in terms of cellular toxin content (fmol/cell) against different growth phases. Cellular toxin content was the sum of number of moles of different PSTs in the sample. As shown in Figure 4.11, the toxin contents were about 28-43 fmol/cell. No significant difference ($p \approx 0.43$) was found between different phases of growth cycles (Appendix A7). Previously, it was suggested that the total toxin contents of different strains of *G. catenatum* were about 0.2-0.6 pmol/cell, which is larger than the results of the present study (Band-Schmidt et al., 2006). It should be noted that different strains were used in this study and this may account for the difference seen. Another possible reason is the difference in culturing temperature. In the present study, the temperature for cultivation was set at 25°C, while it was at 20°C in the study by Band-Schmidt's group. Such difference could lead to different toxin production rates as it is known that low temperature could increase toxin content per cell in the case of *G. catenatum* and *A. catenella* whereas a decreased trend of the growth rate was seen (Ogata et al., 1989). It should also be noted that post-column derivatization of PSTs was used in the study by Band-Schmidt's group, and it is different from pre-column oxidation method used in the present study.

**Figure 4.11.** Cellular toxin content (fmol/cell) of GC-T at different growth phases (Day 2, 8, 18, 38 and 58). Cellular content was kept within the range of 28-43 fmol/cell thought out the growth cycle. (Bars indicate ± S.D. of triplicates)

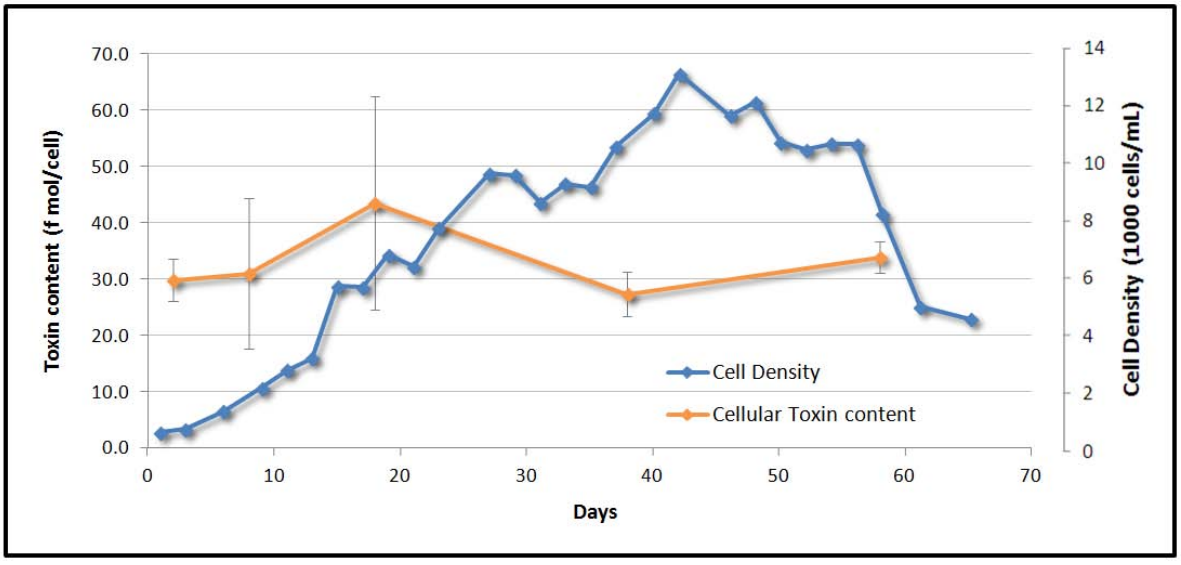

Different from GC-T, the toxin content of AC-T was higher in the exponential phase, compared to the decline phase (Figure 4.12). The cellular toxin content was around 3 fmol/cell in the exponential phase. Like GC-T, the toxin content of AC-T was found to be less than that from the literature. For example, the toxin content of several strains of *A. catenella* isolated from the Southeast China Sea had a toxin level of about 30 fmol/cell (Wang et al., 2006). The same explanations could be applied for the AC-T that variation of toxigenicities exists between different strains. The growing temperature was lower and post-column derivatization was used in the experiment by Wang and coworkers. Figure 4.13 (a) and (b) shows the toxin profiles of AC-N and AT-N. Being as non-toxic species, no PST was detected at any growth phases.

**Figure 4.12.** Cellular toxin content (fmol/cell) of AC-T at different growth phases (Day 8, 18, 38 and 58). Cellular content has a decreasing trend when culture went from log phase to decline phase. (Bars indicate ± S.D. of triplicates)

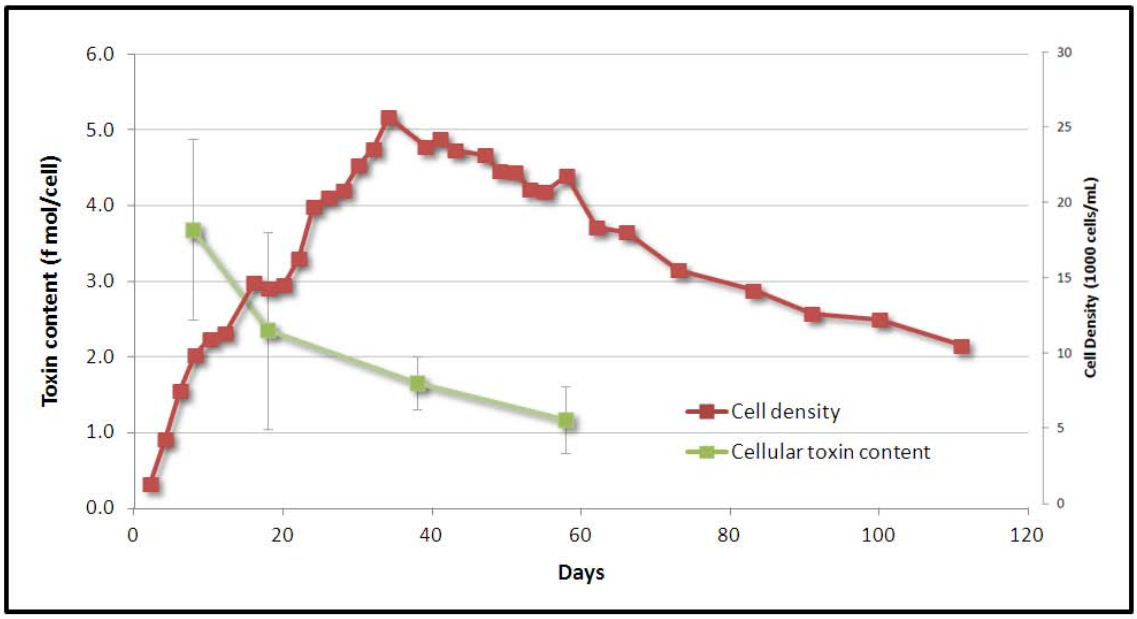


The toxin profiles of the 4 species were combined into a single figure (Figure 4.14). Cellular toxin content in GC-T was almost 10 times higher than that of AC-T. As mentioned above, comparison in toxigenicity could not be made solely with reference to the cell numbers. By averaging the toxin content with cell volume, the amounts of toxin were expressed as

cellular toxin concentration (mM) in Figure 4.15. Cellular toxin concentration of GC-T was ranged from around 1.1-1.8 mM, while AC-T was ranged from 0.2-0.4 mM. The results showed that GC-T had a higher ability to produce toxins than that of AC-T.

**Figure 4.13.** (a) Cellular toxin content (fmol/cell) of AC-N at different growth phases (Day 8, 18 and 38). (b) Cellular toxin content (fmol/cell) of AT-N at different growth phases (Day 2, 8, 18 and 24). No PST was detected from both species at any growth phases.

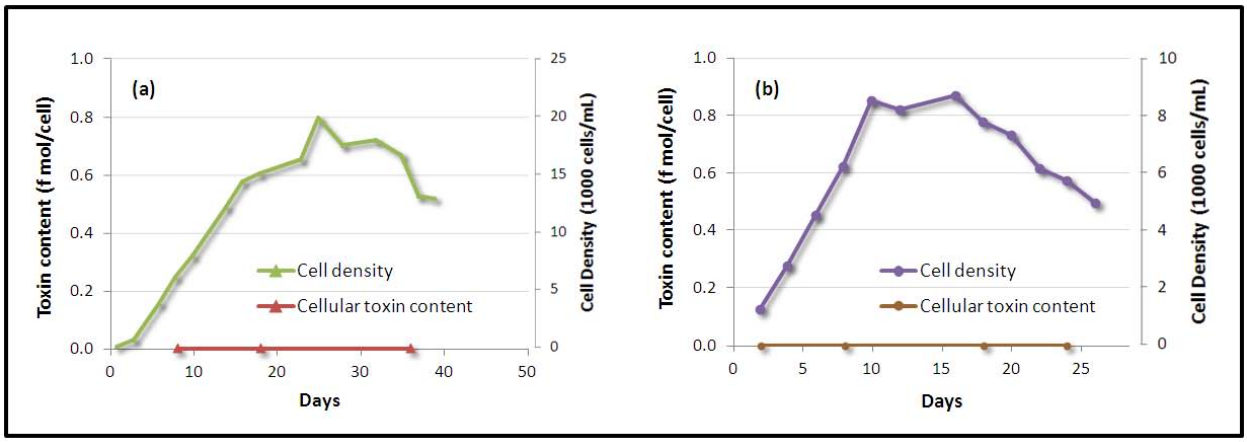


**Figure 4.14.** Cellular toxin contents (fmol/cell) of the 4 dinoflagellates studied. GC-T has about 10 times more PSTs per cell than that of AC-T. AC-N and AT-N show no toxin (Bars indicate ± S.D. of triplicates).

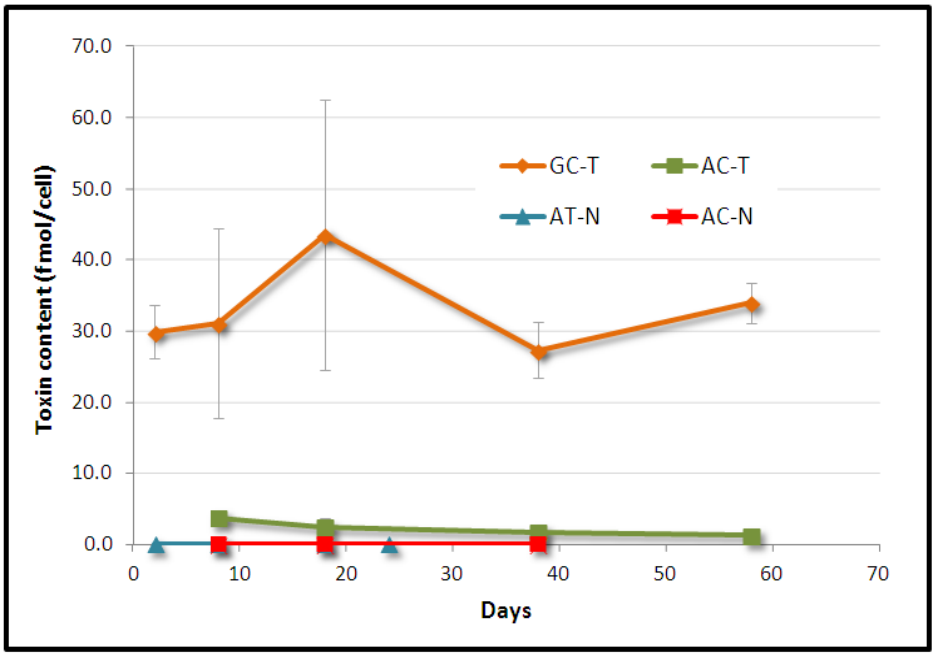

**Figure 4.15.** Cellular toxin concentrations (mM) of the 4 dinoflagellates studied. It can be seen that GC-T has more concentrated PST per cell than AC-T. AC-N and AT-N did not have any PST.

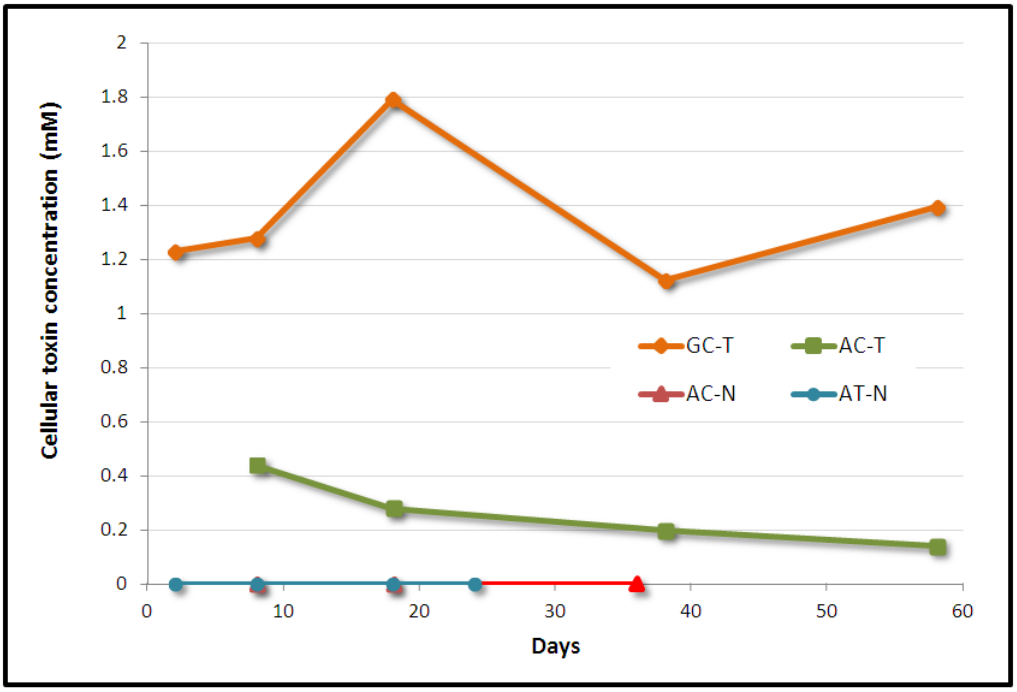


Beside the total toxin content, toxin composition was also studied among different growth phases. Figures 4.16 and 4.17 showed the toxin compositions of GC-T and AC-T respectively. For GC-T, the most abundant PST was NEO and GTX1 and GTX4, composing at least half of the total toxins. While for AC-T, the main toxin was C toxins. Some groups reported that the toxin compositions were constant with different growth phases and changed very little even under changes in the immediate environment (Ogata et al., 1987; Parkhill and Cembella, 1999; Usup et al., 1994). Toxin composition profile of AC-T showed similar characteristics. C toxins are always at around 70-80% of the total toxins. Such composition was also found in the *Alexandrium* isolates from South China Sea reported by Wang's group (2006). The similarity in toxin compositions in these two studies may due to the same source of geographical region as it was reported that toxin composition of dinoflagellate correlated with geographical locations in which the dinoflagellate come from (Cembella, 1998).

**Figure 4.16.** Cellular contents of different PSTs of GC-T at different growth phases. GTX1,4 and NEO composed of at least half of the total toxin content (Bars indicate ± S.D. of triplicates).

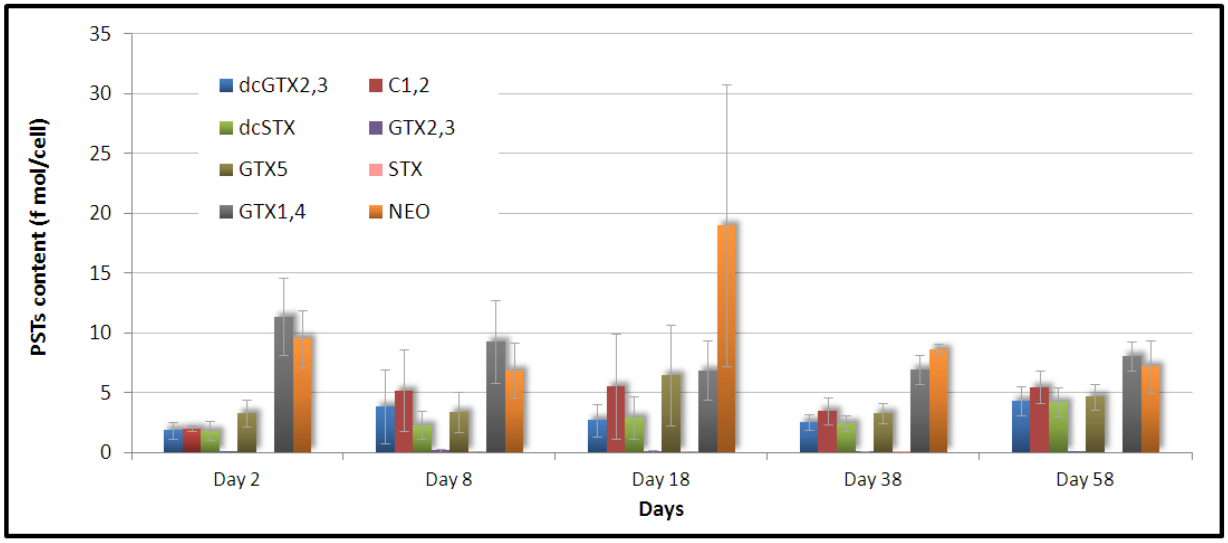


**Figure 4.17.** Cellular contents of different PSTs of AC-T at different growth phases. C toxins dominated the profile with a 70-80% content (Bars indicate ± S.D. of triplicates).

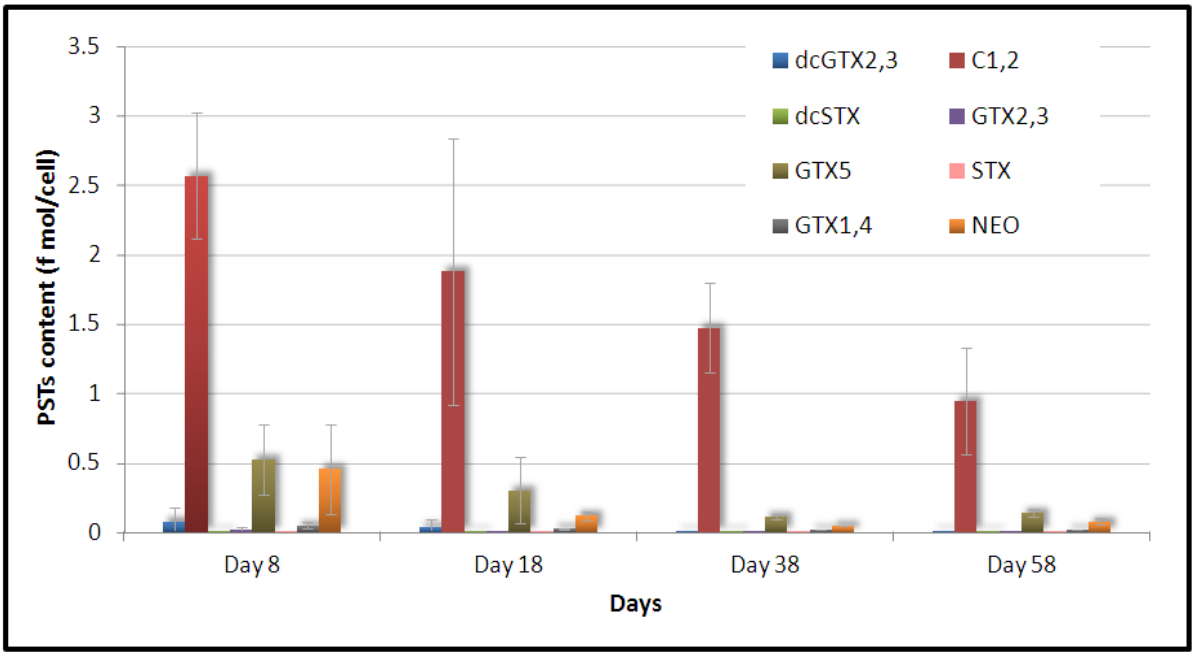

### 4.3.7 Endogenous Arginine Assay

In cyanobacteria, arginine is known to be the precursor of PST. Two arginine molecules are involved in synthesizing one saxitoxin molecule. To further study the relationship between arginine and PSTs production, levels of endogenous free arginine of the dinoflagellates were assayed with the aid of an amino acid analyzer using established methodology (Brief methodology had been included in Chapter 3). Arginine content was measured as the peak area relative to the standard. To ensure the amount of arginine measured was not interfered by intracellular protease activities, the need of the protease inhibitors was examined. A flask of dinoflagellates culture was harvested into two aliquots. Except the addition of a cocktail of protease inhibitors prior to sonication for cell breakage, sample preparation and arginine assessments of the two aliquots were performed with the same protocol as well as the same run. Figure 4.18 showed the difference of the readings between these two aliquots, indicating the importance of the use of protease inhibitors. Without the addition of protease inhibitor, the reading was nearly 10 times more than that of the aliquot with protease inhibitors. The results shows that the actual levels of intracellular free arginine could be exaggerated by the extra arginine released from the intracellular protease activities. To control artifactual generation of arginine, protease inhibitors were added in the experiment thereafter.

**Figure 4.18.** Amino acid analyzer chromatograms of the same flask of culture (GC-T) (a) with the addition of a cocktail of protease inhibitors and (b) without the use of the protease inhibitors. Arginine levels were exaggerated 10 times more if no protease inhibitor was added prior cell disruption.

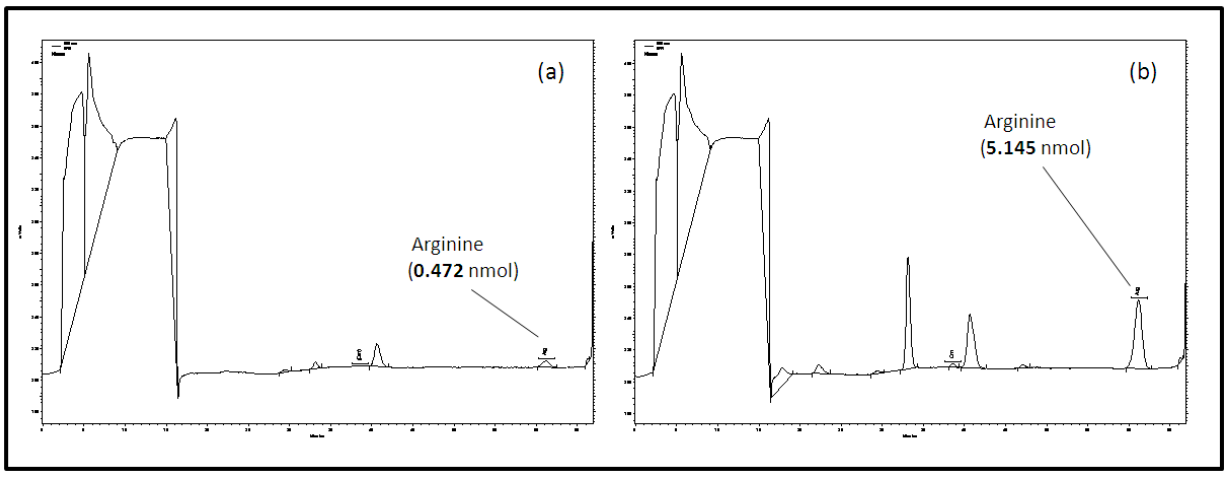

Endogenous levels of arginine in GC-T, AC-T and AT-N were accessed at the toxin sampling time points (Arginine content of AC-N was not accessed due to the failure of the machine afterwards). Its relationship to growth and also toxin content were studied. Figure 4.19 showed the endogenous free arginine content of GC-T at different growth phases. It was found that the arginine content was high, around 230 fmol/cell, during the lag phase and decline phases. On the other hand, the arginine content in exponential phase was significantly lower, around 25-110 fmol/cell. For AC-T shown in Figure 4.20, free arginine content of AC-T was high in lag phase, over 45 fmol/cell. This level was lowered during exponential growth phase to around 15-24 fmol/cell. The arginine content then increased back to 45 fmol/cell in the stationary phase before dropped back to a low level of 10 fmol/cell in the decline phase. Similar pattern of variations of the arginine levels had been reported in *Alexandrium sp.* by Anderson's group (1990). My results in the present study indicated that such variation pattern could also be seen in *Gymnodinium sp.* It was suggested that metabolism was active during exponential phases as there are high rates of protein synthesis and other cellular process that consume arginine. Therefore, the cellular free arginine level was lowered in the exponential phase. On the other hand, these processes were inactive in the lag phase and stationary/decline phase and so cause the accumulation of free arginine. No conclusion to be made about the last drop of arginine content in AC-T.

**Figure 4.19.** Endogenous free arginine content in GC-T at different growth phases. A concave pattern was seen. Arginine level was at low level during the exponential phase (Bars indicate ± S.D. of triplicates).

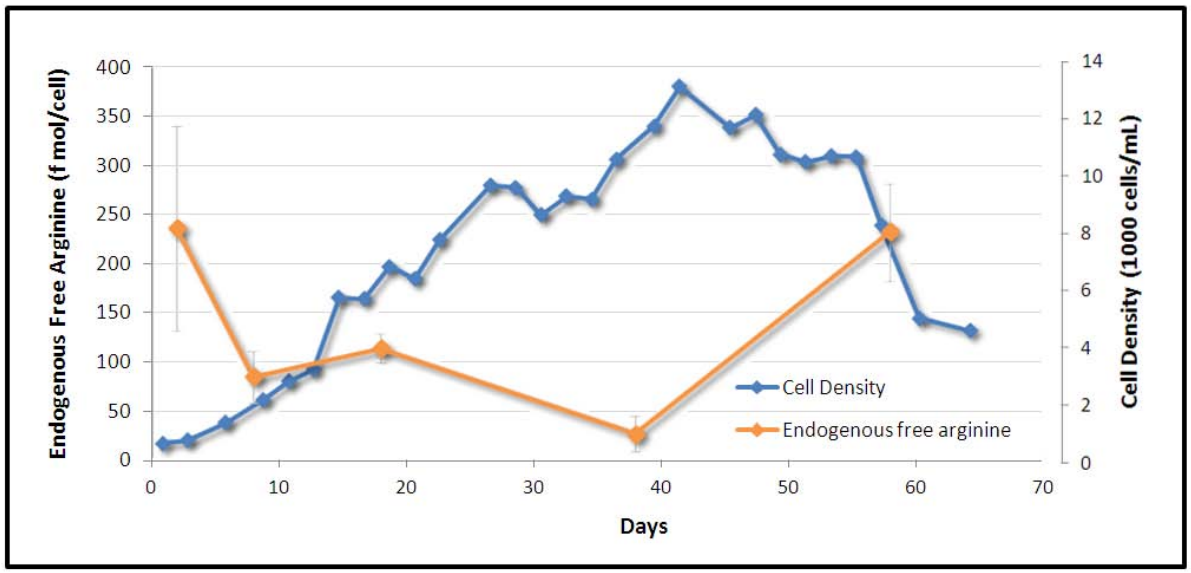


**Figure 4.20.** Endogenous free arginine level in AC-T at different growth phases. A concave pattern was seen in the lag- to exponential- to stationary phases. There is a drop of arginine content in the decline phase (Bars indicate ± S.D. of triplicates).

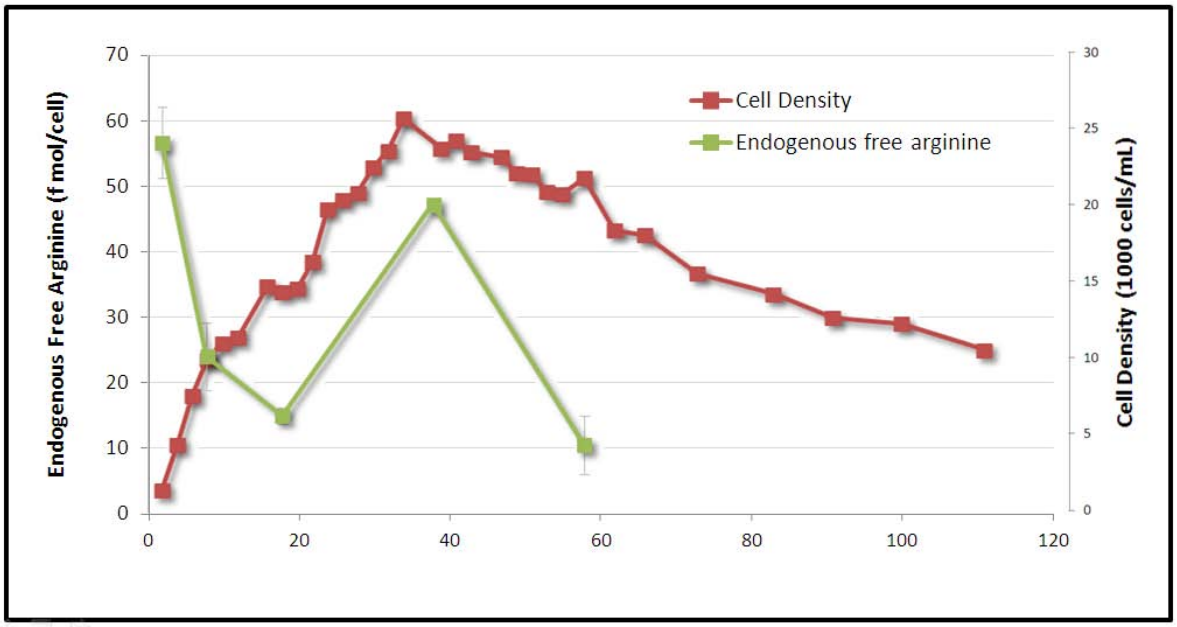

Anderson's and coworkers also suggested that the concave pattern of the arginine levels mirrored the convex pattern of cellular toxin content of the *Alexandrium sp.* because arginine was used in synthesizing toxins. Such relationship was not found in either GC-T or AC-T in the present study. Figures 4.21 and 4.22 showed the relationship between endogenous free arginine content and cellular toxin content of GC-T and AC-T respectively. As mentioned before, there is no significant change of cellular toxin content in different growth phases of GC-T. At the same time, there is neither conserved nor inversed pattern to the free arginine content. For AC-T, the toxin content decreased from exponential to decline phase; while the arginine content was low in the exponential and decline phases but high in stationary phase. The fact that no converse or inverse pattern to toxin content was found indicate that there is no simple dose-dependent relationship between the amounts of endogenous arginine of toxic dinoflagellates with their PSTs contents. Since other cellular processes including protein synthesis also need arginine, the consumption rate of arginine for PST production could not been simply reflected by accessing the free arginine content in the cells. More intensive controlled experiments are needed for further investigation of the relationship.

**Figure 4.21.** Endogenous free arginine content and cellular toxin content at different sampling time point (Day 2, 8, 18, 38 and 58) of GC-T (Bars indicate ± S.D. of triplicates).

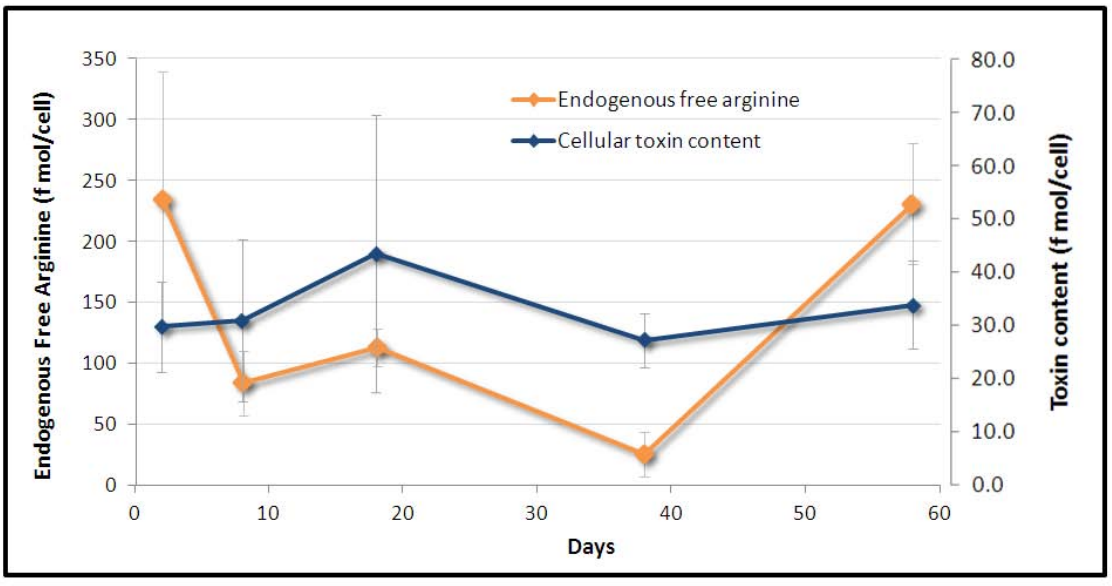

**Figure 4.22.** Endogenous free arginine content and cellular toxin content at different sampling time points (Day 2 (Arginine only); Day 8, 18, 38 and 58) of AC-T (Bars indicate ± S.D. of triplicates).

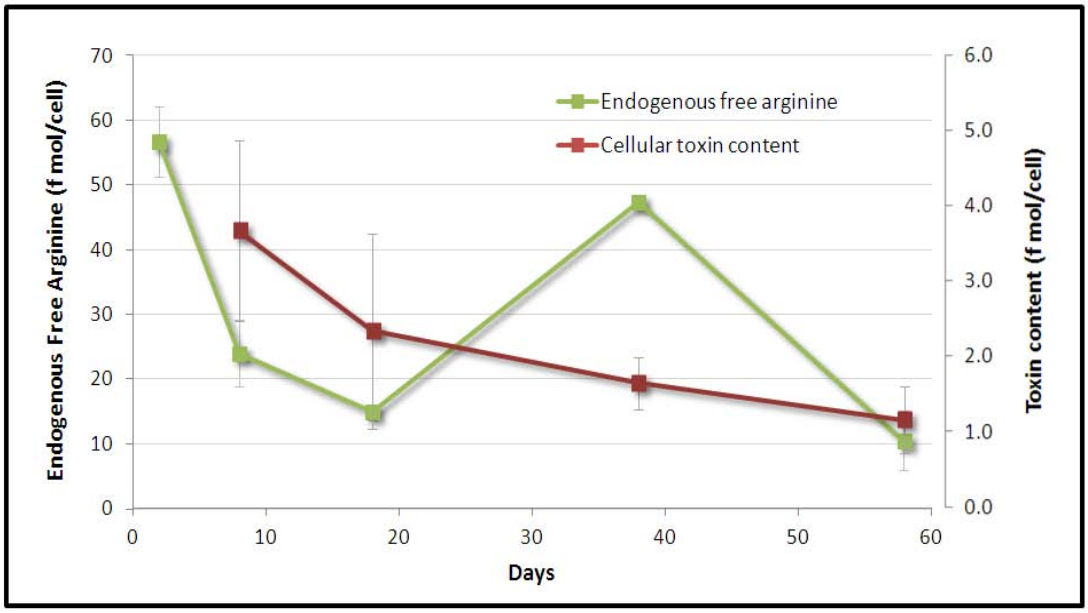


Comparing the endogenous arginine contents between GC-T and AC-T, the level of free arginine in GC-T in terms of fmol/cell was much higher than that of AC-T. It is because GC-T has a larger cell volume which could store more arginine. Considering the difference in cell volume, comparison of arginine contents of the 3 toxic dinoflagellates in terms of molar concentration was shown in Figure 4.23. Arginine contents of GC-T and AC-T varied between 1-9.7 mM and 1.2-6.7 mM respectively. No significant difference ($p \approx 0.19$) was found between these two set of variations. Free arginine content of the non-toxic dinoflagellate AT-N was also assessed in the same way and it varied from 0.8 to 3.6 mM. This level is comparable to that of the toxic species. In the present study, no significant difference of endogenous arginine levels was found among PSTs producing and non-PSTs producing dinoflagellates. Toxin production theoretically should lead to higher consumption rate of arginine in the toxic species than the non-toxic species. Whether toxic PST-producing dinoflagellates produce more free arginine to support toxin production is not clear. If all dinoflagellates produce the same amount of arginine, my results did not support the notion that arginine is involved in the biosynthesize of PSTs in

dinoflagellates. It is also possible that the dinoflagellates are able to maintain the free arginine amount at equilibrium levels despite using some arginine to produce PSTs. Further study is needed to investigate the assimilation of intracellular free arginine and its relationship to toxin production.

A higher amount of intracellular free arginine level than my AC-T and AT-N and at about 7.2 mM in the exponential phase of another toxic *Alexandrium sp.* was reported earlier (John and Flynn, 1999). The difference may due to a different species being studied or the earlier study did not control intracellular protease activities with protease inhibitors when they broke the cells.

**Figure 4.23.** Endogenous arginine concentrations (mM) of GC-T, AC-T and AT-N. The free arginine levels of the three species being studied were not significantly different from each other.

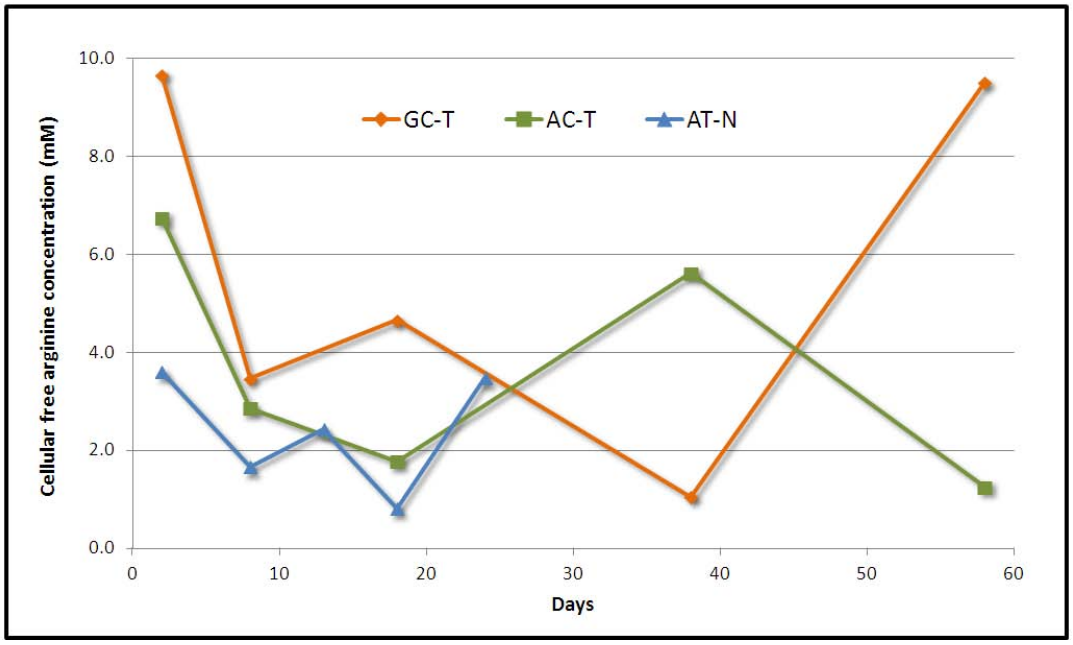

## 4.4 Summary

Two toxic species of dinoflagellates GC-T and AC-T and 2 non-toxic ones AC-N and AT-N were studied and they were positively identified through their rDNA sequences in the ITS1-5.8S-ITS2 region. The intra-species homology of the ribosomal gene sequence was 97%; the inter-species homology was 81-82% and the inter-genus homology was 44-45%. Background information of these 4 species was collected in this chapter. Protein expression profiles were shown to be species specific and the same species (AC-T and AC-N) shared the same major peaks and could act as protein fingerprints for differentiation of the identities between two species. Growth rates were measured and different growth phases could be established. Cell volumes of the dinoflagellates were measured and it was found that GC-T had the largest cell size while AC-T and AC-N are similar in size to each other. Toxin profiles at different growth phases were also documented. Cellular toxin content of GC-T was kept constant throughout the whole growth cycle. The cellular toxin content of AC-T was found to be highest during exponential phase. No PST was found in AC-N and AT-N. GC-T was shown to be more toxic than AC-T, not only because of its larger cell size for toxin accumulation, but also having higher cellular toxin concentration and higher cellular toxicity. C toxins were the dominant PSTs of AC-T. Endogenous free arginine was measured but it is necessary to add protease inhibitors to stop intracellular protease activities during cell disruption. Endogenous free arginine was found to be at low level during exponential growth but relatively high in lag and stationary-decline phases. Amounts of endogenous arginine of the toxic and non-toxic dinoflagellates are similar. In my study, the relationship between endogenous arginine and toxin level is yet to be established in dinoflagellates.

# Chapter 5 Effects of Nitrate Enrichment as well as Limitation, Phosphate Limitation and Exogenous Arginine on Toxin Production of PSTs-producing Dinoflagellates

## 5.1 Introduction

The mechanism of production of PSTs by dinoflagellates has long been the interest of many researchers as the complete pathway of how the toxins are synthesized is still inconclusive. Nonetheless, it was found that certain amino acids including arginine, methionine and acetate are involved in the toxin synthesis as precursors (Shimizu et al., 1984). Study of PST production mechanism in dinoflagellates was hindered by lack of genomic information due to its large genome size (Lin, 2006). With the provision of high-throughput next-generation DNA sequencing machines, the study is becoming easier. As mentioned in the previous chapter, different species of dinoflagellates could have a large variation in their behavior. Therefore, to eliminate complications from genetic variations in the analysis of the experimental results, it is more preferable to study toxic and non-toxic dinoflagellates of the same species. The difference in toxin production rate would be manifested as changes in the expression of proteins related to biosynthesis of PSTs. It is known that, toxigenicity of dinoflagellates could vary with different environmental and nutritional factors. Therefore, it would be a possible strategy to induce a change in the toxin production rate by changing its environmental and nutritional conditions. Comparative proteomic studies could then be performed to pinpoint proteins that may be involved in the biosynthetic process.

### 5.1.1 Effects of Availability of Nitrogen and Phosphate Sources on PST Production

As one of the possible ingredients in the biosynthesis of saxitoxin, effects of the availability of nitrogen source to PST bio-synthesis has been studied by many groups. Most of the studies reported that N-stress by itself caused a decreased in PST production as the cells had reduced growth (Anderson et al., 1990a; John and Flynn, 2000; Strichartz, 1984; Wang and Hsieh, 2002b). However, the extent of changes on PST production was different from study to study. Further, several other studies had reported that when phosphate is in limiting conditions (i.e. high N:P ratio), toxin production was increased (Boyer et al., 1987; Lippemeier et al., 2003; Siu et al., 1997).

Touzet and coworkers stressed that the cells in P-stress should have sufficient soluble protein quotas from adequate nitrogen supply, before the increase in toxin level could be seen (Touzet et al., 2007b). On the contrary, Flynn's group reported that P-limiting cells had decreased synthesis of toxin (Flynn et al., 1994). On the other hand, Wang and Hsieh reported that in the presence of 5 μM of phosphate (i.e. at P-stress), addition of nitrate caused an increase in toxin produced (Wang and Hesieh, 2005). It is particularly interesting to note that Flynn' group reported that N-refeeding of N-deprived cells of *A. minutum* induced the production of maximum amount of PST in 1-2 days afterwards. Further, they reported that P-stress followed by N-stress did not cause the production of PST to come down, implying the availability of phosphate is the regulator of toxin metabolism (Flynn et al., 1994). Lastly, Parkhill and coworkers reported that the amount of toxin produced was independent on changes in nitrate (Parkhill and Cembella, 1999). In 2011, Li's research group reported that in *A. catenella*, N-starved cells preferentially uptake nitrate and ammonium over urea. In addition, the amount of toxin produced was the lowest and comparable to that of control when urea was used as the sole N-source (Li et al., 2011). Taken overall, ratio of N:P and/or P-stress followed by refeeding regimes will induce changes in the levels of PST produced. However, no mechanistic study has been conducted for this parameter.

### 5.1.2 Availability of Arginine on PST Production

Arginine was reported to affect the toxin production. Being one of the precursor ions of PST production, it was found that exogenously added arginine would increase toxin production in *A. fundyense* (John and Flynn, 1999).

Taken overall, in this chapter, effects on PST production due to variations in the availability of nitrate, phosphate and arginine were studied. Two PST-producing dinoflagellates, *Gymnodinium catenatum* (GC-T) and *Alexandrium catenella* (AC-T) were used. It is hoped to deliver a pair of dinoflagellates with different toxigenicities for proteomic analyses in the later part of this thesis.

## 5.2 Materials and Methods

Unless stated otherwise, all the materials and methods used in this part of the study were presented in Chapter 3 already.

## 5.3 Results and Discussion

### 5.3.1 Nitrate Enrichment and Limitation

The effect of nitrate enrichment (10 times of the normal amount of $NO_3$ supply) and limitation (one tenth of normal $NO_3$ supply) on growth and toxicity were studied. For *Gymnodinium catenatum* (GC-T), growth from lag phase to the exponential phase (Day 0-18) under both $NO_3$-enriched (8800 μM or 8.8 mM) and $NO_3$-limited (88 μM) conditions were found to be similar to that of the GC-T in normal medium (Figure 5.1). The three growth curves overlapped partly with each other. Figure 5.2 showed the PST contents and also the PST composition of the exponential culture of GC-T (Day 18) with different amounts of $NO_3$ supply. There is no significant change of the PST contents of GC-T among normal condition, $NO_3$-enriched and $NO_3$-limited conditions. My results are the same as that reported previously by others that growth and toxin contents of GC-T were relatively stable for a range of nitrate supply (Oshima et al., 1993; Reguera and Oshima, 1990). Reguera and Oshima also reported that the *G. catenatum* in their study continued to grow under nitrate-depleted medium for some time, suggesting that *G. catenatum* has a large pool of intracellular nitrate. I found similar results in my study. On the other hand, regarding toxin contents, Reguera and Oshima reported that the toxin composition changed under $NO_3$-limited (110 μM). Oshima also reported that toxin composition of several strains of *G. catenatum* showed stable toxin composition under either $NO_3$ or $PO_4$ starvation (Oshima et al., 1993). The GC-T studied in this study behaved similarly to the strain described in Oshima's study (mentioned above) that it is less reactive to the changes of nitrate supply.

**Figure 5.1.** Growth curves (Day 0 to 18) of GC-T grown in normal medium (880 µM $NO_3$ supply), $NO_3$-limited medium (88 µM $NO_3$ supply) and $NO_3$-enriched medium (8800 µM $NO_3$ supply). No significant difference of growth was found among the three culture conditions (bars indicate ± S.D. of triplicates).

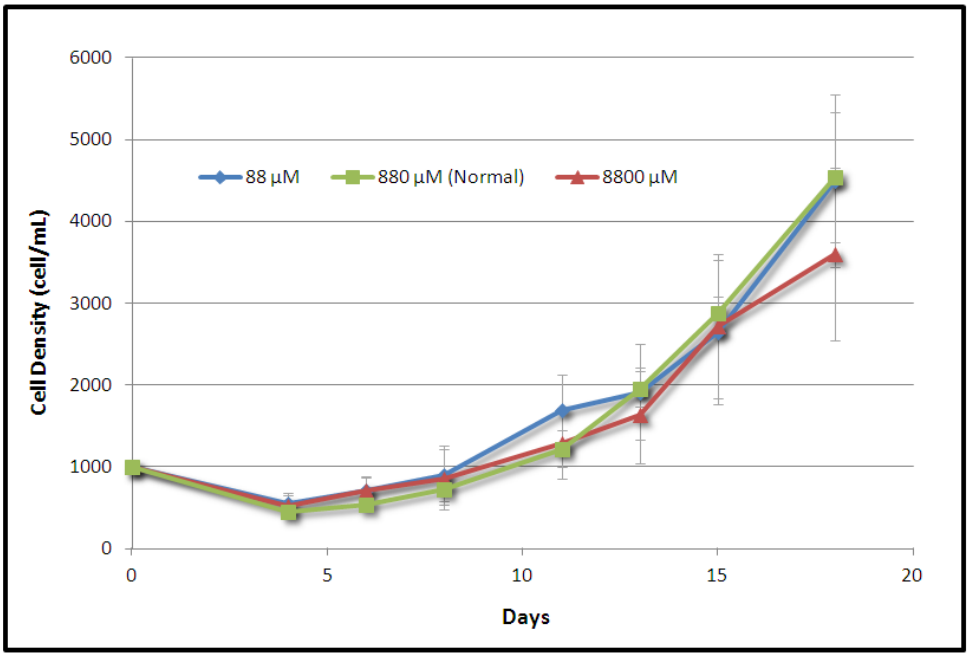


**Figure 5.2.** Cellular PST compositions of GC-T culture at exponential phase (Day 18) under normal $NO_3$ supply (880 µM), limited $NO_3$ supply (88 µM) and enriched $NO_3$ supply (8800 µM). No significant difference was found among the three conditions ($p \approx 0.51$) (bars indicate + S.D. of triplicates).

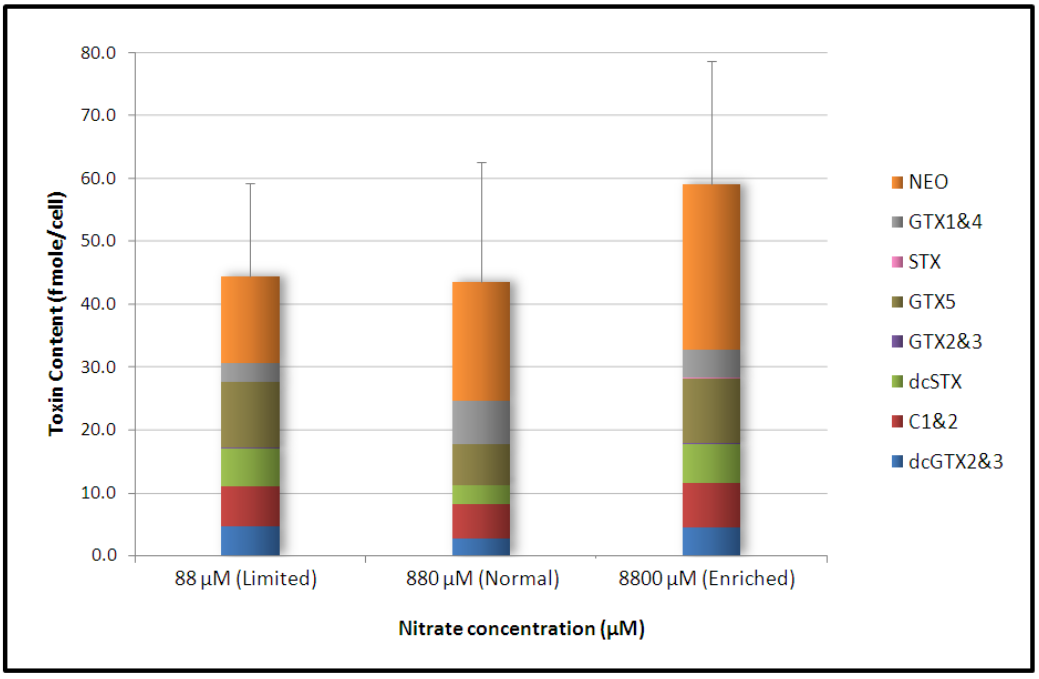

The same set of experiments was performed on *Alexandrium catenella* (AC-T), another PST-producing dinoflagellate. Figure 5.3 showed the growth curves of $NO_3$-enriched culture, $NO_3$-limited culture and the normal culture. It was found that cell densities of Day 18 cultures in both $NO_3$-enriched and limited culture were reduced when compared to that of normal condition. In $NO_3$-enriched culture, maximum cell density was reached at Day 15 and started to decline afterwards. On the other hand, in $NO_3$-limited culture, cell density stopped to increase at Day 7 and began to drop after Day 15. Results of toxin analyses were shown in Figure 5.4. At Day 18, toxin contents of $NO_3$-enriched culture were similar to that of the normal culture, which is about 2.3 fmol/cell. However, in $NO_3$-limited culture, toxins content was found to be about half of the normal (1.1 fmol/cell). Similar studies on *Alexandrium spp.* also reported that growth was retarded when nitrate supplied was reduced (Anderson et al., 1990b; Parkhill and Cembella, 1999; Touzet et al., 2007b; Wang and Hsieh, 2002b). However, in these earlier studies, the toxin contents under nitrate limitation were shown to be comparable to that of normal culture. The difference in response in toxin content of AC-T in the present study may indicate difference in responses in different species or strains of dinoflagellates. It should be noted that the large errors of toxin contents was found and that such changes were not significant enough for proteomic study in later studies ($p \approx 0.24$). On the other hand, the growth of AC-T was negatively affected in the $NO_3$-enriched culture. This negative effect may due to competition from increased number of associated bacteria that grew in the $NO_3$-enriched culture. Under such condition, toxin level in culture with enriched $NO_3$ was found to be similar to that in normal culture.

**Figure 5.3.** Growth curves of AC-T (Day 0 to 18) grown in normal medium (880 µM $NO_3$ supply), $NO_3$-limited medium (88 µM $NO_3$ supply) and $NO_3$-enriched medium (8800 µM $NO_3$ supply) (bars indicate ± S.D. of triplicates).

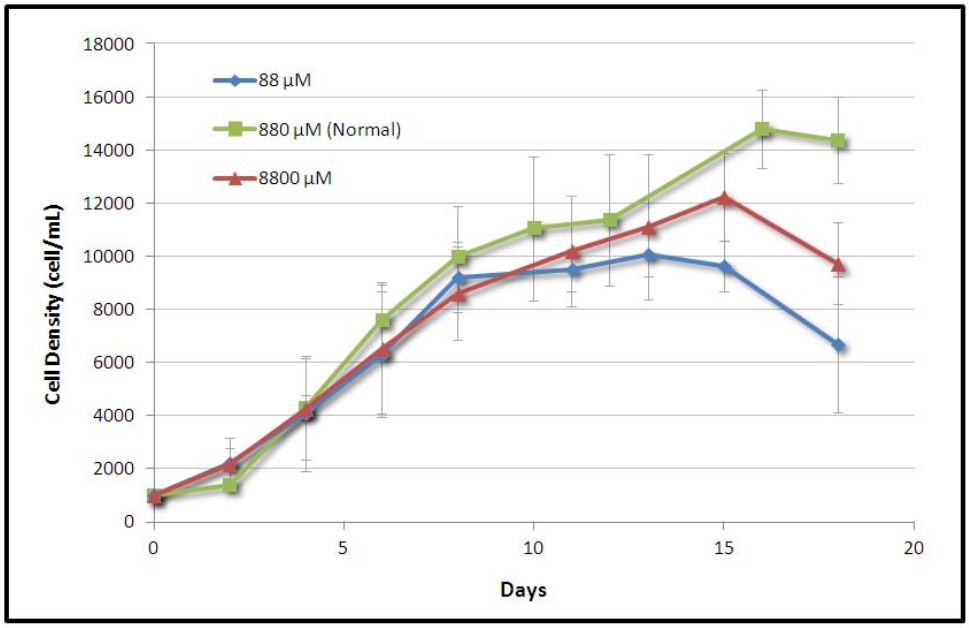


**Figure 5.4.** Cellular PST compositions of AC-T in the exponential culture (Day 18) under normal $NO_3$ supply (880 µM), limited $NO_3$ supply (88 µM) and enriched $NO_3$ supply (8800 µM). PST content was reduced in $NO_3$-limited culture ($p \approx 0.24$) (Bars indicate + S.D. of triplicates).

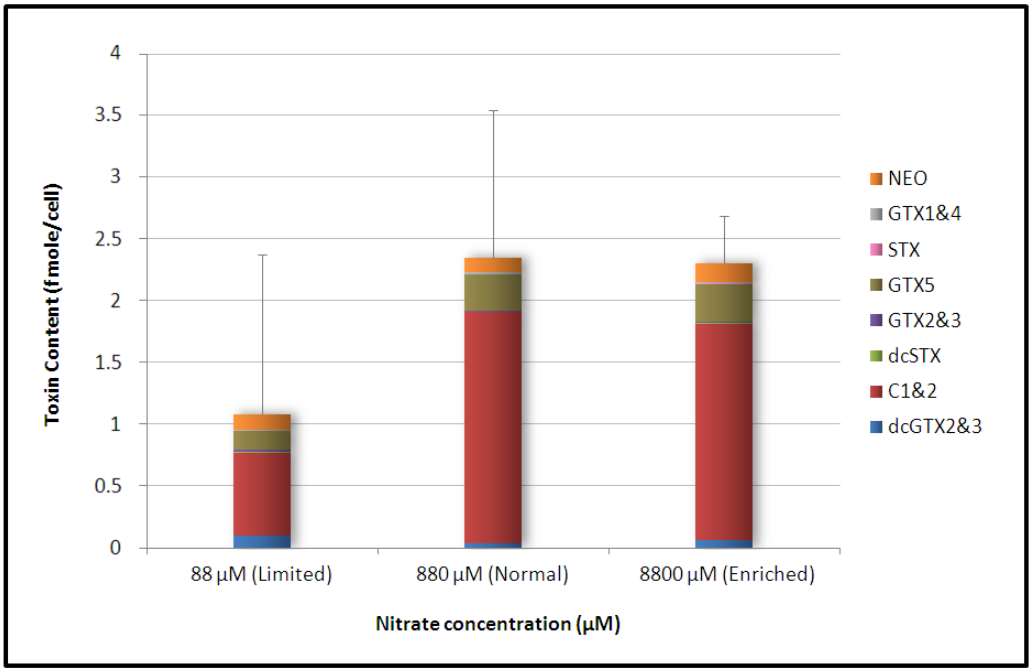

### 5.3.2 Phosphate Limitation

Phosphate is another factor that could affect PSTs production (Anderson et al., 1990a; Boyer et al., 1987). Effects of $PO_4$ limitation on GC-T and AC-T were studied using a phosphate limiting condition (3.6 µM; one tenth of the normal $PO_4$ supply). As shown in Figure 5.5, growth of GC-T (Day 0-20) under phosphate limitation was similar to that in normal condition. Figure 5.6 showed that the PSTs contents of GC-T at exponential phase (Day 18) and under phosphate limitation. There is no significant difference in PST contents between normal and $PO_4$-limited culture ($p \approx 0.96$). Results in the present study showed that the first 20 days of growth of GC-T and its toxin content was not affected by reduced phosphate supply. It is consistent with the suggestion that *Gymnodinium sp.* has a large pool of intracellular nutrients, including nitrate and phosphate (Boyer et al., 1987; Reguera and Oshima, 1990). It could grow at its optimal level for some time under nutrient-reduced environment.

**Figure 5.5.** Growth curves (Day 0 to 18) of GC-T grown in normal medium (36 µM $PO_4$ supply) and $PO_4$-limited medium (3.6 µM $NO_3$ supply). No significant difference of growth was found between the two conditions (Bars indicate ± S.D. of triplicates).

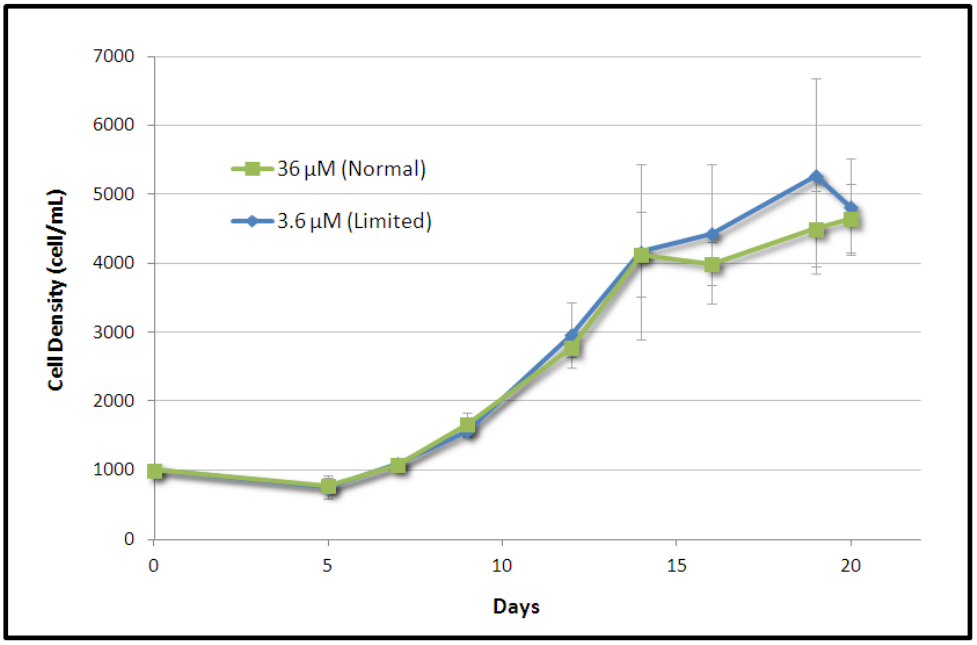

**Figure 5.6.** Cellular PST compositions of GC-T in exponential phase (Day 18) in normal $PO_4$ supply (36 µM) and limited $PO_4$ supply (3.6 µM). PSTs content of $PO_4$-limited culture was comparable to that in normal condition (Bars indicate + S.D. of triplicates).

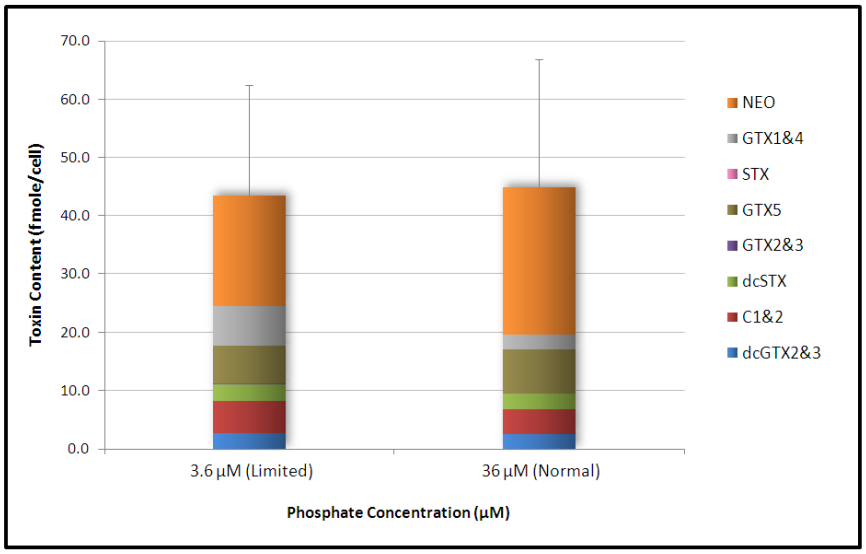


In contrast, there is significant change in growth and toxin contents when AC-T grown ordinarily in normal condition was made to grow under phosphate limitation. As shown in Figure 5.7, AC-T under $PO_4$-limited culture reached maximum cell density at 8100 cell/mL at Day 7 and its growth started to have a gradual decrease. The cell density of $PO_4$-limited culture at Day 20 (5700 cell/mL) is less than half of that of normal culture (14600 cell/mL). Results of toxin contents analysis of AC-T under phosphate limitation were shown in Figure 5.8. The PST contents of $PO_4$-limited culture at Day 10 and Day 20 was increased by about 360% ($p \approx 0.04$) and 400% ($p \approx 0.01$) of the normal culture respectively. C toxins were always the dominant PSTs. My results are consistent with others that in *Alexandrium spp.*, toxin contents were increased under $PO_4$-limited condition (Touzet et al., 2007b; Wang and Hesieh, 2005; Wang et al., 2006). It was suggested that phosphate limitation caused DNA synthesis to stop and no cell division occurred. Subsequently, nutrients were used to build up cell volume but not cell number. This resulted in an increase of cell size and with concomitant accumulation of toxins intracellularly (Touzet et al., 2007b). Another suggestion is that the cease of cell division would reduce the competition of arginine and other toxin precursors by cell growth. More of these molecules became available for PST production and so increase the toxin content (Wang et al., 2006).

**Figure 5.7.** Growth curves of AC-T (Day 0 to 20) grown on normal medium (36 µM $PO_4$ supply) and $PO_4$-limited medium (3.6 µM $NO_3$ supply). Cell density stopped to increase after Day 7 under $PO_4$-limited medium (bars indicate ± S.D. of triplicates).

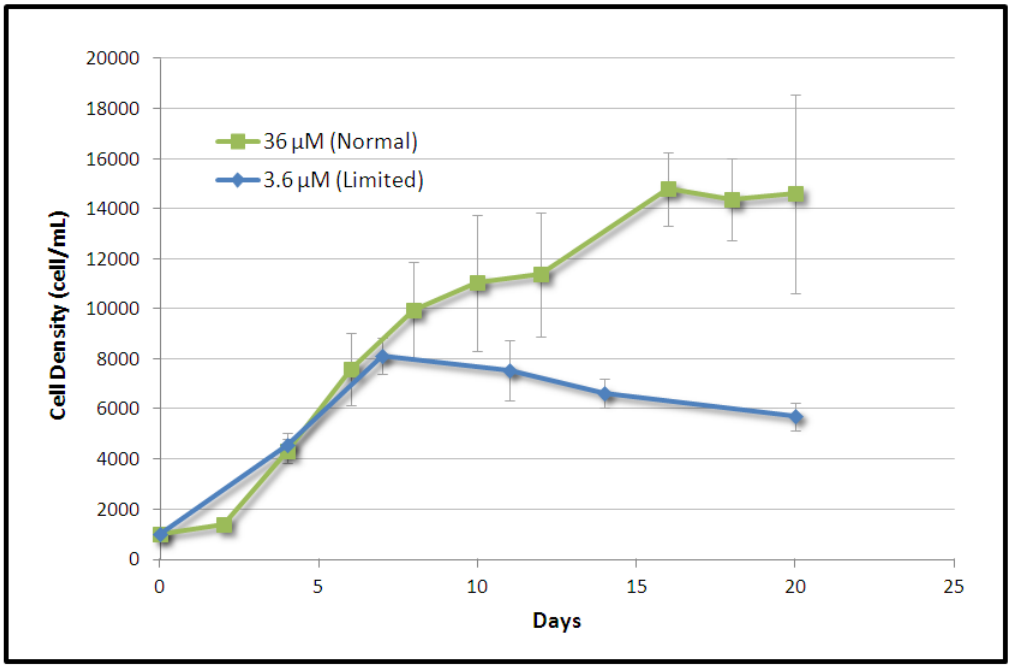


**Figure 5.8.** Cellular and PST composition of AC-T at Day 10 and Day 20 under normal $PO_4$ supply (36 µM) and limited $PO_4$ supply (3.6 µM). At Day 20, PST content of $PO_4$-limited culture was increased to about 400% of that of normal (p≈0.01) (bars indicate + S.D. of triplicates).

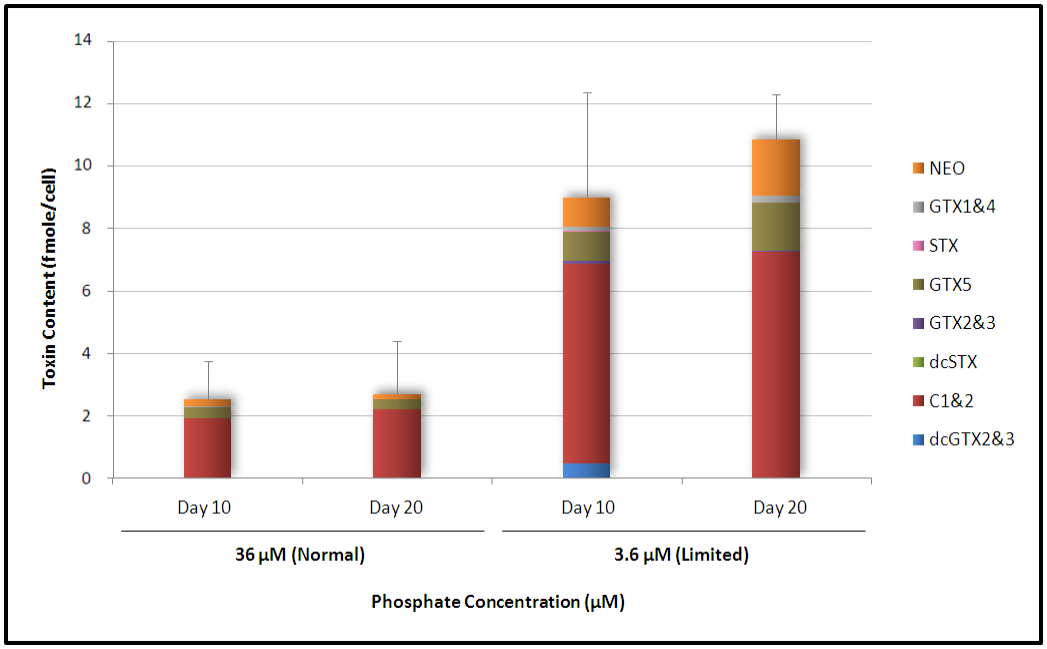

To investigate whether the increase of PST contents of AC-T under $PO_4$ limitation is due to an increase in cell size or a really increase in the concentration of toxins, cell volume of AC-T under $PO_4$ limitation were measured. As shown in Figure 5.9, cell volume increased under $PO_4$-limited culture while cell volume was constant in normal culturing condition. There is nearly a double of cell size at Day 20. Taking cell volume into account, PST contents in terms of concentration (mM) were calculated and shown in Figure 5.10. PST concentration of AC-T was constant at 0.30-0.33 mM in the normal culture. However, PST concentration was increased to about 0.61-0.86 mM in $PO_4$-limited culture. These results indicated that the higher toxicity in $PO_4$-limited cultured cells was not only due to a larger cell size, but also an elevated production of toxins under such condition.

Besides cell size, rate of protein synthesis was also considered as an indicator of growth. Cellular protein concentrations of the cultures were measured and the ratios of cellular toxin per cellular protein (fmol/ng) were estimated by mathematical conversion and were illustrated in Figure 5.11. It was found that the toxin/protein ratio were constant at around 9 fmol/ng in normal culture while it increased to about 23-24 fmol/ng under phosphate limitation. The increase in ratios indicated that the toxin production rate is higher than that of protein synthetic rate under phosphate limitation. Hence, the difference in toxin content at Day 20 between the normal culture and $PO_4$-limited culture were significant and such difference could be used in the comparative proteomic studies in later parts of this thesis.

**Figure 5.9.** (a) Cell volumes of AC-T in normal and $PO_4$-limited culturing conditions. There is a significant increase of cell volume of AC-T under phosphate limitation at Day 20 (bars indicate ± S.D. of triplicates); (b) microscopic images of AC-T in normal and $PO_4$-limited culturing conditions. The increase in cell size could be seen by larger cell dimensions seen under microscope examination.

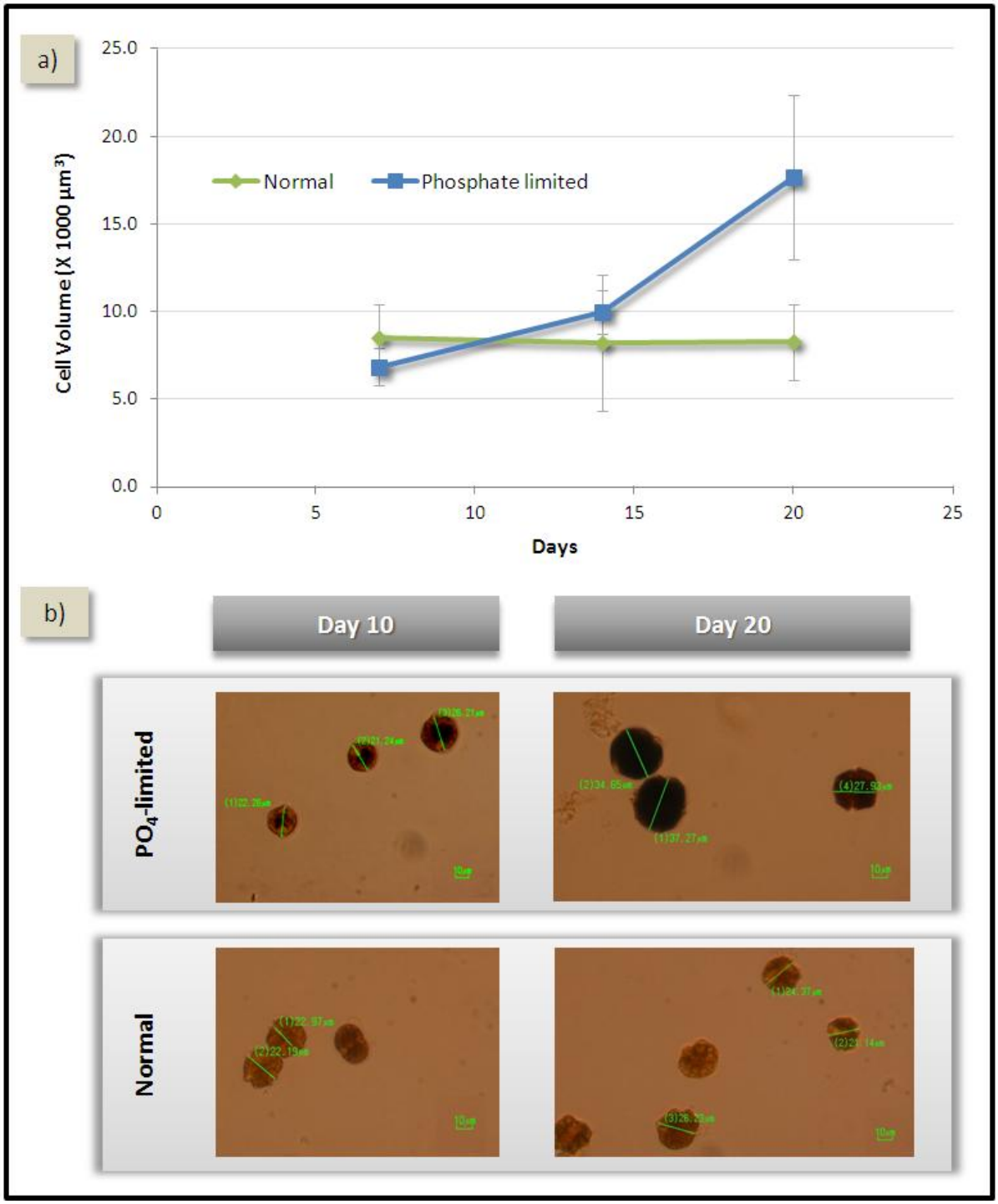

**Figure 5.10.** Cellular toxin concentrations of AC-T in normal and $PO_4$-limited culturing condition. Toxin concentrations were higher in $PO_4$-limited culture.

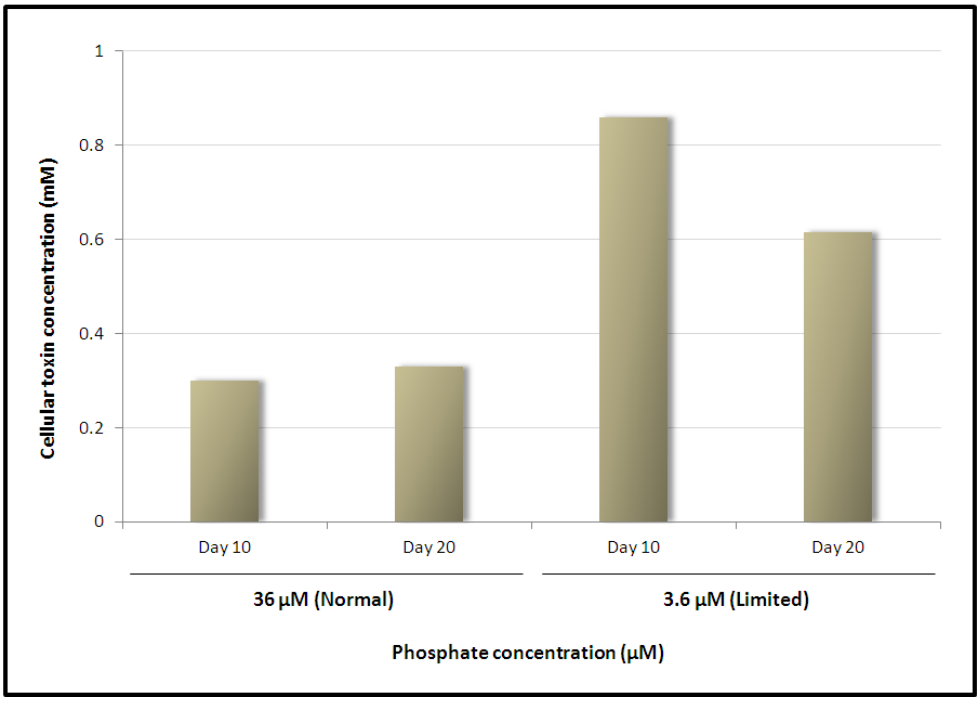


**Figure 5.11.** Toxin/Protein ratios of AC-T in normal and $PO_4$-limited culturing conditions. The ratios were higher in $PO_4$-limited culture.

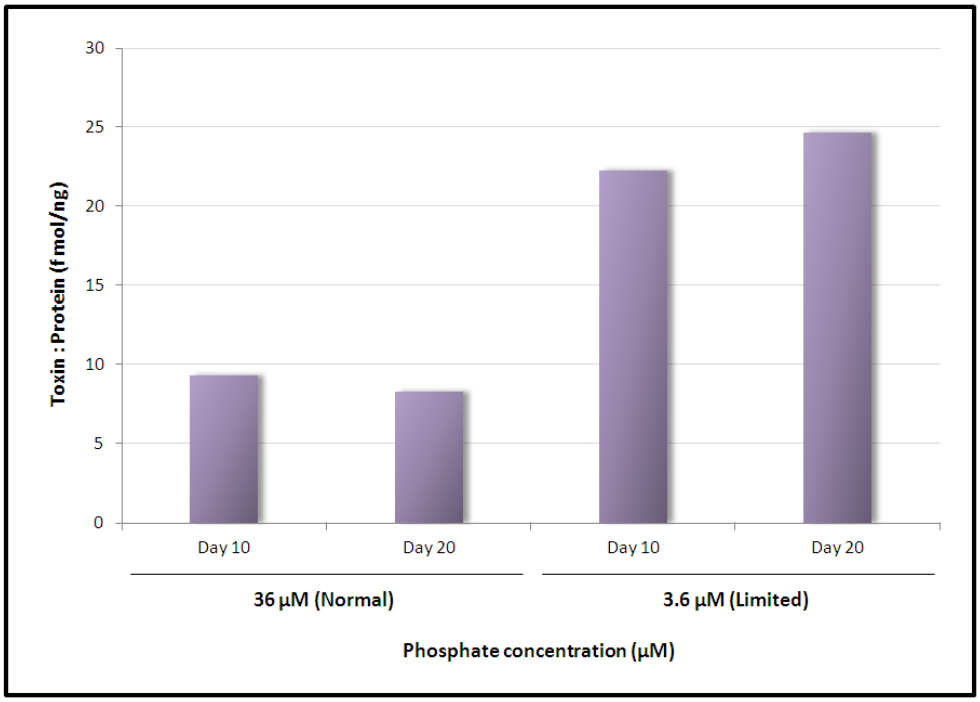

### 5.3.3 Exogenous Arginine

Arginine was found to be the precursor of saxitoxin and other PST analogs in cyanobacteria (Shimizu et al., 1990). Effect of arginine supplement on toxicity was examined. A preliminary experiment was performed to investigate the upper limit of exogenously added arginine that the dinoflagellates could sustain. It was found that the growth rate was highest in culture with 12 µM of arginine added. This concentration was then used for the experiments thereafter. Figure 5.12 showed the growth of GC-T (Day 0-30) with 12 µM arginine supplement. In comparison with normal culture, a longer lag phase (Day 0-7) was found. The growth rate of exponential phase to Day 30 was 0.12 $day^{-1}$, which is comparable to that of normal culture (0.11 $day^{-1}$). Toxin analysis was performed on the exponential culture (Day 18). As illustrated in Figure 5.13, the toxin content was decreased to about 25 fmol/cell. Toxin composition was found to be different with the normal culture – the actual amount of NEO presented was decreased to about 37% of that of normal. While the GTX1,4 contents were increased about 16%. However, the decrease of cellular PST content was not significant as large errors exist ($p \approx 0.28$).

**Figure 5.12.** Growth curves (Day 0 to 30) of GC-T grown in normal (L1) and arginine-supplemented medium (L1 + 12 µM arginine). In comparison with normal culture, a longer lag phase was found in arginine-supplemented culture. The growth rate of arginine-supplemented culture cells (0.12 $day^{-1}$; Day 3-30) was similar to normal culture (0.11 $day^{-1}$) (bars indicate ± S.D. of triplicates).

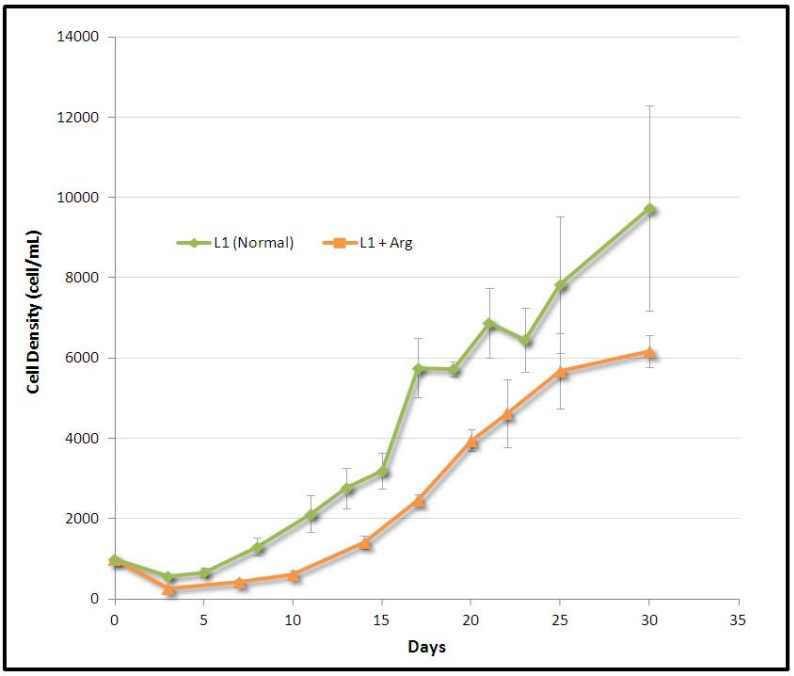

**Figure 5.13.** Cellular PSTs compositions of GC-T in exponential phase (Day 18) in normal (L1) and arginine-supplemented medium (L1 + 12 µM arginine). No significant change of PST content was found when exogenous arginine was added (p≈0.28) (bars indicate + S.D. of triplicates).

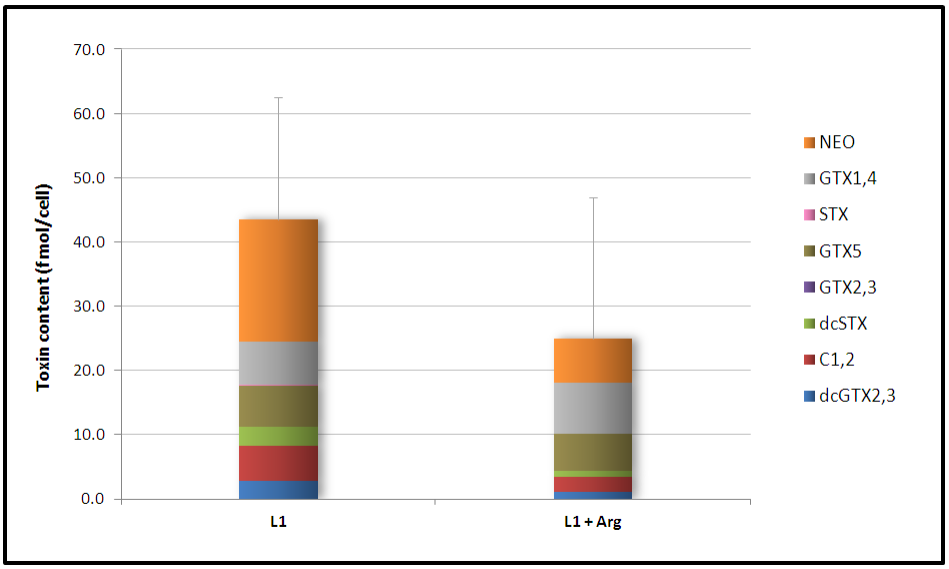


For AC-T, the effect of exogenous arginine on growth was shown in Figure 5.14. A longer lag phase was also found in arginine-enriched culture. But the exponential growth rate of arginine-supplemented culture was decreased to about 0.10 $day^{-1}$, which is less than that of normal culture (0.18 $day^{-1}$). As shown in Figure 5.15, there is no significant difference in PST contents between normal culture and arginine-enriched culture (p≈0.61). Although it was reported earlier that toxin content in dinoflagellates was increased to almost 3 folds of the normal culture after addition of a very high concentration of exogenous arginine (John and Flynn, 1999). However, AC-T did not give the same response. The discrepancy may either due to the difference in amounts of arginine used or the different species used in these studies.

**Figure 5.14.** Growth curves (Day 0 to 30) of AC-T grown in normal medium (L1) and arginine-supplemented medium (L1 + 12 µM arginine). In comparison with normal culture, a longer lag phase was found in arginine-supplemented culture. The exponential growth rate (0.10 $day^{-1}$) (Day 0 to Day 30) was found to be less than that of normal culture (0.18 $day^{-1}$) (bars indicate ± S.D. of triplicates).

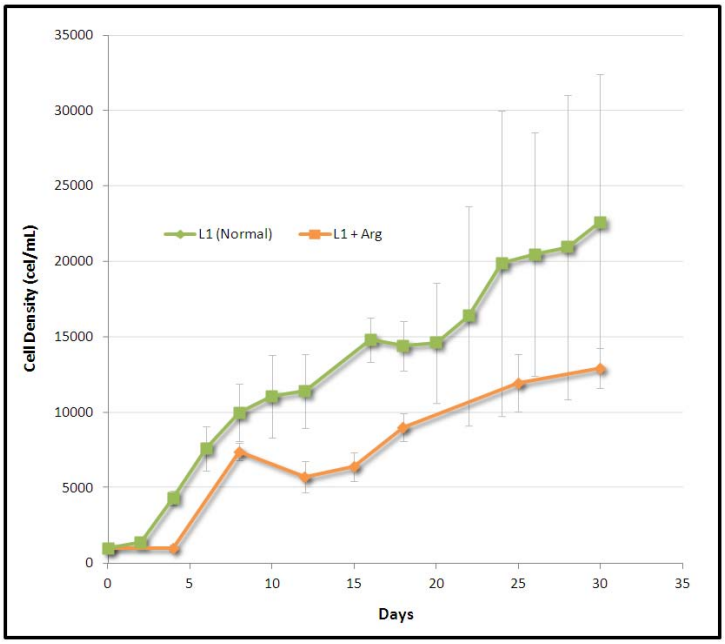


**Figure 5.15.** Cellular PST composition of AC-T at exponential phase (Day 18) in normal medium (L1) and arginine-supplemented medium (L1 + 12 µM arginine). In comparison with control culture, no significant difference in PST content was found when exogenous arginine was added (p≈0.61) (bars indicate + S.D. of triplicates).

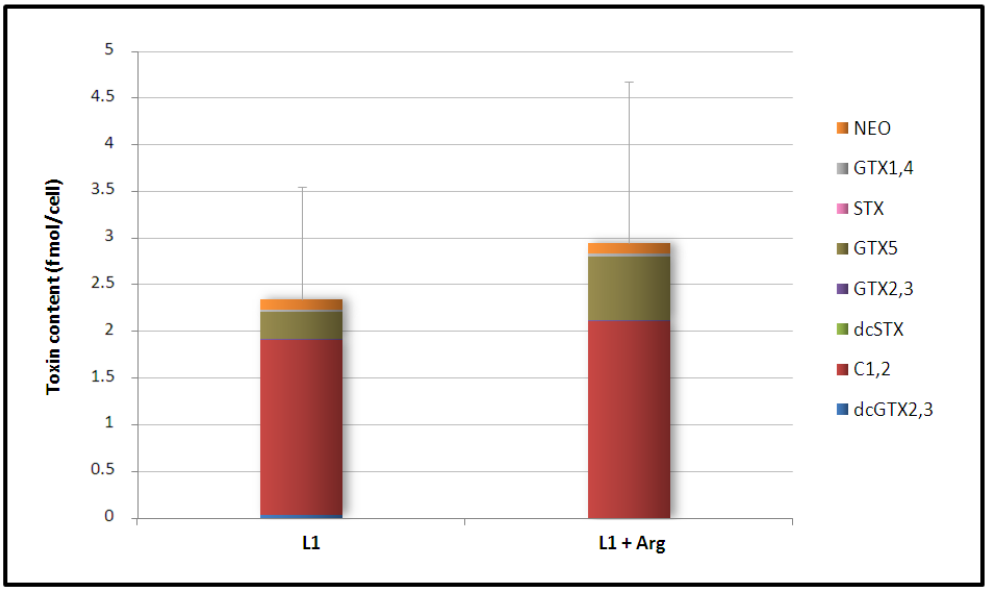

From the results of on the effects of nutrient availabilities in GC-T and AC-T, PSTs contents were not increased with exogenously added arginine. It may indicate that arginine is not the only factor to change toxin production in dinoflagellates. Flynn and coworkers has studied the relationship between cellular toxin content and other intracellular free amino acids of *Alexandrium minutum* (Flynn et al., 1994). They reported that several amino acids including arginine, taurine, glycine and glutamine showed similar relationship to toxin contents, suggesting that the availability of intracellular free arginine is not the only factor to control toxin synthesis. Further, since arginine was not the only precursor that used for PST production, other unknown factors which may be involved in PST production could be limiting and regulated the toxin production process. More detailed and controlled experiments may be needed to investigate the assimilation and utilization of arginine for PST production. On the other hand, the growths of arginine-supplemented culture of both species were negatively reduced. The suppression of growth may be related to the growth of associated bacteria when the medium were enriched with arginine supplements.

## 5.4 Summary

Toxicity of dinoflagellates was known to vary with different environmental and nutritional factors. In this study, the effect on toxin production of nitrate-enrichment, -limitation, phosphate limitation and exogenous arginine were investigated with two PST-producing dinoflagellates, *Gymnodinium catenatum* (GC-T) and *Alexandrium catenella* (AC-T). GC-T did not show any significant changes in cellular toxin contents in exponential phases (Day 18) in any of the nutrient-enriched and nutrient-limiting experiments. Limitation of nitrate supply (10% of normal supply) halved the PST content in AC-T. Under phosphate limitation, AC-T growth was stopped at Day 7 and toxin contents were significantly increased to around 4 folds of that of normal both in Day 10 and Day 20. Increase of cellular toxin content was not only due to the increase of cell volume under phosphate limitation, but also higher production of PSTs as cellular toxin concentrations were increased. Supplements of exogenous arginine to the culture of both GC-T and AC-T did not cause any significant increase of toxin contents. In summary, as significant increase of toxin content were shown by AC-T in phosphate limitation, the following study would then focus on investigating the pathway of PST production on AC-T using comparative proteomic analysis. A pair of AC-T (in normal culturing condition and $PO_4$-limited condition), together with a strain of non-toxic *Alexandrium catenella* (AC-N) were used in later comparative proteomic studies.

# Chapter 6 Comparative Proteomic Studies between Cultures of *Alexandrium catenella* of different toxigenicities

## 6.1 Introduction

Subsequent to previous work in this thesis (Chapters 4 and 5), a strain of *G. catenatum* and several strains of *Alexandrium spp.* of different toxicities were found. Especially for the *Alexandrium spp.*, we have one toxic strain of *A. catenella* (AC-T) and a non-toxic *A. catenella* (AC-N). These two strains have very similar growth rates, cell size, protein expression profiles and ribosomal ITS gene sequences (97% homology, Figures 4.4-4.5 in Chapter 4). The only substantial difference is the toxicity. Further, from my work, it is found that with $PO_4$-limiting condition, the toxicity of AC-T increased in both the amount and concentration. Moreover, we also have a non-toxic strain of *A. tamarense* (AT-N). These strains may be used in my comparative proteomic studies. However, it should be noted that GC-T is very different from AC-T, AC-N and AT-N as they only shared 44%-45% of homology in their ITS regions. Therefore, if one uses GC-T to compare to the others in comparative proteomic investigations, it is impossible to pinpoint meaningful differentially expressed proteins without complication from their highly different genetic makeup. Hence, GC-T was not used in the comparative proteomic investigations. Similarly, although both AC-N and AT-N are non-toxic, it seems irrelevant to compare them. Hence, in order to find possible proteins of interest that may be related to biosynthesis of PSTs and also to eliminate complications in interpretation of experimental data due to difference in genetic makeup among different strains, it would be more logical to compare AC-T and AC-N as they shared a high homology of 97% in their ITS regions. Further, protein expressions in AC-T with and without phosphate-stress would also be performed.

It is my aim to document if there are differentially expressed proteins among these strains so as to pinpoint proteins/enzymes that are involved in the biosynthesis of PSTs. Because of the lack of whole genome database of dinoflagellates, shot-gun proteomics with non-gel based analysis is not feasible. Therefore, the classical 2-dimensional gel electrophoresis (2-DE) was used to document any differentially expressed proteins among these strains. Although shortcomings such as poor representation of highly hydrophobic and/or membrane proteins as they do not go into the polyacrylamide gel, 2-DE is a simple preparative method to

study global changes of protein expression in these dinoflagellates. With the aid of image analyzing computer software, expression level of a particular protein across different gels (ran with different samples) could be compared and differentially expressed proteins pinpointed. Subsequently, matrix-assisted laser desorption/ionization time-of-flight tandem mass spectrometry (MALDI-TOF-TOF MS) and liquid chromatography electrospray ionization ion-trap tandem mass spectrometry (LC ESI-ion-trap MS/MS) were used to find partial amino acid sequences of the differentially expressed proteins of interest. With the amino acid sequences, identities of proteins of interest may be found and their putative functions predicted.

## 6.2 Materials and Methods

Two major sets of proteomic comparison were performed: (a) AC-T against AC-N, (b) AC-T in normal medium against AC-T in phosphate-limited medium. Unless stated otherwise, all the materials and methods used in this chapter were presented to Chapter 3 already. Unless stated otherwise, all chemicals used are of the highest grade in purity and they are from Sigma, USA.

### 6.2.1 Two Dimensional Gel Electrophoresis (2-DE), Gel Staining and Imaging Analysis

Protein expression of dinoflagellates in the 2 sets of comparison was examined by two-dimensional gel electrophoresis (2-DE). 2-DE was divided into 3 main steps: rehydration, isoelectric focusing (IEF) and SDS-PAGE analysis. For rehydration, 340 μL of sample buffer containing either 80 μg protein for silver staining or 1 mg protein for comassie blue staining), 1 % v/v of IPG buffer pH 4-7, small amount of dithiothreitol (DTT) (USB, USA) and the remaining volume of rehydration buffer (7 M urea, 2 M thiourea, 4 % CHAPS (USB, USA), 5 % glycerol (USB, USA) and 10 % isopropanol (International Laboratory, USA)) was used to rehydrate the IPG strip (18 cm) pH 4-7 (Bio-Rad, USA) for 16-20 hours at 20$^{o}$C. Subsequently, IEF was performed on the rehydrated IPG strip, using Protean-IEF cell (Bio-Rad, USA), according to the following protocol: 500 V for 3 hours, 1000 V for 6 hours, 8000 V for 3 hours and finally with a total of 120000 voltage hours. Before going to the SDS-PAGE step, the strip was allowed to incubate for 15-minutes with the equilibration buffer (50 mM Tris pH 8.8, 6 M urea, 30 % glycerol, 2 % SDS (USB, USA) and trace amount of bromophenol blue) containing 1 % DTT and 2.3 % iodoacetamine

(IAA) respectively. The second dimension of SDS-PAGE was performed in 12 % polyacrylamide gel using the PROTEAN® II xl cell (Bio-Rad, USA) and voltage of 35 mA/gel. Subsequently, the gel was fixed in 10 % v/v acetic acid, 40% v/v methanol.

Visualization of protein was either performed with silver staining or comassie blue staining. Silver staining was performed in 3 steps. Fixed gel was sensitized for 30 minutes (8 mM sodium thiosulphate and 30 % v/v methanol). After several rounds of washing with water, silver nitrate solution (14.7 mM) was added onto the gel before allowed to a 20-minute incubation. Subsequently, the gel was then washed twice for 1 minute, before being developed with a 0.24 M sodium carbonate solution (USB, USA) in 0.004 ‰ v/v formaldehyde. Development was finally stopped by adding EDTA (USB, USA) solution (35mM) when the stain was adequate. Coomassie blue staining was performed by 1-hour staining and several rounds of destaining, using the 0.1 % coomassie blue stain and destain solution (5 % methanol and 7 % aceic acid) respectively. The 2-D gels which were either silver stained or coomassie blue stained were scanned before image analyses with software called Melanie III software (GeneBio, Switzerland). Differentially expressed proteins can be identified and their difference in expression levels calculated.

### 6.2.2 In-gel Digestion

Gel-plugs containing the proteins of interest pinpointed by 2-D gel image analysis were excised from the coomassie stained gel for in-gel tryptic digestion before MALDI-TOF-TOF mass spectrometry. The excised coomassie blue stained gel plugs about 1 mm X 1mm size were washed with 25 mM ammonium bicarbonate ($NH_4HCO_3$) solution in 50 % acetonitrile (ACN) for three times. After dehydrating with 100 % ACN, the gel pieces were reduced and alkylated by incubating with 10 mM DTT (55$^{o}$C for 45 minutes) and 55 mM IAA (room temperature; in dark for 30 minutes) respectively. Solutions of DTT and IAA were prepared with 25 mM $NH_4HCO_3$. Gel plugs were subsequently washed and dried again. Aliquots of 3 µl of freshly prepared trypsin (Promega, USA) solution (20 ng/ml) were then added onto the dried gel pieces. After 30-minute incubation on ice, the trypsin-gel-plugs were left at 37$^{o}$C overnight. Digested peptides inside the gels were eluted with 0.1 % trifluoroacetic acid (TFA) in 50 % ACN with the aid of

ultra-sonication. The peptide solution was then dried under vacuum before resuspending the dried peptide fragments in 2 µl of 0.1 % TFA with ACN (2:1).

### 6.2.3 MALDI-TOF-TOF Mass Spectrometry

Prior to adding samples onto the target plate (anchor-chip, Bruker, USA), each spot on the anchor-chip was firstly coated with 1 µl saturated (2 mg $ml^{-1}$) matrix solution (α-cyano-4-hydroxycinnamic acid in 0.1 % TFA with ACN (2:1)). The resuspended peptides samples were then introduced onto the dried anchor spots and allowed to dry again. Followed with brief washing of 0.1 % TFA, samples were subsequently recrystallized with 0.5 µl of a mixture of ethanol (Merck, Germany), acetone (Lab-Scan, Poland) and 0.1 % TFA in a volume of ratio 6:3:1. Samples were then ready for MALDI-TOF MS analysis with Autoflex III (Bruker, USA). Reflector mode over a mass range of 700-3000 Da was used after calibration with a peptide calibration standard (Bruker, USA) as external calibrants. Peptide mass fingerprints (PMF) were generated from the combined spectra of 1000 shots of each sample. Peptide ions visualized in the spectra might be further fragmented into its constituent amino acids with post-source decay in the LIFT mode. The MS/MS spectra generated were analyzed by the de novo sequencing function of the software Biotools 3.2 (Bruker, USA) to construct its amino acid sequences. The PMF and amino acid sequence tags of unknown proteins may be searched after searching the NCBI non-redundant database with the MASCOT software.

### 6.2.4 N-terminal Sulfonation

De-novo peptides sequencing could be facilitated with the aid of N-terminal sulfonation before MS/MS analysis. To perform sulfonation, several extra steps were introduced after trypsin digestion. After drying the tryptic digest of protein of interest under vacuum, sulfonation were performed by incubating the peptide fragments with 10 mg/ml 4-sulfophenyl isothiocyanate (SPITC) in 20 mM sodium biocarbonate at pH 9.5, in 55$^{o}$C for 30 minutes. The reaction was stopped with 0.5 % TFA. Sulfonated peptide fragments mixture was absorbed onto C-18 zip-tips before being cleaned and eluted with 2 µl 0.1 % TFA with ACN (2:1). Eluted samples were directly targeted onto the anchor-spots in which matrix had been already applied. Successfully sulfonated peptides would have an increased mass of 215 Da. MALDI-TOF-TOF analysis

mentioned before was performed of the sulfonated peptides to generate the MS/MS spectra. Followed-up de novo sequences were then analyzed with Biotools 3.2.

### 6.2.5 Liquid Chromatography Electrospray Ionization (LC-ESI) Ion-trap MS/MS analysis

Although non-gel based whole proteome investigation is not feasible without a corresponding whole genome database of dinoflagellate, LC-ESI ion-trap MS/MS can also be used to obtain amino acid sequence tags of peptides/proteins of interest. When performing the LC-ESI-ion-trap MS/MS, each tryptic peptide mixture of protein of interest (which was suspended in 5 µL of 2% ACN and 0.1% formic acid) was loaded into a 15-cm nanoflow C18 column (LC Packings, Netherlands). The column was equilibrated earlier with 0.1% formic acid. Peptides in the sample were eluted with and elution buffer (20% $H_2O$, 80% ACN & 0.001% formic acid) at a flow rate of nL/min and column temperature 40$^{o}$C. ESI-ion-trap MS/MS for the peptides eluted was performed with an ion-trap mass spectrometer from Bruker (HCT ultra, Bruker, USA). Positive mode with 1400V of capillary voltage and 80-120 nA current were maintained in the ion-trap mass spectrometer. Temperature was set at 150$^{o}$C and the accumulation time for the peptide ions in the ion-trap was set to be 50 ms. Nitrogen was introduced at a flow rate of 6 L/min. MS/MS spectra obtained were analyzed with Data Analysis 3.4 (Bruker, USA) and Biotools 3.2 to construct the amino acid sequences. Finally, putative identification of proteins of interest was performed by searching against the NCBInr database.

### 6.2.6 Transcriptomic Analysis

To support reliable information for the construction of *de-novo* amino acid sequence tags of proteins of interest of the AC and AT strains that being studied, a transcriptome database constructed commercially with a strain of *A. catenella* was obtained. This strain (CS-300) has a more than 97% homology with the *A. catenella* strains in this study (Appendix B1). Construction of the transcriptome database of CS-300 was performed by BGI and commissioned by my Chief Supervisor. I was involved in sample preparation of the transcriptome. RNA was isolated from cells in the exponential phase (Day 18) of the culture by treatment with Trizol (Roche, Switzerland). After homogenization of the dinoflagellates in Trizol, pure RNA was harvested by centrifugation before being sent for sequencing. cDNA library was constructed from the mRNA

and sequencing were performed with HiSeq 2000 (illumina, USA). The transcriptome database was constructed by BGI before being installed into our SQL database in-house. Because the database was commissioned by my supervisor, I was able to use that for protein identification. Statistics of assembly and annotation was listed in the Appendix B2 and B3. MS/MS sequence tags of proteins of interest which have no significant match from the NCBInr database in the public domain, were allowed to search against the transcriptomes database.

## 6.3 Results and Discussion

Two sets of proteomic comparison were performed: (a) AC-T against AC-N and (b) AC-T with and without phosphate-stress. Before the authentic proteomic comparison, preliminary experiments had to be performed to find optimal conditions for running 2DE with the dinoflagellates samples being studied. Two factors are of important considerations: (1) resolution and (2) numbers of observed spots in the 2D gel. Proteins were separated by their isoelectric point (pI) and molecular weight (MW) in 2-DE. By adjusting suitable ranges of pIs and MW for examination, analysis of differential proteins could be facilitated. Figure 6.1 showed the 2D gel of AC-T with a pH range of 3-10. Nearly all proteins were located in the middle part (pH 4-7) of the 2D gel. Such results had been reported by literature that proteins of dinoflagellates were mostly located within this range of pI (Chan et al., 2005; Chan et al., 2004). pH range 4-7 were then chosen for 2-DE analysis. Further, Figure 6.2 showed the 2D profiles of AC-T with difference percentages of acrylamide used in the second dimension of 2DE. 10%, 12% and 15% of acrylamide were tried and it was found that most proteins were located within the range of 15-120 kDa. 10% polyacrylamide gel was not chosen for 2-DE analysis as proteins below 20 kDa were not seen in the profile. Further, comparing protein expression profiles as analyzed by 12% gel and 15% gel, it was found that 12% polyacrylamide gel gave better resolution. Hence, 2-DE analyses described in this thesis thereafter were performed with a pH range of 4-7 and with 12% polyacrylamide gel.

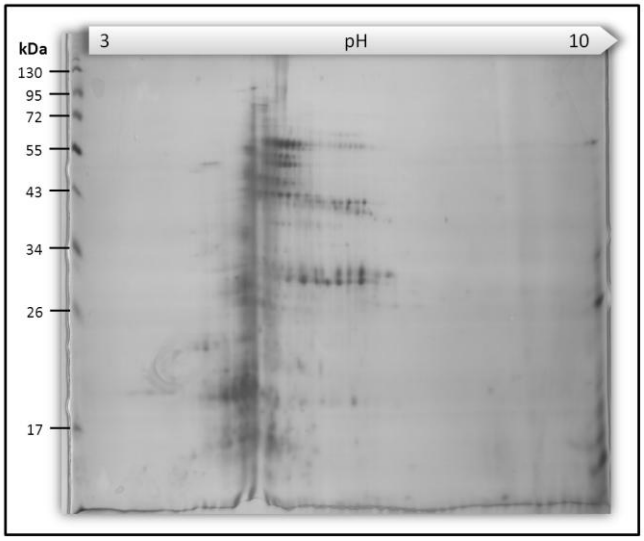


**Figure 6.1.** 2-DE protein expression profiles of AC-T over pH range of 3-10. Most of the proteins were located in the middle part of pH range 4-7.

**Figure 6.2.** 2-DE protein expression profiles of AC-T over pH range of 4-7 with the 2nd dimension performed with 10%, 12% and 15% acrylamide gel. Most proteins were included in the molecular range of 10-120 kDa. All these proteins could be visualized in 12% gel with relatively good resolution, compared to 15% gel.

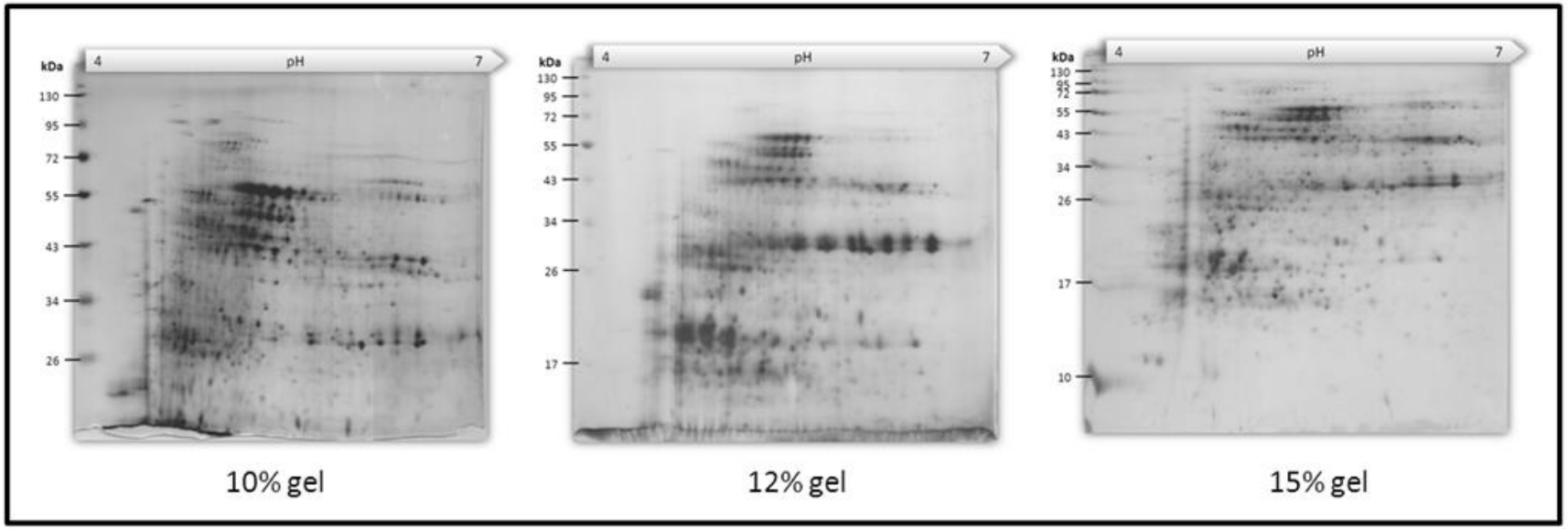

### 6.3.1 Differential Protein Expressions Between Toxic AC-T and Non-toxic AC-N

In order to examine the difference in protein expression between the toxic and non-toxic *A. catenella*, 2-DE was performed on cells in the exponential phase (Day 18) of AC-T and AC-N. 2-DE of the dinoflagellates studied at the same exponential growth phase was performed in triplicates with the same protocol. Same amount of proteins (120 μg) were loaded onto each 2D gel. Gel images were scanned into computer and analyzed by computer software Melanie 3. Difference of the intensities of silver staining of each gel was normalized with standard markers. Matching of spots between the two groups were performed by the software and arbitrarily double checked. Over 300 matched spots of proteins were found among the gels. 65 spots of proteins were found to be differentially expressed with at least 2 folds of difference between AC-T and AC-N. Of the 65 differentially expressed protein spots, 44 were found to have higher expression in AC-T and the other 21 were found to have higher expression in AC-N. Table 6.1 and 6.2 shows the pI, molecular weight and the fold of change of each differential spot. Corresponding position and the quantity of each spots were illustrated in Figure 6.3-6.5.

**Table 6.1.** Upregulated proteins found in AC-T (with ≥2-fold changes) when compared to AC-N.

| Spot | Isoelectric point (pI) | Molecular weight (kDA) | Folds of change |
|---|---|---|---|
| 27 | 5.4 | 60 | 5.2 |
| 28 | 5.4 | 60 | 5.2 |
| 31 | 5.5 | 60 | 4.7 |
| 32 | 5.6 | 60 | 4.1 |
| 33 | 5.7 | 60 | 3.2 |
| 38 | 6.6 | 60 | 5.9 |
| 54 | 5.4 | 55 | 2.5 |
| 62 | 5.3 | 50 | 2.8 |
| 63 | 5.4 | 50 | 2.2 |
| 65 | 5.5 | 50 | 2.2 |
| 68 | 5.6 | 50 | 2.2 |
| 73 | 5.0 | 48 | > 100^ |
| 78 | 5.3 | 47 | 3.0 |
| 96 | 5.3 | 43 | 5.5 |
| 97 | 5.4 | 43 | 4.5 |
| 98 | 5.5 | 43 | 2.9 |
| 104 | 6.5 | 43 | 7.9 |
| 105 | 6.6 | 43 | 7.7 |
| 108 | 6.4 | 43 | 6.1 |
| 117 | 6.4 | 42 | 4.7 |
| 118 | 6.6 | 42 | 7.0 |
| 123 | 6.7 | 42 | 8.2 |
| 125 | 6.4 | 42 | 6.9 |
| 126 | 6.9 | 42 | 22.6 |
| 170 | 6.8 | 30 | 2.8 |
| 173 | 6.6 | 30 | 3.2 |
| 174 | 6.9 | 30 | 8.7 |
| 175 | 6.5 | 30 | 3.0 |
| 177 | 6.0 | 30 | 3.0 |
| 183 | 5.7 | 28 | 7.2 |
| 188 | 6.0 | 28 | 3.1 |
| 189 | 6.0 | 28 | 4.1 |
| 190 | 6.8 | 29 | 2.4 |
| 191 | 5.8 | 29 | 2.4 |
| 193 | 6.5 | 29 | 2.7 |
| 251 | 6.1 | 20 | 5.0 |
| 257 | 5.0 | 19 | 2.4 |
| 266 | 5.0 | 19 | 2.0 |
| 267 | 4.1 | 19 | 7.3 |
| 271 | 5.1 | 18 | 3.1 |
| 296 | 4.9 | 16 | 2.1 |
| 300 | 5.1 | 16 | 2.2 |
| 303 | 5.2 | 16 | 4.0 |
| 309 | 5.9 | 17 | 9.9 |

^ The spot of protein was not detectable in AC-N

**Table 6.2.** Downregulated proteins found in AC-T (with ≥2-fold changes) when compared to AC-N.

| Spot | Isoelectric point (pI) | Molecular weight (kDA) | Folds of change |
|---|---|---|---|
| 10 | 5.2 | 80 | 6.1 |
| 11 | 5.2 | 80 | 4.3 |
| 12 | 5.3 | 80 | 4.2 |
| 14 | 5.2 | 78 | 6.5 |
| 15 | 5.3 | 78 | 7.7 |
| 16 | 4.9 | 72 | > 100[#] |
| 17 | 4.9 | 72 | > 100[#] |
| 18 | 5.0 | 72 | > 100[#] |
| 19 | 5.0 | 72 | > 100[#] |
| 20 | 4.9 | 70 | > 100[#] |
| 21 | 5.0 | 70 | > 100[#] |
| 22 | 5.0 | 70 | > 100[#] |
| 85 | 4.6 | 50 | > 100[#] |
| 86 | 4.6 | 50 | > 100[#] |
| 87 | 4.7 | 50 | > 100[#] |
| 131 | 4.0 | 40 | > 100[#] |
| 132 | 4.5 | 40 | > 100[#] |
| 133 | 4.3 | 40 | > 100[#] |
| 134 | 4.4 | 40 | > 100[#] |
| 137 | 4.5 | 40 | > 100[#] |
| 249 | 5.7 | 21 | 2.6 |

[#] The spot of protein was not detectable in AC-T

**Figure 6.3.** Representative 2-DE gel of protein extracts of exponential culture of AC-T (left) and AC-N (right). Circled regions are where many proteins were found to be differentially expressed between the two strains.

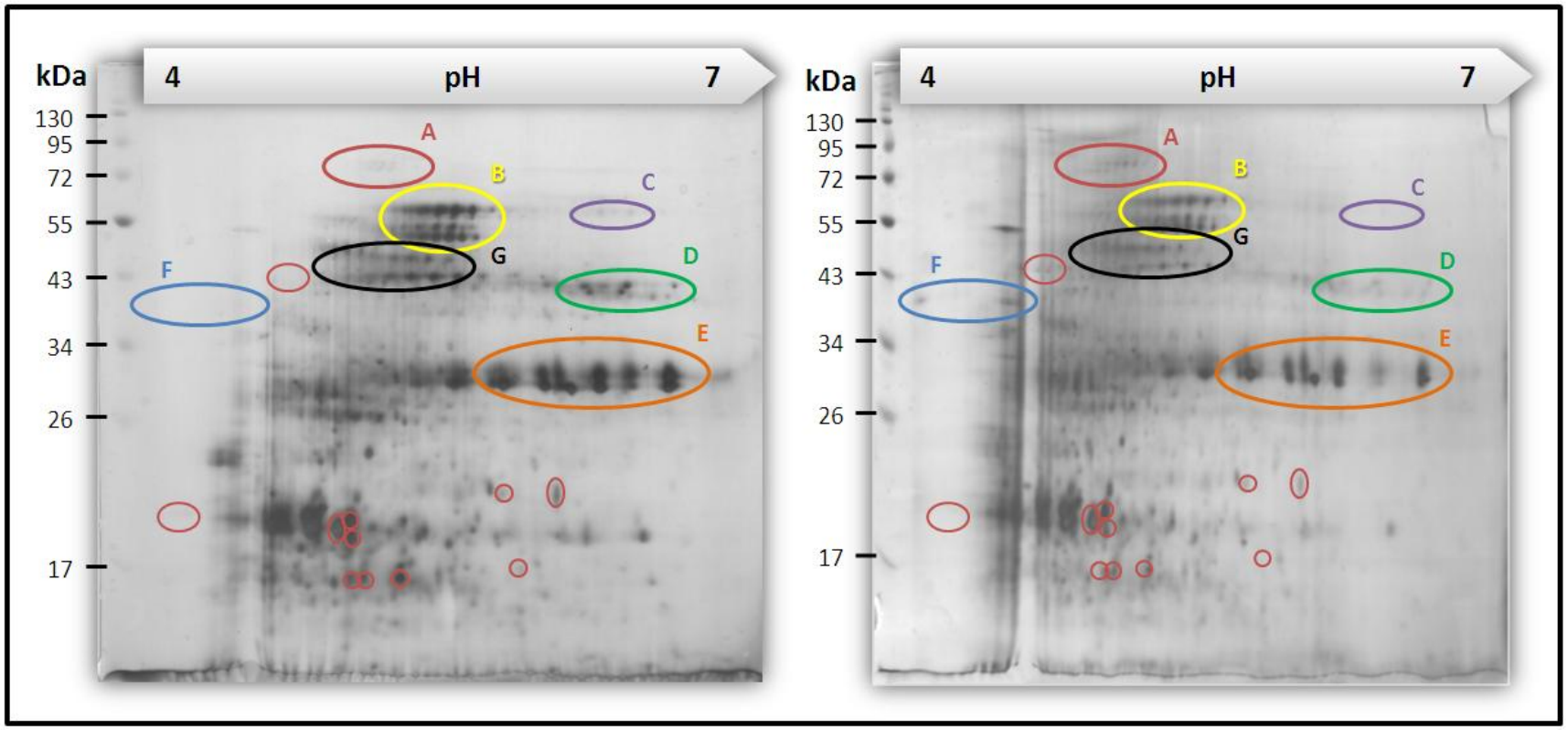

**Figure 6.4.** Enlarged images of region A-E in Figure 6.3. For regions A to D, the left penal is results of the AC-T strain while the right panel is that of AC-N. For region E, the upper penal is for AC-T while the lower penal is for AC-N.

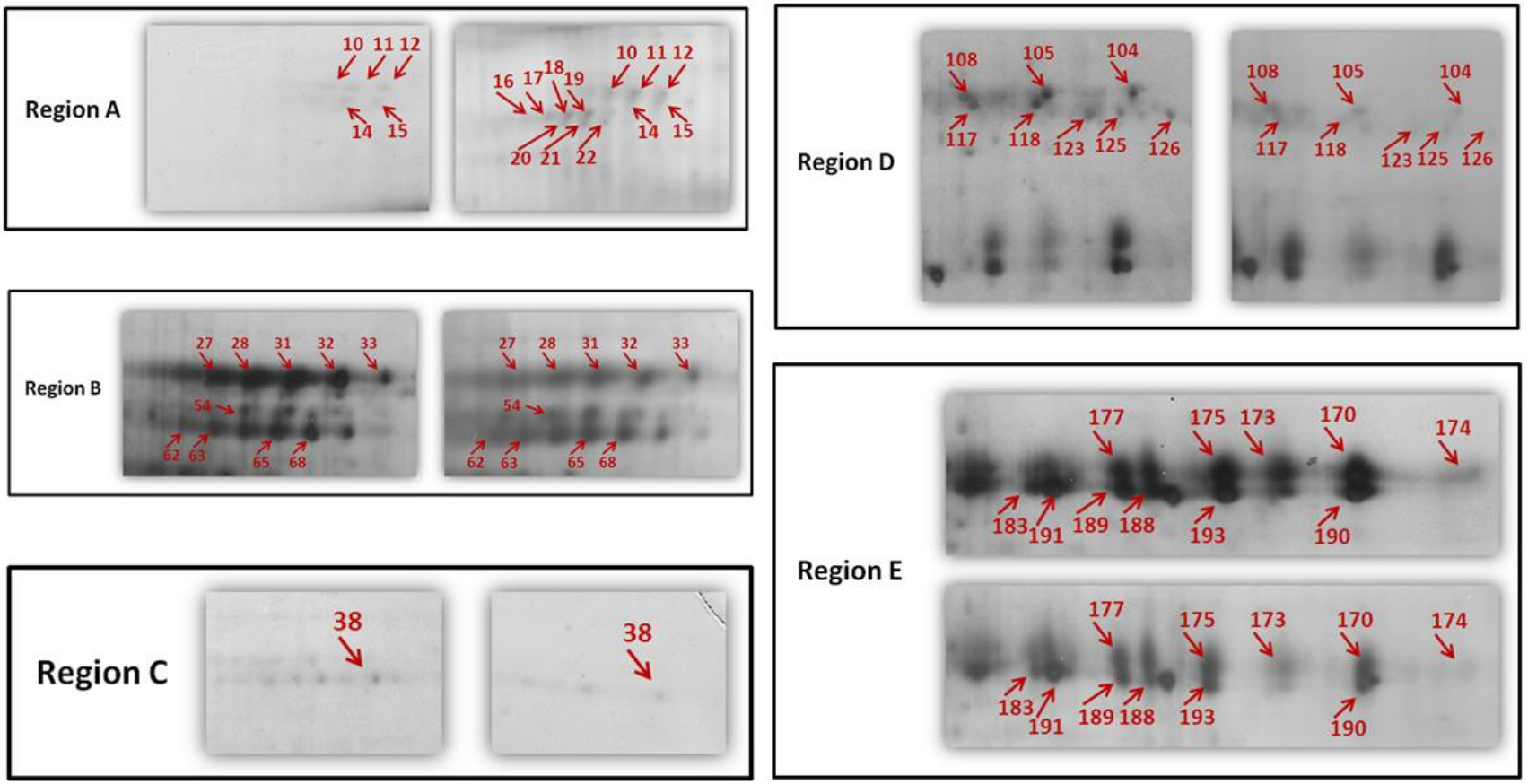

**Figure 6.5.** Enlarged images of region F, G and other circled regions in Figure 6.3. The left panel is results of the AC-T strain while the right panel is that of AC-N.

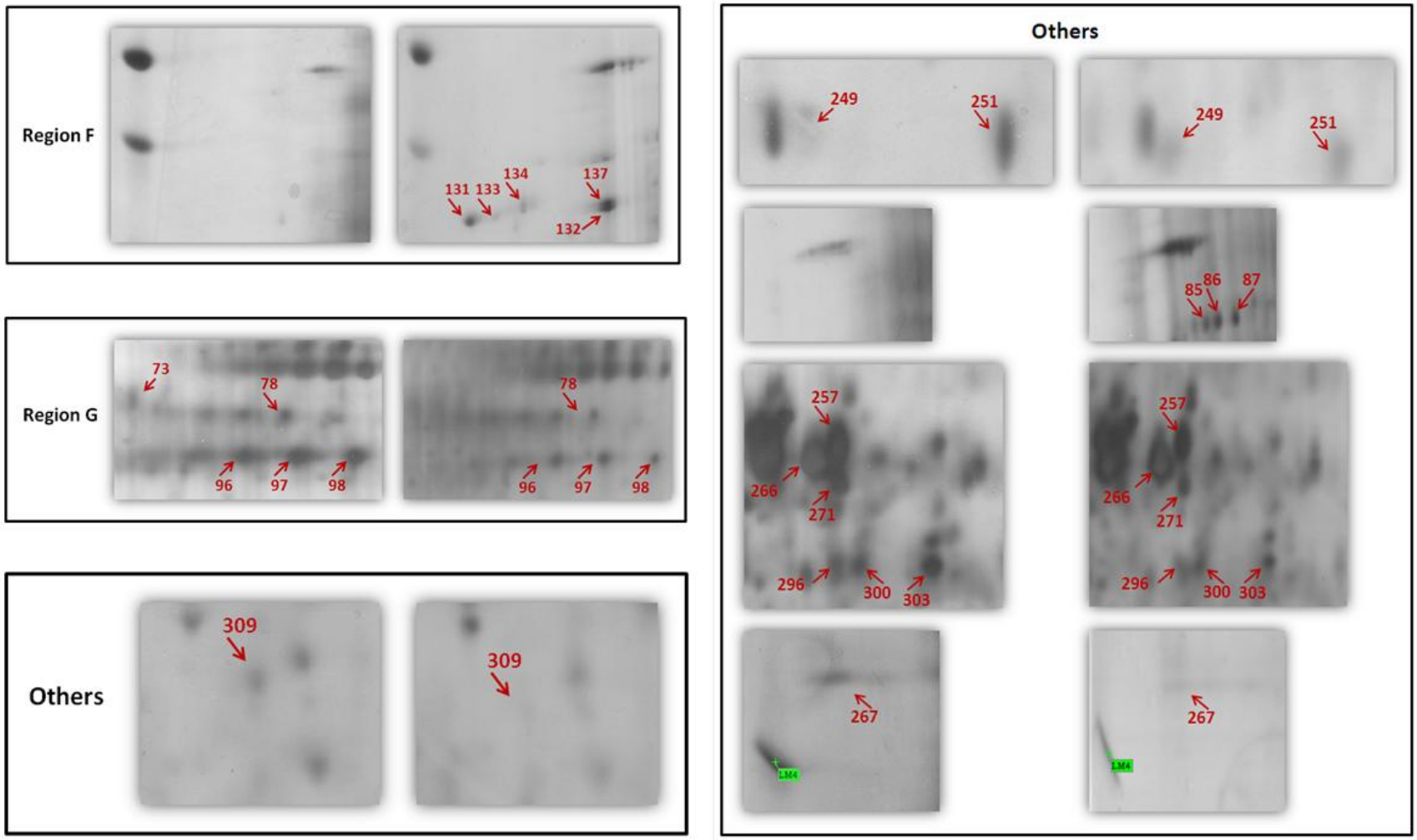

### 6.3.2 Differentially Protein Expressions of *A. catenella* (AC-T) Under Phosphate Limitation

As said earlier, results from the previous chapter showed that when AC-T was grown under phosphate limitation, cellular toxin content was significantly increased four times. Cultures of AC-T under phosphate limitation were harvested at Day 18. 2-DE analysis of these protein extracts were performed as previously mentioned. 22 spots were found to be differentially expressed with at least 2-folds changes. All of these 22 proteins spots were down-regulated proteins found in AC-T with phosphate limitation. Figure 6.6-6.7 showed the corresponding position and the quantity of the differentially expressed protein spots. The pIs, molecular weights and the folds of change were listed in Table 6.3.

**Figure 6.6.** Representative 2-DE gels of protein extracts of normal culture (left) and $PO_4$-limited culture (right) of AC-T. Circled spots are the proteins found to be differentially expressed between the two strains.

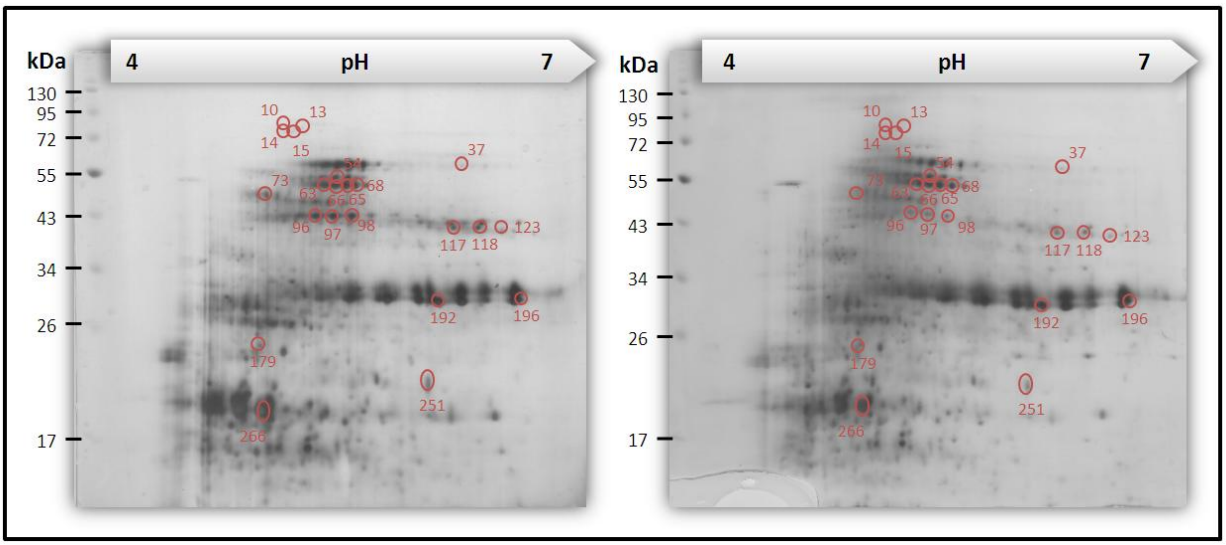

**Figure 6.7.** Enlarged images circled regions in Figure 6.6. Left penal is for normal culture (AC-T) and right penal is for phosphate limitation.

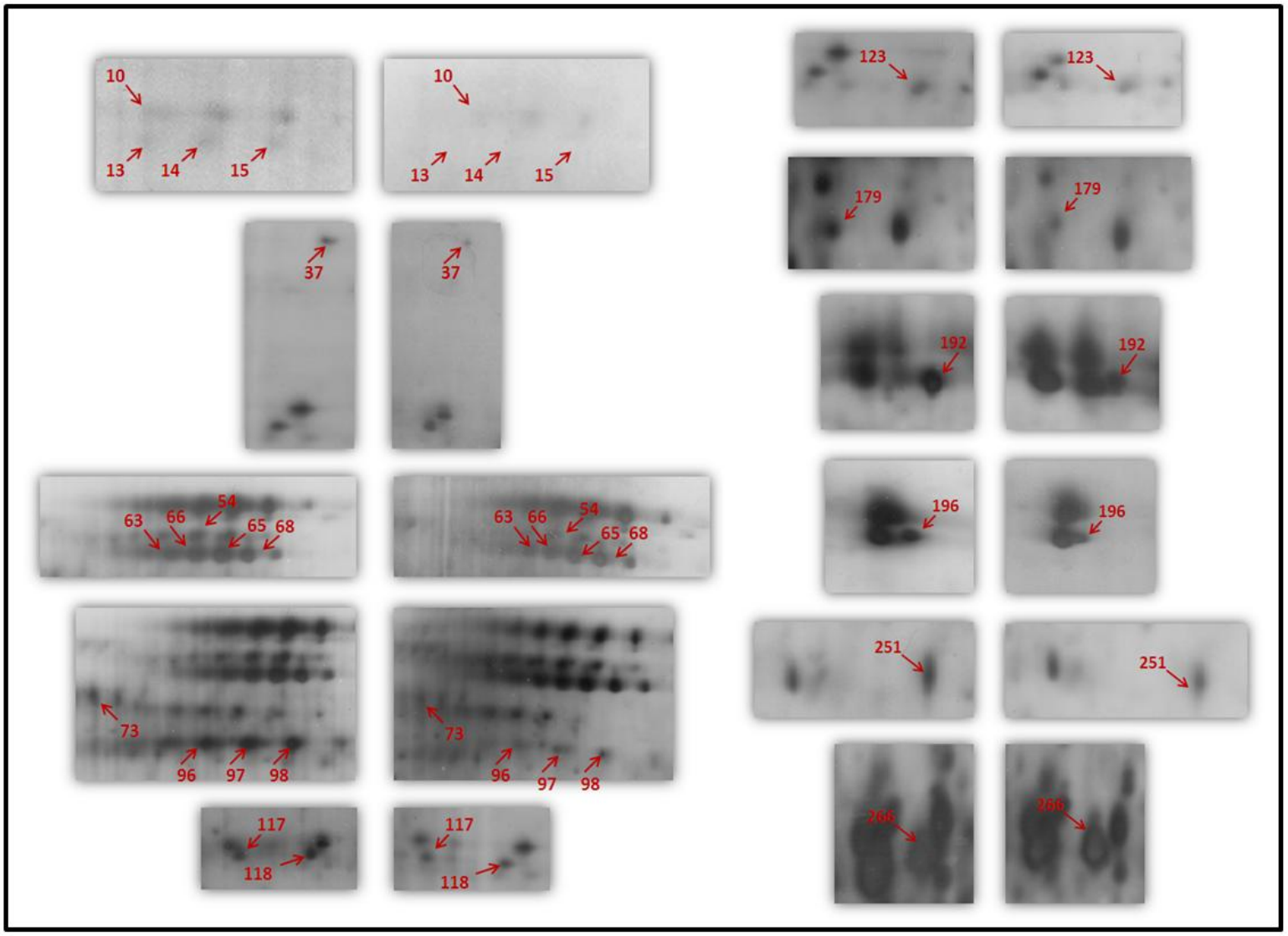

**Table 6.3.** Differentially expressed proteins (with ≥2-fold changes) of AC-T under phosphate limitation.

| Spot | Isoelectric point (pI) | Molecular weight (kDA) | Protein expression level* | Folds of change |
|---|---|---|---|---|
| 10 | 5.2 | 80 | ↓ | 3.7 |
| 13 | 5.2 | 78 | ↓ | 4.2 |
| 14 | 5.2 | 78 | ↓ | 2.5 |
| 15 | 5.3 | 78 | ↓ | 7.2 |
| 37 | 6.4 | 60 | ↓ | 7.0 |
| 54 | 5.4 | 55 | ↓ | 3.7 |
| 63 | 5.4 | 50 | ↓ | 5.9 |
| 65 | 5.5 | 50 | ↓ | 2.1 |
| 66 | 5.5 | 50 | ↓ | 2.0 |
| 68 | 5.6 | 50 | ↓ | 2.0 |
| 73 | 5 | 50 | ↓ | 3.7 |
| 96 | 5.4 | 43 | ↓ | 7.3 |
| 97 | 5.5 | 43 | ↓ | 7.7 |
| 98 | 5.6 | 43 | ↓ | 6.1 |
| 117 | 6.4 | 42 | ↓ | 3.0 |
| 118 | 6.6 | 42 | ↓ | 2.9 |
| 123 | 6.7 | 42 | ↓ | 2.4 |
| 179 | 5.0 | 24 | ↓ | 2.5 |
| 192 | 6.3 | 28 | ↓ | 4.2 |
| 196 | 6.8 | 29 | ↓ | 3.5 |
| 251 | 6.1 | 20 | ↓ | 3.2 |
| 266 | 5.0 | 19 | ↓ | 2.2 |

* Expressed levels of spots in cells with $PO_4$ limitation (Expression in AC-T is the reference).

↓ = Expressed level is down-regulated under phosphate limitation

From Tables 6.1-6.3, there are 16 protein spots that were differentially expressed in both comparisons. These results are summarized in Figure 6.8. Further, 3 of these 16 spots (#10, #14, #15) were also down-regulated in AC-T cells when compared to AC-N cells (Table 6.2). More importantly, as all of the differentially expressed proteins between AC-T cells with and without phosphate-limitation are down-regulated and the toxicity in phosphate-limited AC-T cell cultures was increased by about 4 times, it seems that the increased in toxicity is not due to increased enzyme activities in AC-T cells during phosphate-stress. In addition, as discussed earlier, because of the intrinsic deficit of 2DE analysis, some important proteins related to the PST-biosynthetic pathway may not go into the gel matrix and hence not being detected.

**Figure 6.8.** Summary of differentially expressed protein spots in proteomic (1) comparison between AC-T and AC-N; and (2) comparison between AC-T cells with and without $PO_4$-limiting conditions. There are 16 spots which showed differential expression in both cases.

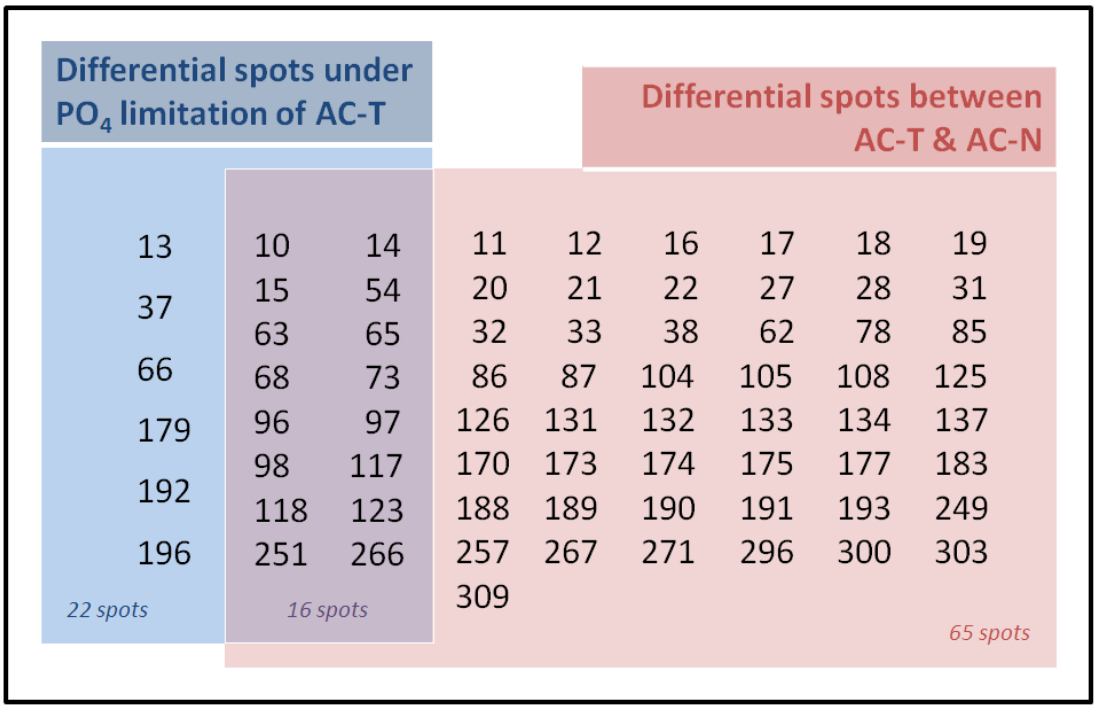

### 6.3.3 Identification of Differentially Expressed Proteins by MALDI-TOF-MS

Attempts to identify protein spots with significant differential expression as listed in Figure 6.8 were performed with MALDI-TOF-MS. Peptide mass fingerprints (PMFs) were generated for each spots after tryptic digestion before attempts to search against the NCBInr database with the aid of MASCOT. However, none of the spots could be identified. (Detailed results of PMFs of spots with sufficient materials were presented in Appendix B.) There are several reasons that no significant hit from the database could be obtained. Firstly, there is neither whole genome DNA database nor protein database for the genus *Alexandrium* or even for dinoflagellates. The principle of protein identification with PMF is to compare masses of the spectral peaks of the peptides experimentally generated with that of the peptides generated by *in-silico* digestion of proteins/DNA from the sequence databases (Song et al., 2007). Without an established whole genome or protein database for dinoflagellates, data available for searching is limited to those DNA sequences and protein sequences already submitted to public domain. Another possible reason is that for the proteins carrying the same function, the sequence of that protein in dinoflagellates may not have sufficient homology to be recognized.

Since protein identification purely with PMF generated was not successful, attempt to obtain amino acid sequence tags with MALDI-MS/MS was made. Abundant peptides peaks of each PMF were selected for MS/MS analysis in order to obtain the amino acid sequences to help the identification process. In addition, in order to promote the generation of y-type ions in the MS/MS spectrum and free from much interference from ions of other series, MALDI-MS/MS was performed with sulfonation. When sulfonation was successfully performed, sequences of the selected peptides could be deduced from the mass difference between the ion peaks in the MS/MS spectra using the Biotools 3.2 software (Bruker, USA). Mass tolerance for deduction was set to ± 0.3 Da. A minimum amino acid sequence tag with 7 successive amino acids would allow MASCOT search against the NCBInr database. Because of the comparatively modest sensitivity of the MALDI-TOF-TOF (Autoflex III, Bruker, USA) in our laboratory, a strongly coomassie blue stained gel plug is needed for the MALDI-MS/MS analysis. Hence, protein spots #10-22, #174, #249, #267, #309 which did not have sufficient protein material, were not selected for MALDI-MS/MS analysis. Detailed results of MASCOT search results with significant protein hits and

sequence coverage were presented in Appendix B. Five proteins were identified with the sequence tags generated from the MS/MS Spectra. The first one is spot 38, which is up-regulated in AC-T, to about 6 folds of AC-N. From the PMF of spot 38, peptide 1458.874 m/z was selected for sulfonation and the corresponding peptide ion in the sulfonated PMF was 1673.597 m/z (Figure 6.9). Fragment ions were obtained in the MS/MS spectrum. Amino acid residues were deduced from the analysis of the mass difference between the fragment ions. Since amino acid residue isoleucine (I) and leucine (L) have the same molecular mass (113.17 g/mol), analysis from MS/MS spectrum could not differentiate them. Such mass difference (± 0.3 Da mass tolerance) will be expressed as [I/L]. Sequence tag F[I/L][I/L]NPQGDAG[I/L]TGR was deduced (Figure 6.10). Two proteins were reported to have matched significantly to the sequence submitted in the MASCOT bioinformatic search. Both were methionine adenosyltransferase, with one of them isolated from *Nucula proxima* (Accession no.: gi|46909371) with sequence FIINPQGDAGLTGR and the other from *Danio rerio* (Accession no.: gi|94536641) with sequence FLLNPQGDAGLTGR.

**Figure 6.9.** PMFs of spot #38: (a) with sulfonation and (b) without sulfonation. Peptide ion 1458.847 m/z was successfully sulfonated to 1673.597 m/z with an increased mass of 215 Da.

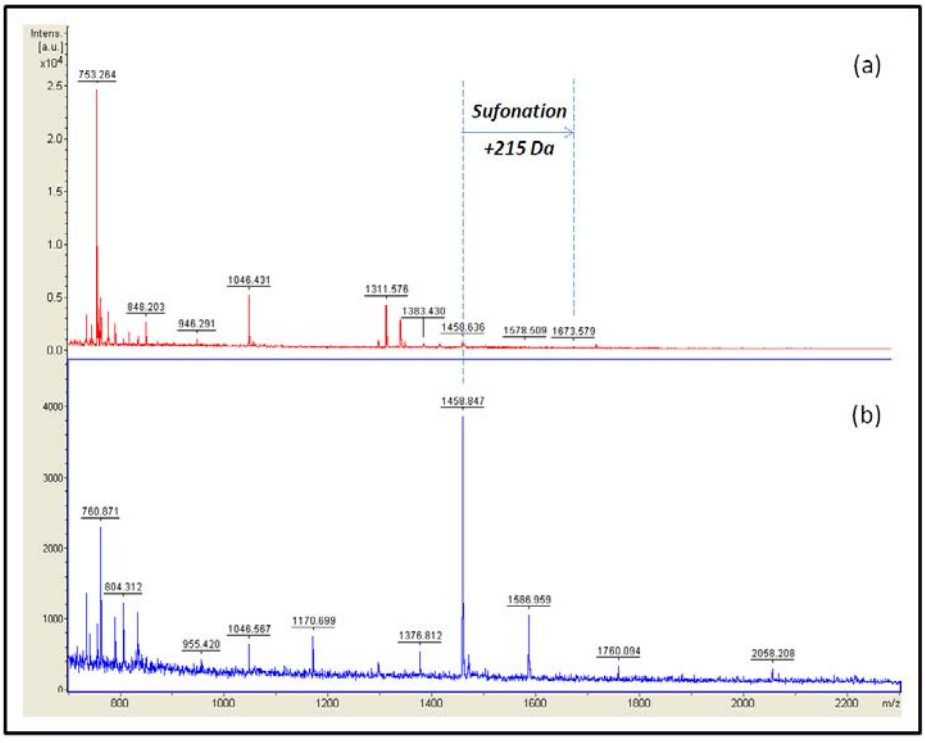

**Figure 6.10.** MS/MS spectrum of sulfonated peptide ion 1673.597 m/z of spot #38. Peptide 1458.4 m/z was the native peptide ion. Amino acid sequence F[I/L][I/L]NPQGDAG[I/L]TGR was deduced by the mass differences between the adjacent peaks of y-ions with mass tolerance of ± 0.3 Da. Amino acid isoleucine (I) and leucine (L) have the same molecular mass (113.17 g/mol) and the gaps of such mass difference in the spectrum was expressed as [I/L].

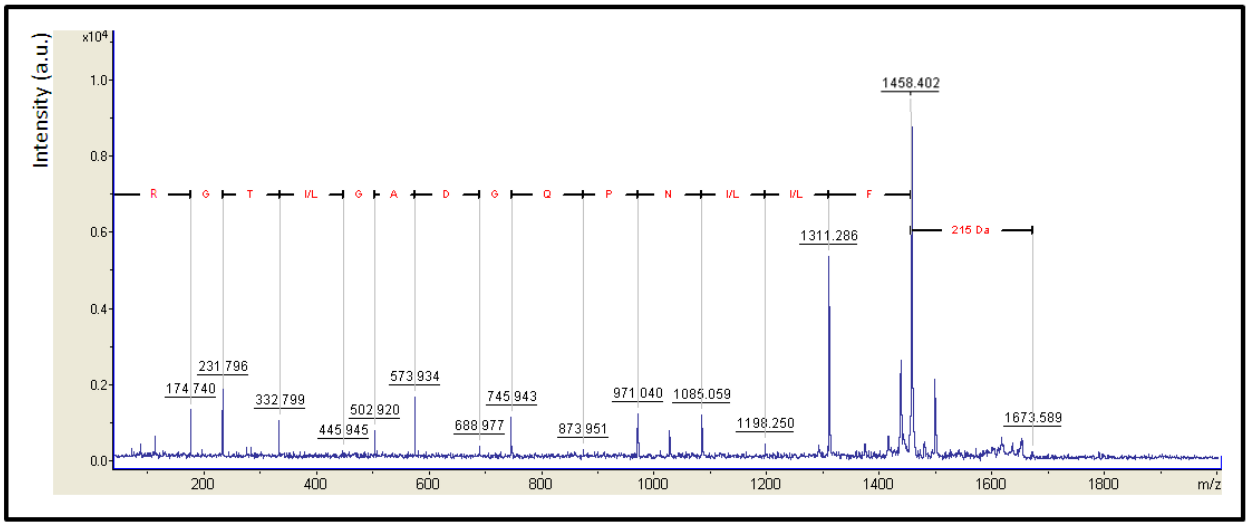


Another protein that could be successfully identified was spot #104, which is also up-regulated 8 folds in AC-T (as compared to AC-N). Peptide 1557.862 m/z and 1788.875 m/z were analyzed by MS/MS and the sequence tags found were VSVVD[I/L]T and SWYDNEWGYSNR respectively (Figure 6.11). With MASCOT bioinformatic searches, two significant hits were found for the former sequence tag and another two significant hits were found for the later one. All of them were reported to be glyceraldehyde-3 phosphate dehydrogenase. The accession numbers were gi|1151182 and gi|56188 (for VSVVDLT) and gi|5219 and gi|32454979 (for SWYDNEWGYSNR) respectively. When both sequences were submitted together as parts of one protein, the protein was identified as glyceraldehyde-3 phosphate dehydrogenase.

Spot #257 was also identified by the same strategy. It was found to be upregulated in AC-T and was about 2.4 folds that of AC-N. Peptide 957.474 m/z were sulfonated to 1172.464 m/z (Figure 6.12). Sequence tag [I/L]DAE[I/L]A[I/L]GR was obtained (Figure 6.13). The only significant hit by MASCOT searching was putative transcriptional regulator (IDAELALGR) that was discovered in *Frankia alni* with accession number gi|111223593.

**Figure 6.11.** (a) MS/MS spectrum of peptide 1557.862 m/z of spot #104. Sequence VSVVD[I/L]T was deduced from the y-ions with mass tolerance of ± 0.3 Da. (b) PMF of spot #104 in which peptide 1557.862 m/z (green circle) and 1788.875 m/z (red circle) were analyzed further by MS/MS. (c) MS/MS spectrum of peptide 1788.875 m/z of spot #104. Sequence SWYDNEWGYSNR was deduced from the y-ions with mass tolerance of ± 0.3 Da.

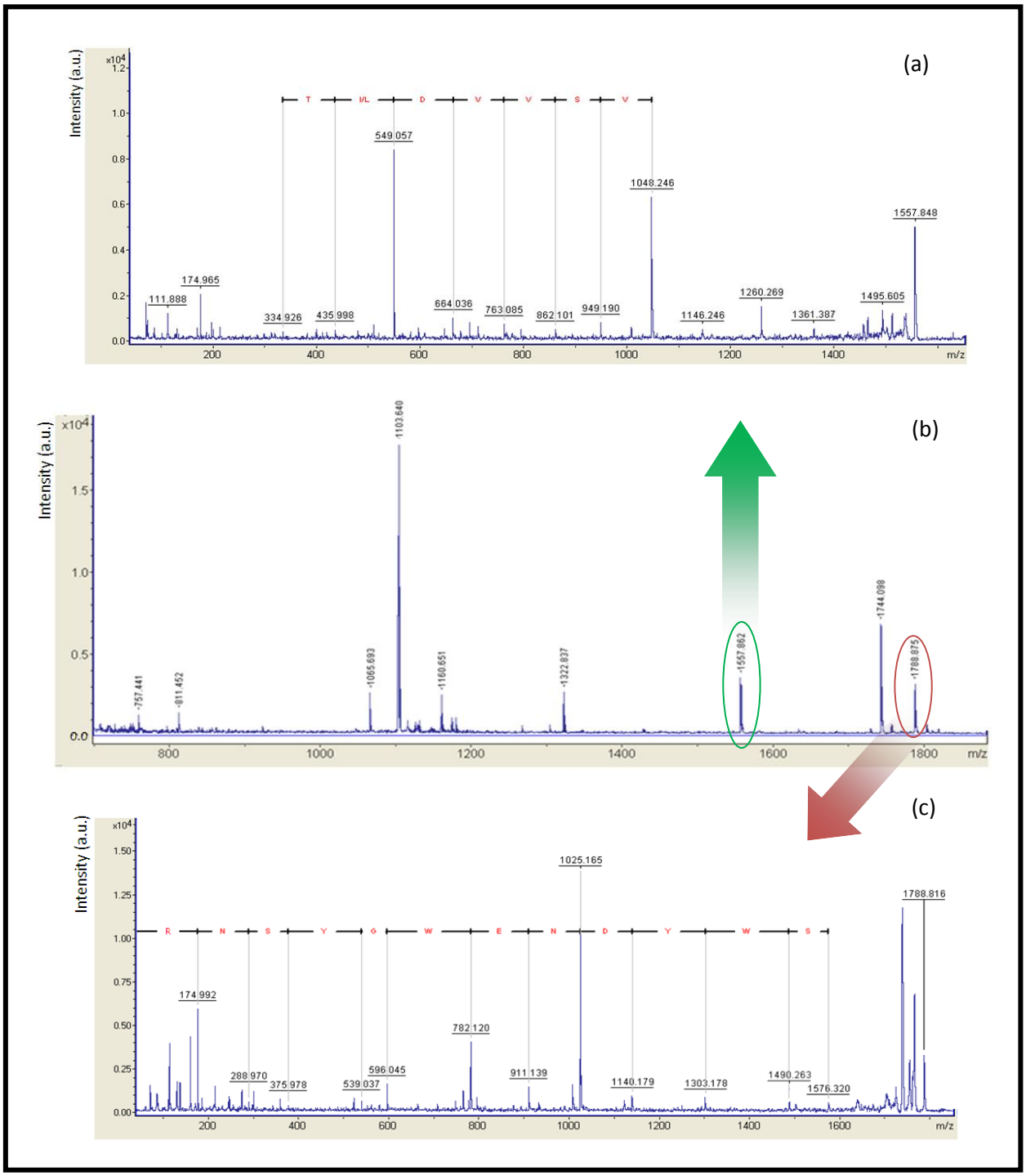

**Figure 6.12.** PMFs of spot #257 (a) with sulfonation and (b) without sulfonation. Peptide ion 957.474 m/z was successfully sulfonated to 1172.464 m/z with an increased mass of 215 Da.

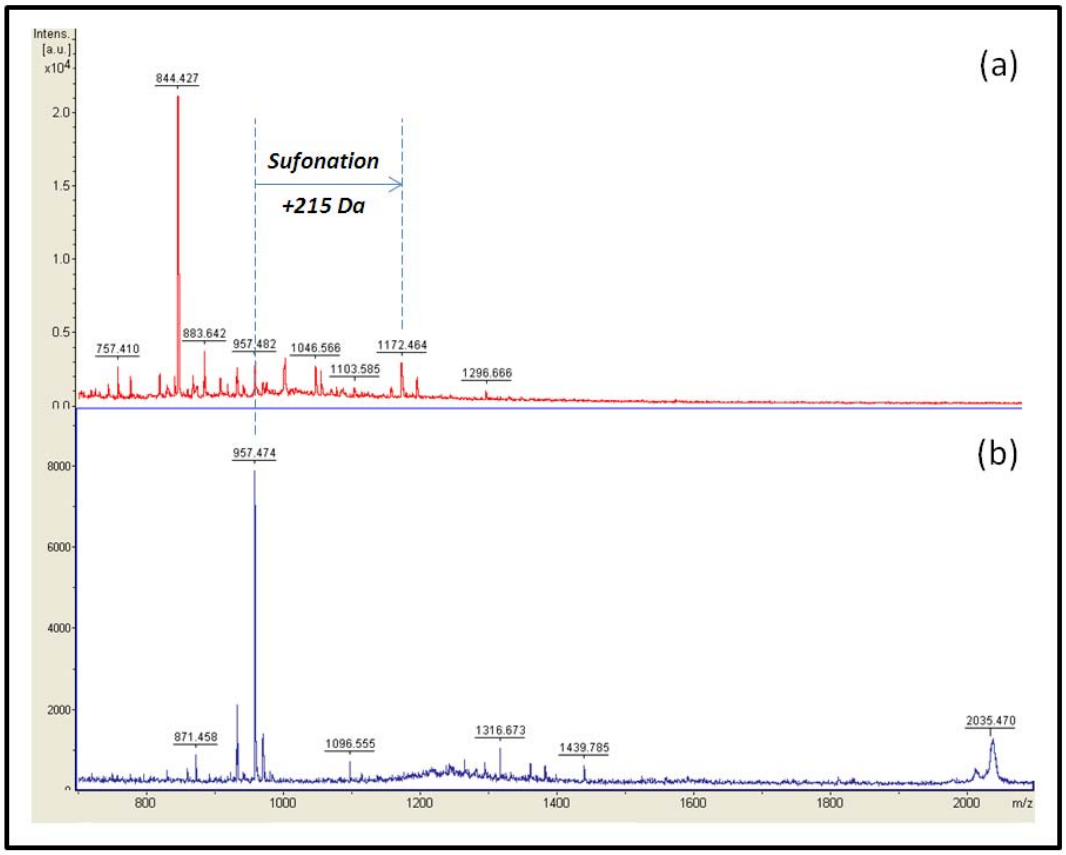


**Figure 6.13.** MS/MS spectrum of sulfonated peptide ion 1172.464 m/z of spot #257. Peptide 957.232 m/z was the native peptide ion. Amino acid sequence [I/L]DAE[I/L]A[I/L]GR was deduced from the y-ions with mass tolerance of ± 0.3 Da.

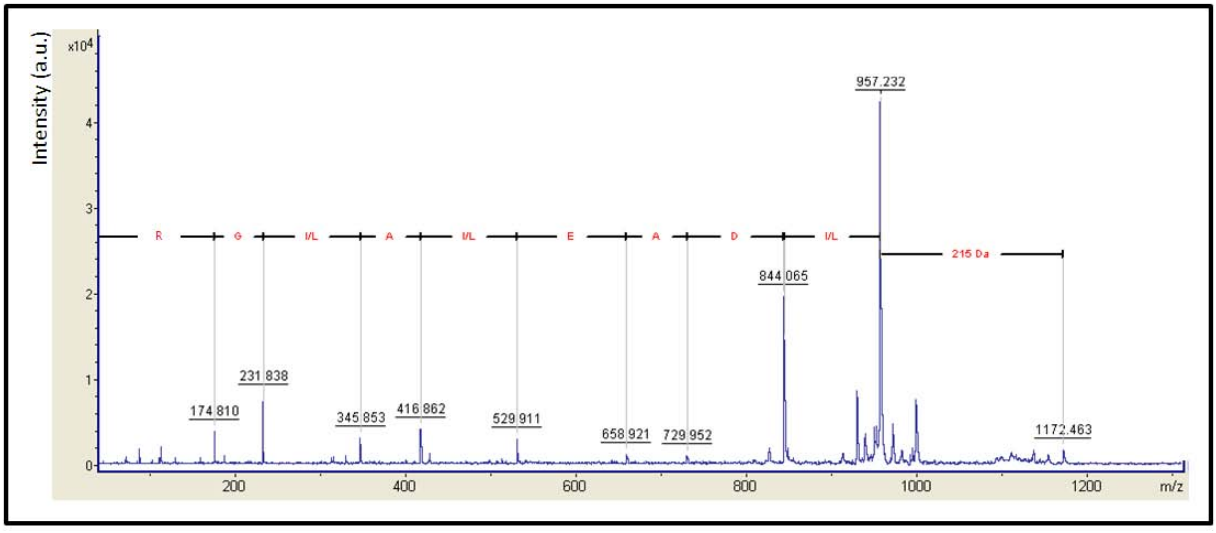

Beside using the MASCOT search engine, protein identification was also performed with the "protein blast" (Basic Local Alignment Search Tool) option provided by the National Centre for Biotechnology Information (NCBI). Protein sequences submitted would be regarded as successfully identified if a significant score (E value<0.05) which proteins in the database is achieved. Spot #27 was successfully identified through this system. It was shown to have 5-fold higher expression level in the AC-T than the AC-N. Peptide 1000.328 m/z was sulfonated and the peptide 1215.692 m/z gives the sequence QF[I/L]HYHR (Figure 6.14). Another sequence GHGAVTS came from the non-suulfonated peptide 1254.805 m/z (Figure 6.15). Using the protein blast system, all the exact matches with significant score to both sequences (QFLHYHR and GHGAVTS) were shown by ribulose 1,5-bisphosphate carboxylase/oxygenase II (Rubisco II) that come from *Prorocentrum minimum* (Accession no.: AAO13045.1, AAO13070.1, AAO13066.1 & AAO13077.1). Spots #28, #31, #32 and #33 were probably the isoforms of spot #27 as they share several major peaks in their PMFs and they were at neighboring positions on the 2D gel and hence were Rubisco II also (Figures 6.16 and 6.4).

**Figure 6.14.** MS/MS spectrum of sulfonated peptide ion 1215.692 m/z of spot #27. Peptide 1000.328 m/z was the native peptide ion. Amino acid sequence QF[I/L]HYHR was deduced from the y-ions with mass tolerance of ± 0.3 Da.

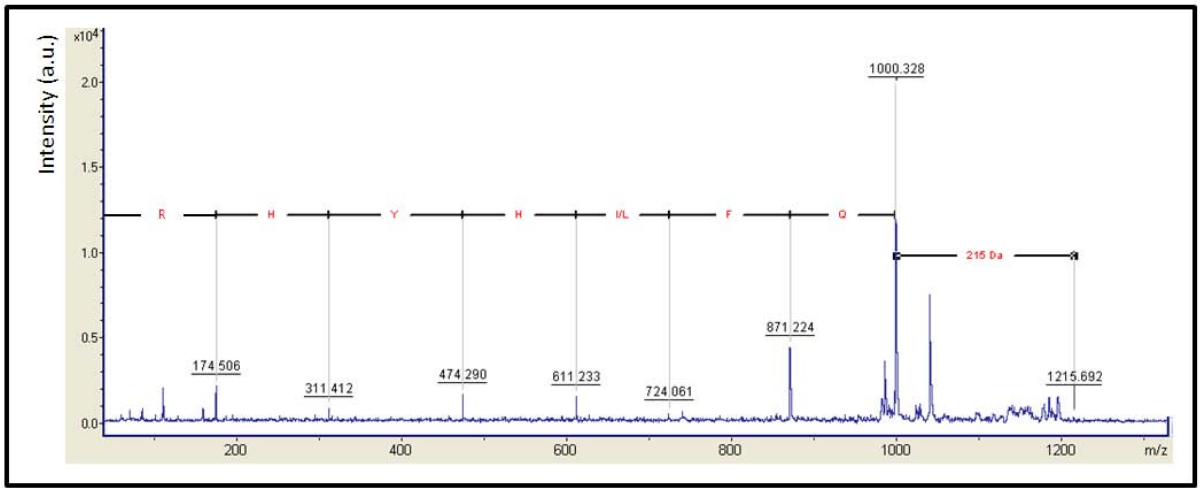

**Figure 6.15.** MS/MS spectrum of non-sulfonated peptide ion 1254.805 m/z of spot #27. Amino acid sequence GHGAVTS was deduced from the y-ions with mass tolerance of ± 0.3 Da.

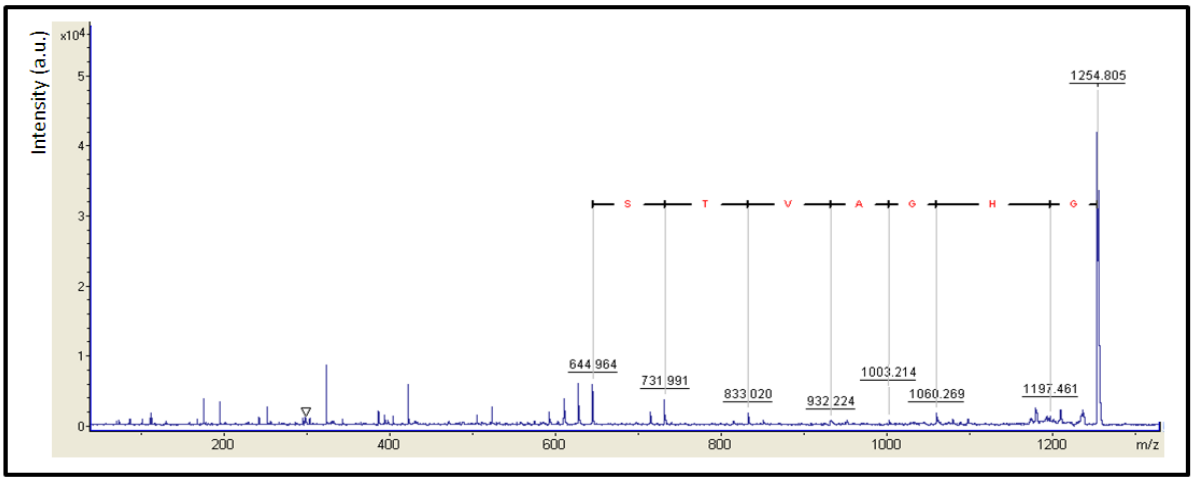


**Figure 6.16.** PMF spectra of spot (a)#27, (b)#28, (c)#31, (d)32 and (e)#33. Similar patterns were observed that some major peaks (highlighted regions) were conserved.

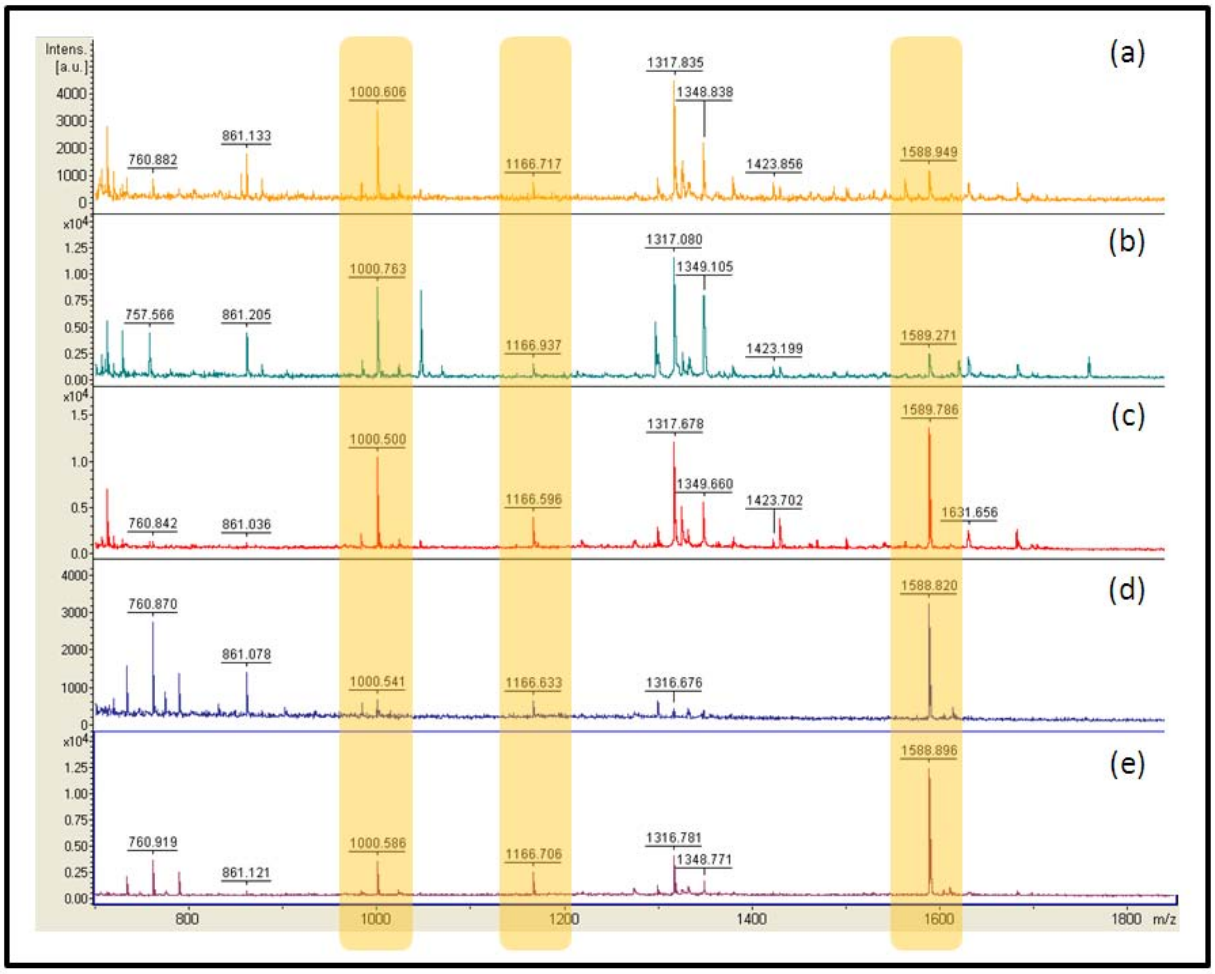

Spot #196 was also successfully identified with the blast function in the NCBI database. Spot #196 was down-regulated by 3.5 folds in phosphate limit culture of AC-T. The peptide 1813.884 m/z was selected for MS/MS analysis. Sequence tag QYSQ[I/L]TYNQVR was found (Figure 6.17). 100% significant match was reported with protein plastid oxygen-evolving enhancer 1-2 precursor (QYSQLTYNQVR) found in *Alexandrium funyense* (Accession no.: ABO47876.1).

Protein spot #118 which was up-regulated in AC-T, compared to AC-N, was also found to be up-regulated in normal AC-T culture than in that with 100% phosphate. Sequence tag [I/L]G[I/L]NGFGR was deduced from the sulfonated peptide 1317.951 m/z (Figure 6.18) and it was reported to be glyceraldehyde-3 phosphate dehydrogenase (IGINGFGR) from *Pfiesteria piscicida* (Accession no.:ABI14256.1). It probably is the isoform of spot #104 as they have similar pI value and molecular weight.

**Figure 6.17.** MS/MS spectrum of non-sulfonated peptide ion 1813.884 m/z of spot #196. Amino acid sequence QYSQ[I/L]TYNQVR was deduced from the y-ions with mass tolerance of ± 0.3 Da.

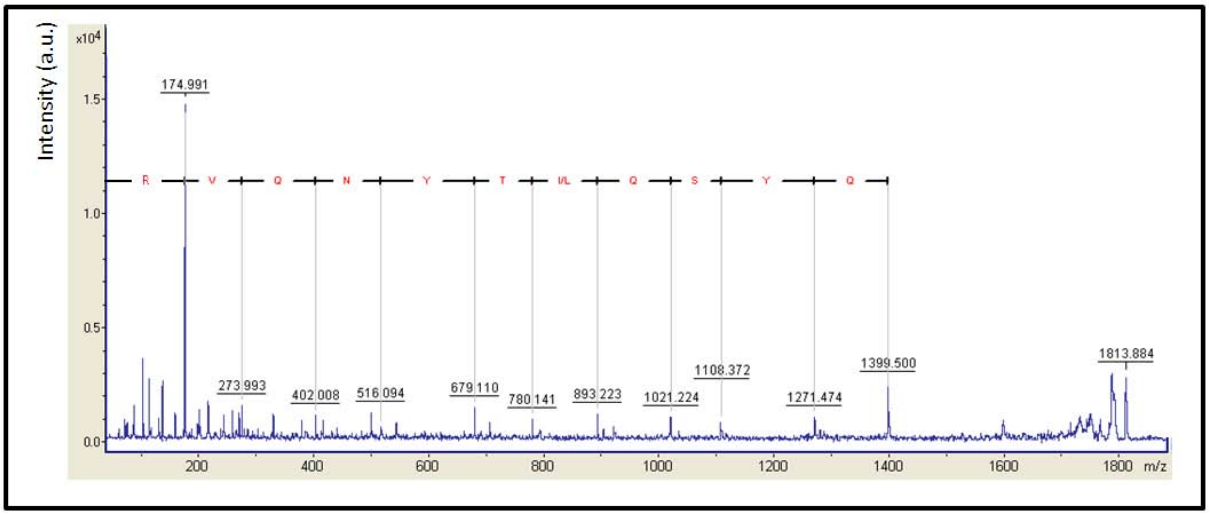

**Figure 6.18.** MS/MS spectrum of non-sulfonated peptide ion 1813.884 m/z of spot #118. Amino acid sequence [I/L]G[I/L]NGFGR was deduced from the y-ions with mass tolerance of ± 0.3 Da.

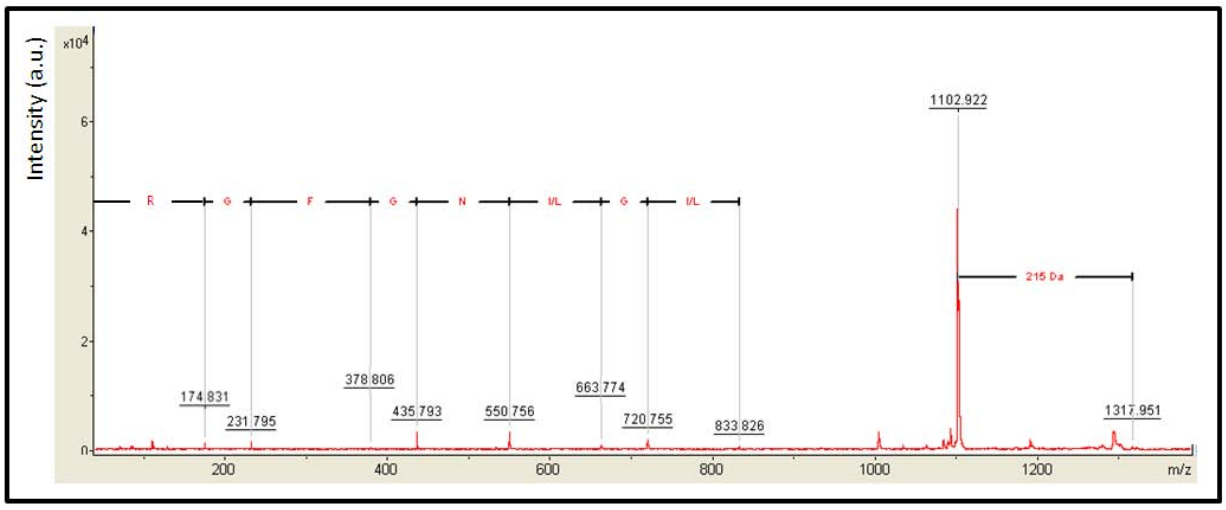


### 6.3.4 Identification of Differentially Expressed Proteins by LC-ESI-Ion-trap MS/MS

Due to the fact that only a small portion of the differentially expressed proteins were identified by the combination of PMF, MALDI-TOF MS/MS analysis as well as sulfonation, additional LC-ESI-ion-trap MS/MS was performed with the hope of more identification. Several additional proteins were identified. One of them is spot #96. It has a higher expression levels in AC-T than AC-N and is by 5.5 folds. On the other hand, it showed a down-regulation when AC-T was under phosphate-stress. Sequence tags TGIAINGFGR, IM*LDPTFVK, SGNIIPSST were obtained from the peptide 1076.585 m/z, 1207.639 m/z & 1344.712 m/z respectively (M* stands for oxidized methionine) (Figures 6.19-21). Most significant matches were shown by glyceraldehyde-3 phosphate dehydrogenase from *Gonyaulax polyedra* (Accession no.: gi|4103871), *Alexandrium catenella* (Accession no.: gi|117959253) and *Scrippsiella trochoidea* (gi|35210480). The three peptides and the corresponding sequence tags were also found from PMFs of spot #97 and spot #98. They are also glyceraldehyde-3 phosphate dehydrogenase.

**Figure 6.19.** Deduction of amino acid sequence tag from MS/MS spectrum of peptide 1076.585 m/z of spot #96 by Biotools 3.2. Successive amino acid sequence TGIAINGFGR was derived from y- and b-ions.

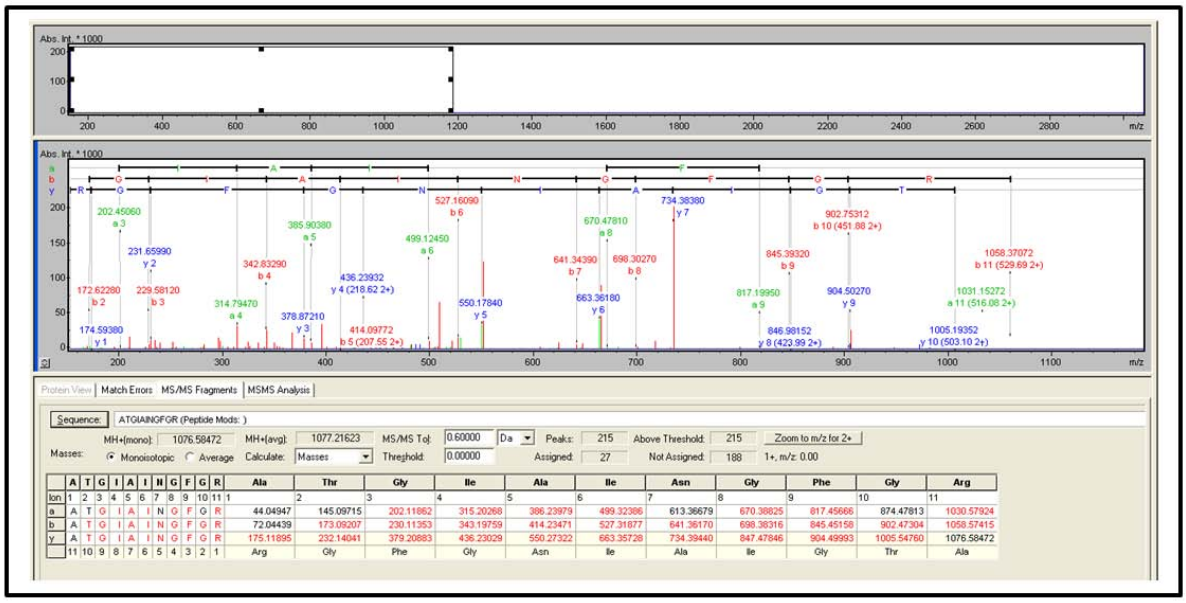

**Figure 6.20.** Deduction of amino acid sequence tag from MS/MS spectrum of peptide 1207.639 m/z of spot #96 by Biotools 3.2. Successive amino acid sequence IM*LDPTFVK was derived from y- and b-ions. (M*, oxidized methionine)

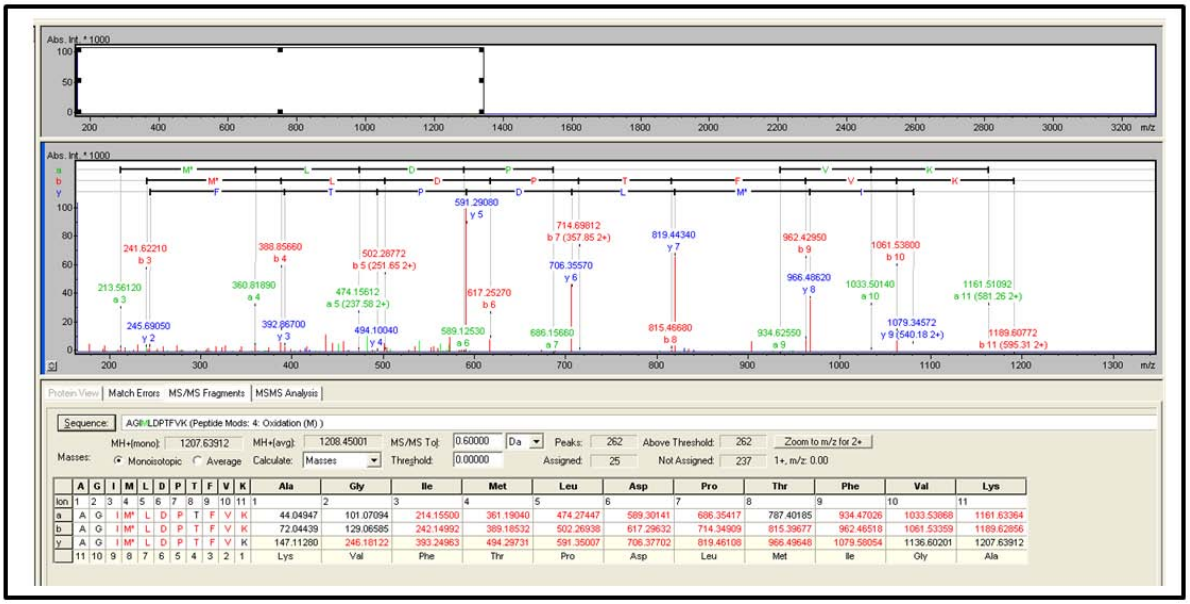

**Figure 6.21.** Deduction of amino acid sequence tag from MS/MS spectrum of peptide 1344.712 m/z of spot #96 by Biotools 3.2. Successive amino acid sequence SGNIIPSST was derived from y- and b-ions.

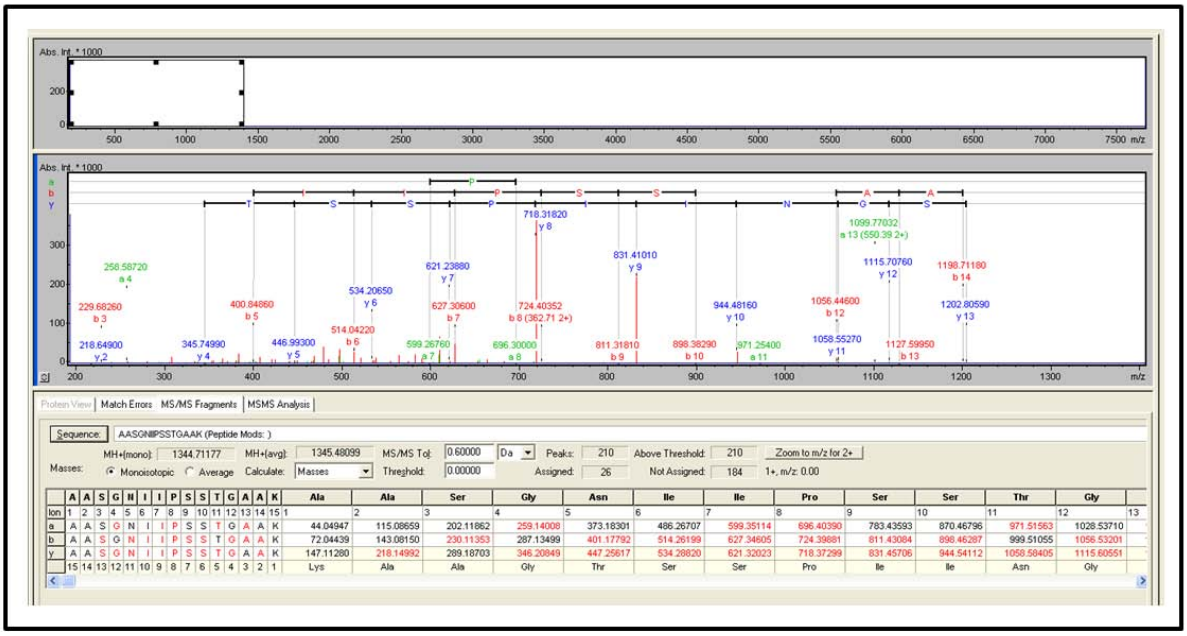


Another protein identified was spot #175, which was up-regulated by 3 folds in AC-T when compared to AC-N. Bioinformatic searches using its sequence tag INEPTAAAL from peptide 1659.895 m/z returned heat shock protein 70 from *Cryptosporidium andersoni* (Accession no.: gi|61969374) and *Euplotes aediculatus* (Accession no.: gi|3169833, gi|3169841) (Figure 6.22).

Spot #192 showed a 4.2-fold down-regulation under phosphate limitation in AC-T. Sequence tag PTVESQGSSV was deduced from the peptide 2131.045 m/z (Figure 6.23) and it was identified as plastid oxygen-evolving enhancer 1-2 precursor from *Alexandrium fundyense* (Accession no.: gi|134037072) which is the same as spot #196 described previously.

**Figure 6.22.** Deduction of amino acid sequence tag from MS/MS spectrum of peptide 1659.895 m/z of spot #175 by Biotools 3.2. Successive amino acid sequence INEPTAAAL was derived from y- and b-ions.

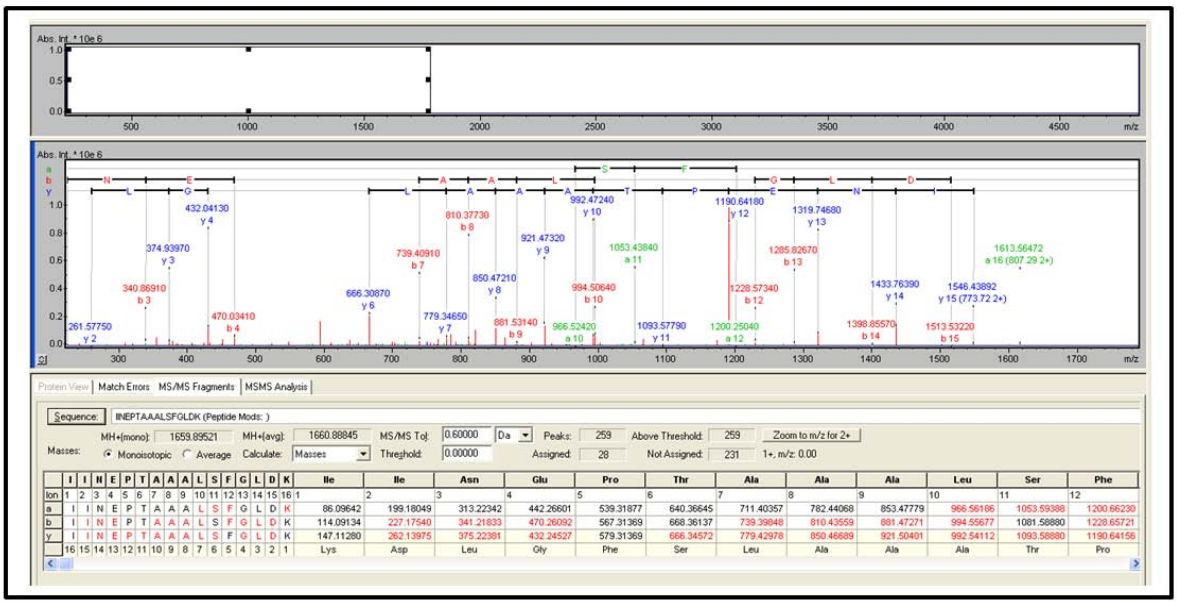


**Figure 6.23.** Deduction of amino acid sequence tag from MS/MS spectrum of peptide 2131.045 m/z of spot #175 by Biotools 3.2. Successive amino acid sequence PTVESQGSSV was derived from y- and b-ions.

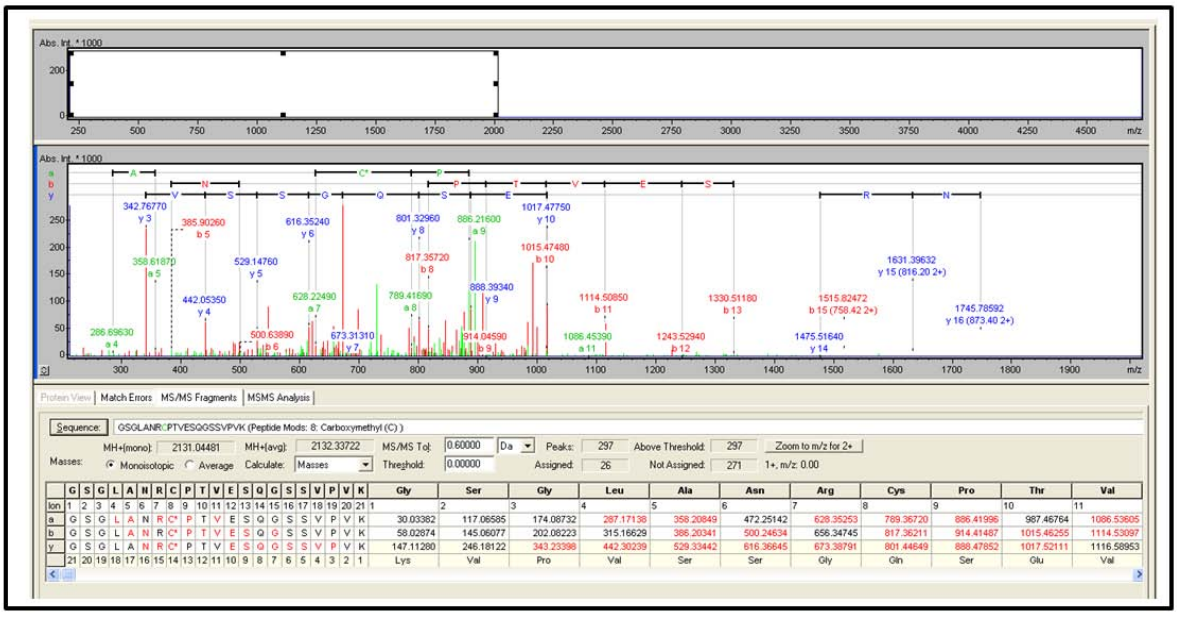

Spot #266 was identified as light-harvesting related proteins. Comparing AC-T and AC-N, it has a higher expression level in AC-T than AC-N by 2 folds. Its expression level was dropped by 2.2 folds under phosphate limiting condition. Matching sequence tags DIPNGLGAI and ATM*GYITP were deduced from peptides 1376.706 m/z and 1841.939 m/z respectively (Figures 6.24-25). Significant protein hits included light-harvesting polyprotein precursor from *Amphidinium carterae* (Accession no.: gi|3355306), light-harvesting chlorophyll a-c binding protein also from *A. carterae* (Accession no.: gi|757520) and chloroplast light harvesting complex protein from *Heterocapsa triquetra* (Accession no.: gi|58613557). By comparing the molecular weights of the protein hits, spot #266 has a similar size to light-harvesting chlorophyll a-c binding protein, with both of them at around 20 kDa. Light-harvesting polyprotein precursor actually contains several long strings of amino acids with similar sequences. The molecular weight of chloroplast light harvesting complex protein is 16 kDa (Appendix B).

**Figure 6.24.** Deduction of amino acid sequence tag from MS/MS spectrum of peptide 1376.706 m/z of spot #266 by Biotools 3.2. Successive amino acid sequence DIPNGLGAI was derived from y- and b-ions.

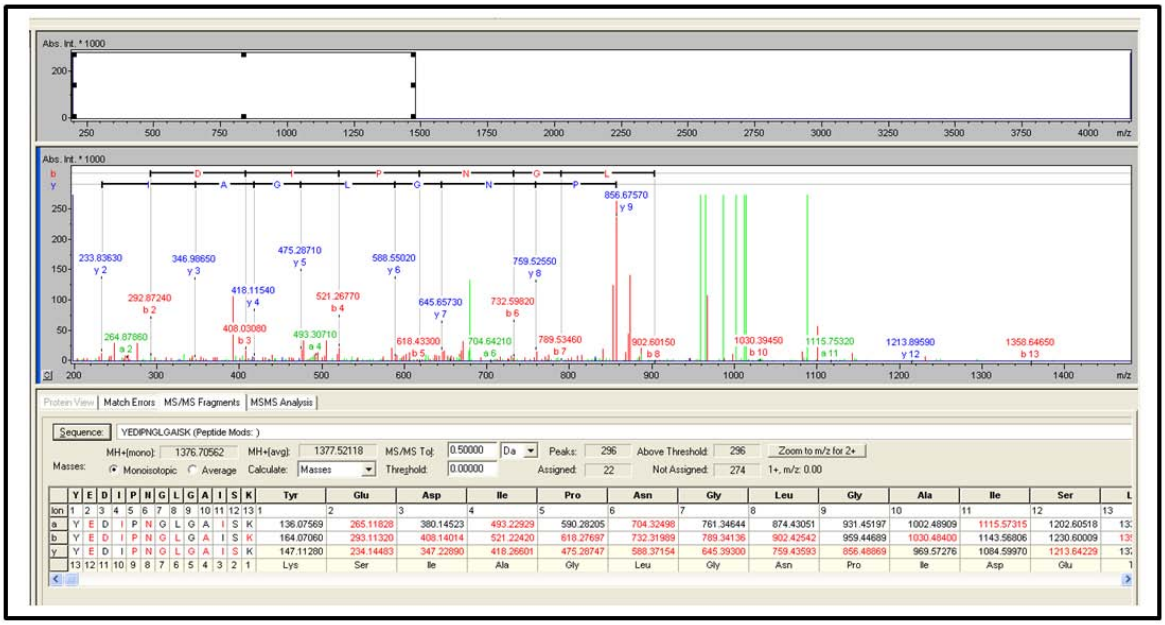

**Figure 6.25.** Deduction of amino acid sequence tag from MS/MS spectrum of peptide 1841.939 m/z of spot #266 by Biotools 3.2. Successive amino acid sequence ATM*GYITP was derived from y- and b-ions.

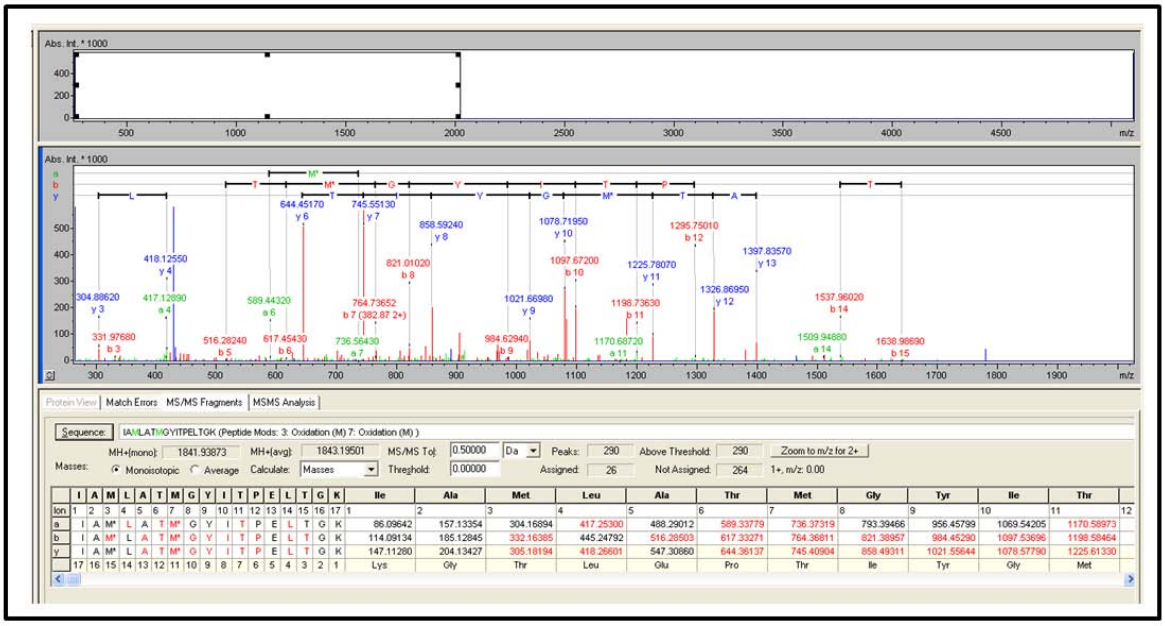


It is noteworthy to mention that two categories of protein hits were reported for spot #73. It was highly expressed in AC-T as it was not found in AC-N. However, it was down-regulated by 3.7 folds in AC-T exposed to phosphate-limited condition. By MS/MS analysis of peptides 1088.635 m/z, 1435.754 m/z & 1573.779 m/z, sequence tags VDLLAFYAK, TQAGSEVSALLGR & VYGQMNEPPGA were obtained. These tags were matched to ATP synthase subunit beta (Figures 6.26-28). On the other hand, peptides 1679.798 m/z and 1707.862 m/z gave the sequence tag M*DLEPGTM*D and TVPELTQQM*FDA which were matched with beta-tubulin (Figures 6.29-30). Although the pI value and molecular weight of spot #73 (i.e. pI 5.0 & 48 kDa) was similar to ATP synthase subunit beta (pI 5.2 and 53.2 kDa), there is no sufficient information for eliminating the possibility of beta-tubulin. Further, co-migration of two proteins in 2-DE may occur if the two proteins have similar pI and also molecular weight. They may be very close or even overlap to each other. Hence the identity of spot #73 could not be confirmed and would not be further discussed in the later section.

**Figure 6.26.** Deduction of amino acid sequence tag from MS/MS spectrum of peptide 1088.635 m/z of spot #73 by Biotools 3.2. Successive amino acid sequence VDLLAFYAK was derived from y- and b-ions.

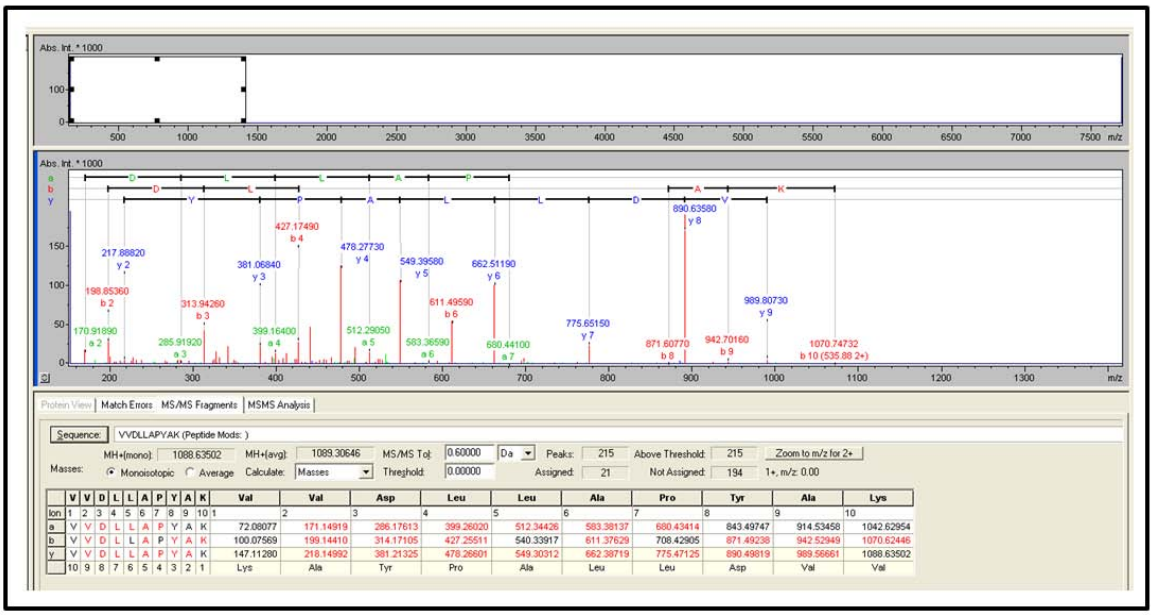


**Figure 6.27.** Deduction of amino acid sequence tag from MS/MS spectrum of peptide 1435.754 m/z of spot #73 by Biotools 3.2. Successive amino acid sequence TQAGSEVSALLGR was derived from y- and b-ions.

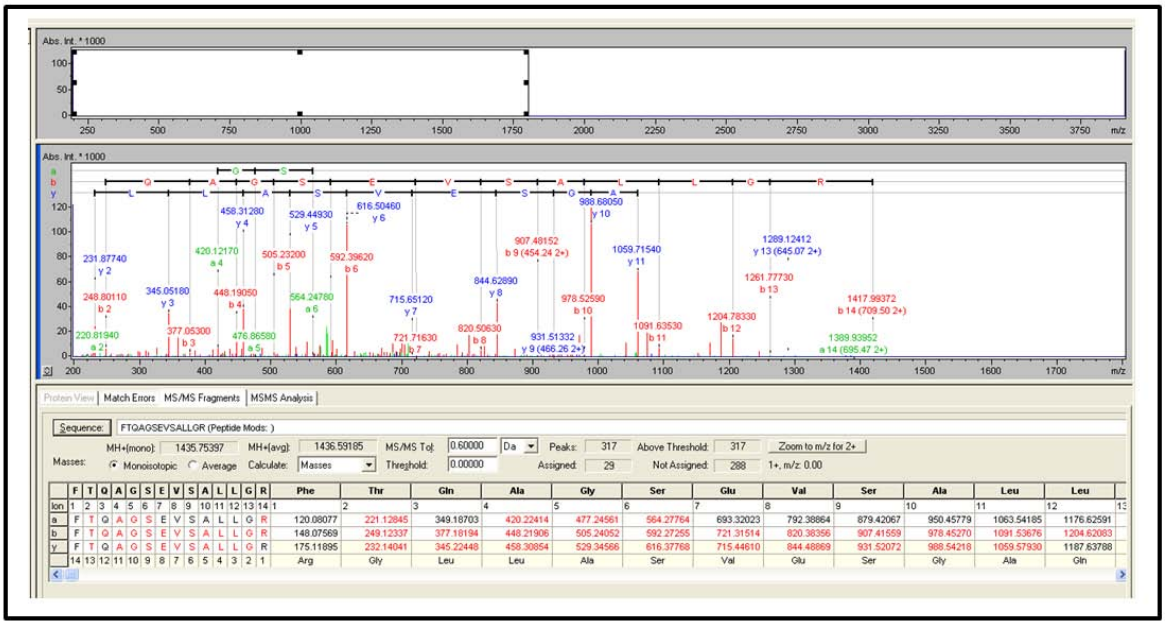

**Figure 6.28.** Deduction of amino acid sequence tag from MS/MS spectrum of peptide 1573.779 m/z of spot #73 by Biotools 3.2. Successive amino acid sequence VYGQMNEPPGA was derived from y- and b-ions.

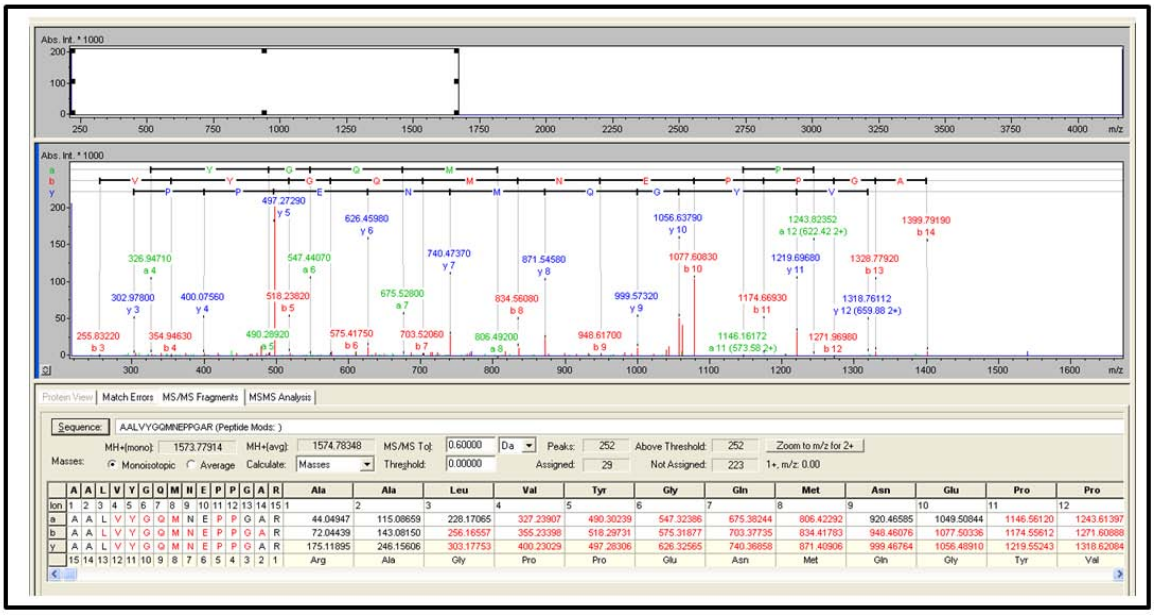


**Figure 6.29.** Deduction of amino acid sequence tag from MS/MS spectrum of peptide 1679.798 m/z of spot #73 by Biotools 3.2. Successive amino acid sequence M*DLEPGTM*D was derived from y- and b-ions.

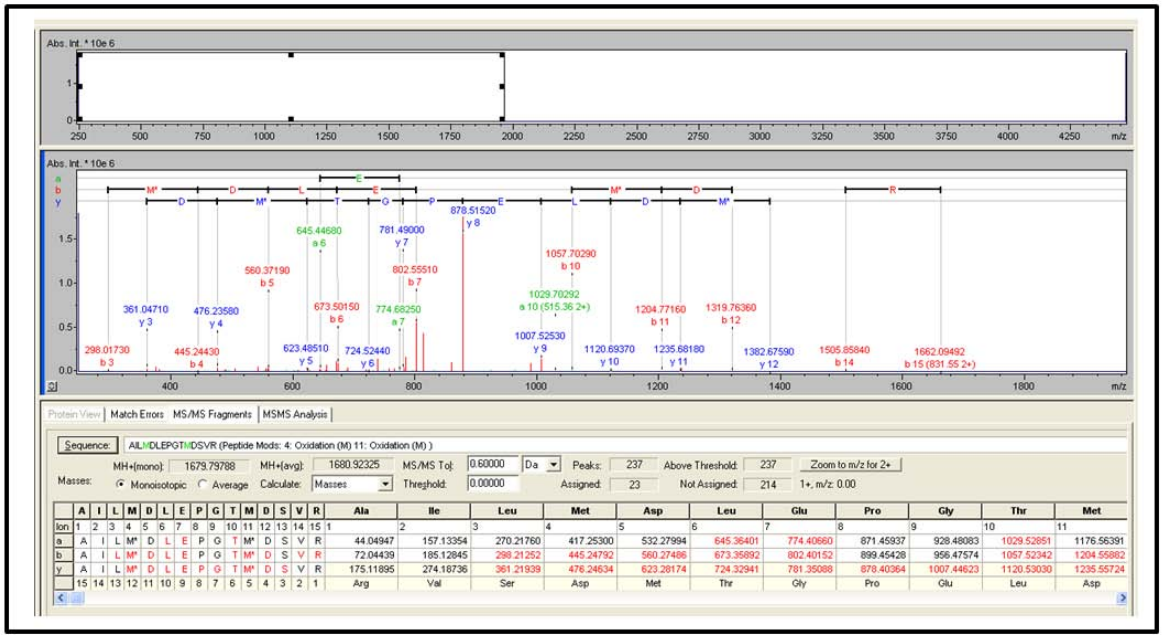

**Figure 6.30.** Deduction of amino acid sequence tag from MS/MS spectrum of peptide 1707.862 m/z of spot #73 by Biotools 3.2. Successive amino acid sequence TVPELTQQM*FDA was derived from y- and b-ions.

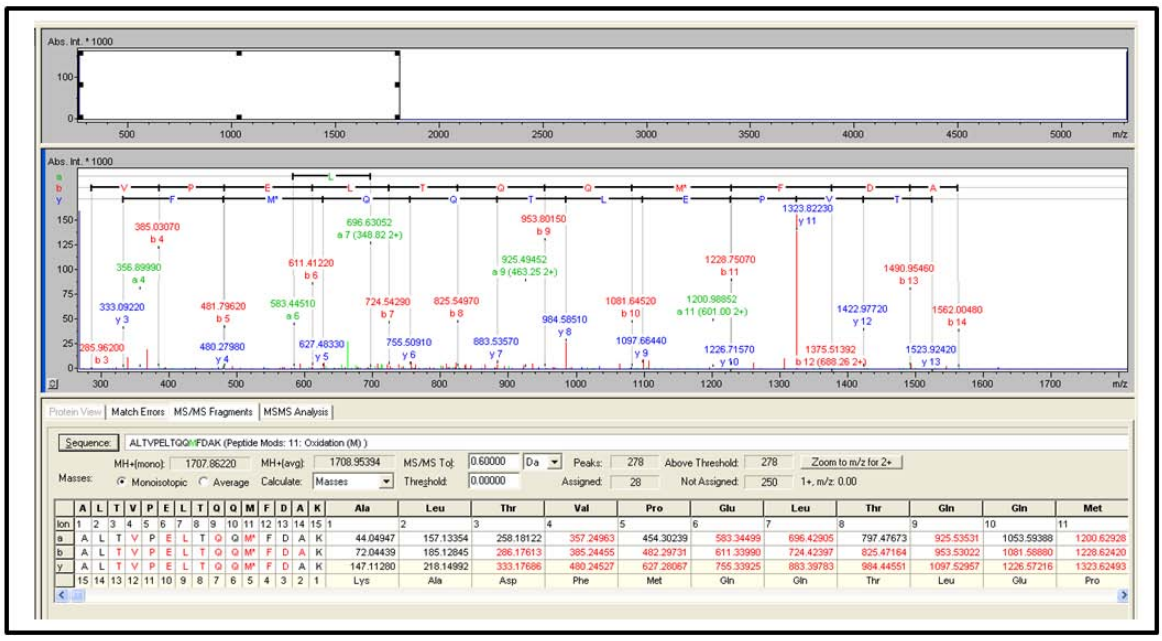


Similar cases were found for spot #66, which is down regulated by 2 folds in AC-T in phosphate limiting condition. Peptides 1076.585 m/z, 1207.639 m/z and 1344.712 m/z which were found in spot #96, #97, #98 were found again. Same amino acid sequence tags were deduced and the results were matched as glyceraldehyde-3 phosphate dehydrogenase also. On the other hand, another two sequence tags ALLFVPR and VDSEDLPLNIS were deduced from peptides 815.514 m/z and 1513.786 m/z respectively (Figure 6.31-32). The two sequence tags matched with the amino acid sequences of heat shock protein 90. Similar to spot #73, spot #66 would not be discussed in the following section since the identity could not be confirmed.

**Figure 6.31.** Deduction of amino acid sequence tag from MS/MS spectrum of peptide 815.514 m/z of spot #66 by Biotools 3.2. Successive amino acid sequence ALLFVPR was derived from y- and b-ions.

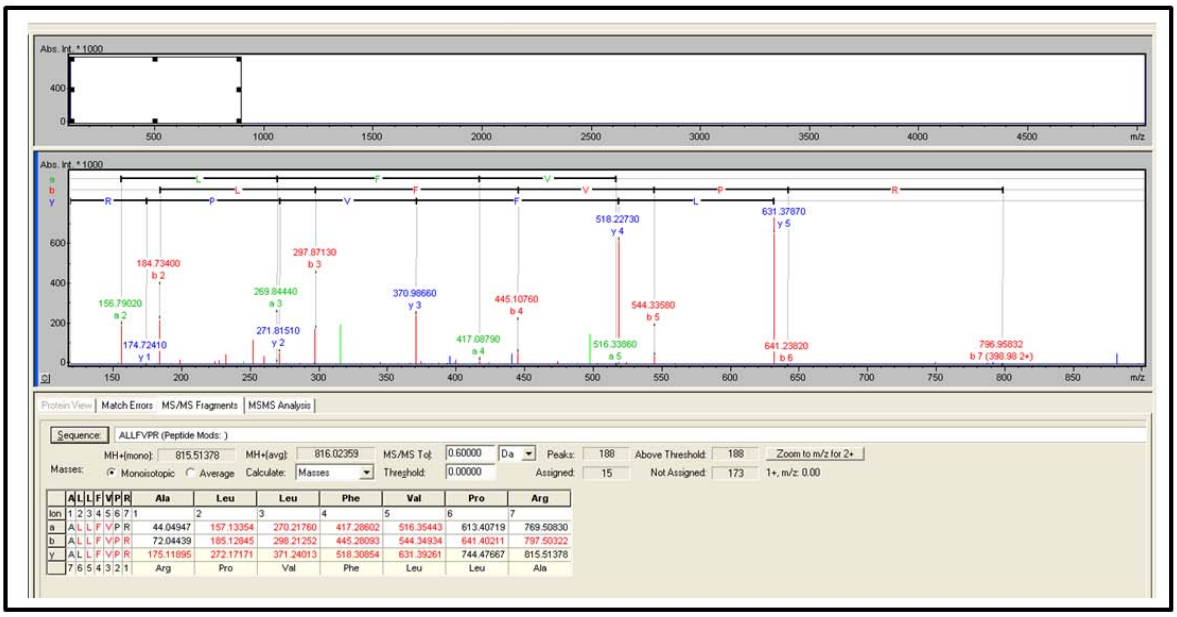


**Figure 6.32.** Deduction of amino acid sequence tag from MS/MS spectrum of peptide 1513.786 m/z of spot #66 by Biotools 3.2. Successive amino acid sequence VDSEDLPLNIS was derived from y- and b-ions.

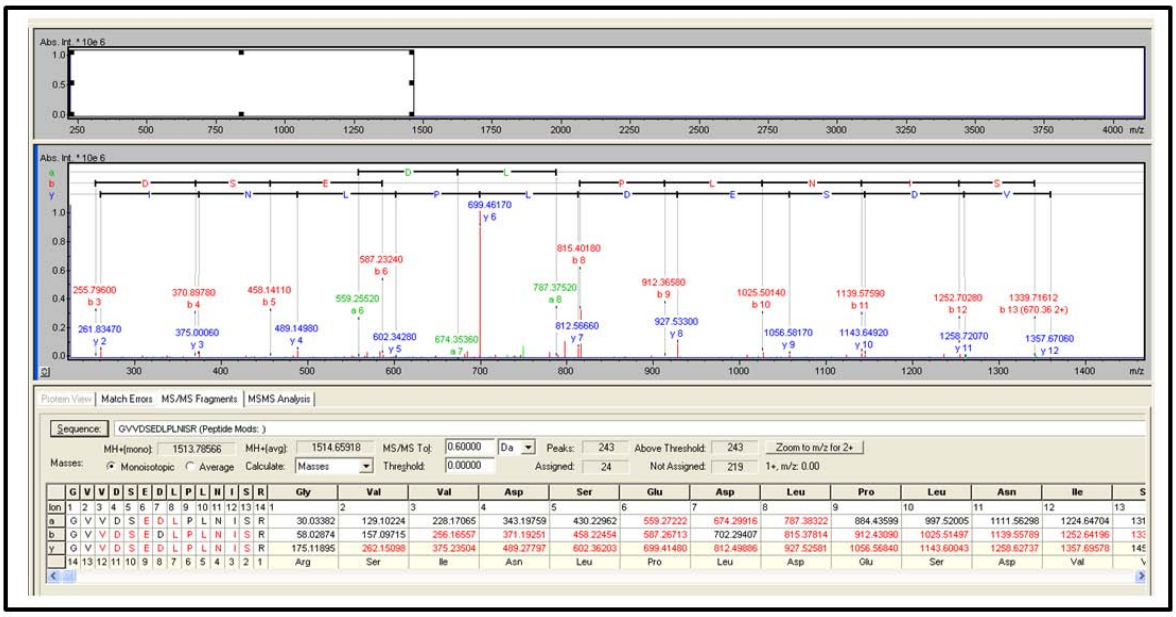

### 6.3.5 Identification By Searching Against the Transcriptome of *Alexandrium catenella*

In addition to searching sequence tag from the NCBInr database, sequence tags generated from MALDI-TOF/TOF analysis with sulfonation were allowed to search against the transcriptome of *A. catenella* (CS-300) constructed by BGI. One of the protein spots was found to have high homology to deduced protein sequence of an expressed gene in the transcriptome. Sequence tag EVDWNAEYFAR was generated from a sulfonated peptide 1613.513 m/z of spot #175 (Figure 6.33). No significant search was reported with the sequence from neither MASCOT nor blast search engine. By searching the sequence against the transcriptome database of *A. catenella*, high similarity was found to a sequence EVDWNADYFKA from the gene peridinin chlorophyll-a binding protein apoprotein precursor (annotated using homology from *Symbiodinium sp. RKT-203*). Figure 6.34 showed the alignment results obtained from EMBOSS Water of European Bioinformatics Institute (EBI) when the EVDWNADYFKA sequence was submitted. Eight amino acids were identical in the two sequences. E (glutamate) and D (aspartate) are similar that they both have negatively charged side chain. Together with the results from the ESI-ion-trap MS/MS analysis, two protein candidates were reported for spot #175.

Together with all the results of identification, Tables 6.4 and 6.5 summarized all the information of the proteins identified using various methodologies.

**Figure 6.33.** MS/MS spectrum of sulfonated peptide ion 1613.513 m/z of spot #175. Peptide 1398.410 m/z was the native peptide ion. Amino acid sequence EVDWNAEYFAR was deduced from the y-ions with mass tolerance of ± 0.3 Da.

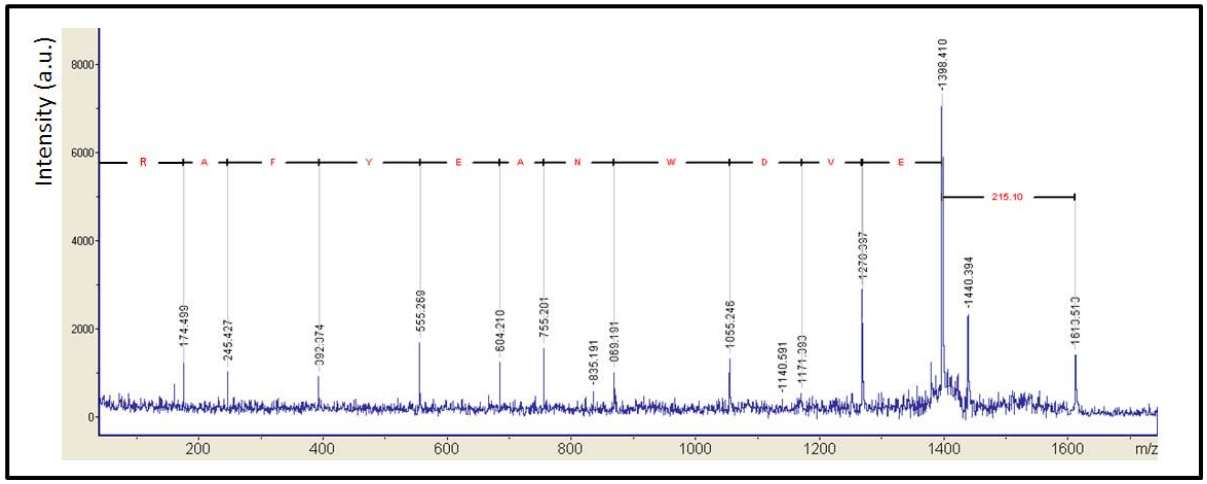


**Figure 6.34.** Sequence alignment of EVDWNAEYFAR (from spot #175) and EVDWNADYFKA (from transcriptome of *A. catenella*). High homology was reported between them.

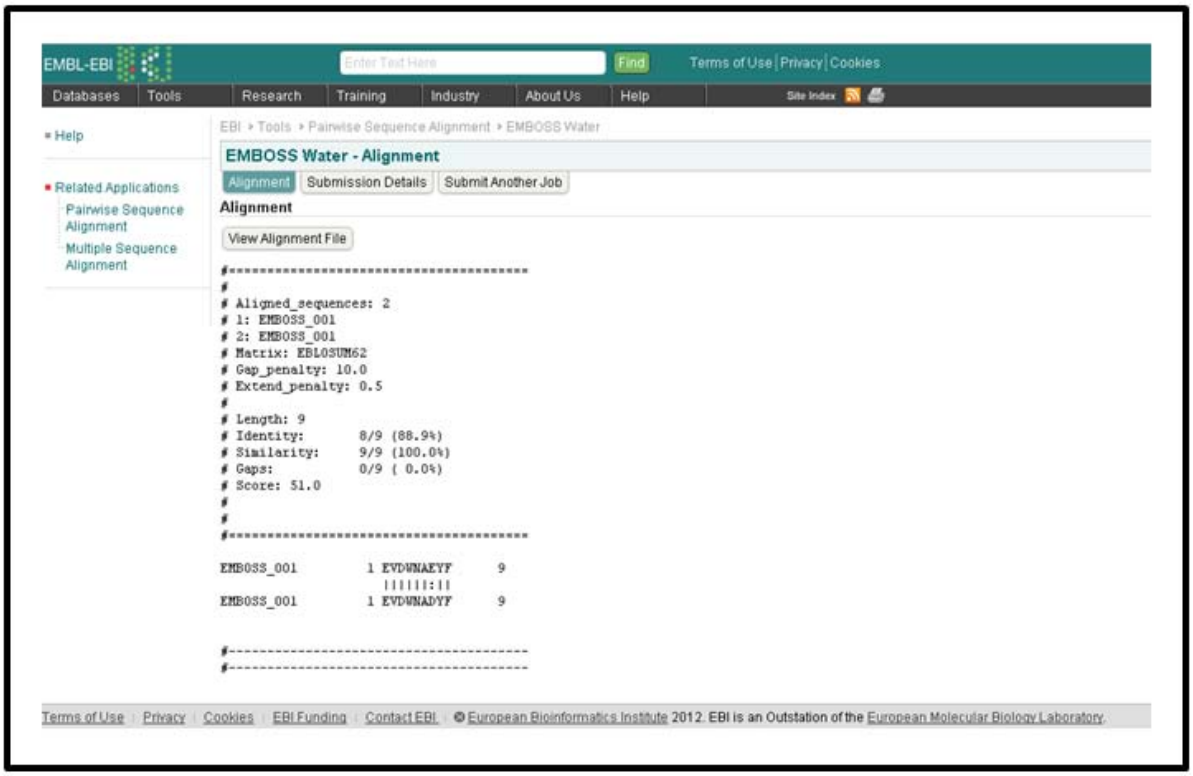

**Table 6.4.** A summary of proteins successfully identified by the various methodologies. These proteins were found to be differentially expressed in the toxic *Alexandrium catenella* (AC-T), when compared to the non-toxic *A. catenella* (AC-N).

| Protein identity | Spot number | Differential expression | Folds of change |
|---|---|---|---|
| Ribulose 1,5-bisphosphate carboxylase/oxygenase II (Rubisco II) | 27 | ↑ | 5.2 |
| | 28 | | 5.2 |
| | 31 | | 4.7 |
| | 32 | | 4.1 |
| | 33 | | 3.2 |
| Methionine adenosyltransferase | 38 | ↑ | 5.9 |
| ATP synthase subunit beta or beta-tubulin | 73 | ↑ | >100* |
| Glyceraldehyde-3 phosphate dehydrogenase | 96 | ↑ | 5.5 |
| | 97 | | 4.5 |
| | 98 | | 2.9 |
| | 104 | | 7.9 |
| | 118 | | 7.0 |
| Heat shock protein 70 or peridinin chlorophyll-a binding protein apoprotein precursor | 175 | ↑ | 3.0 |
| Transcriptional regulator | 257 | ↑ | 2.4 |
| Light-harvesting protein | 266 | ↑ | 2.0 |

↑ Up-regulated expression in AC-T, compared to AC-N

*The spot of protein was not detectable in AC-N

**Table 6.5.** Proteins identified by various methodologies. These proteins are found to be differentially expressed in the toxic *Alexandrium catenella* (AC-T) in phosphate-limiting condition, as compared to the AC-T cells in normal cultivation medium.

| Protein identity | Spot number | Differential expression | Folds of change |
|---|---|---|---|
| Glyceraldehyde-3 phosphate dehydrogenase or Heat shock protein 90 | 66 | ↓ | 2.0 |
| ATP synthase subunit beta or beta-tubulin | 73 | ↓ | 3.7 |
| Glyceraldehyde-3 phosphate dehydrogenase | 96 | ↓ | 7.3 |
| | 97 | | 7.7 |
| | 98 | | 6.1 |
| | 118 | | 2.9 |
| plastid oxygen-evolving enhancer 1-2 precursor | 192 | ↓ | 4.2 |
| | 196 | | 3.5 |
| Light-harvesting protein | 266 | ↓ | 2.2 |

↓ down-regulated expression under phosphate limitation

### 6.3.6 Significance of Identified Proteins and PSTs Production

Researches focusing on elucidating mechanisms of the production of saxitoxin and other paralytic shellfish toxins have started decades before. However, the lack of whole genome information hinders progress of these studies. The occurrence of post-translational modification in dinoflagellates introduces additional difficulties to studies of PST production through genomic approach (Fagan et al., 1999). Until a decade ago, more knowledge regarding PST biosynthesis was disclosed with proteomic techniques. Several proteins were reported to be differentially expressed between toxic and non-toxic *Alexandrium minutum* (Chan et al., 2005). However, identities of these proteins were unknown. These previous studies were performed by former members of our research group. The biggest hurdle in the identification process was the lack of genomic information and there was no other method available then to help them. With the advancement of mass spectrometry, techniques including sulfonation, LIFT technology in the MALDI-TOF-TOF, transcriptome database to support LC-ESI-ion-trap MS became available to me in the course of this thesis. Therefore, a total of 7 differentially expressed proteins were positively identified in the present study. Six of these proteins were upregulated when AC-T was compared to AC-N while some of the same proteins became down-regulated when the AC-T culture cells were exposed to phosphate-stress (Tables 6.4 and 6.5). Comparison between AC-T and AC-N will broadly represent difference in genetic makeup which enable or otherwise the production of PSTs. As the AC-T cells experiencing phosphate-stress became 4 times more toxic than the AC-T cells in normal medium, the insights provided by the 3 down-regulated proteins between AC-T cells with and without phosphate-stress are very important. I shall discuss these proteins in the following.

6 differentially expressed proteins were identified from the comparison of protein expression between toxic AC-T and non-toxic AC-N. All of these 6 proteins were upregulated in AC-T cells. Among these 6 proteins, 3 of them were involved in photosynthesis. Ribulose 1,5-bisphosphate carboxylase/oxygenase II (Rubisco II) is the chief enzyme for autotrophic $CO_2$ fixation and it is the initial as well as the rate-limiting step in the Calvin cycle. With an added carbon from $CO_2$ to ribulose-1,5-bisphosphate (RuBP), 2 molecules of 3-phosphoglycerate (3-PGA) come out. The same active site of the enzyme is also responsible for the first oxygenation

step in photorespiration that one 3-PGA and one 2-phosphoglycolate (2-PG) molecules are formed after $O_2$ is reacted with RuBP (Tabita et al., 2008). The molecular structure of Rubisco II in dinoflagellates is not the same as those (form I) in the green plants, although they have the same biological role. Form II Rubisco is a dimer of two large subunits. Due to its important role in photosynthesis, its concentration in dinoflagellates is reasonably high. From the 2D gel profiles in this study, spot #27, #28, #31 to #33 were found to be Rubisco II. Normalized with the total proteins expressed in the 2-D gel profiles, the amount of Rubisco II was about 8.9 % of the total cellular proteins in AC-T cells in the exponential phase. For similar cell volumes and cell densities at the same growth phase, AC-N only process about 1.9 % protein amount of Rubisco II. This may indicate that there are some differences of photosynthetic ability between AC-T and AC-N. One can also infer that the difference in photosynthetic ability may relate to PST production as AC-T is toxic while AC-N is not.

Another differentially expressed protein that is upregulated when AC-T is compared to AC-N is glyceraldehyde-3 phosphate dehydrogenase (G3PD). It is the enzyme that catalyze the reversible interconversion between glyceraldehyde-3-phosphate (G3P) and 1,3-diphosphoglycerate (1,3-BPG), depending on which biological pathway is involved. One of these pathways is the Calvin cycle. After an inorganic phosphate group from ATP is added to 3-PGA, 1,3-BPG is formed and the plastid G3PD is responsible for converting the molecule to G3P with NADPH. The other possible pathways that is involved with G3P and 1,3-BPG interconversion is glycolysis/gluconeogenesis in which cytosolic G3PD is involved. However, previous studies reported that several cytosolic and plastid-targeted G3PD were processed in dinoflagellates (Takishita et al., 2005). Further, no full amino acid sequence of the differentially expressed G3PD was generated for alignment to those in the database. No conclusion could be made whether the G3PD which showed differentially expression are actually cytosolic or plastid-targeted. Nevertheless, the up-regulation of G3PD in AC-T indicates that the metabolic activities between AC-T and AC-N would probably be different, even at the same growth phase at similar cell density and size. Whether the difference in metabolic rate manifested in difference in PST production is not yet known.

Thirdly, Spot #266 was shown to be upregulated in AC-T and it was found to be light-harvesting protein (LHP). LHP is the protein part of light-harvesting complex (LHC), which forms reaction center of the photosystem and is important for transfer of energy efficiently (Prezelin and Alberte, 1978). LHP in the complex are transmembrane proteins in the thylakoids and are pigment-bound. LHP assists energy transfer by holding the pigments in specific three-dimensional arrays. Light dependent reaction occurs in the LHC and ATP as well as NADPH are generated for the other part of photosynthesis. AC-T expressed comparatively more LHP than AC-N and again such difference would be another indicator of different photosynthetic ability between the two strains.

About half of dinoflagellates are photosynthetic in nature (Ishida and Green, 2002). A higher capability of carrying photosynthesis reflects a higher carbon uptake for cellular metabolism. Fast-growing dinoflagellates have a comparatively higher photosynthetic rate than slow-growing species as more carbon is needed for a high rate of biomass production. From the results of differential protein expression between AC-T and AC-N, Rubisco II, G3PD and LHP all play vital roles in various parts of photosynthesis. All of these proteins were found to have a higher expression in AC-T than AC-N. However, from observations in my background studies in Chapter 4, both AC-T and AC-N have similar cell sizes and cell densities at Day 18 (the sampling point) and also in most part of the exponential phases. The growth rates in this period of the two strains were the same also. No obvious difference in carbon gain between AC-T and AC-N were found from observation of their growth and biomass accumulation. But the presence of PSTs in AC-T but not in AC-N reflects a difference of carbon usage between them. Carbon is the main component of STX (about 40 % of its molecular weight). A higher photosynthetic ability of AC-T may account for the extra expenditure of carbon in PST production. Besides, ATP-dependent enzyme is found to be involved for interconversion of PSTs (John and Flynn, 2002). Energy consumption is thus involved in toxin synthesis and this may be the possible reason of higher requirement of photosynthesis in AC-T than AC-N. Further, it was reported earlier that a strain of *Alexandrium lusitanicum* lost its PSP toxigenicity of a formerly toxic clone (Martins et al., 2004) and the loss of toxigenicity was associated with a reduced growth capability, indicating that the metabolic activities were changed concurrently with the ability of toxin

production. These observations linked toxigenicities of dinoflagellates with their metabolic or photosynthetic activities. This is not a novel idea. In 2010, research has been done on the relationship between photosynthesis and PST production in dinoflagellate *Alexandrium minutum* (Maas and Brooks, 2010). By incubating the culture in dark for 22 days, toxin profiles changed and STX production disappeared completely. Although the levels of other PSTs such as GTX1-4 and NEO were not changed, it is noteworthy that photosynthesis does have some effects in toxin production of dinoflagellates. Such findings bring along the followed-up question. Why dinoflagellates process toxin production which in fact is energy consuming? Several explanations could be proposed. The simplest and most direct rationale is that PSTs could actually bring some advantages to the organism. Because of such value, it is worthwhile or even necessary for dinoflagellates to use part of its energy gained from photosynthesis for toxin production. However, such advantage is yet to be found and substantiated in field studies. Also, the free existence of non-toxic strain in the natural environment cast doubt on the possible importance of such 'advantages'. Another explanation of the phenomenon is the existence of PST is a by-product. PSTs may be the by-product of some kind of treatments of removal or transformation of some unwanted substances produced from the toxic dinoflagellates. However, one may imagine that similar problem existed in non-toxic strains and how are these substances being dealt with in non-toxic strains? Are they changed to other non-toxic molecular structures other than PST or no such substances are produced in these strains? The third proposed explanation could be the consumption of extra metabolic energy. Due to the higher intrinsic photosynthetic capabilities of the toxic strains, energy gained from photosynthesis may be in excess, much more than the actual need for cell growth and other metabolic activities. The excess energy was not stored but consumed with some cellular processes, resulting in PSTs formation. All of these proposed explanation needed to be tested by further investigation which will be discussed in the later part of this thesis.

In addition to proteins involved in photosynthesis, methionine adenosyltransferase (MAT) was also found to be upregulated in AC-T than in AC-N. Expression level of MAT in AC-T is about 6 folds of AC-N. MAT is the enzyme involved in synthesis of S-adenosylmethionine (SAM) with methionine and ATP in the methionine cycle (Figure 6.35) in which methionine and

homocystiene could be interconverted. The product of MAT reaction, SAM, participates in many cellular processes. The principal function of SAM is methylation and it could occur in proteins, lipids and nucleic acids. SAM participates in the repairing function of spontaneous protein degradation as well. It is noteworthy that methylation of DNA is one kind of regulation of gene transcription.

**Figure 6.34.** Methionine cycle. Methionine adenosyltransferase is responsible for synthesize of SAM from methionine

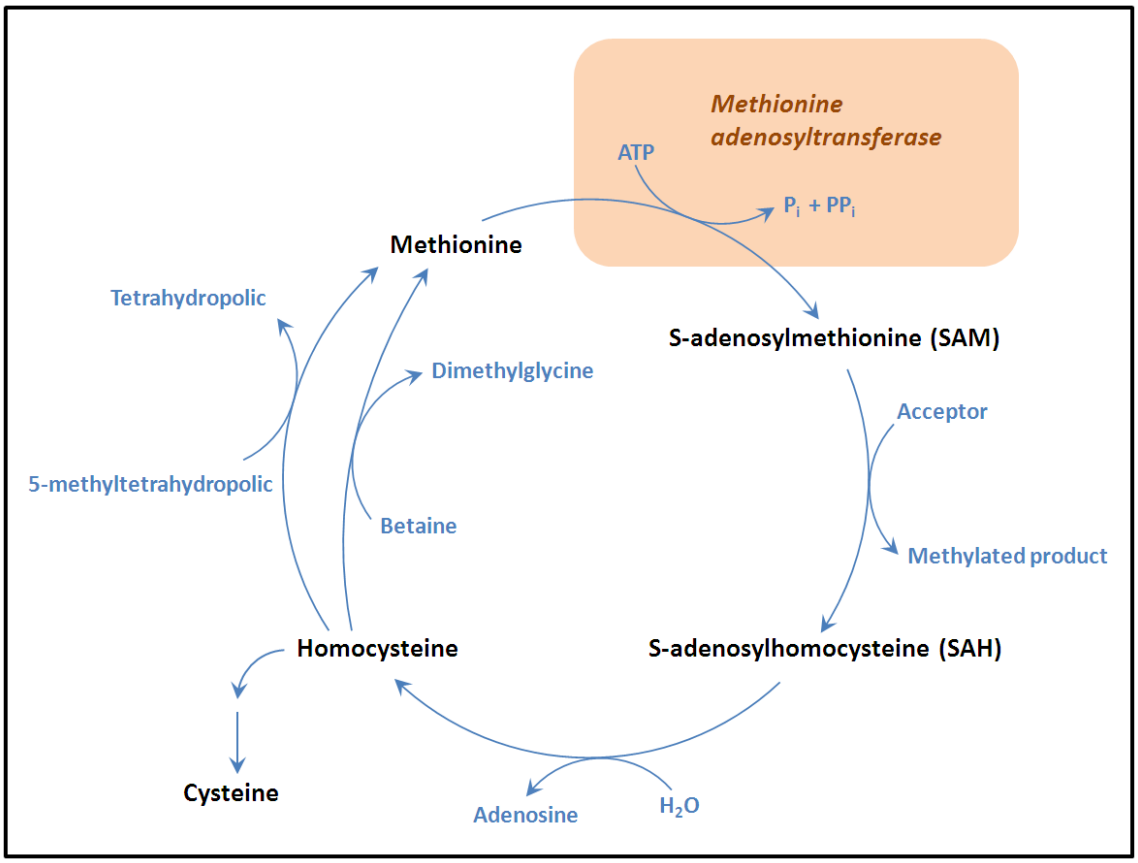


In PSTs producing dinoflagellates, SAM was reported to play a role in PST synthesis. The methyl group of methionine (through SAM) was reported to be one of the precursors of proposed STX synthetic pathway (Shimizu, 1993). In the proposed mechanism, a side chain methyl group was added to the heterocyclic skeleton of the molecule by SAM after cyclization reactions. Previous study on PSTs production reported that the gene of another SAM relating enzyme, adenosylhomocysteinase (AHS), was differentially expressed during toxin synthesis

(Taroncher-Oldenburg and Anderson, 2000). The findings of a higher MAT expression in AC-T in this study appeared to be coherent to its toxigenic characteristic that an additional portion of SAM is consumed during toxin synthesis (Figure 6.36) and that it did not occur in the non-toxic AC-N strain. Hence, for toxin production in toxic dinoflagellates, SAM needed to be regenerated in a higher rate and hence a higher expression of MAT. However, such direct relationship between SAM and toxigenicity could be argued against with the wide range of biological roles of SAM. As mentioned, SAM is also involved in DNA methylation for transcriptional regulation. Higher expression of SAM between the toxic and non-toxic strain could be explained with the differential regulation of 'PSTs related genes'. Methylation of 'PSTs related genes' in AC-T may induce its expression and result in toxin production. In depth investigation is needed to confirm the significance of MAT and SAM in PSTs production.

The other upregulated protein, spot #175, were found to be either peridinin-chlorophyll a protein (PCP) by the transcriptomic approach or heat shock protein 70 (HSP70) by the amino acid sequence tags approach. It is known that peridinin is the carotenoid that is uniquely found in dinoflagellates (Rowan et al., 1996a). Because of peridinin, dinoflagellates could capture light and transfer energy efficiently, even at low light levels in the marine environment. Upregulation of PCP in AC-T is consistent with the upregulation of other photosynthesis relating proteins mentioned before, indicating a difference in photosynthetic capabilities between AC-T and AC-N. On the other hand, if spot #175 is HSP70, its interference is different. HSP70 is known to take part in many cellular processes including protein folding, protection of cells from thermal or oxidative stress and also signal transduction (Uribe et al., 2008). However, increased expression of HSP70 in toxic dinoflagellates is contradictory that reported in the literature (Pomati et al., 2006). In that study, comparison of transcriptional profiles between a toxic and a non-toxic strain of *Anabaena circinalis* was performed. Gene expression of HSP70 in the non-toxic strain was found to be higher than that of the toxic counterpart and the authors suggested that heat shock proteins have a role in PSTs production regulation. It should be noted that *Anabaena circinalis* is a prokaryote and is genetically distant to dinoflagellates. The role of HSP70 in prokaryote and eukaryote may be very different. Further, due to the non-specificity of

**Figure 6.35.** Simplified proposed biosynthetic pathway for saxitoxin as suggested by Shimizu (1993), showing methylation through SAM is involved for STX production (highlighted region).

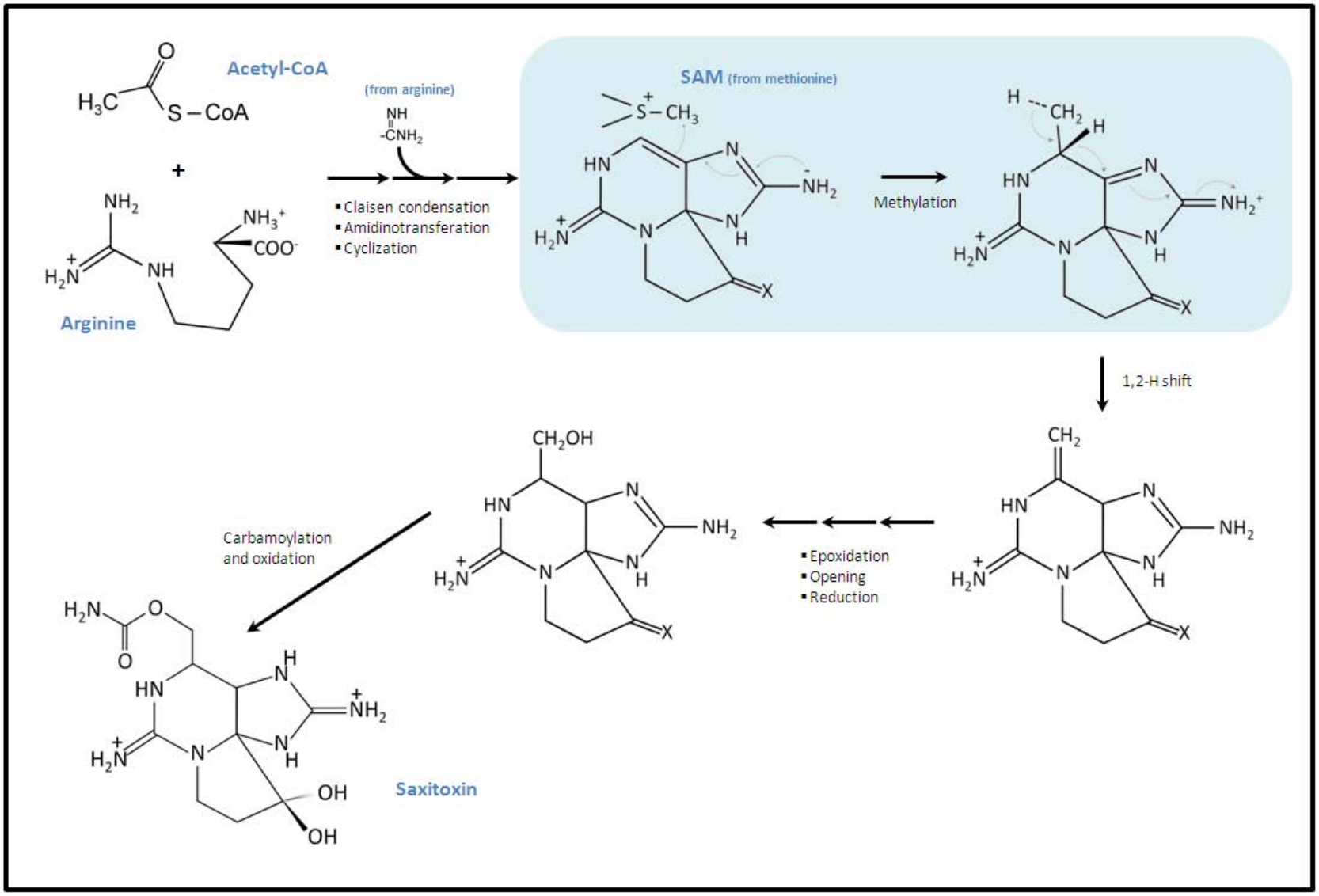

functions of HSP70, the linkage between the expression of HSP70 and toxigenicities of dinoflagellates remains elusive and further investigation is needed to find its role in PSTs production.

Spot #257 was the last protein found to be upregulated and successfully identified when protein expression in AC-T was compared to that of AC-N. It was identified as a putative transcriptional regulator homologous to that of a bacterium *Frankia alni*. Upregulation of this transcriptional regulator in AC-T may indicate that it has higher gene regulation/expression. Previous experiment focusing on the comparison of expressed sequence tag (EST) of a toxic and a non-toxic *A. minutum* found that there were 192 genes that were differentially expressed between the two strains (Yang et al., 2010). Such difference could be linked to different levels of transcriptional proteins between them. Further, a recent study showed that a *sxtA* gene is responsible for PSTs production in the toxic *A. tamarense*/*catenella*/*fundyense* complex (Stuken et al., 2011). This implied that the inability of PSTs production in AC-N may due to some kind of *sxt* genes suppression. Such explanation could also fit to the proposed reason why *A. lusitanicum* lost its toxicity after many generations of sub-culturing. There may be an 'unknown factor' which leads to shut down of expression of the *sxt* genes and loss of toxicity. Nonetheless, understanding of the role of transcriptional regulator(s) in AC-T may give insight into the production of PSTs.

On another front, 3 differentially expressed proteins (all down-regulated) were successfully identified in AC-T cells in phosphate limiting condition in comparison with AC-T in normal medium. Two of these 3 proteins were discussed previously when AC-T was compared to AC-N. They are glyceraldehyde-3 phosphate dehydrogenase (G3PD) and light-harvesting protein (LHP). AS elaborated previously, G3PD is the metabolic enzyme that is involved in Calvin cycle, glycolysis and gluconeogenesis. The lower expression of G3PD in $PO_4$-limited culture apparently related to the retarded growth of the culture due to the unavailability of phosphate for cell division. As there was not enough phosphate to support growth (e.g. new DNA synthesis), there was less demand for metabolic energy to support growth of the culture and hence there was less expression of G3PD. The second protein LHP found to be down-regulated

in $PO_4$-limited AC-T culture. As elaborated earlier, LHP is involved in photosynthesis by binding to light-capturing pigments and aid energy transfer in the photosystem. Lower expression of LHP may indicate the photosynthetic activity become lower as the energy requirement or the reduced growth became less. To understand further the effects of LHP, discussion with the third protein identified is needed. The third protein that was identified is plastid oxygen-evolving enhancer (OEE) 1-2 precursor, another protein that related to photosynthesis. OEE is located on the thylakoid lumen and has a stabilizing function for the tetra-manganese cluster for water oxidation in photosystem II (Ishida and Green, 2002). It also serves as a protection of reaction centre of D1 protein from oxidizing actions of oxygen radicals. OEE is highly conserved in phototrophic organisms. A lower expression of OEE 1-2 precursor was found under phosphate limitation in the present study, indicating that the photosynthetic activities were lower under the condition of phosphate stress. Together with LHP, my results showed that under phosphate limitation, growth was retarded after several days of culturing. Photosynthetic activities were decreased concomitantly. Results reported in the literature support this inference. It was found that the fluorescence-based photochemical efficiency of $PO_4$-limited culture of *A. minutum* was decreased (Lippemeier et al., 2003). It was suggested that such drop was the result of reduction of the requirement of ATP and this lead to a pH gradient across the thylakoid membranes and hence resulted in nonphotochemical quenching. Regarding toxicity, in the study by Lippemeier and coworkers as well as the present study, cellular toxin content were increased in the $PO_4$-limited culture, showing an inverse relationship to photosynthetic activities. The relationship between photosynthesis and toxin content may have some correlations to the fact that light intensity could affect toxin synthesis of dinoflagellates. As photosynthesis could be affected by light intensity, the toxin production at various light intensities may be one kind of effect of changes of photosynthesis of dinoflagellates. However, it is hard to deduce the mechanism of such interrelationship at this moment as this kind of effect is not seen in GC-T in the present study as well as that reported by Usup and coworkers (Usup et al., 1994). Further, the inverse relationship of photosynthesis and cellular toxin content was in contradictions with the suggestion that the product or process of photosynthetic capabilities is required for toxin synthesis. It also disagreed with the

suggestion that the ability of toxin synthesis is solely metabolism-driven. A possible explanation to this conflicting phenomenon could be that there is more than one mechanism in controlling PST production. Beside the pathway which is responsible for toxin synthesis, another mechanism may exist for the removal or detoxification of PSTs. Non-toxic AC-N is intrinsically unable to carry out toxin synthesis but toxic AC-T seems to have the genetic machinery to produce PSTs. On the other hand, PSTs removal or detoxification mechanism is somehow disabled under phosphate limiting condition in AC-T and hence caused the accumulation of toxins in the toxic dinoflagellates. It should also be noted that toxin detoxification mechanism in toxic dinoflagellates is not yet identified but could be possible as this was found from other toxin producing microorganism (Lefebvre et al., 2008; Shilo M. and Aschner, 1953). If this is also true for PSTs producing *Alexandrium*, will it be an energy-consuming process that require specific transportation? Is the accumulation of the toxins actually the result of reduction in metabolism and such transport? Certainly, further investigation is needed to confirm this hypothesis and also its effects as induced by phosphate limitation.

## 6.4 Summary

65 proteins were found to be differentially expressed between the 2D expression profiles of AC-T and AC-N in the exponential phase (Day 18). 7 proteins were identified with MALDI-TOF/TOF and ESI-ion-trap MS analysis and they are all upregulated in AC-T. Some of these proteins are known to be involved in photosynthesis and they are ribulose 1,5-bisphosphate carboxylase/oxygenase, glyceraldehyde-3 phosphate dehydrogenase, peridinin-chlorophyll a protein and light harvesting protein. Others are methionine adenosyltransferase, heat shock protein 70 and transcriptional regulator. 22 proteins were found to be differentially expressed with the 2D expression profiles of AC-T under phosphate limitation. 3 of them were identified and they are downregulated, including glyceraldehyde-3 phosphate dehydrogenase, plastid oxygen-evolving enhancer 1-2 precursor and light harvesting protein. The results suggested that the toxin content of *A. catenella* may have some correlations to the photosynthetic activities of the dinoflagellates.

## Chapter 7 Concluding Remarks and Further Studying Approaches

In the ultimate aim to understand the mechanism for PST production, four strains of dinoflagellates were selected for studying their growths, cell sizes, intracellular toxin contents and endogenous free arginine contents. A strain of *Gymnodinium catenatum* (GC-T) and toxic strain of *Alexandrium catenella* (GC-T) were found to contain PSTs, while no toxin was found in the non-toxic strain of *A. catenella* (AC-N) and *A. tamarense* (AT-N). GC-T was found to be more toxic than AC-T in terms of both intracellular toxin content and cellular toxin concentration. However, environmental variations (including nitrate enrichment/limitation, phosphate limitation and the addition of exogenous arginine) could not induce any significant charge in toxin content in GC-T. On the other hand, toxin content of AC-T under phosphate limitation was increased to about 400% of that of normal. 2-DE proteins expression of AC-T and AC-N were compared and 65 proteins were found to be differentially expressed. 6 differentially expressed proteins were identified with the aid of MALDI-TOF-TOF MS and LC-ESI-ion-trap MS/MS. Some of the proteins are known to be involved in photosynthesis (i.e. Rubisco II, G3PD, LHP and PCP) and one of them is involved in the methionine cycle (i.e. MAT). 2-DE proteins expression of AC-T under phosphate limitation was also examined and photosynthetic proteins were found to be differentially expressed again. These results imply that there may have some correlations between photosynthesis capabilities and toxin synthesis in *A. catenella*.

To build on my results and to understand mechanism of PST production ultimately, several possible experiments are suggested.

1) Firstly, expression levels of the differentially expressed proteins identified in this study should be validated by either genetic method (e.g. quantitative real-time PCR), western blotting with antibodies and classical biochemical approach.
2) Secondly, several photosynthetic proteins were reported to have some implications in toxin synthesis, effects on toxigenicity of the dinoflagellates by specific inhibition of the photosynthetic pathway at different stages should be performed. Ultra-violet radiation, 3-(3,4-dichlorophenyl)-1,1-dimethylurea (DCMU) and methyl parathion were the substance reported to cause inhibition of photosynthesis (Helbling et al., 2008; Saroja and Bose, 1983;

Staats et al., 2000; Sukenik et al., 2002). With the addition of these substances at different extent and time points, toxin content of dinoflagellates at their optimal and sub-optimal levels of photosynthesis could be investigated.

3) Methionine adenosyltransferase (MAT) was also reported to have higher expression in toxic dinoflagellates. It was suggested that this was the result of higher requirement of S-adenosylmethionine (SAM) for methylation during toxin synthesis. The effect on toxigenicity of surplus methionine or SAM should be studied.
4) Another further studying approach could be performed by investigation of toxin content after blocking the gene expression of MAT. With the limited supply of SAM, the pathway for toxin production is supposed to be hampered at some stages and expression of the relating enzyme would be affected.
5) Based on the results of the analyses of the 2D profiles of AC-T and AC-N and $PO_4$-limited AC-T, it is proposed that more than one mechanism are involved in controlling or balancing the intracellular toxin content of the dinoflagellates. To test the hypothesis, interaction of the PST molecules with other cellular components should be found out. Column binding experiment with immobilized PST molecules could be performed to find out what components in the dinoflagellates are involved in reacting or transporting the toxins. This studying approach could help elucidate the biological role of PSTs.
6) Recently, more and more researchers studying dinoflagellates with transcriptomic approach, with the development of more powerful sequencing technologies (Yang et al., 2010). The information of the transcriptome could compensate limitations of the proteomic analysis of dinoflagellates in which no full genomic database is established. Full sequence of the protein candidates found from proteomic analysis could be known from the corresponding transcriptomic information. Besides, comparative study with the transcriptomes could provide a global view about the physiology of toxin producing mechanism of the dinoflagellates in any one time.

# Appendices

## Appendix A

**Appendix A1.** Growth curve of GC-T.

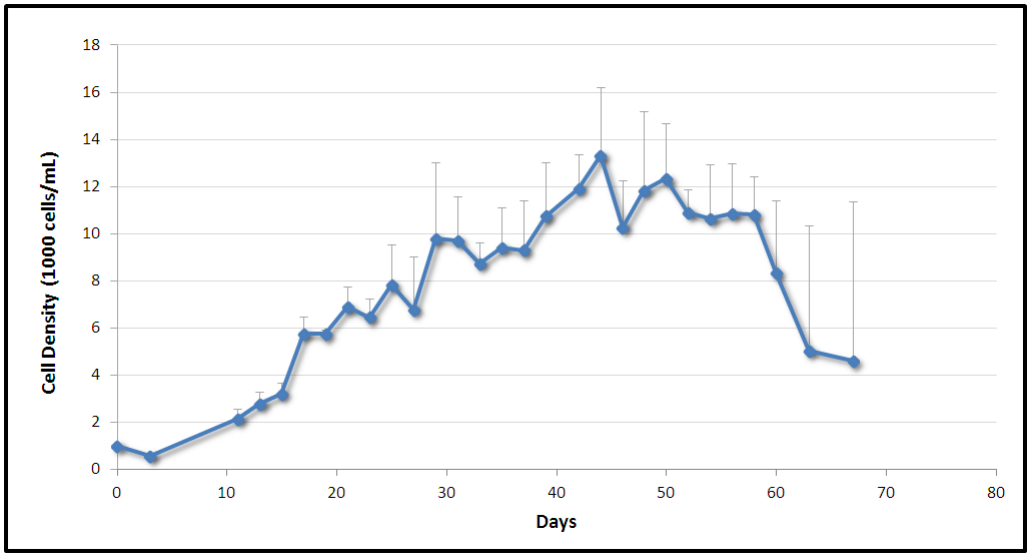


**Appendix A2.** Growth curve of AC-T.

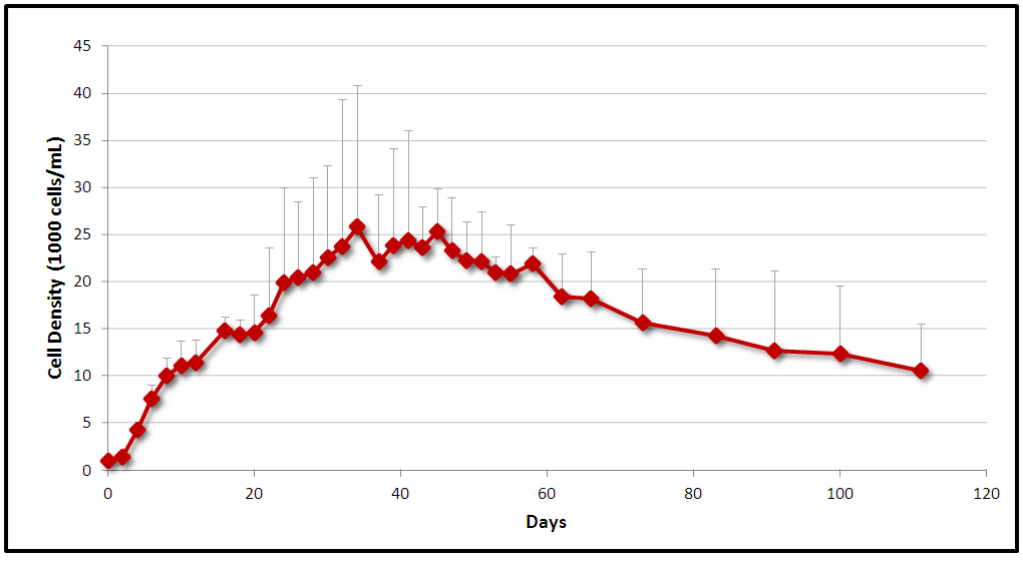

**Appendix A3.** Growth curve of AT-N.

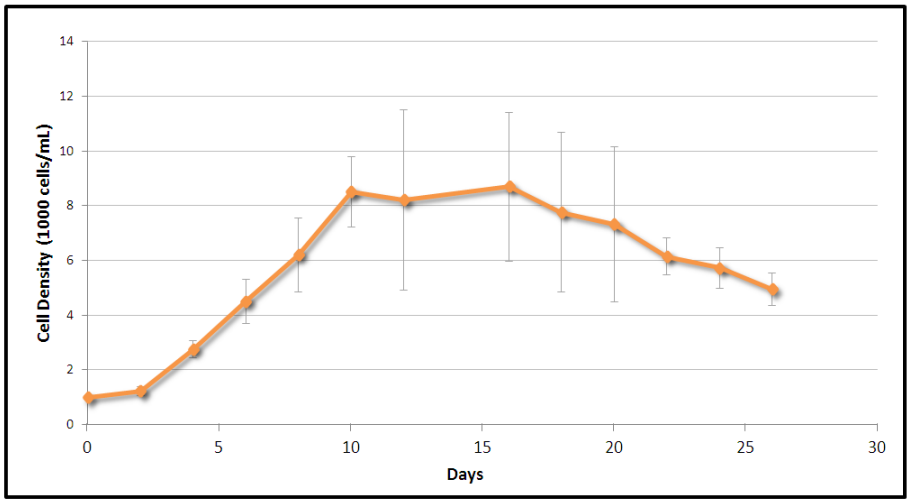


**Appendix A4.** Growth curve of AC-N.

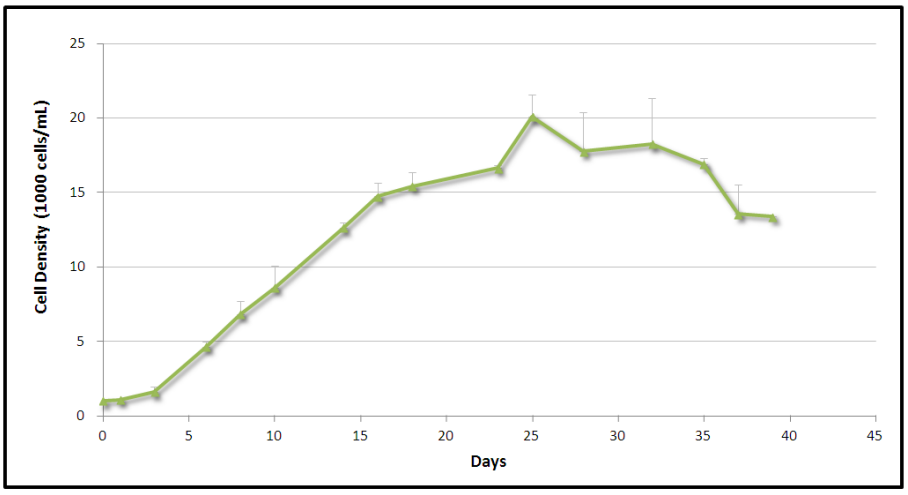


**Appendix A5.** Standard curves of neuroblastoma assay using STX as the standard.

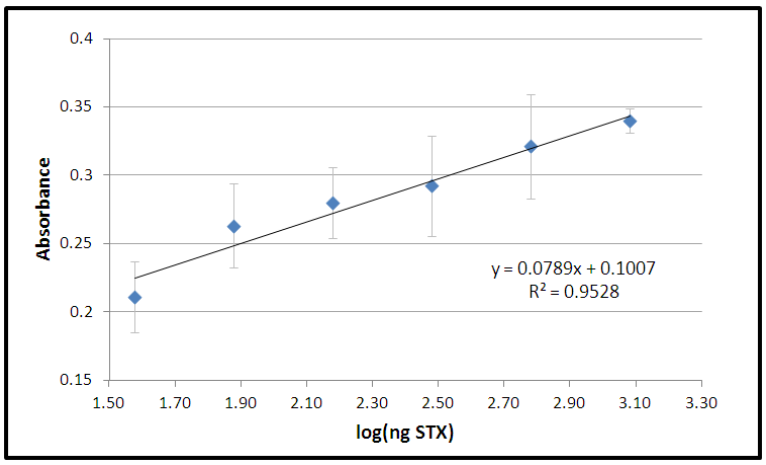

**Appendix A6.** UPLC standard curves of different PSTs.

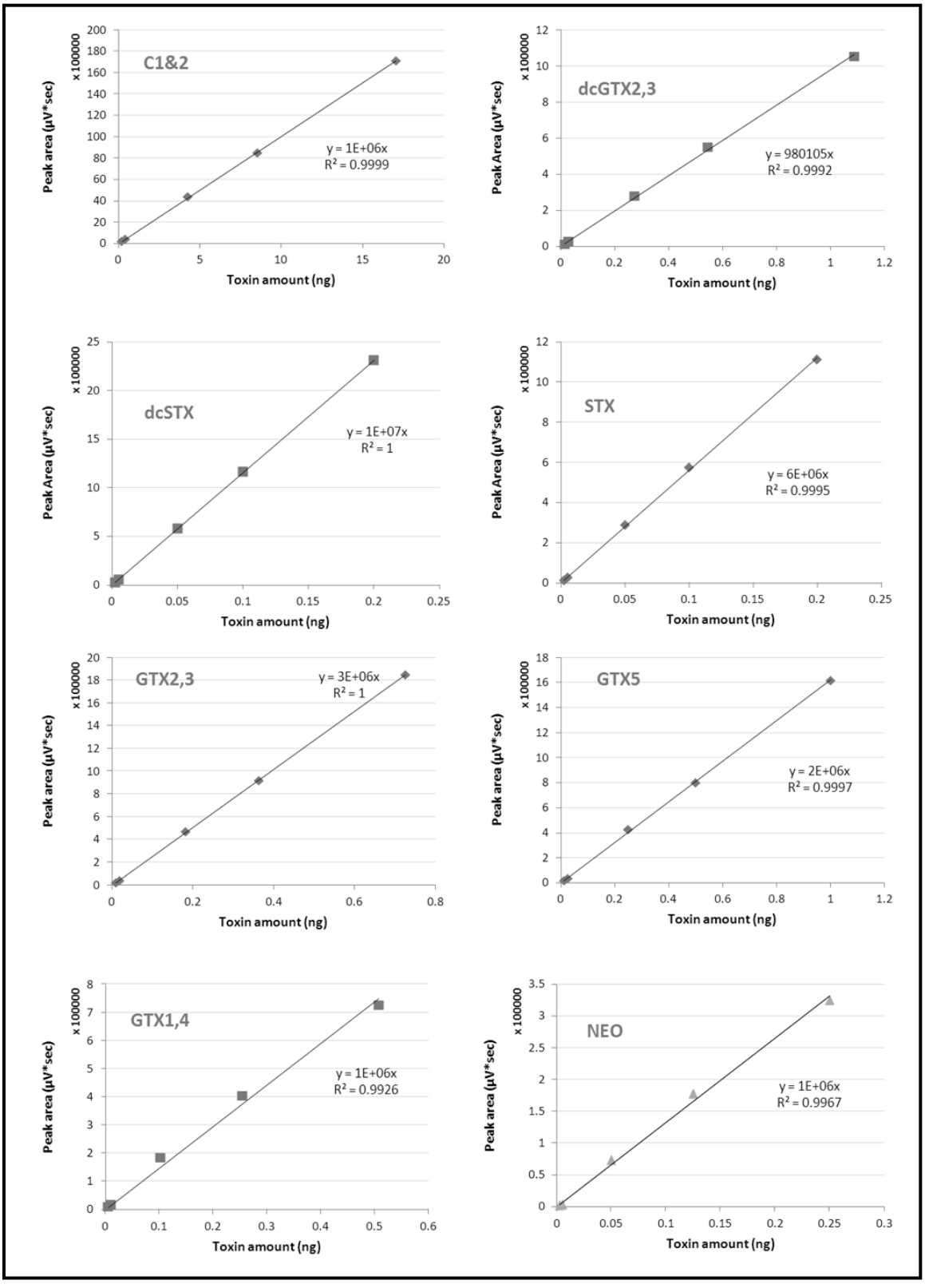

**Appendix A7.** Analysis of variance with SPSS program of toxin data of GC-T at different growth phases. p≈0.43 means there is no significant difference of toxin content between different growth phases.

**Tests of Between-Subjects Effects**

Dependent Variable:Data

| Source | Type III Sum of Squares | df | Mean Square | F | Sig. |
|---|---|---|---|---|---|
| Corrected Model | 5.750E8 | 4 | 1.438E8 | 1.043 | .429 |
| Intercept | 1.731E10 | 1 | 1.731E10 | 125.532 | .000 |
| Group | 5.750E8 | 4 | 1.438E8 | 1.043 | .429 |
| Error | 1.516E9 | 11 | 1.379E8 | | |
| Total | 2.032E10 | 16 | | | |
| Corrected Total | 2.092E9 | 15 | | | |

a. R Squared = .275 (Adjusted R Squared = .011)

**Appendix A8.** Analysis of variance with SPSS program of arginine measurements of GC-T, AC-T and AT-N. p≈0.19 means there is no significant difference of arginine concentration between the three dinoflagellates.

**Tests of Between-Subjects Effects**

Dependent Variable:VAR00001

| Source | Type III Sum of Squares | df | Mean Square | F | Sig. |
|---|---|---|---|---|---|
| Corrected Model | 27.429[a] | 2 | 13.715 | 1.888 | .194 |
| Intercept | 228.931 | 1 | 228.931 | 31.519 | .000 |
| VAR00002 | 27.429 | 2 | 13.715 | 1.888 | .194 |
| Error | 87.160 | 12 | 7.263 | | |
| Total | 343.520 | 15 | | | |
| Corrected Total | 114.589 | 14 | | | |

a. R Squared = .239 (Adjusted R Squared = .113)

**Appendix A9.** Post Hoc tests between the different sampling time points of arginine measurement of GC-T. The highlighted column shows the p values. $p<0.05$ means there is significantly difference between the two compared groups at 95% confidence level. Results shows that the arginine content in Day 2 (log phase) and Day 58 (decline phase) samples were different from the levels in Day 8, 18 & 38 (exponential phase). And no significant variation of arginine levels was found within the different sampling points (Day 8, 18 & 38) of exponential phases.

**Multiple Comparisons**

VAR00001
LSD

| (I) VAR00002 | (J) VAR00002 | Mean Difference (I-J) | Std. Error | Sig. | 95% Confidence Interval | |
|---|---|---|---|---|---|---|
| | | | | | Lower Bound | Upper Bound |
| Day18 | Day2 | -122.0833* | 43.52717 | .023 | -222.4572 | -21.7095 |
| | Day38 | 87.7167 | 43.52717 | .079 | -12.6572 | 188.0905 |
| | Day58 | -117.9667* | 38.93189 | .016 | -207.7438 | -28.1896 |
| | Day8 | 29.0667 | 38.93189 | .477 | -60.7104 | 118.8438 |
| Day2 | Day18 | 122.0833* | 43.52717 | .023 | 21.7095 | 222.4572 |
| | Day38 | 209.8000* | 47.68163 | .002 | 99.8460 | 319.7540 |
| | Day58 | 4.1167 | 43.52717 | .927 | -96.2572 | 104.4905 |
| | Day8 | 151.1500* | 43.52717 | .008 | 50.7762 | 251.5238 |
| Day38 | Day18 | -87.7167 | 43.52717 | .079 | -188.0905 | 12.6572 |
| | Day2 | -209.8000* | 47.68163 | .002 | -319.7540 | -99.8460 |
| | Day58 | -205.6833* | 43.52717 | .001 | -306.0572 | -105.3095 |
| | Day8 | -58.6500 | 43.52717 | .215 | -159.0238 | 41.7238 |
| Day58 | Day18 | 117.9667* | 38.93189 | .016 | 28.1896 | 207.7438 |
| | Day2 | -4.1167 | 43.52717 | .927 | -104.4905 | 96.2572 |
| | Day38 | 205.6833* | 43.52717 | .001 | 105.3095 | 306.0572 |
| | Day8 | 147.0333* | 38.93189 | .005 | 57.2562 | 236.8104 |
| Day8 | Day18 | -29.0667 | 38.93189 | .477 | -118.8438 | 60.7104 |
| | Day2 | -151.1500* | 43.52717 | .008 | -251.5238 | -50.7762 |
| | Day38 | 58.6500 | 43.52717 | .215 | -41.7238 | 159.0238 |
| | Day58 | -147.0333* | 38.93189 | .005 | -236.8104 | -57.2562 |

Based on observed means.
The error term is Mean Square(Error) = 2273.538.

*. The mean difference is significant at the .05 level.

**Appendix A10.** Analysis of variance with SPSS program of toxin analysis of GC-T under different nitrate supply. p≈0.51 means there is no significant difference of toxin content between the three conditions.

**Tests of Between-Subjects Effects**

Dependent Variable:VAR00001

| Source | Type III Sum of Squares | df | Mean Square | F | Sig. |
|---|---|---|---|---|---|
| Corrected Model | 4.810E8 | 2 | 2.405E8 | .732 | .514 |
| Intercept | 2.355E10 | 1 | 2.355E10 | 71.674 | .000 |
| VAR00002 | 4.810E8 | 2 | 2.405E8 | .732 | .514 |
| Error | 2.300E9 | 7 | 3.286E8 | | |
| Total | 2.624E10 | 10 | | | |
| Corrected Total | 2.781E9 | 9 | | | |

a. R Squared = .173 (Adjusted R Squared = -.063)

**Appendix A11.** Independent sample t-test with SPSS program of toxin analysis of AC-T under (1) normal and (2) $NO_3$-limited contdition. p≈0.24 means there is no significant difference of toxin content between the two groups.

**Independent Samples Test**

| | | Levene's Test for Equality of Variances | | t-test for Equality of Means | | | | | | |
|---|---|---|---|---|---|---|---|---|---|---|
| | | | | | | | | | 95% Confidence Interval of the Difference | |
| | | F | Sig. | t | df | Sig. (2-tailed) | Mean Difference | Std. Error Difference | Lower | Upper |
| VAR00001 | Equal variances assumed | .090 | .776 | 1.340 | 5 | .238 | 1268.26169 | 946.75956 | -1165.46124 | 3701.98462 |
| | Equal variances not assumed | | | 1.321 | 4.220 | .254 | 1268.26169 | 960.04653 | -1343.44868 | 3879.97205 |

**Appendix A12.** Independent sample t-test with SPSS program of toxin analysis of GC-T under (1) normal and (2) $PO_4$-limited contdition. p≈0.96 means there is no significant difference of toxin content between the two groups.

**Independent Samples Test**

| | | Levene's Test for Equality of Variances | | t-test for Equality of Means | | | | | | |
|---|---|---|---|---|---|---|---|---|---|---|
| | | | | | | | | | 95% Confidence Interval of the Difference | |
| | | F | Sig. | t | df | Sig. (2-tailed) | Mean Difference | Std. Error Difference | Lower | Upper |
| VAR00001 | Equal variances assumed | .189 | .682 | .057 | 5 | .957 | 1328.54527 | 23484.83242 | -59041.13835 | 61698.22889 |
| | Equal variances not assumed | | | .061 | 4.922 | .954 | 1328.54527 | 21776.35238 | -54915.94161 | 57573.03216 |

**Appendix A13.** Independent sample t-test with SPSS program of toxin analysis of AC-T under (1) normal and (2) $PO_4$-limited contdition, at Day 10. p≈0.04 means there is a significant difference of toxin content between the two groups.

**Independent Samples Test**

| | | Levene's Test for Equality of Variances | | t-test for Equality of Means | | | | | | |
|---|---|---|---|---|---|---|---|---|---|---|
| | | | | | | | | | 95% Confidence Interval of the Difference | |
| | | F | Sig. | t | df | Sig. (2-tailed) | Mean Difference | Std. Error Difference | Lower | Upper |
| VAR00001 | Equal variances assumed | 4.636 | .098 | -3.117 | 4 | .036 | -6432.16238 | 2063.63623 | -12161.73511 | -702.58966 |
| | Equal variances not assumed | | | -3.117 | 2.480 | .068 | -6432.16238 | 2063.63623 | -13851.73463 | 987.40986 |

**Appendix A14.** Independent sample t-test with SPSS program of toxin analysis of AC-T under (1) normal and (2) $PO_4$-limited contdition, at Day 20. p≈0.01 means there is a significant difference of toxin content between the two groups.

**Independent Samples Test**

| | | Levene's Test for Equality of Variances | | t-test for Equality of Means | | | | | | |
|---|---|---|---|---|---|---|---|---|---|---|
| | | | | | | | | | 95% Confidence Interval of the Difference | |
| | | F | Sig. | t | df | Sig. (2-tailed) | Mean Difference | Std. Error Difference | Lower | Upper |
| VAR00001 | Equal variances assumed | .134 | .738 | -5.877 | 3 | .010 | -8182.35593 | 1392.30045 | -12613.27735 | -3751.43452 |
| | Equal variances not assumed | | | -5.595 | 1.930 | .033 | -8182.35593 | 1462.50103 | -14698.75932 | -1665.95255 |

**Appendix A15.** Independent sample t-test with SPSS program of toxin analysis of GC-T under (1) normal and (2) arginine-supplemented contdition. p≈0.28 means there is no significant difference of toxin content between the two groups.

**Independent Samples Test**

| | | Levene's Test for Equality of Variances | | t-test for Equality of Means | | | | | | |
|---|---|---|---|---|---|---|---|---|---|---|
| | | | | | | | | | 95% Confidence Interval of the Difference | |
| | | F | Sig. | t | df | Sig. (2-tailed) | Mean Difference | Std. Error Difference | Lower | Upper |
| VAR00001 | Equal variances assumed | .004 | .949 | 1.200 | 5 | .284 | 18523.53782 | 15435.81909 | -21155.49836 | 58202.57399 |
| | Equal variances not assumed | | | 1.171 | 4.038 | .306 | 18523.53782 | 15815.36158 | -25225.98815 | 62273.06378 |

**Appendix A16.** Independent sample t-test with SPSS program of toxin analysis of AC-T under (1) normal and (2) arginine-supplemented contdition. p≈0.61 means there is no significant difference of toxin content between the two groups.

**Independent Samples Test**

| | | Levene's Test for Equality of Variances | | t-test for Equality of Means | | | | | | |
|---|---|---|---|---|---|---|---|---|---|---|
| | | | | | | | | | 95% Confidence Interval of the Difference | |
| | | F | Sig. | t | df | Sig. (2-tailed) | Mean Difference | Std. Error Difference | Lower | Upper |
| VAR00001 | Equal variances assumed | .777 | .418 | -.548 | 5 | .607 | -601.27265 | 1097.25476 | -3421.85580 | 2219.31050 |
| | Equal variances not assumed | | | -.515 | 3.398 | .638 | -601.27265 | 1166.67836 | -4079.89473 | 2877.34943 |

## Appendix B

**Appendix B1.** Alignment of the complete sequence of ITS1-5.8S-ITS2 region of the selected strain (CS-300) of *Alexandrium catenella* for transcriptomic analysis with AC-T and AC-N in the study.

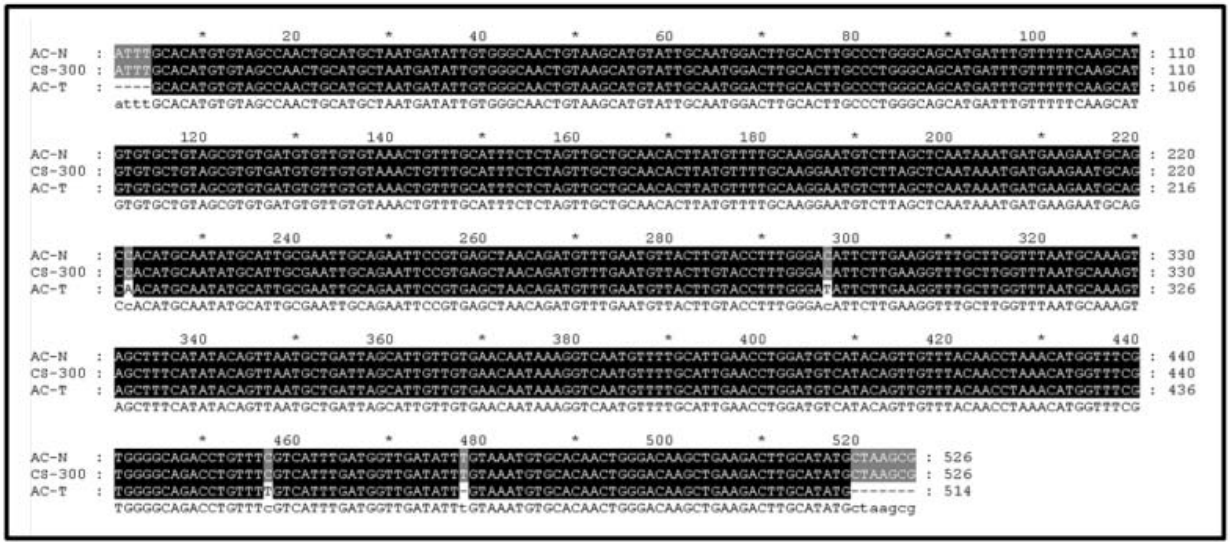

**Appendix B2.** Statistics of transcriptome assembly of *A. catenella*

| | |
|---|---|
| Raw Data | 5 976 312 840 bp |
| G+C content | 59.86% |
| Number of contigs | 133 556 |
| Number of contigs' bases | 112 486 653 bp |
| Number of sequences with 400-1000 bp | 95 854 |
| Number of sequences with 1001-2000 bp | 31 615 |
| Number of sequences with > 2000 bp | 6 384 |
| Contig *N50* | 1 049 |
| Contig length mean | 842 |
| Number if unigenes | 108 596 |
| Number of bases in unigenes | 89 716 414 bp |
| Number of unigenes with 400-1000 bp | 78 764 |
| Number of unigenes with 1001-2000 bp | 25 050 |
| Number of unigenes with >2000 bp | 4 782 |
| Unigene *N50* | 1 032 |
| Unigene length mean | 826 |

**Appendix B3.** Statistics of gene annotation of the transcriptome of *A. catenella*

| | |
|---|---|
| Number annotated unigenes | 71 110 |
| Number of blast CDs | 71 053 |
| Number of sequences with 200-1000 bp | 62 347 |
| Number of sequences with 1000-2000 bp | 7 857 |
| Number of sequences with > 2000 bp | 1 665 |
| Number of EST scan CDs | 18 637 |
| Number of sequences with 200-1000 bp | 16 747 |
| Number of sequences with 1000-2000 bp | 1 803 |
| Number of sequences with > 2000 bp | 87 |

**Appendix B4.** PMF of spot # 10.

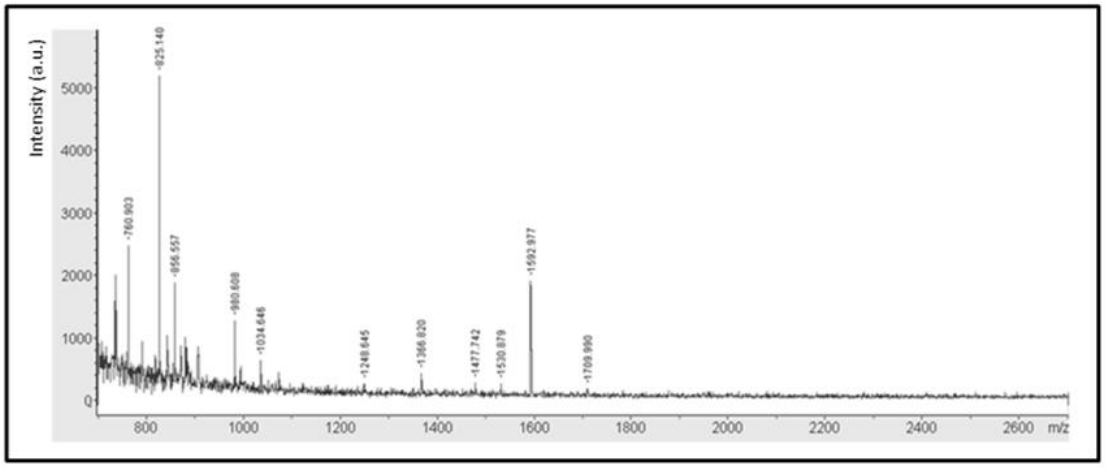


**Appendix B5.** PMF of spot #11.

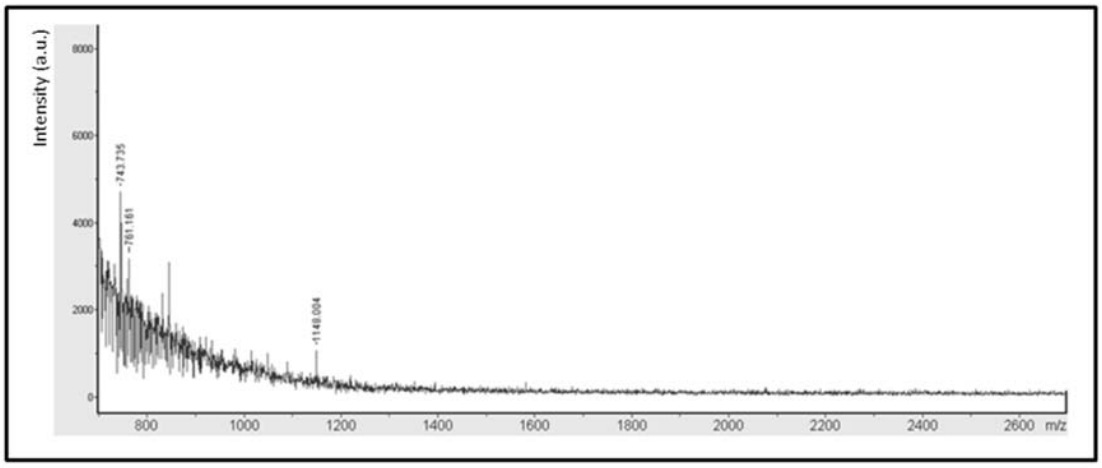

**Appendix B6.** PMF of spot #12.

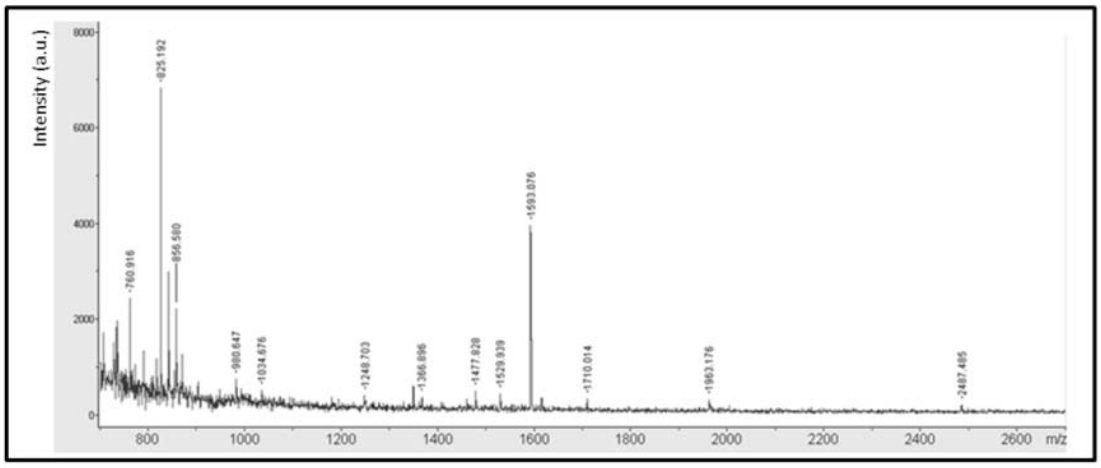


**Appendix B7.** PMF of spot #13.

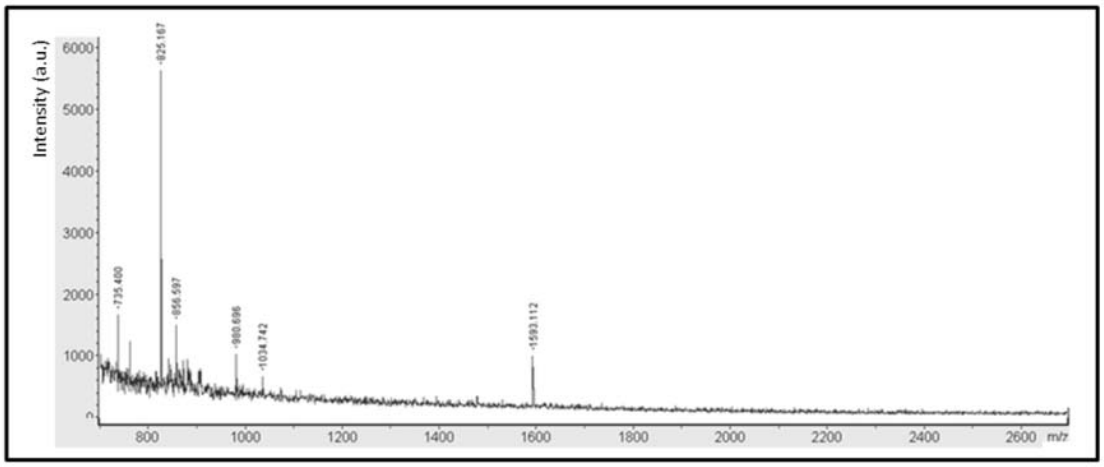


**Appendix B8.** PMF of spot #14.

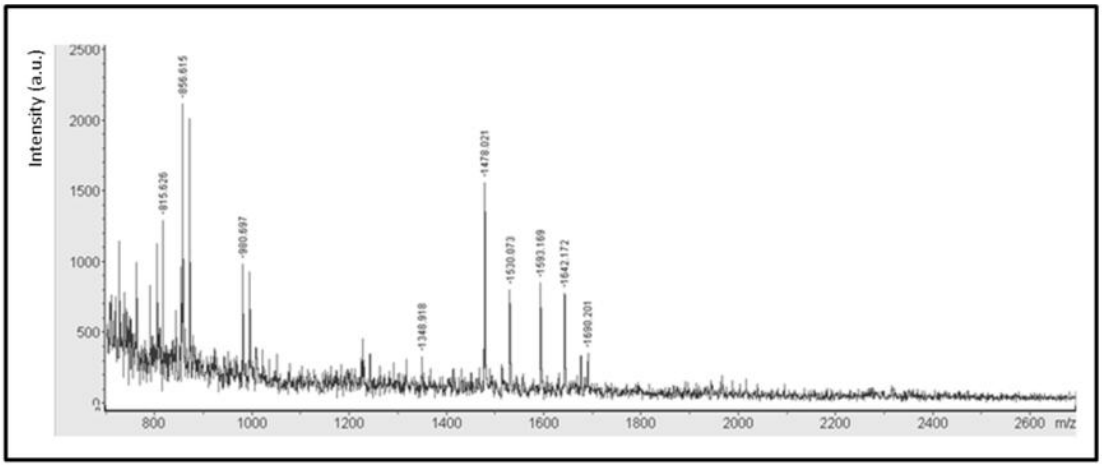

**Appendix B9.** PMF of spot #15.

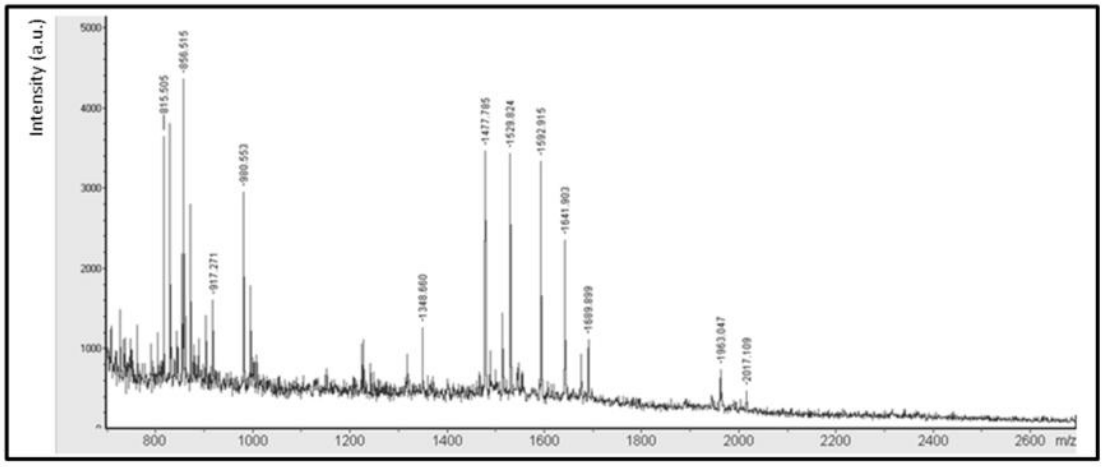


**Appendix B10.** PMF of spot #16.

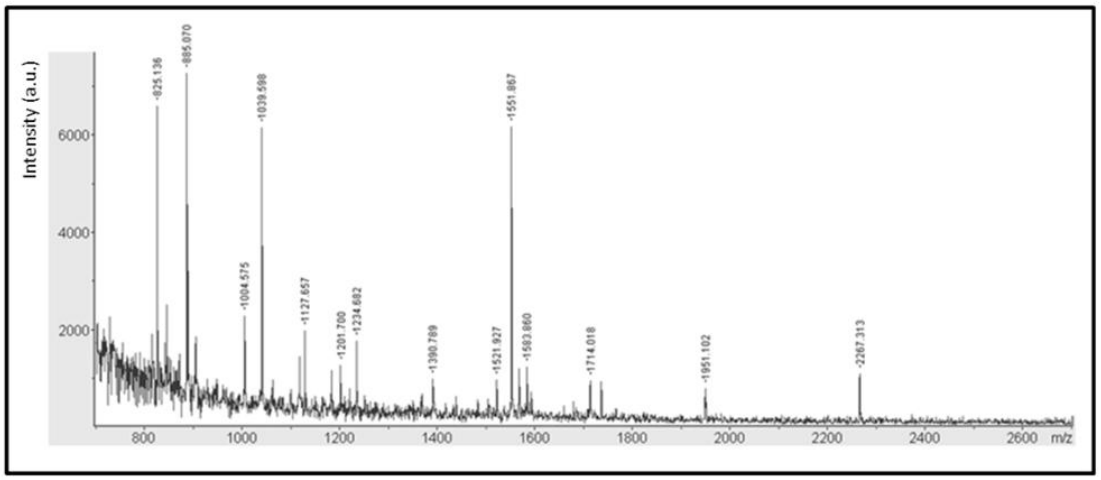


**Appendix B11.** PMF of spot #17.

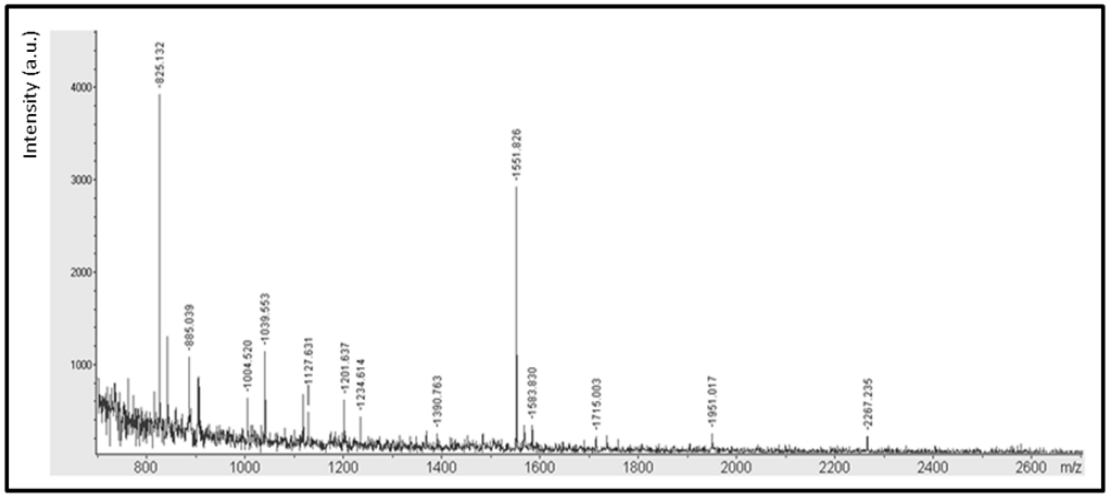

**Appendix B12.** PMF of spot #18.

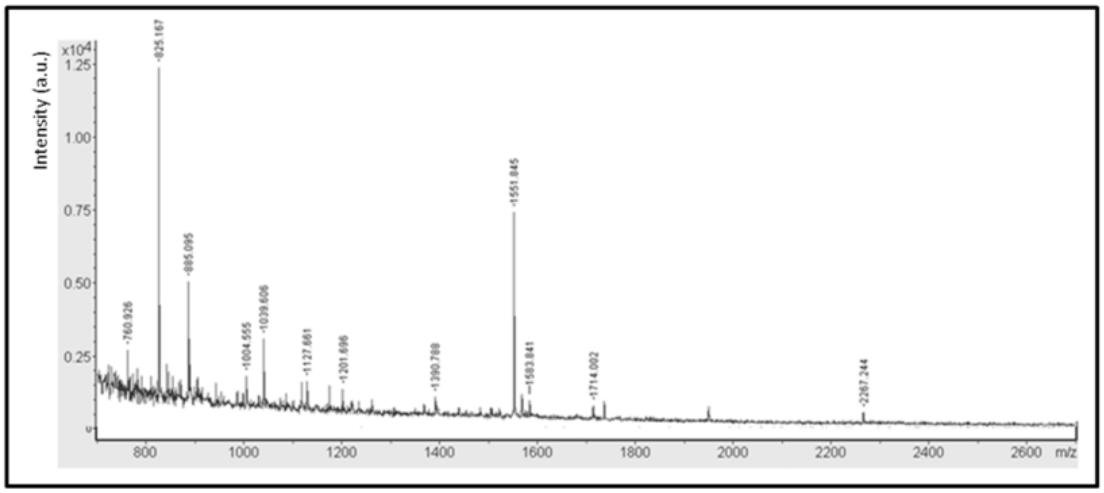


**Appendix B13.** PMF of spot #19.

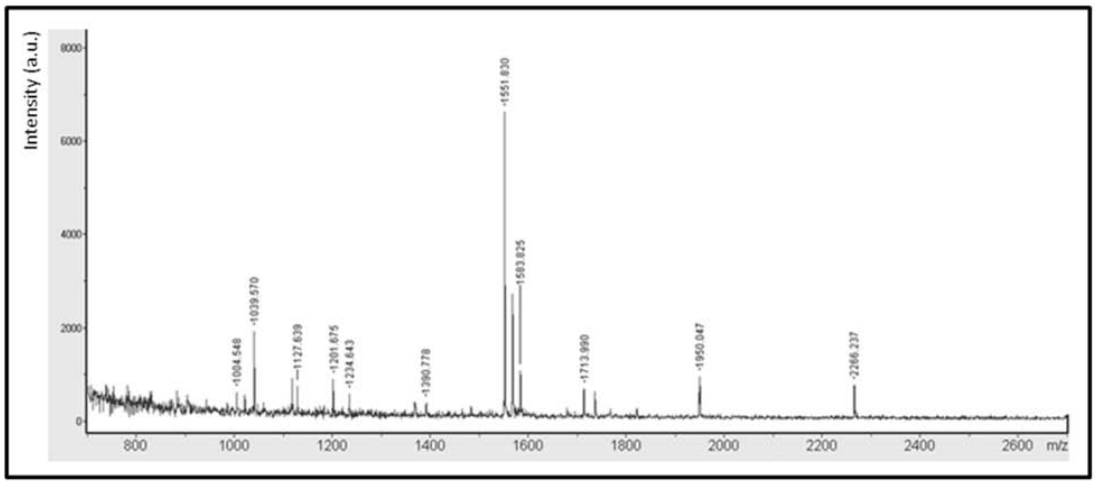


**Appendix B14.** PMF of spot #20.

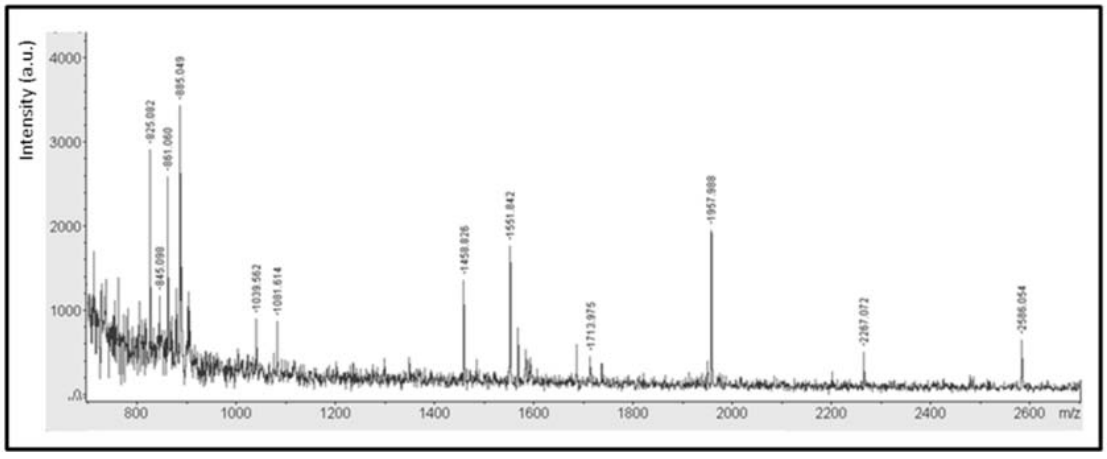

**Appendix B15.** PMF of spot #21.

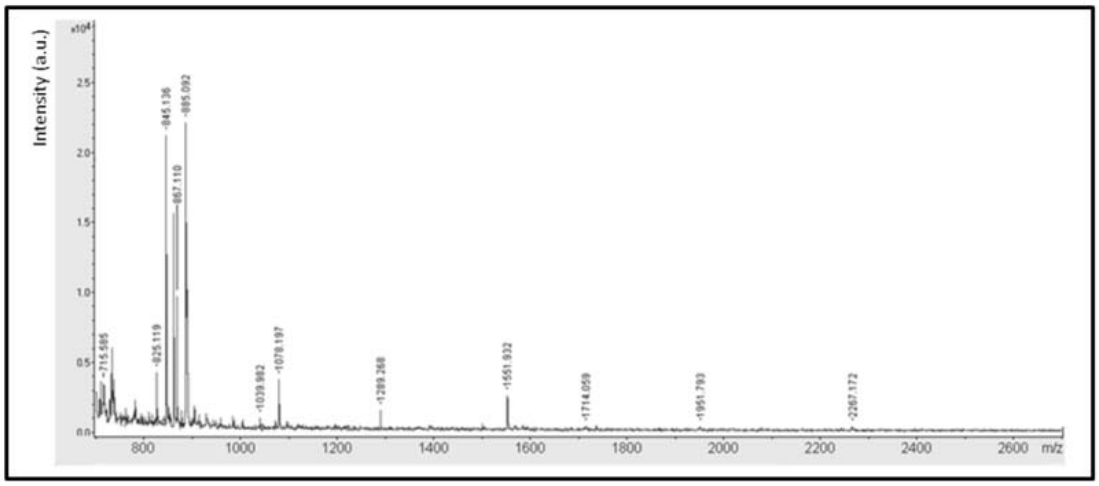


**Appendix B16.** PMF of spot #22.

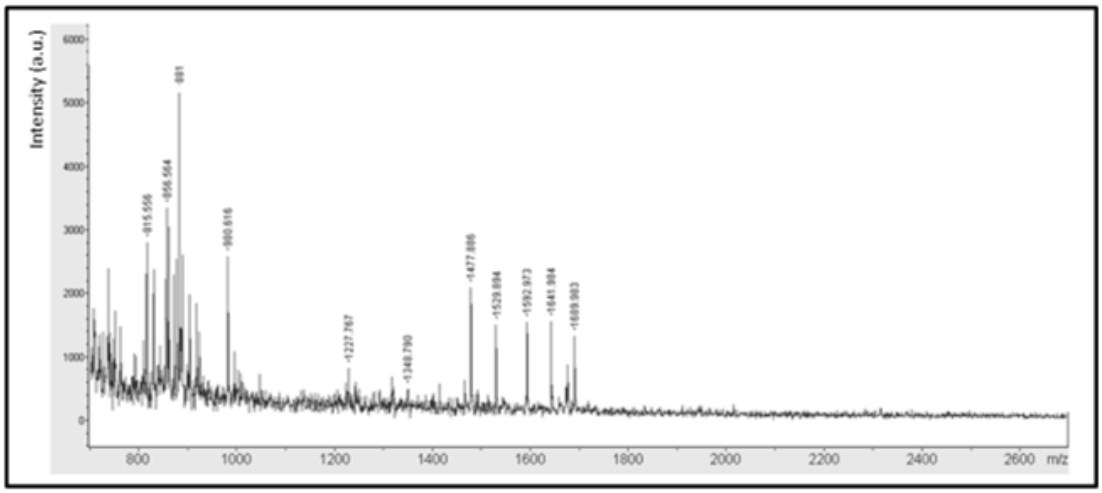


**Appendix B17.** PMF of spot #27.

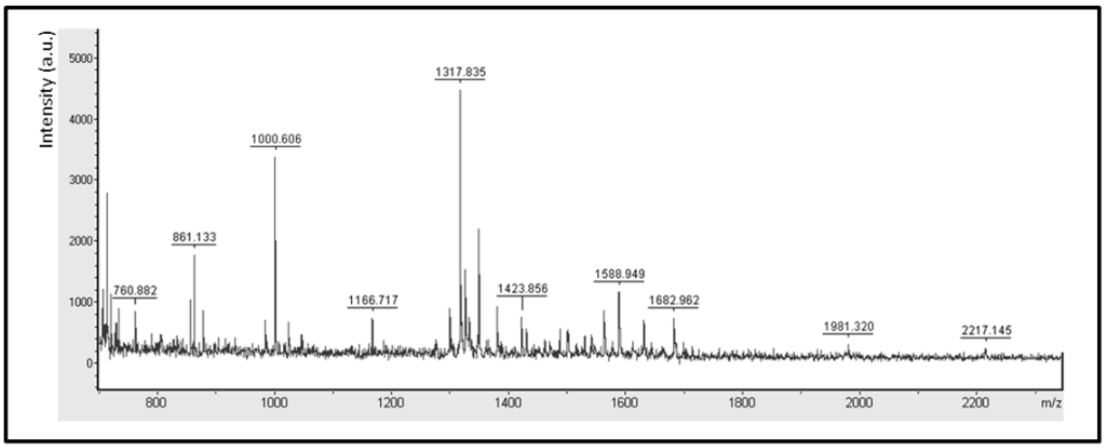

**Appendix B18.** PMF of spot #28.

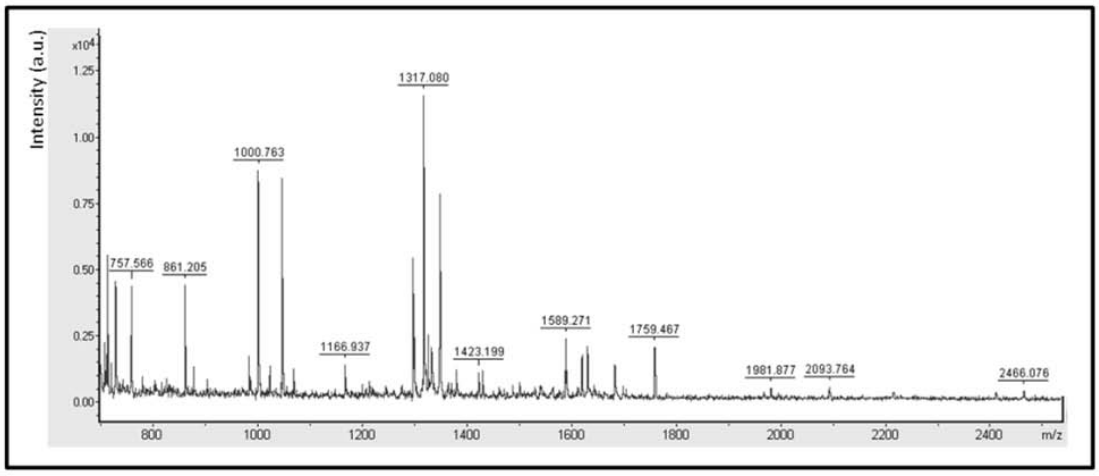


**Appendix B19.** PMF of spot #31.

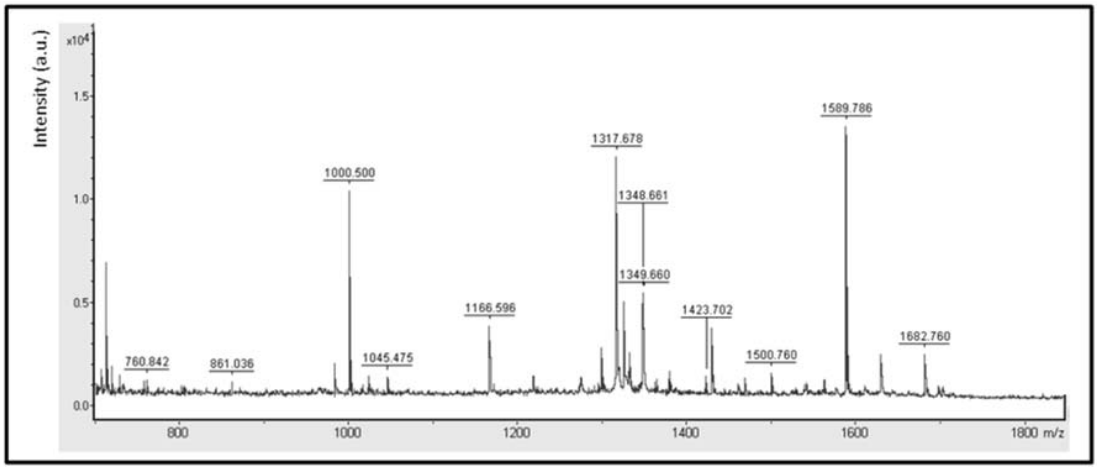


**Appendix B20.** PMF of spot #32.

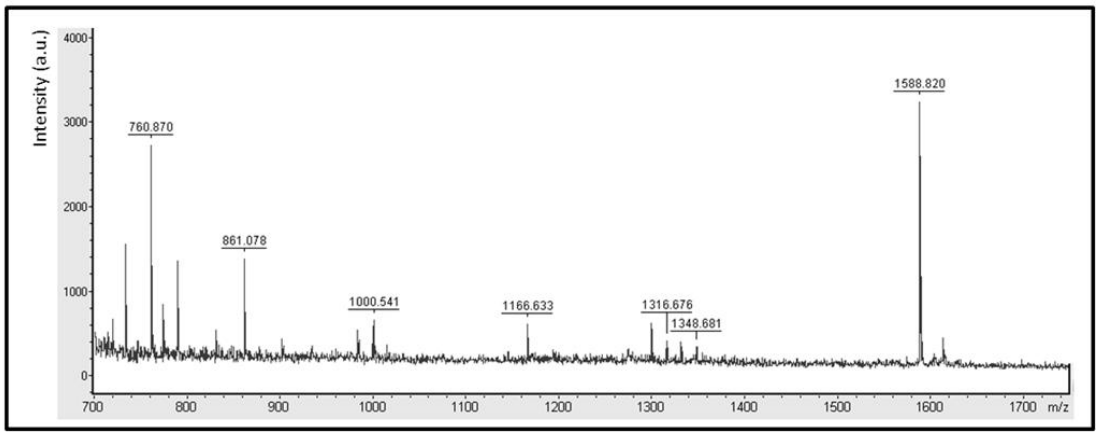

**Appendix B21.** PMF of spot #33.

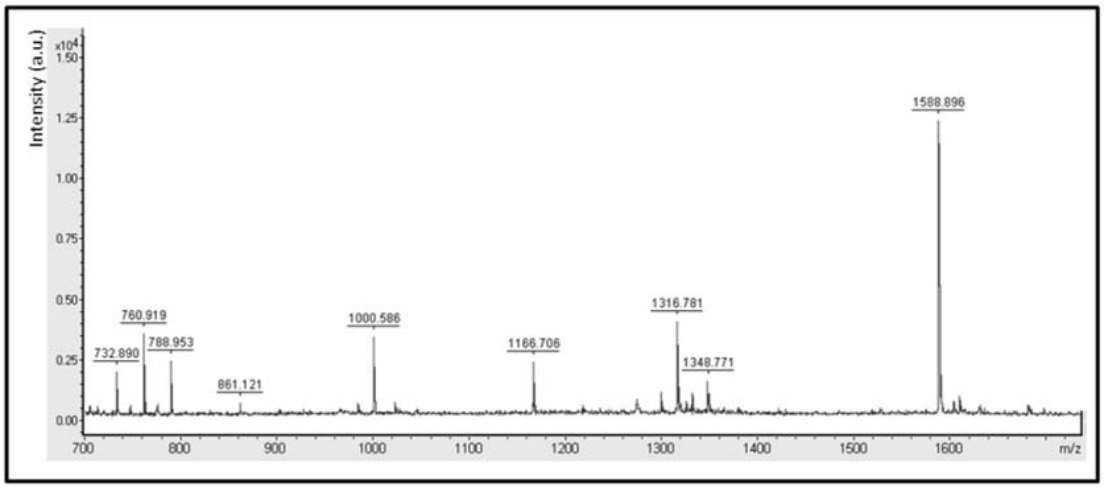


**Appendix B22.** PMF of spot #37.

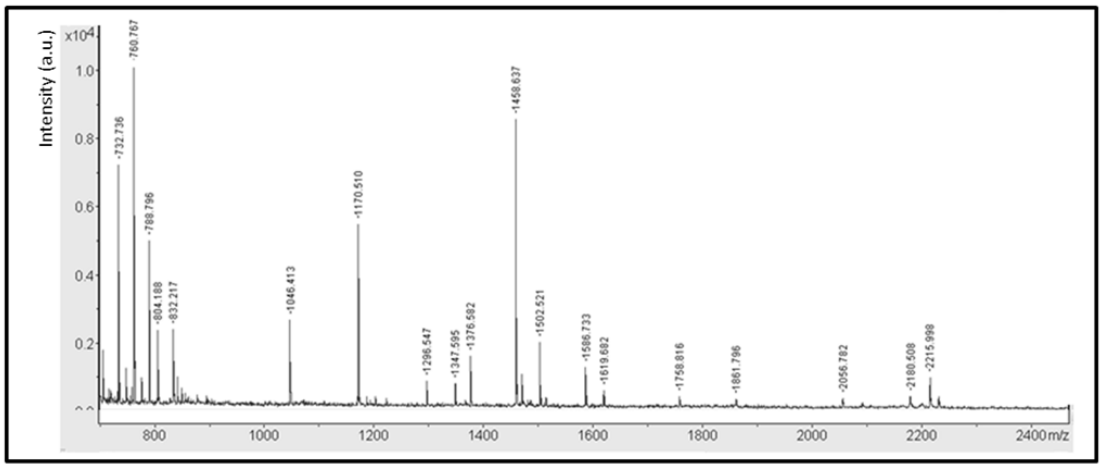


**Appendix B23.** PMF of spot #38.

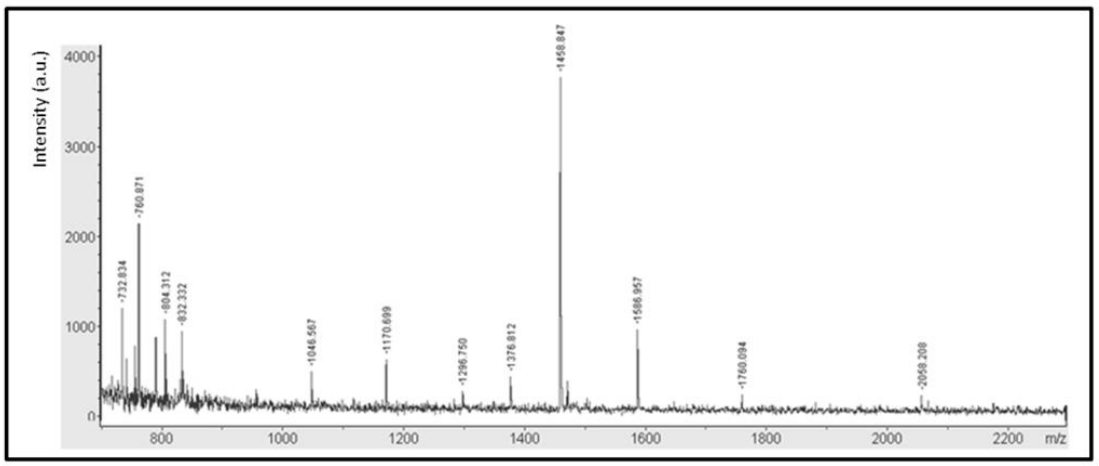

**Appendix B24.** PMF of spot #54.

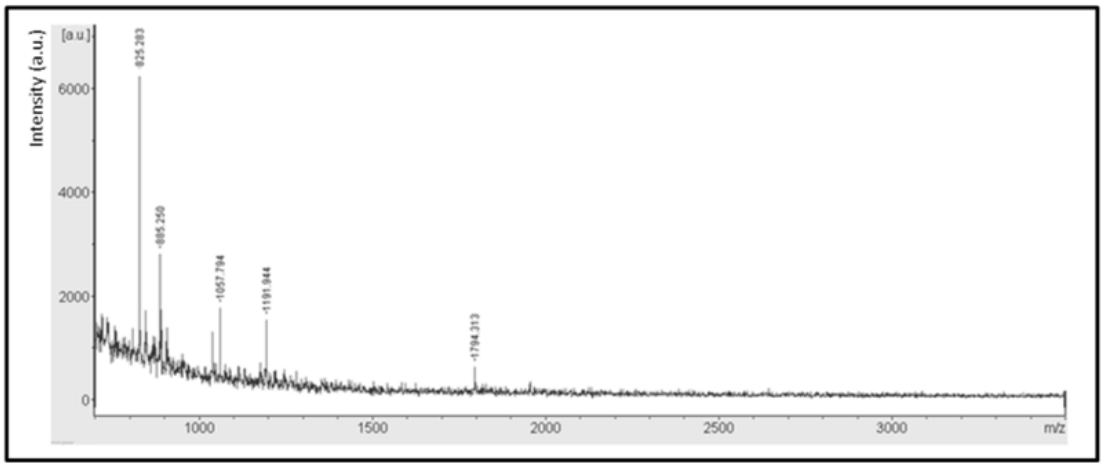


**Appendix B25.** PMF of spot #62.

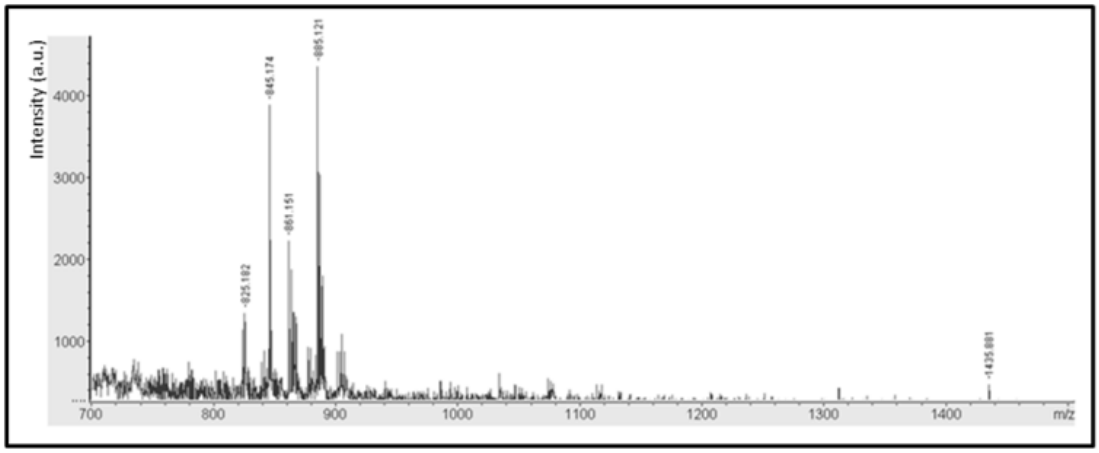


**Appendix B26.** PMF of spot #63.

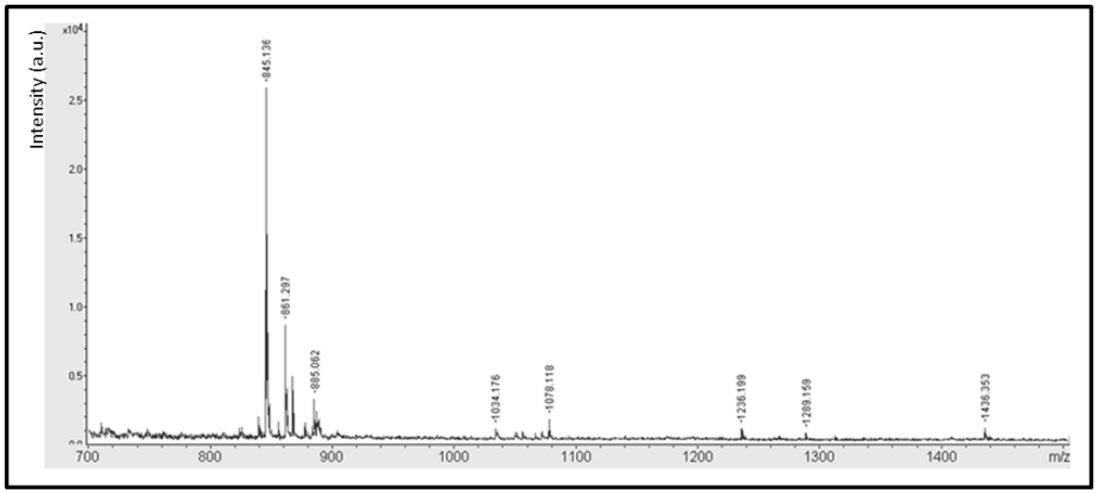

**Appendix B27.** PMF of spot #65.

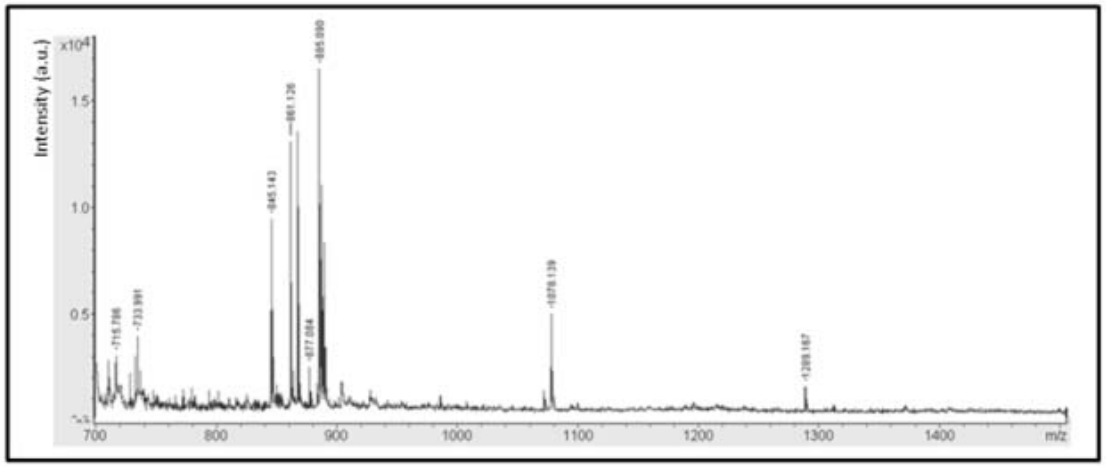


**Appendix B28.** PMF of spot 66.

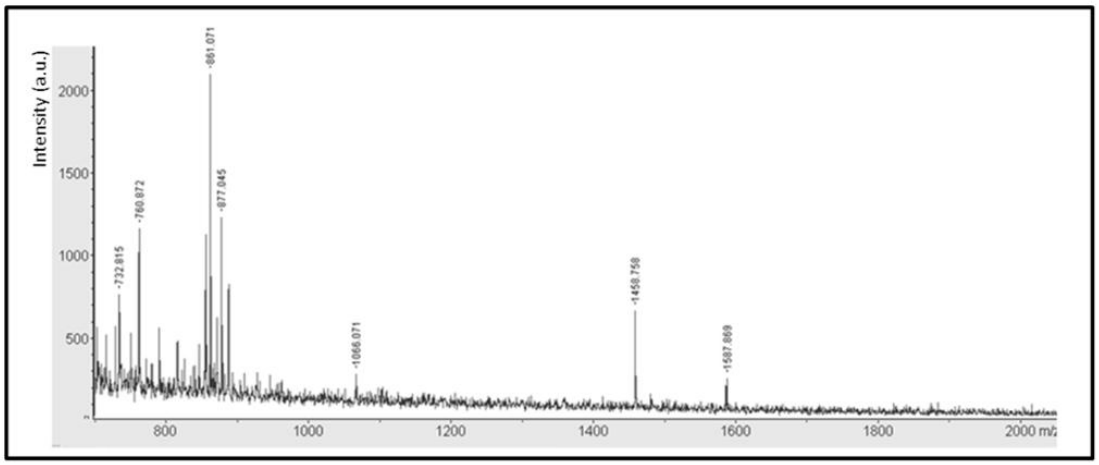


**Appendix B29.** PMF of spot #68.

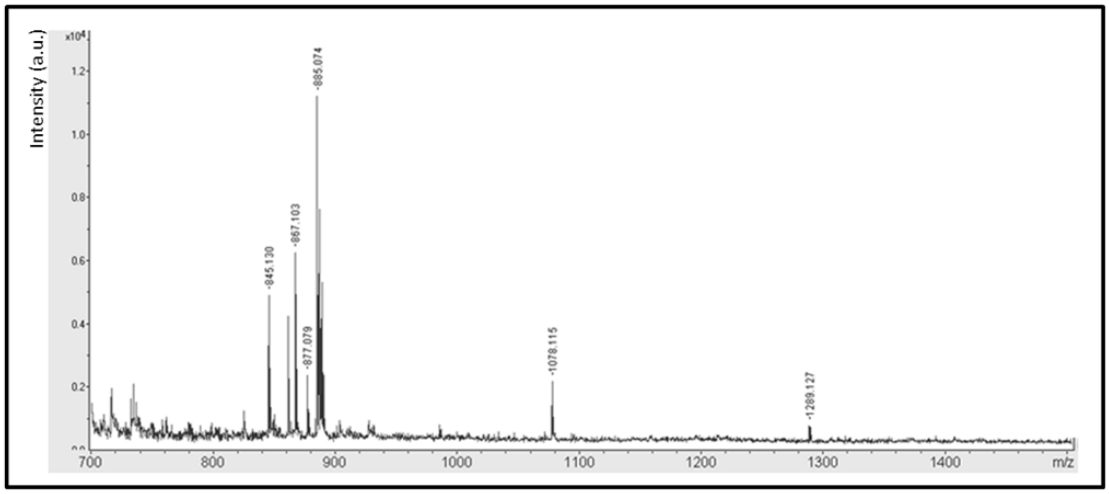

**Appendix B30.** PMF of spot #73.

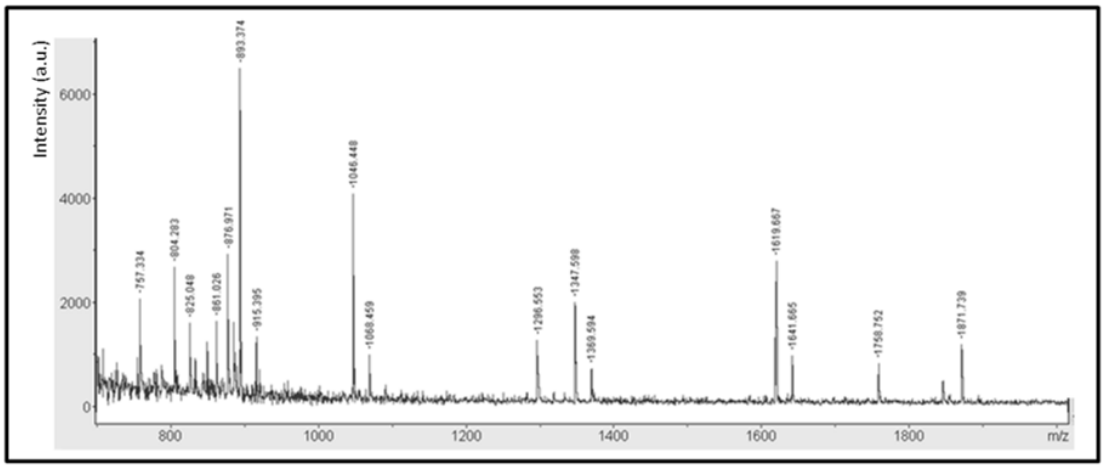


**Appendix B31.** PMF of spot #78.

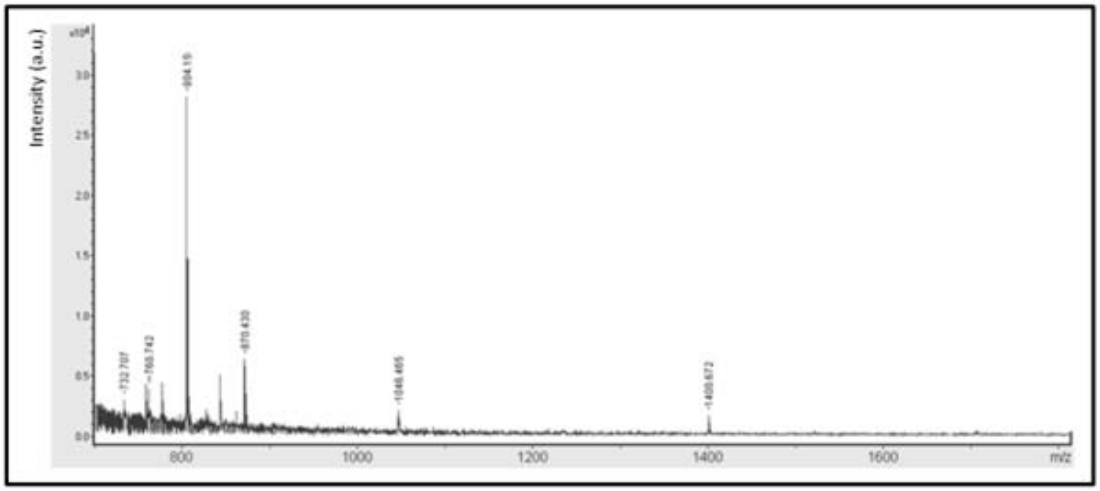


**Appendix B32.** PMF of spot #85.

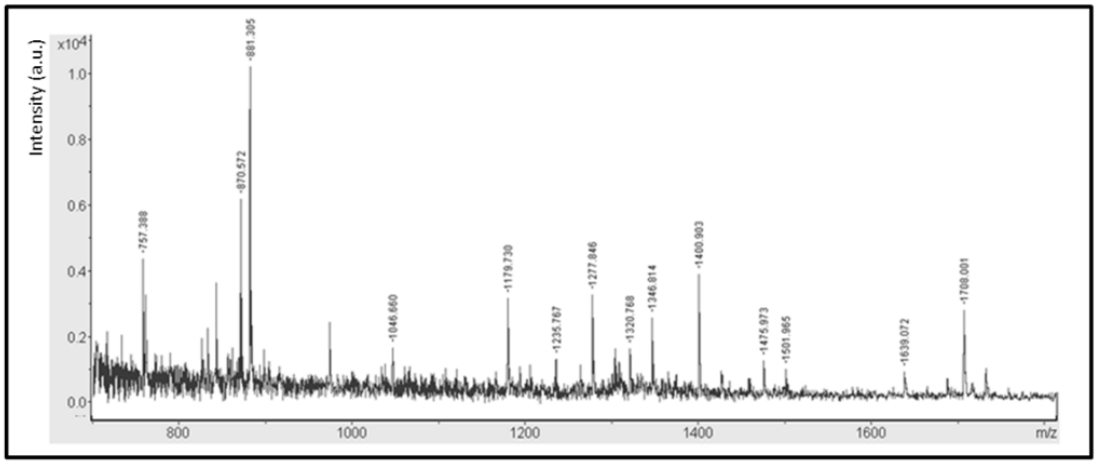

**Appendix B33.** PMF of spot #86.

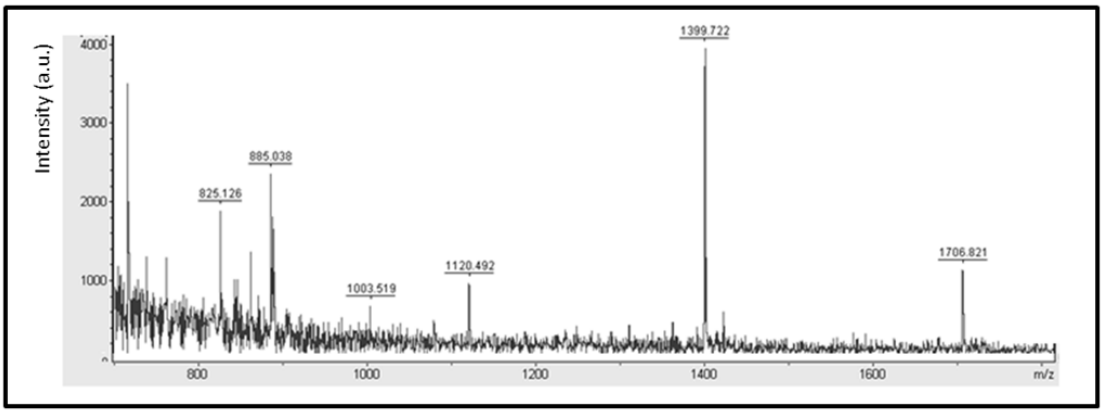


**Appendix B34.** PMF of spot #87.

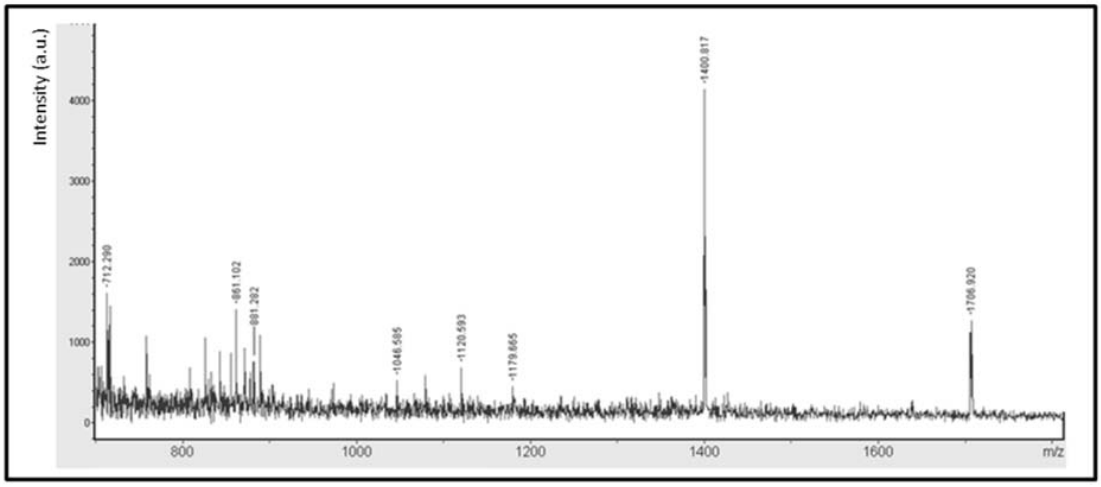


**Appendix B35.** PMF of spot #96.

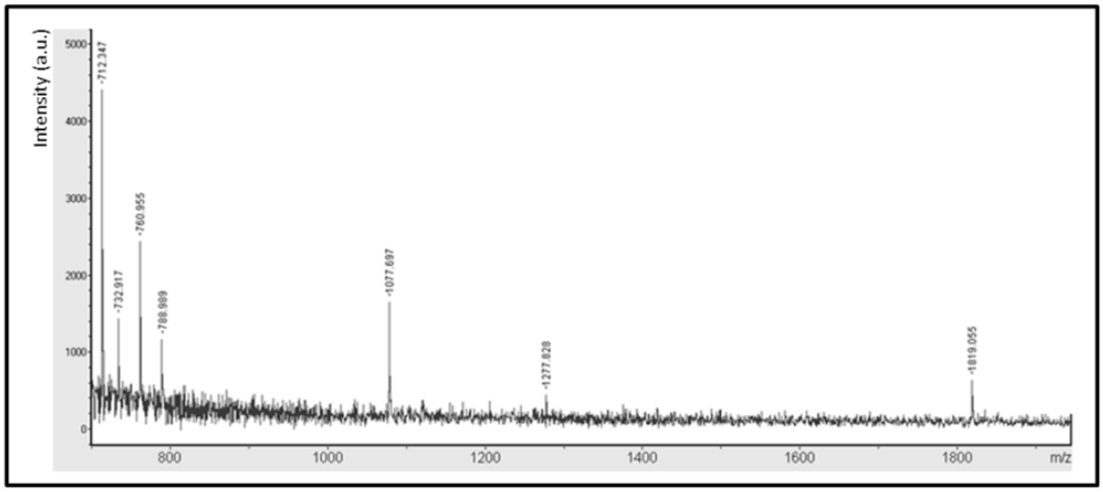

**Appendix B36.** PMF of spot #97.

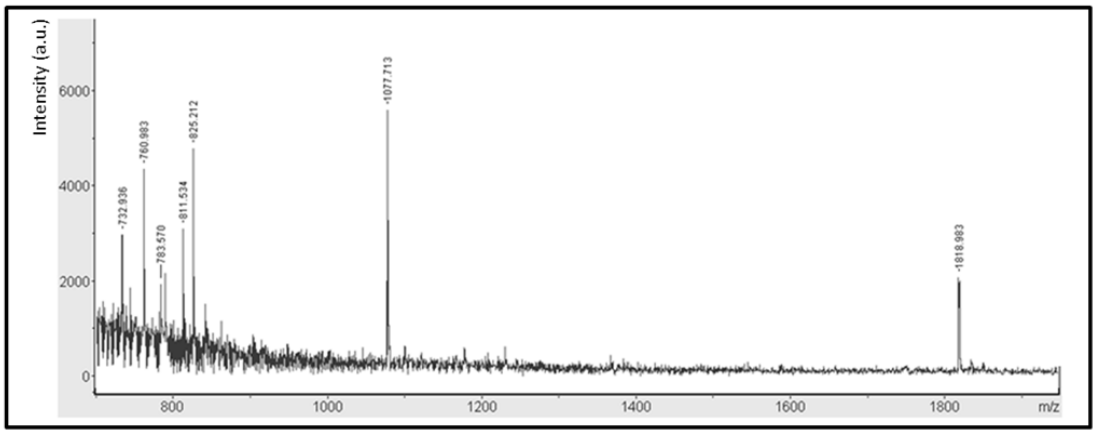


**Appendix B37.** PMF of spot #98.

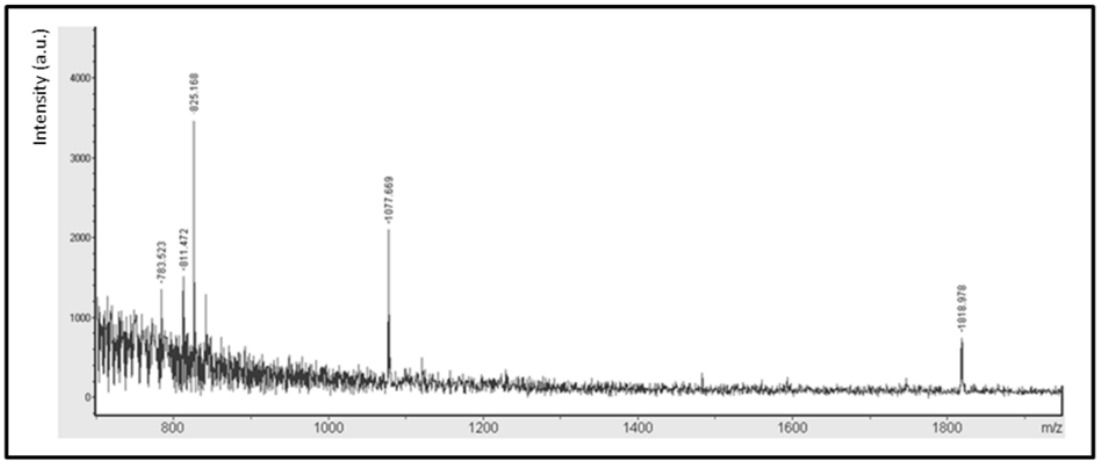


**Appendix B38.** PMF of spot #105.

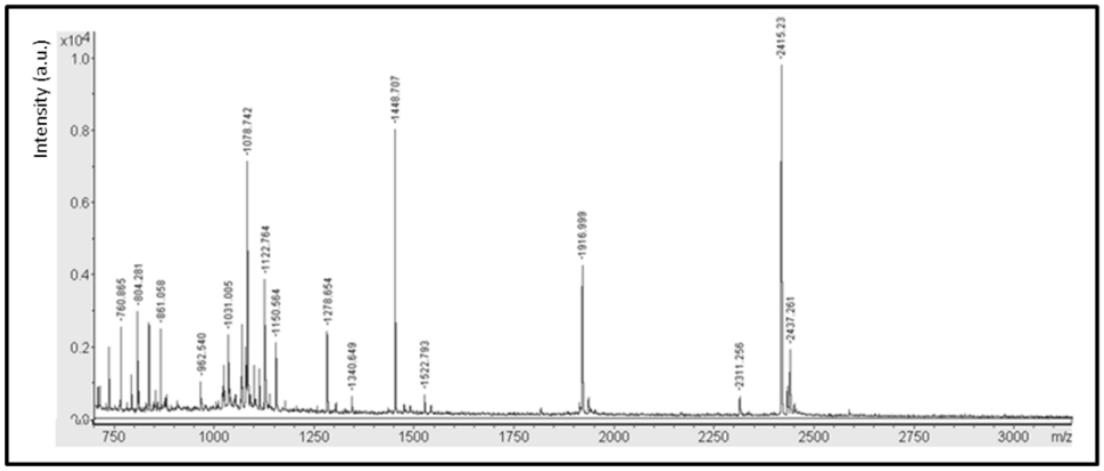

**Appendix B39.** PMF of spot #108.

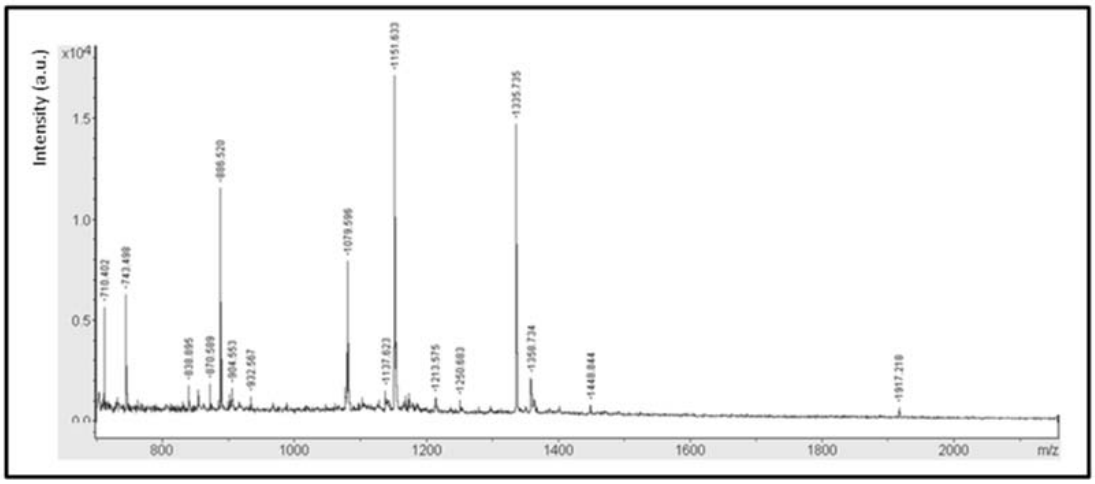


**Appendix B40.** PMF of spot #117.

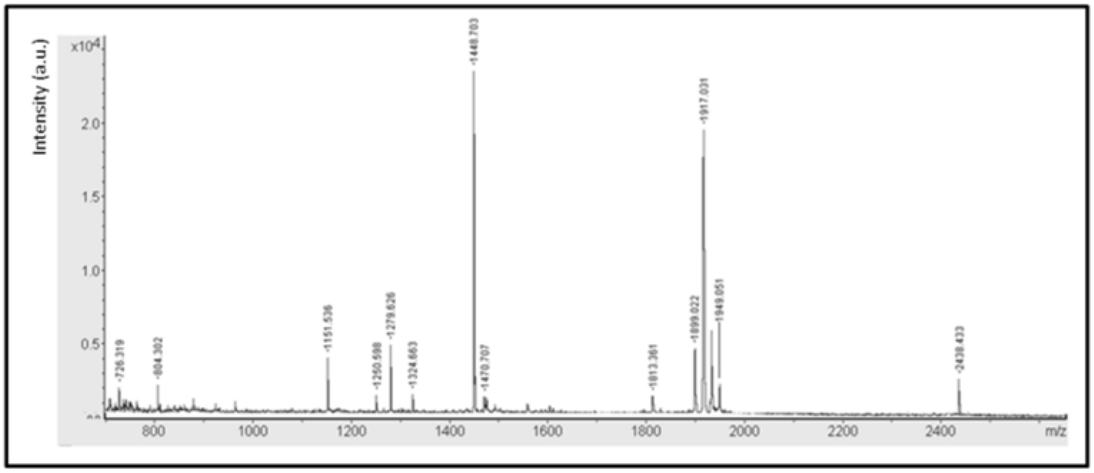


**Appendix B41.** PMF of spot #118.

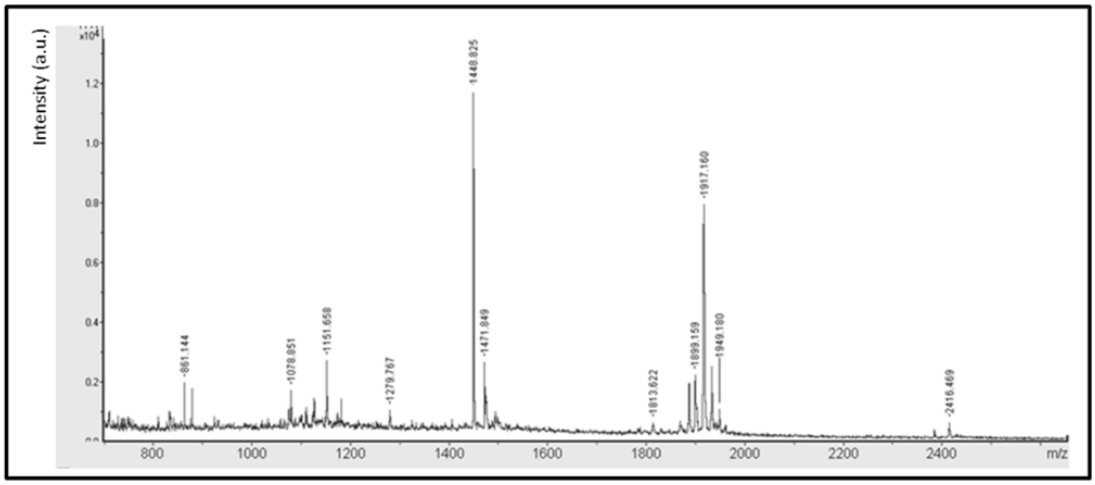

**Appendix B42.** PMF of spot 123.

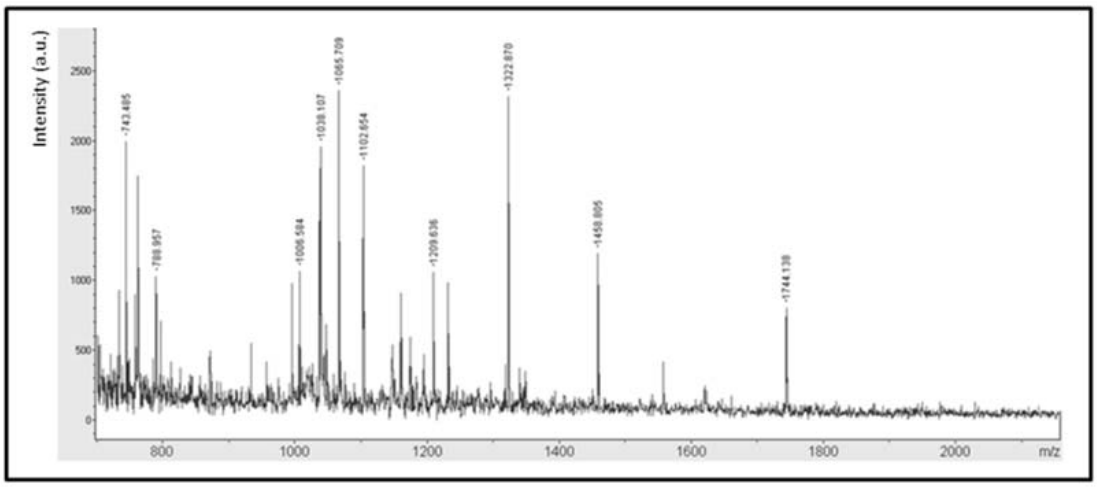


**Appendix B43.** PMF of spot #125.

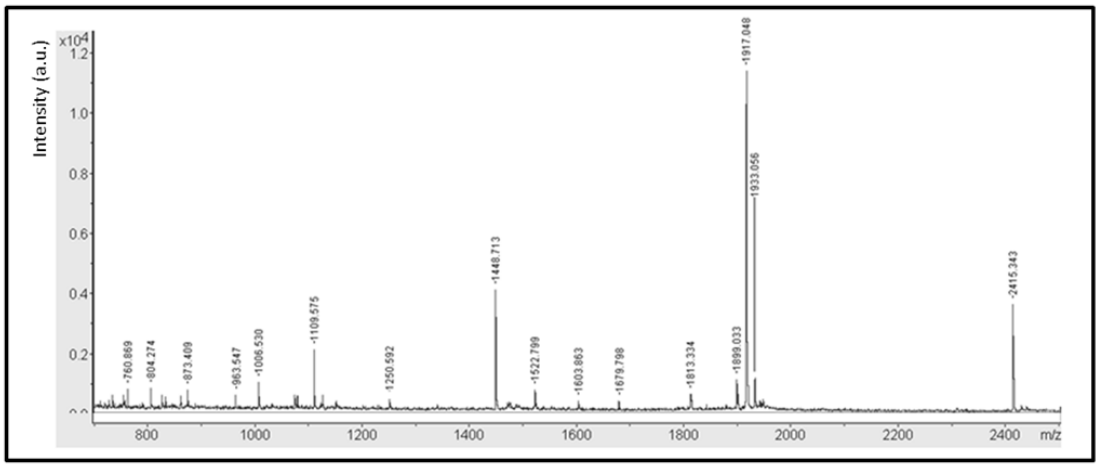


**Appendix B44.** PMF of spot #126.

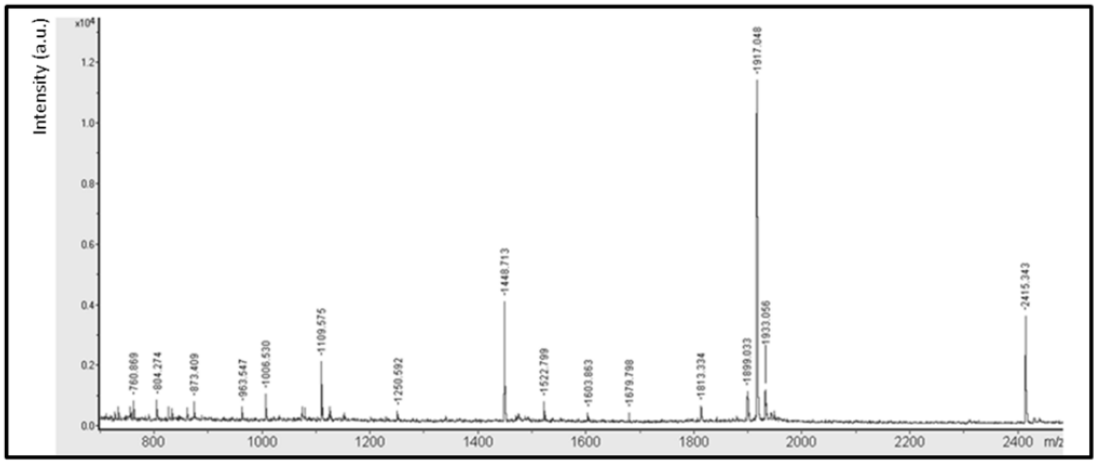

**Appendix B45.** PMF of spot #131.

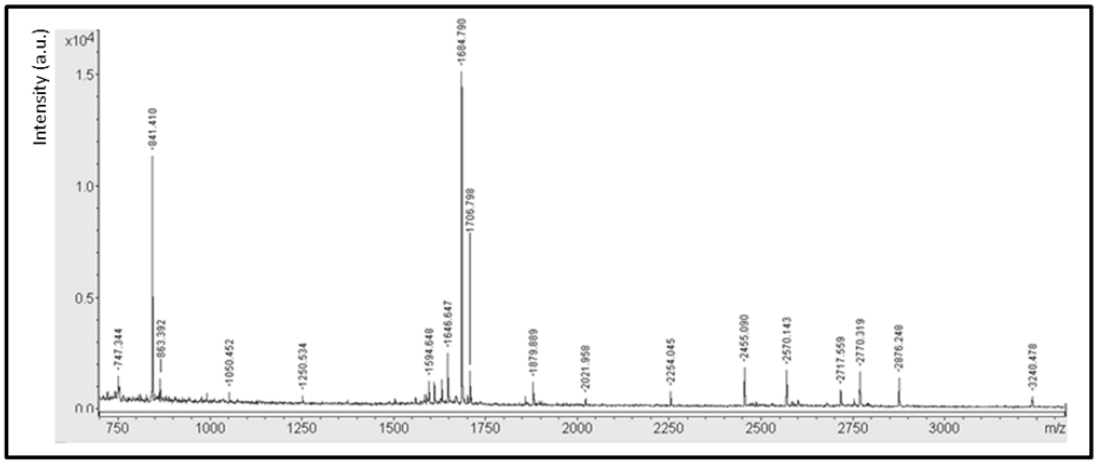


**Appendix B46.** PMF of spot #132.

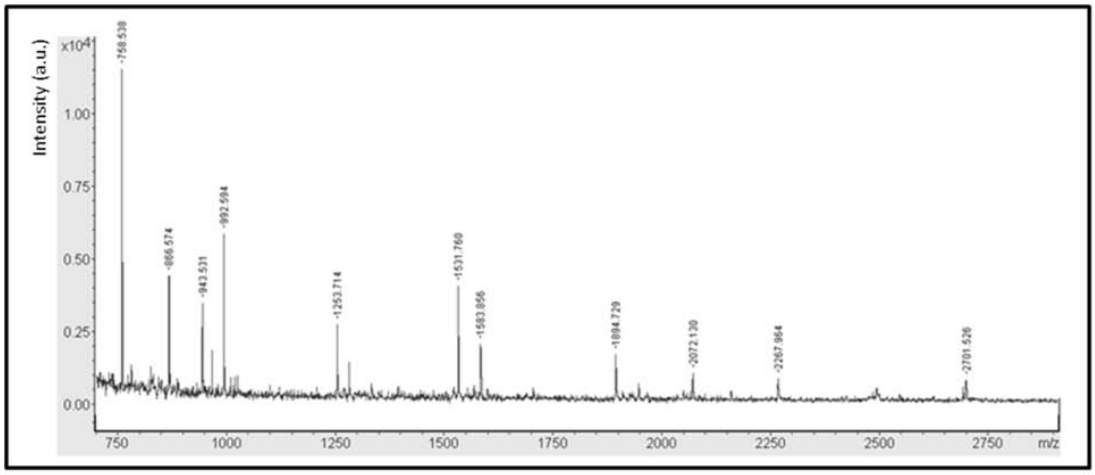


**Appendix B47.** PMF of spot #133.

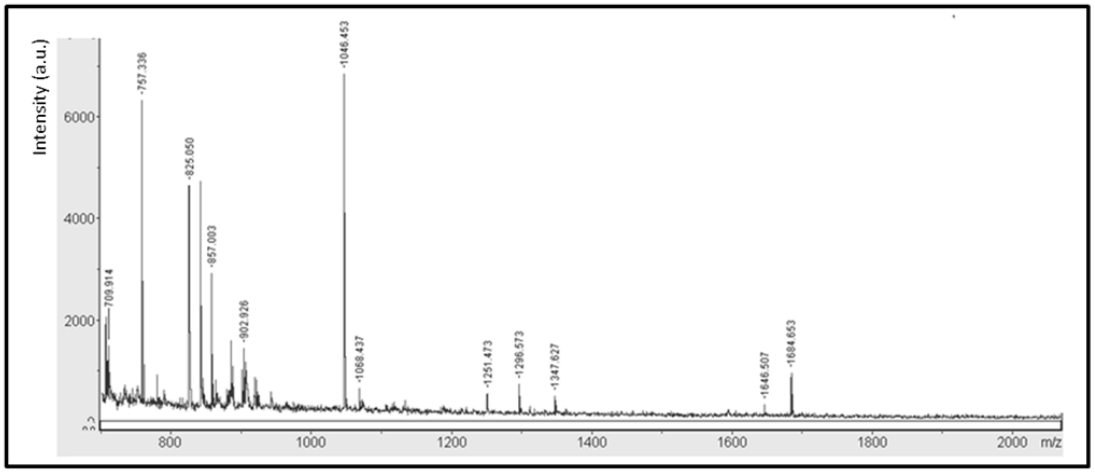

**Appendix B48.** PMF of spot #134.

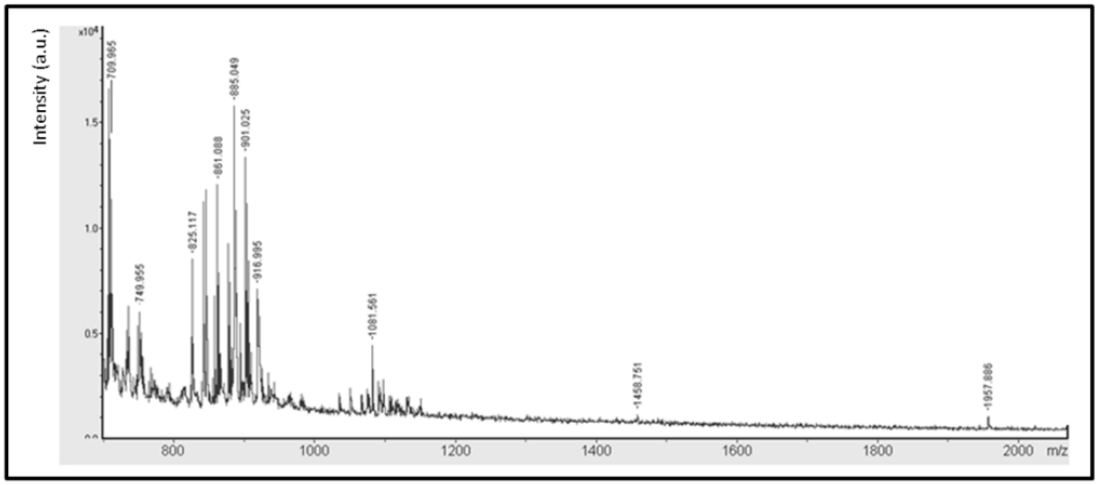


**Appendix B49.** PMF of spot #137.

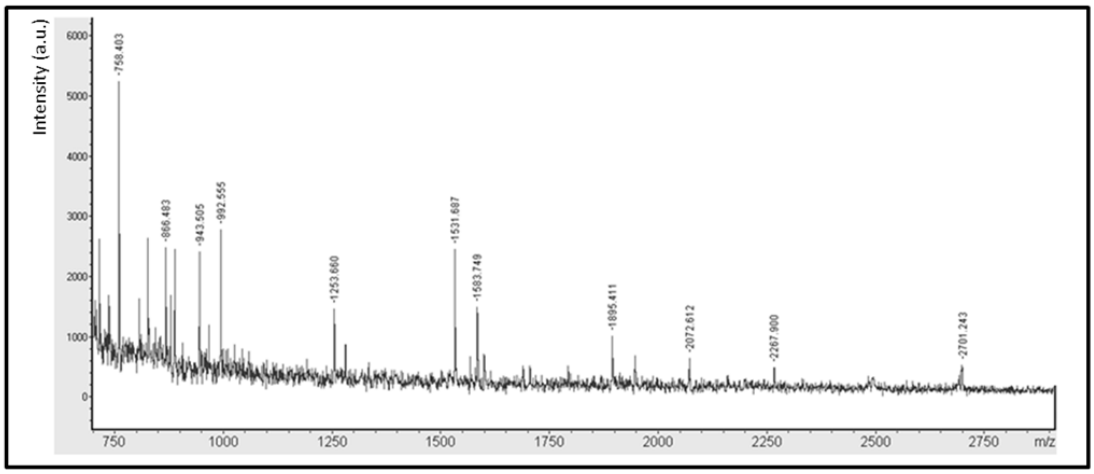


**Appendix B50.** PMF of spot #170.

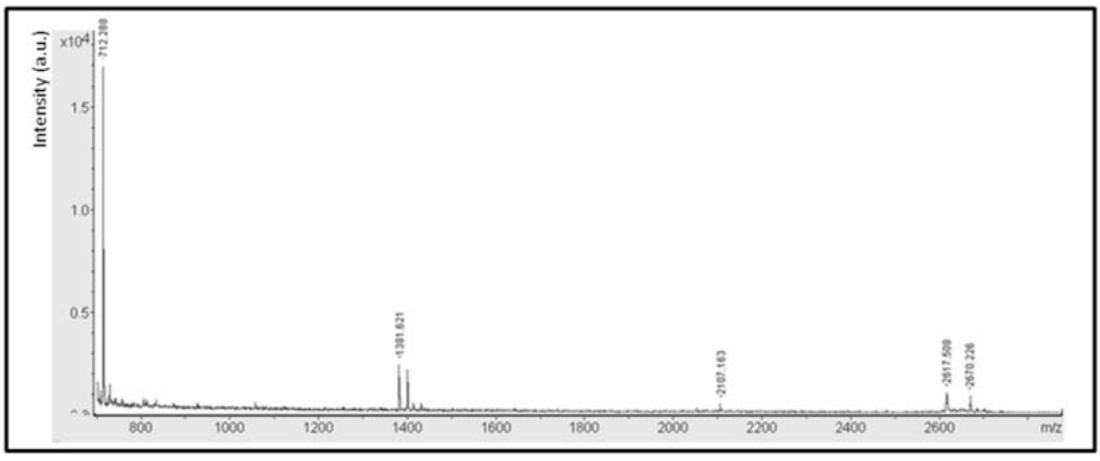

**Appendix B51.** PMF of spot #173.

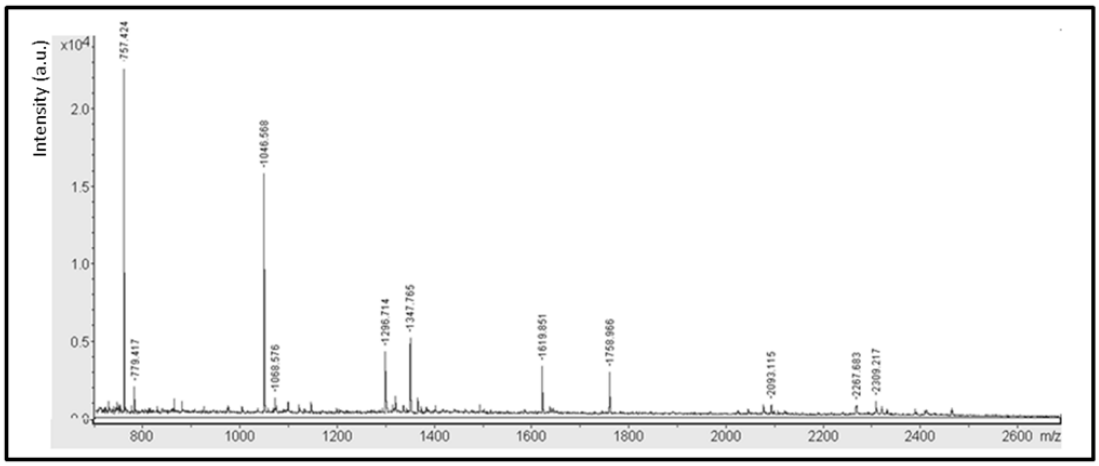


**Appendix B52.** PMF of spot #174.

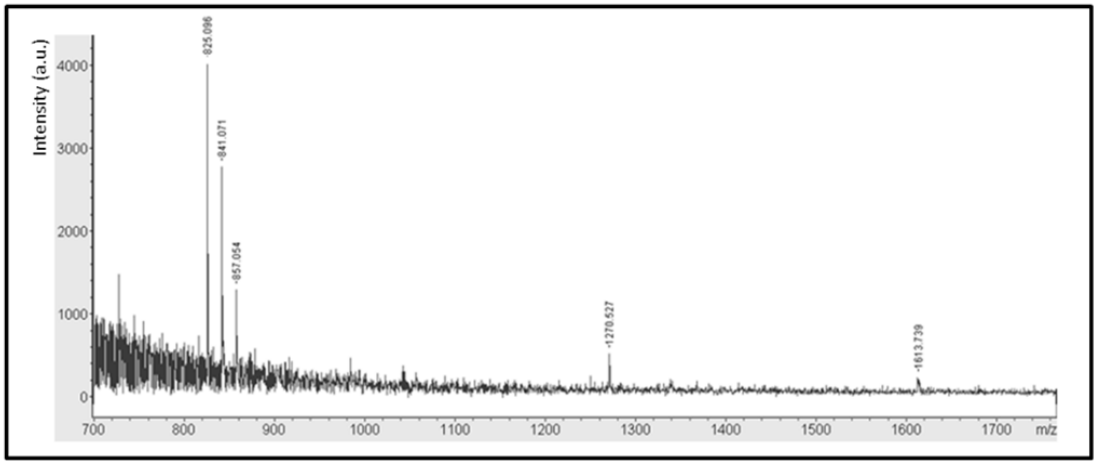


**Appendix B53.** PMF of spot #175.

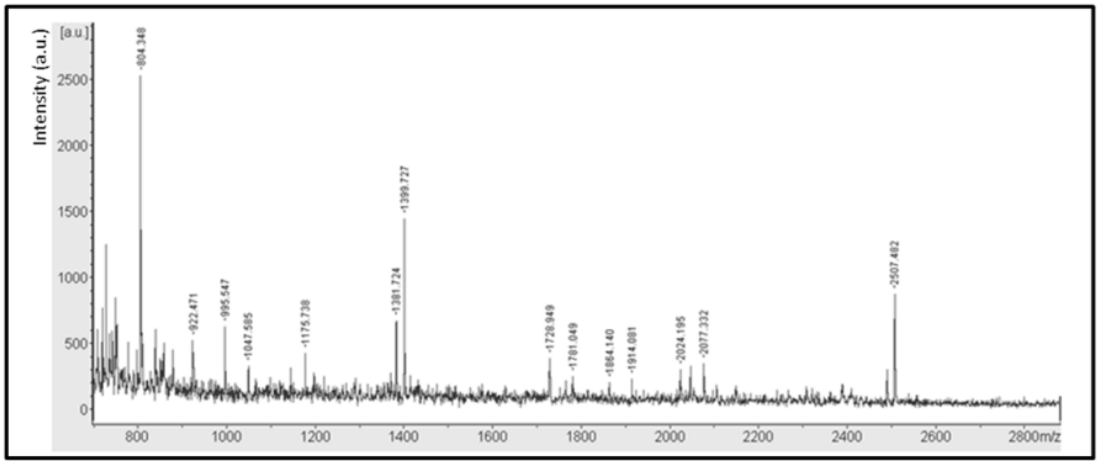

**Appendix B54.** PMF of spot #177.

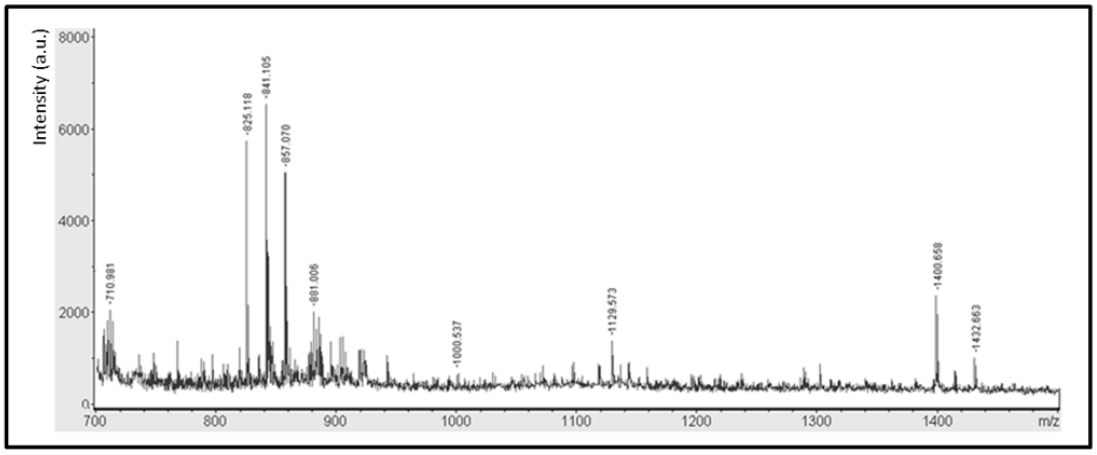


**Appendix B55.** PMF of spot #179.

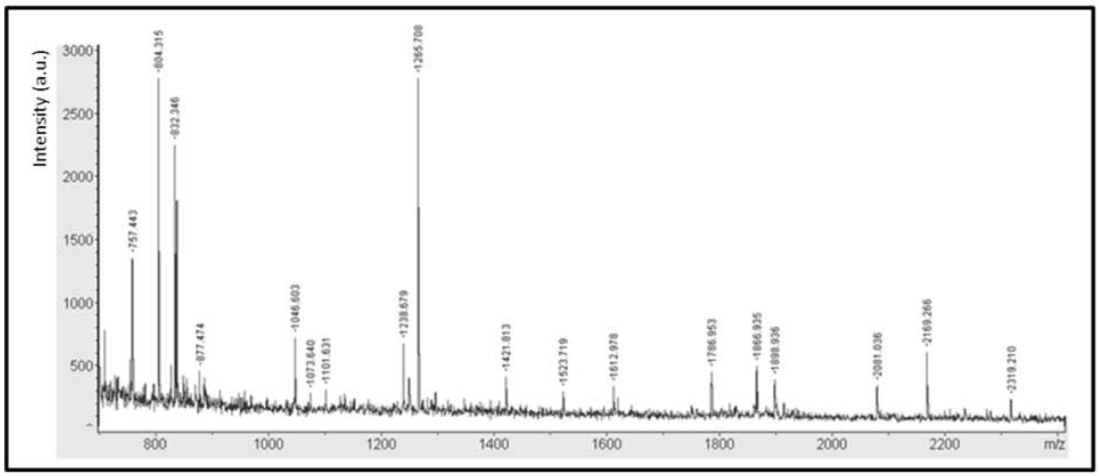


**Appendix B56.** PMF of spot #183.

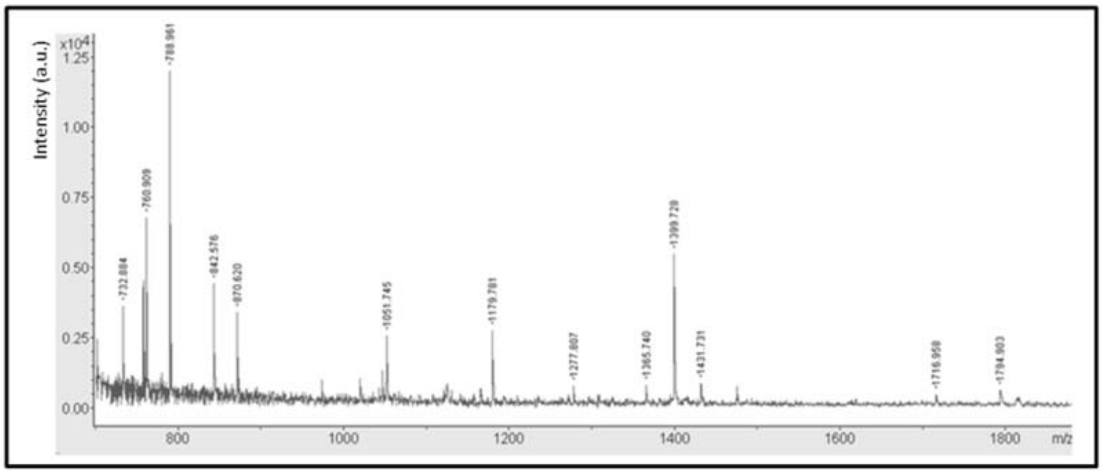

**Appendix B57.** PMF of spot #188.

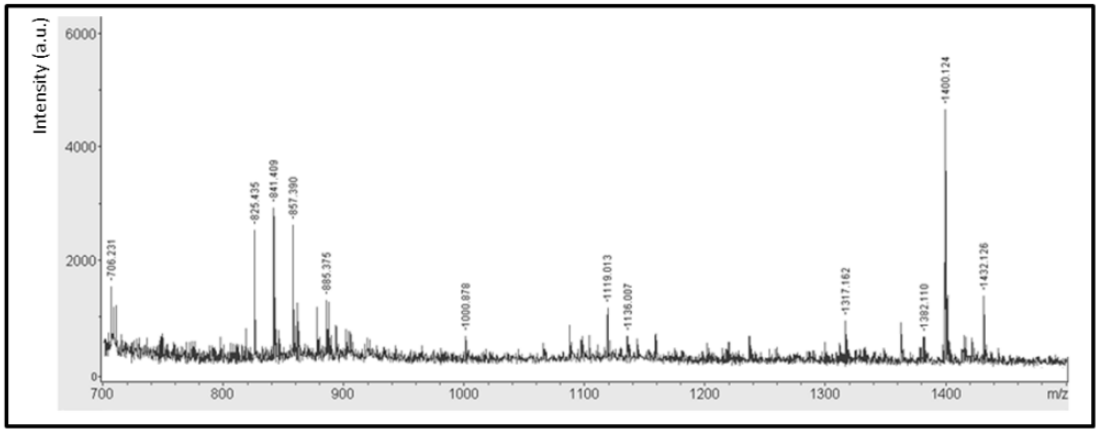


**Appendix B58.** PMF of spot #189.

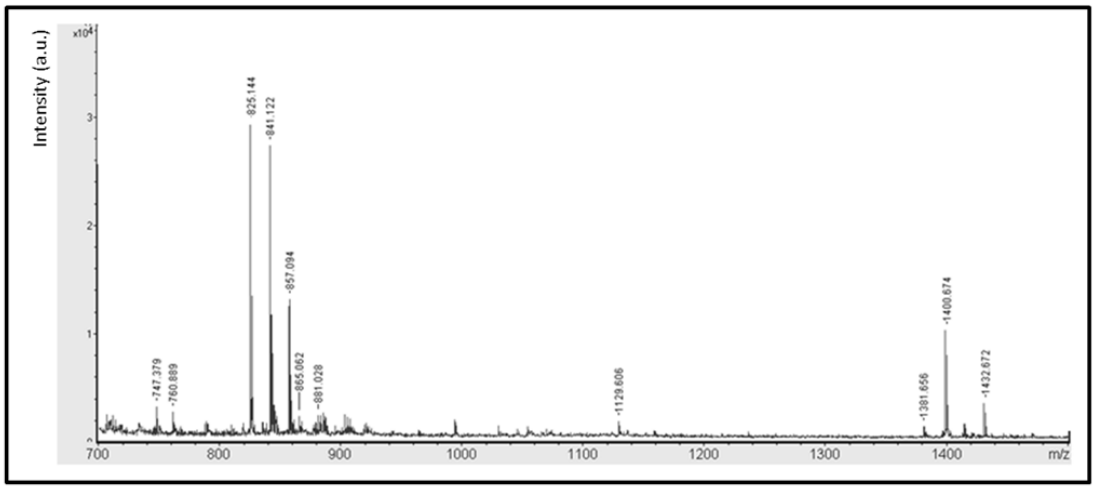


**Appendix B59.** PMF of spot #190.

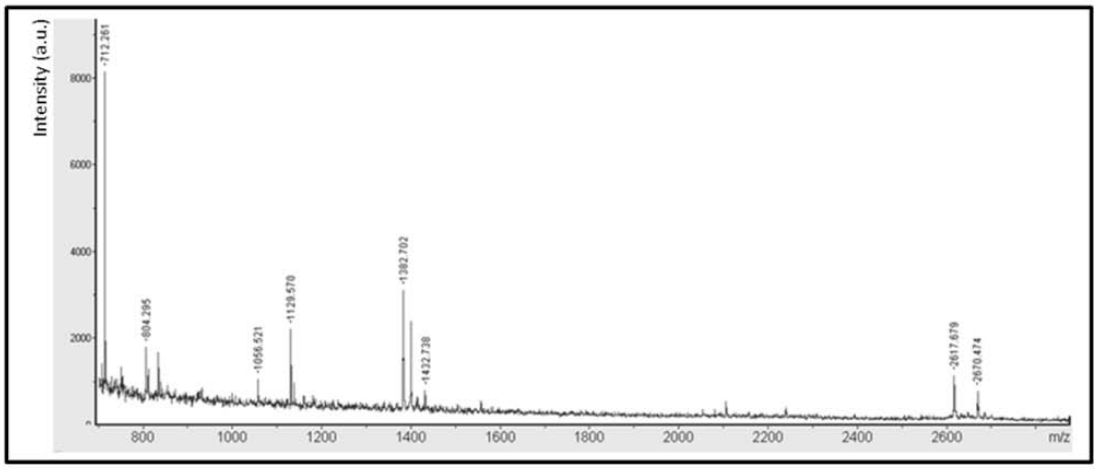

**Appendix B60.** PMF of spot #191.

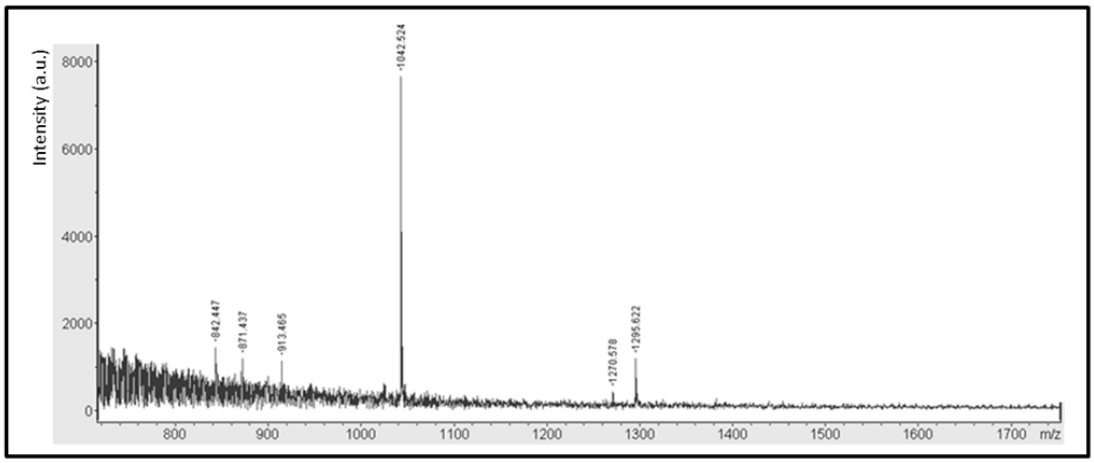


**Appendix B61.** PMF of spot #192.

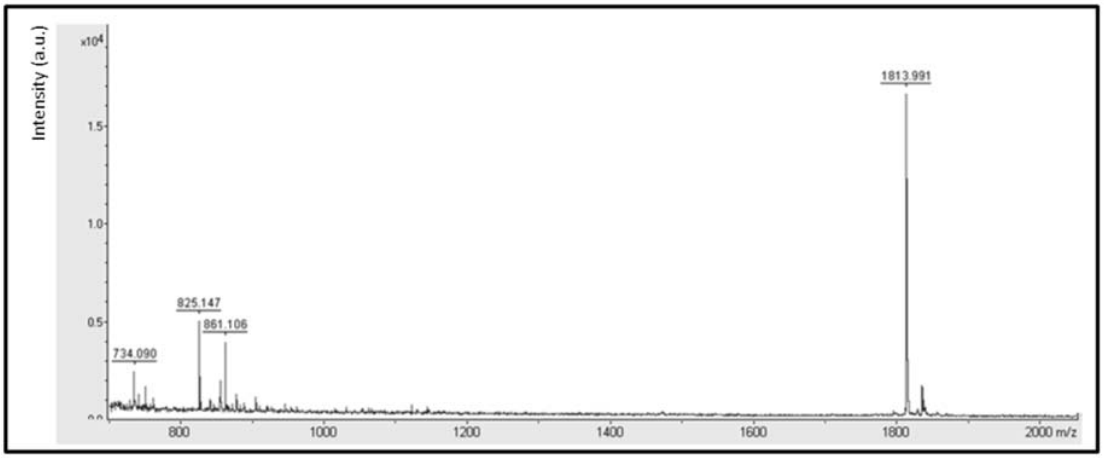


**Appendix B62.** PMF of spot #193.

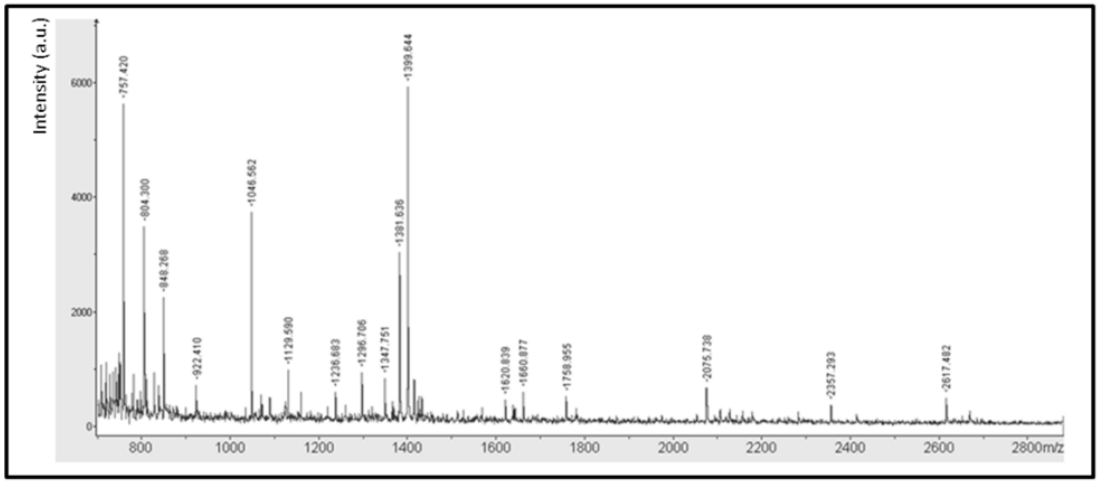

**Appendix B63.** PMF of spot #196.

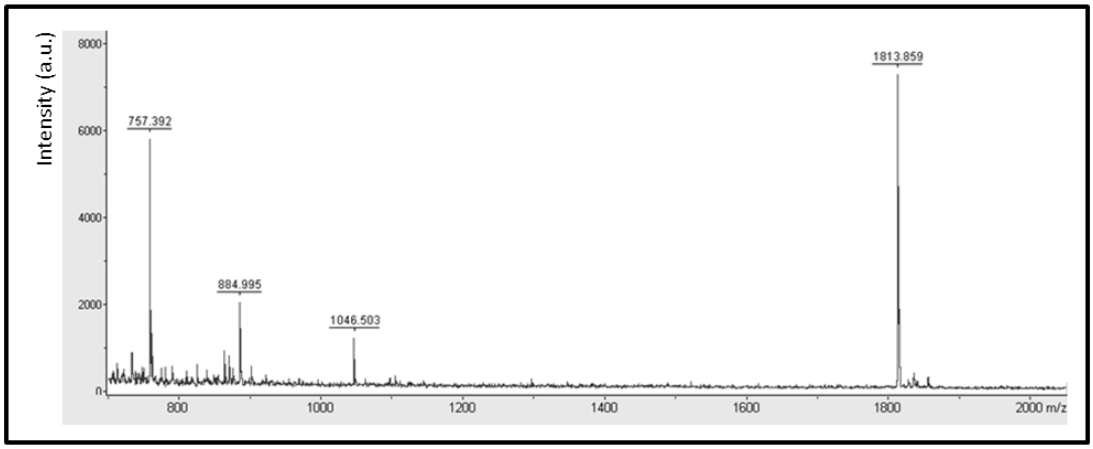


**Appendix B64.** PMF of spot #249.

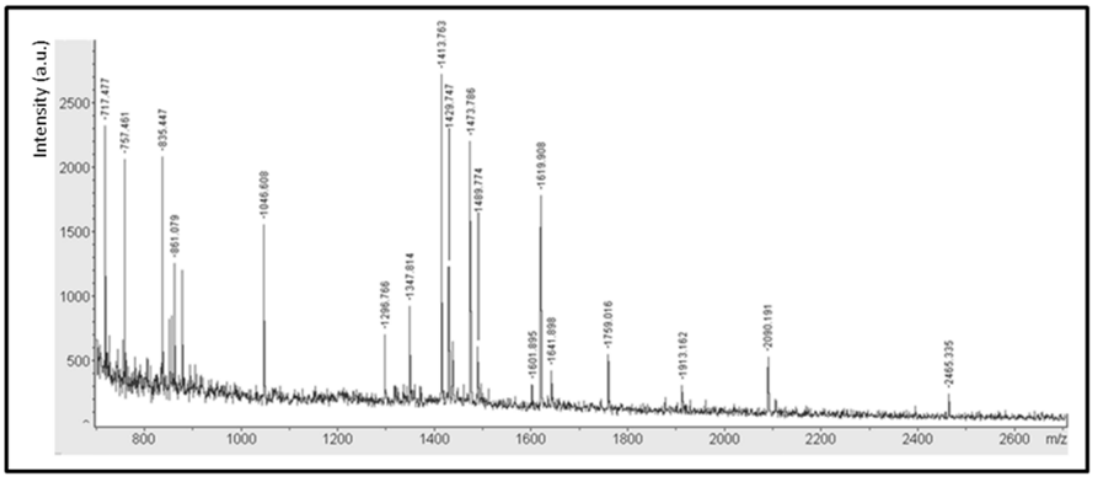


**Appendix B65.** PMF of spot #251.

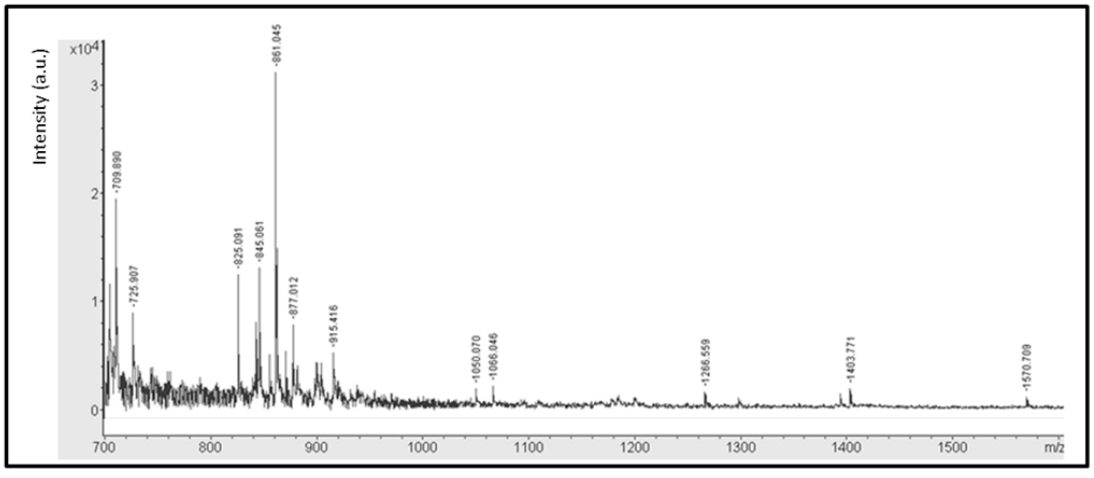

**Appendix B66.** PMF of spot #257.

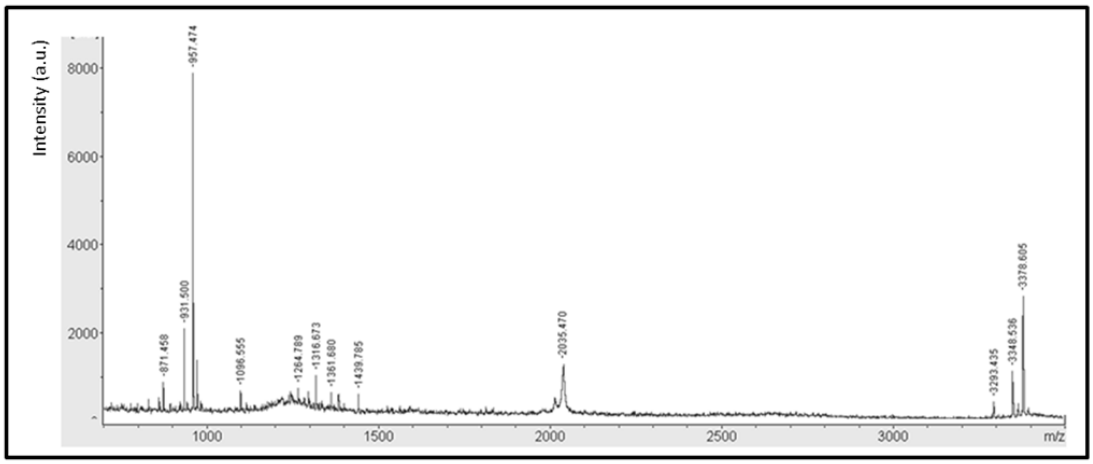


**Appendix B67.** PMF of spot #266.

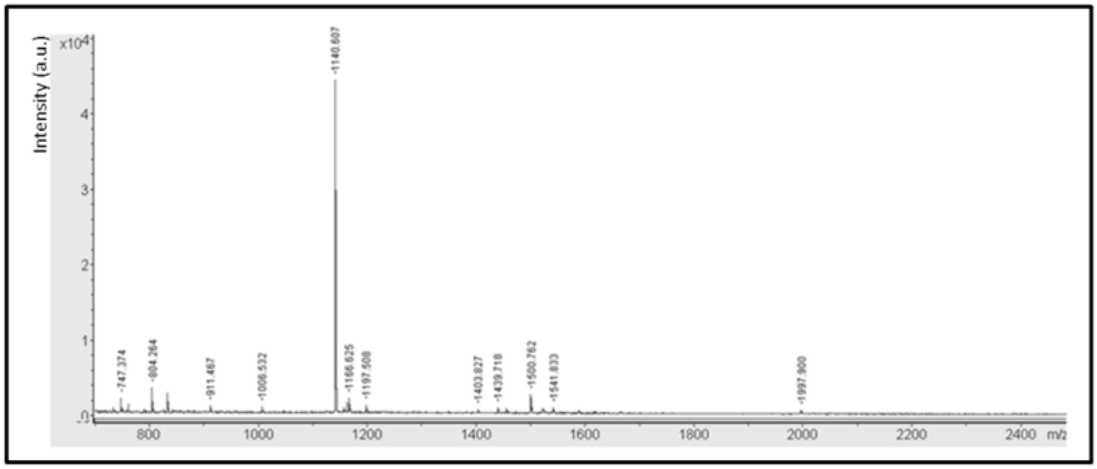


**Appendix B68.** PMF of spot #267.

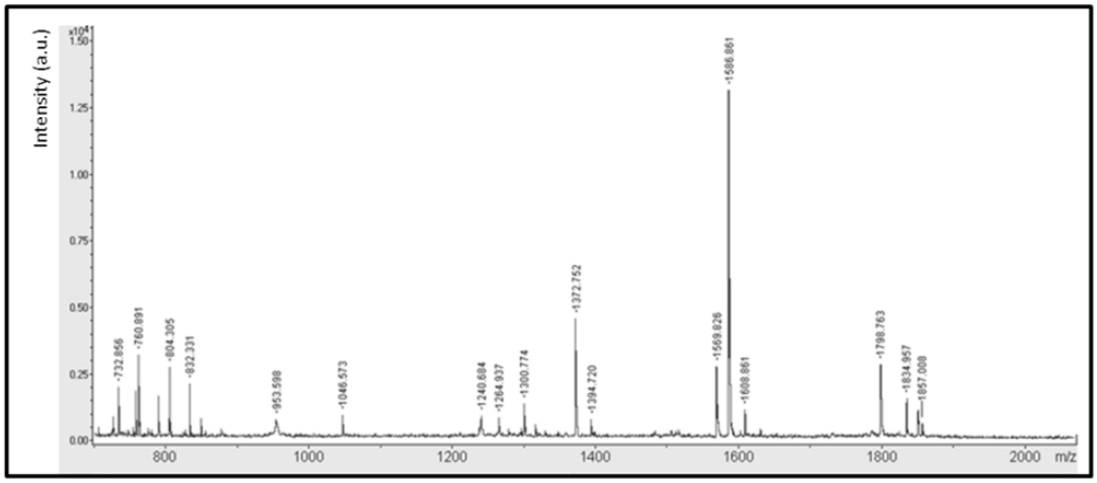

**Appendix B69.** PMF of spot #271.

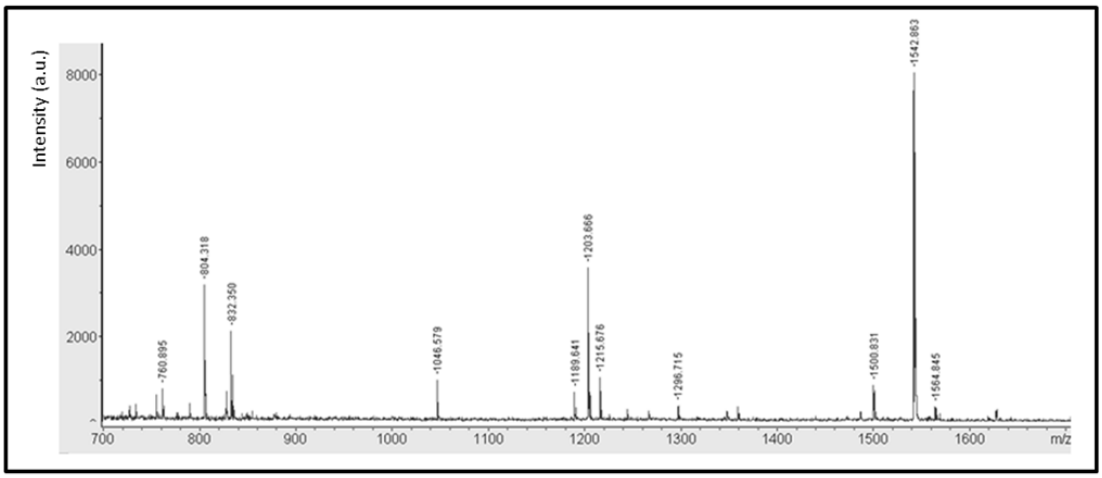


**Appendix B70.** PMF of spot #296.

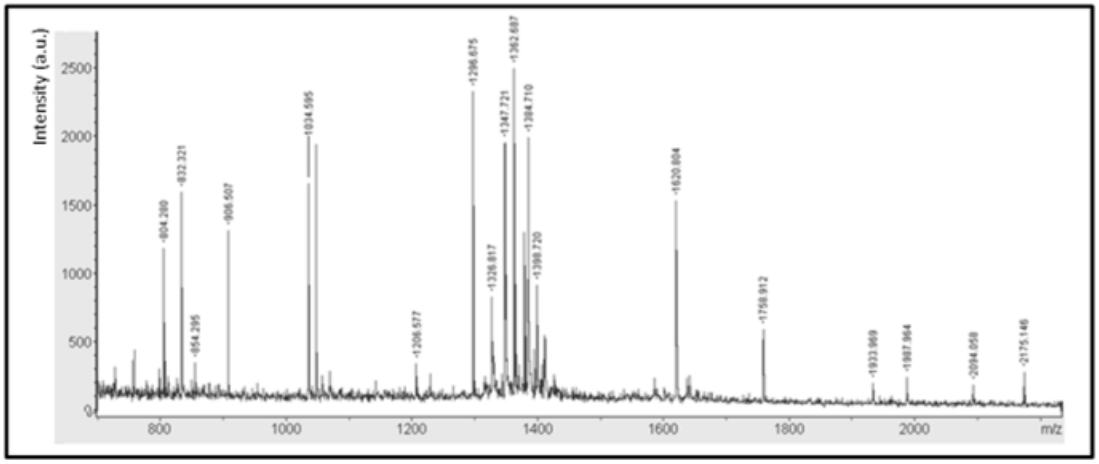


**Appendix B71.** PMF of spot #300.

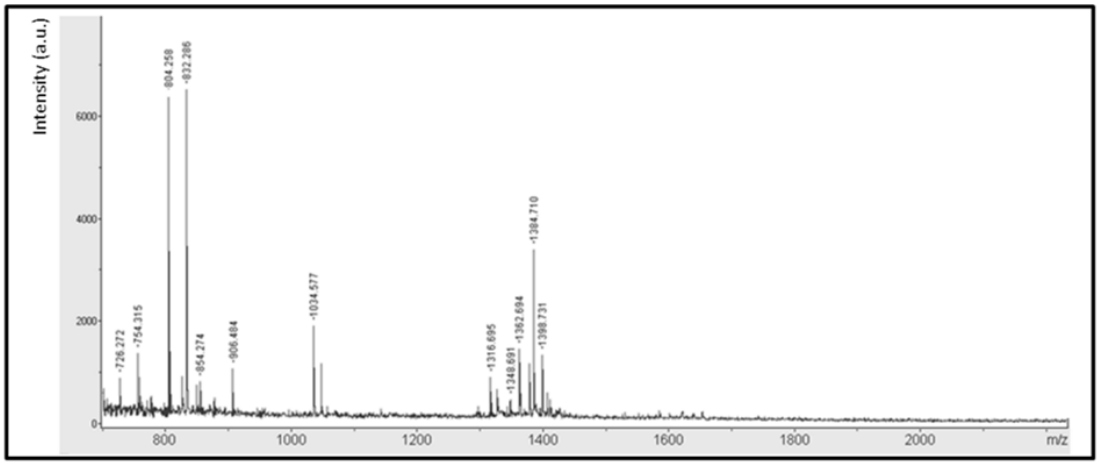

**Appendix B72.** PMF of spot #303.

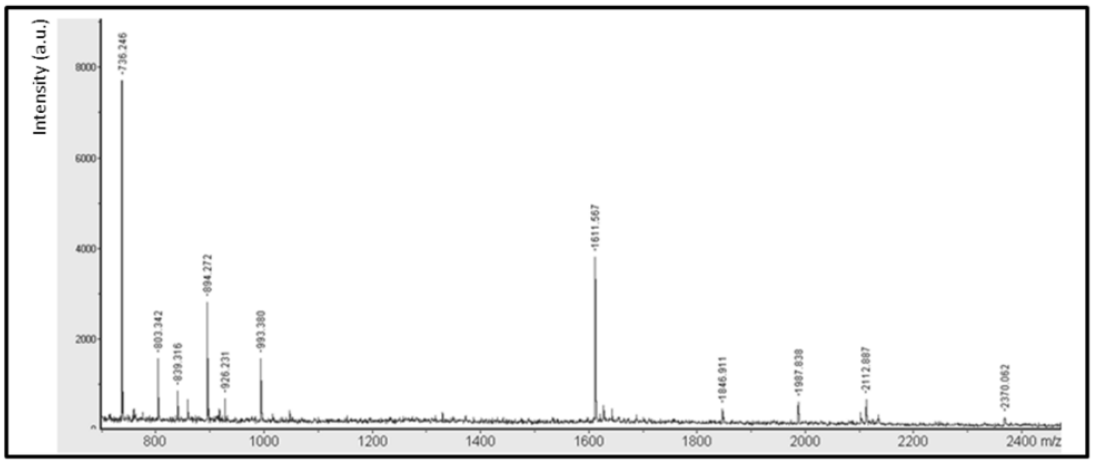


**Appendix B73.** PMF of spot #309.

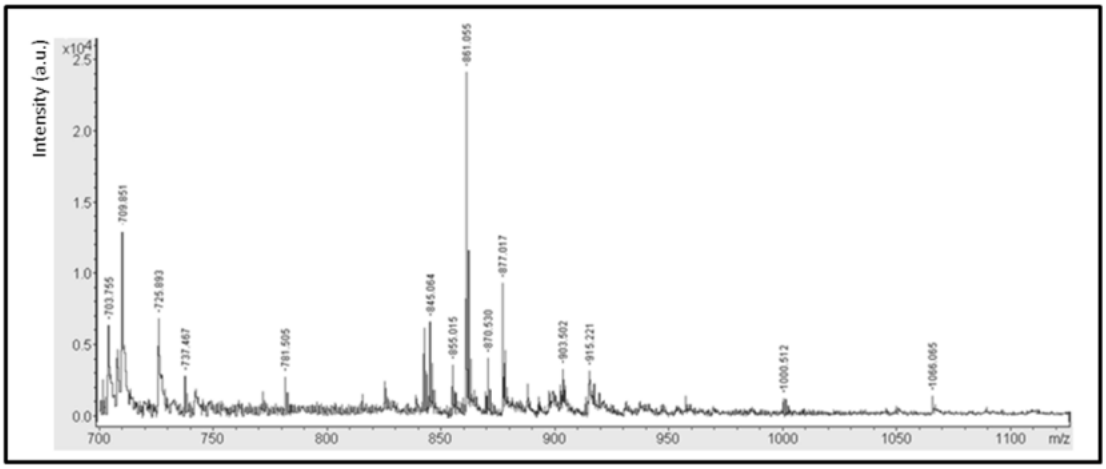

**Appendix B74.** Mascot search result of peptide 1673.597 m/z of spot #38 and the protein sequence of methionine adenosyltransferase (gi|46909371) in the NCBInr database. Highlighted region is the matched sequence tag.

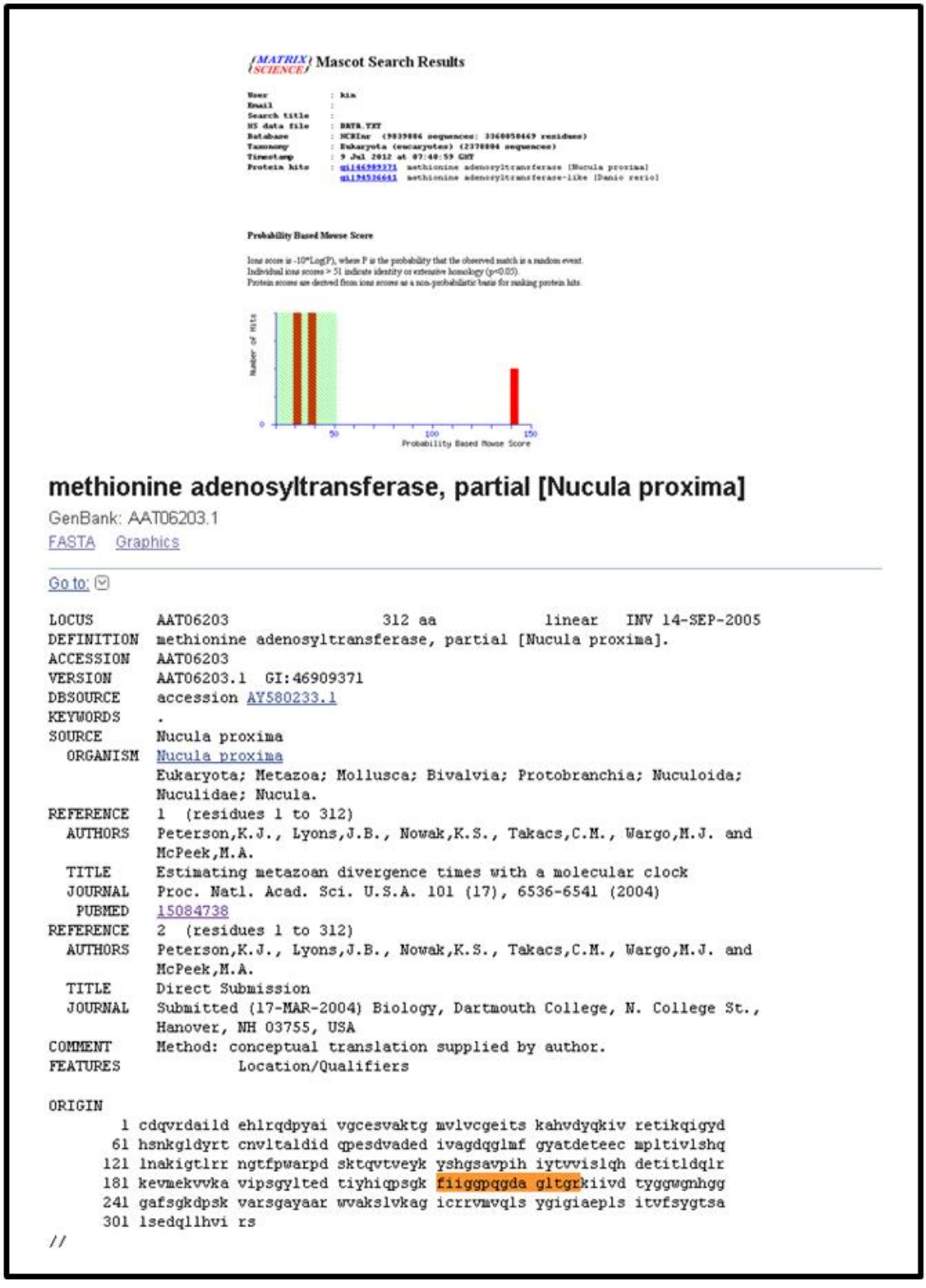

Mascot Search Results

User : kin
Email :
Search title :
MS data file : DATA.TXT
Database : NCBInr (9839886 sequences; 3360050449 residues)
Taxonomy : Eukaryota (eucaryotes) (2370804 sequences)
Timestamp : 9 Jul 2012 at 07:40:59 GMT
Protein hits : gi|46909371 methionine adenosyltransferase [Nucula proxima]
gi|194536641 methionine adenosyltransferase-like [Danio rerio]

Probability Based Mowse Score

Ions score is -10*Log(P), where P is the probability that the observed match is a random event.
Individual ions scores > 51 indicate identity or extensive homology (p<0.05).
Protein scores are derived from ions scores as a non-probabilistic basis for ranking protein hits.



## methionine adenosyltransferase, partial [Nucula proxima]

GenBank: AAT06203.1
FASTA Graphics

Go to:

```
LOCUS       AAT06203                312 aa            linear   INV 14-SEP-2005
DEFINITION  methionine adenosyltransferase, partial [Nucula proxima].
ACCESSION   AAT06203
VERSION     AAT06203.1  GI:46909371
DBSOURCE    accession AY580233.1
KEYWORDS    .
SOURCE      Nucula proxima
  ORGANISM  Nucula proxima
            Eukaryota; Metazoa; Mollusca; Bivalvia; Protobranchia; Nuculoida;
            Nuculidae; Nucula.
REFERENCE   1  (residues 1 to 312)
  AUTHORS   Peterson,K.J., Lyons,J.B., Nowak,K.S., Takacs,C.M., Wargo,M.J. and
            McPeek,M.A.
  TITLE     Estimating metazoan divergence times with a molecular clock
  JOURNAL   Proc. Natl. Acad. Sci. U.S.A. 101 (17), 6536-6541 (2004)
   PUBMED   15084738
REFERENCE   2  (residues 1 to 312)
  AUTHORS   Peterson,K.J., Lyons,J.B., Nowak,K.S., Takacs,C.M., Wargo,M.J. and
            McPeek,M.A.
  TITLE     Direct Submission
  JOURNAL   Submitted (17-MAR-2004) Biology, Dartmouth College, N. College St.,
            Hanover, NH 03755, USA
COMMENT     Method: conceptual translation supplied by author.
FEATURES             Location/Qualifiers

ORIGIN
        1 cdqvrdaild ehlrqdpyai vgcesvaktg mvlvcgeits kahvdyqkiv retikqigyd
       61 hsnkgldyrt cnvltaldid qpesdvaded ivagdqglmf gyatdeteec mpltivlshq
      121 lnakigtlrr ngtfpwarpd sktqvtveyk yshgsavpih iytvvislqh detitldqlr
      181 kevmekvvka vipsgylted tiyhiqpsgk fiiggpqgda gltgrkiivd tyggwgnhgg
      241 gafsgkdpsk varsgayaar wvakslvkag icrrvmvqls ygigiaepls itvfsygtsa
      301 lsedqllhvi rs
//
```

**Appendix B75.** Mascot search result of peptide 1673.597 m/z of spot #38 and the protein sequence of methionine adenosyltransferase (gi|94536641) in the NCBInr database. Highlighted region is the matched sequence tag.

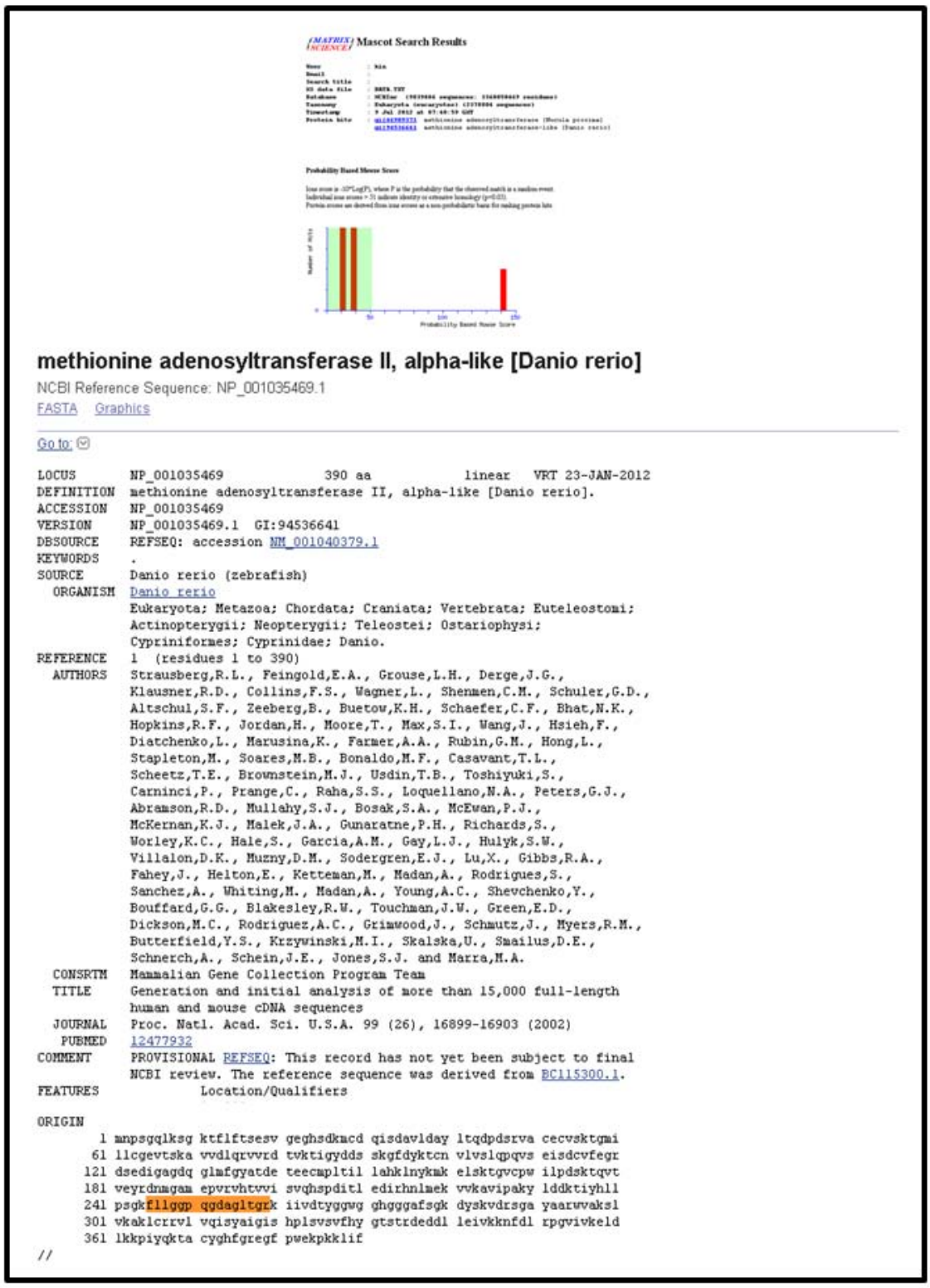

Mascot Search Results

## methionine adenosyltransferase II, alpha-like [Danio rerio]

NCBI Reference Sequence: NP_001035469.1

FASTA Graphics

Go to:

```
LOCUS       NP_001035469            390 aa            linear   VRT 23-JAN-2012
DEFINITION  methionine adenosyltransferase II, alpha-like [Danio rerio].
ACCESSION   NP_001035469
VERSION     NP_001035469.1  GI:94536641
DBSOURCE    REFSEQ: accession NM_001040379.1
KEYWORDS    .
SOURCE      Danio rerio (zebrafish)
  ORGANISM  Danio rerio
            Eukaryota; Metazoa; Chordata; Craniata; Vertebrata; Euteleostomi;
            Actinopterygii; Neopterygii; Teleostei; Ostariophysi;
            Cypriniformes; Cyprinidae; Danio.
REFERENCE   1  (residues 1 to 390)
  AUTHORS   Strausberg,R.L., Feingold,E.A., Grouse,L.H., Derge,J.G.,
            Klausner,R.D., Collins,F.S., Wagner,L., Shenmen,C.M., Schuler,G.D.,
            Altschul,S.F., Zeeberg,B., Buetow,K.H., Schaefer,C.F., Bhat,N.K.,
            Hopkins,R.F., Jordan,H., Moore,T., Max,S.I., Wang,J., Hsieh,F.,
            Diatchenko,L., Marusina,K., Farmer,A.A., Rubin,G.M., Hong,L.,
            Stapleton,M., Soares,M.B., Bonaldo,M.F., Casavant,T.L.,
            Scheetz,T.E., Brownstein,M.J., Usdin,T.B., Toshiyuki,S.,
            Carninci,P., Prange,C., Raha,S.S., Loquellano,N.A., Peters,G.J.,
            Abramson,R.D., Mullahy,S.J., Bosak,S.A., McEwan,P.J.,
            McKernan,K.J., Malek,J.A., Gunaratne,P.H., Richards,S.,
            Worley,K.C., Hale,S., Garcia,A.M., Gay,L.J., Hulyk,S.W.,
            Villalon,D.K., Muzny,D.M., Sodergren,E.J., Lu,X., Gibbs,R.A.,
            Fahey,J., Helton,E., Ketteman,M., Madan,A., Rodrigues,S.,
            Sanchez,A., Whiting,M., Madan,A., Young,A.C., Shevchenko,Y.,
            Bouffard,G.G., Blakesley,R.W., Touchman,J.W., Green,E.D.,
            Dickson,M.C., Rodriguez,A.C., Grimwood,J., Schmutz,J., Myers,R.M.,
            Butterfield,Y.S., Krzywinski,M.I., Skalska,U., Smailus,D.E.,
            Schnerch,A., Schein,J.E., Jones,S.J. and Marra,M.A.
  CONSRTM   Mammalian Gene Collection Program Team
  TITLE     Generation and initial analysis of more than 15,000 full-length
            human and mouse cDNA sequences
  JOURNAL   Proc. Natl. Acad. Sci. U.S.A. 99 (26), 16899-16903 (2002)
   PUBMED   12477932
COMMENT     PROVISIONAL REFSEQ: This record has not yet been subject to final
            NCBI review. The reference sequence was derived from BC115300.1.
FEATURES             Location/Qualifiers

ORIGIN
        1 mnpsgqlksg ktflftsesv geghsdkmcd qisdavlday ltqdpdsrva cecvsktgmi
       61 llcgevtska vvdlqrvvrd tvktigydds skgfdyktcn vlvslqpqvs eisdcvfegr
      121 dsedigagdq glmfgyatde teecmpltil lahklnykmk elsktgvcpw ilpdsktqvt
      181 veyrdnmgam epvrvhtvvi svqhspditl edirhnlmek vvkavipaky lddktiyhll
      241 psgkfllggp qgdagltgrk iivdtyggwg ghgggafsgk dyskvdrsga yaaruvaksl
      301 vkaklcrrvl vqisyaigis hplsvsvfhy gtstrdeddl leivkknfdl rpgvivkeld
      361 lkkpiyqkta cyghfgregf pwekpkklif
//
```

**Appendix B76.** Mascot search result of peptide 1557.862 m/z of spot #104 and the protein sequence of glyceraldehyde-3 phosphate dehydrogenase (gi|1151182) in the NCBInr database. Highlighted region is the matched sequence tag.

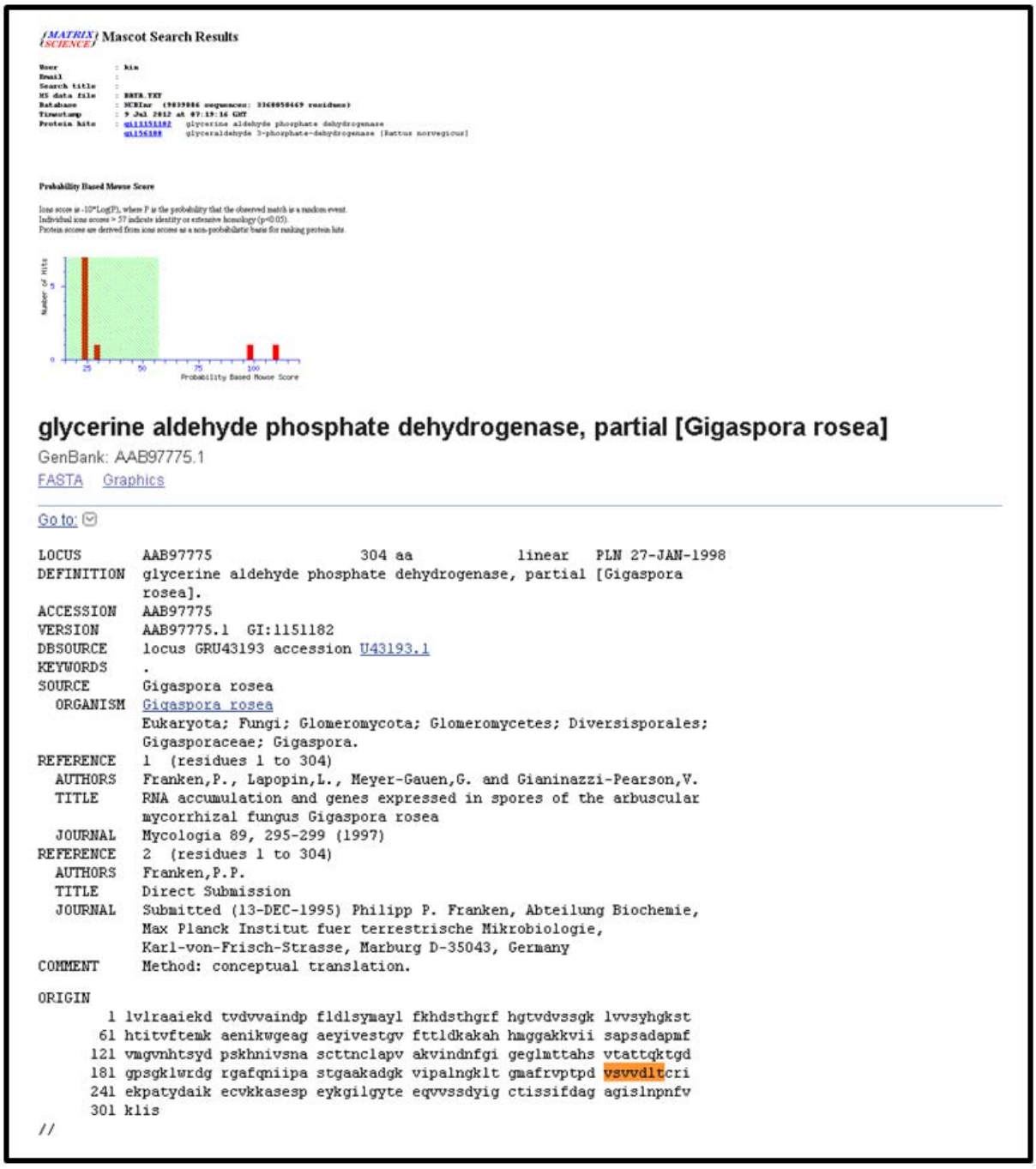

Mascot Search Results

User : kin
Email :
Search title :
MS data file : BRTA.TXT
Database : NCBInr (9839886 sequences; 3368050469 residues)
Timestamp : 9 Jul 2012 at 07:19:16 GMT
Protein hits : gi|1151182 glycerine aldehyde phosphate dehydrogenase
gi|156188 glyceraldehyde 3-phosphate-dehydrogenase [Rattus norvegicus]

Probability Based Mowse Score

Ions score is -10*Log(P), where P is the probability that the observed match is a random event.
Individual ions scores > 37 indicate identity or extensive homology (p<0.05).
Protein scores are derived from ions scores as a non-probabilistic basis for ranking protein hits.




## glycerine aldehyde phosphate dehydrogenase, partial [Gigaspora rosea]

GenBank: AAB97775.1
FASTA Graphics

Go to:

```
LOCUS       AAB97775                304 aa            linear   PLN 27-JAN-1998
DEFINITION  glycerine aldehyde phosphate dehydrogenase, partial [Gigaspora
            rosea].
ACCESSION   AAB97775
VERSION     AAB97775.1  GI:1151182
DBSOURCE    locus GRU43193 accession U43193.1
KEYWORDS    .
SOURCE      Gigaspora rosea
  ORGANISM  Gigaspora rosea
            Eukaryota; Fungi; Glomeromycota; Glomeromycetes; Diversisporales;
            Gigasporaceae; Gigaspora.
REFERENCE   1  (residues 1 to 304)
  AUTHORS   Franken,P., Lapopin,L., Meyer-Gauen,G. and Gianinazzi-Pearson,V.
  TITLE     RNA accumulation and genes expressed in spores of the arbuscular
            mycorrhizal fungus Gigaspora rosea
  JOURNAL   Mycologia 89, 295-299 (1997)
REFERENCE   2  (residues 1 to 304)
  AUTHORS   Franken,P.P.
  TITLE     Direct Submission
  JOURNAL   Submitted (13-DEC-1995) Philipp P. Franken, Abteilung Biochemie,
            Max Planck Institut fuer terrestrische Mikrobiologie,
            Karl-von-Frisch-Strasse, Marburg D-35043, Germany
COMMENT     Method: conceptual translation.

ORIGIN
        1 lvlraaiekd tvdvvaindp fldlsymayl fkhdsthgrf hgtvdvssgk lvvsyhgkst
       61 htitvftemk aenikwgeag aeyivestgv fttldkakah hmggakkvii sapsadapmf
      121 vmgvnhtsyd pskhnivsna scttnclapv akvindnfgi geglmttahs vtattqktgd
      181 gpsgklwrdg rgafqniipa stgaakadgk vipalngklt gmafrvptpd vsvvdltcri
      241 ekpatydaik ecvkkasesp eykgilgyte eqvvssdyig ctissifdag agislnpnfv
      301 klis
//
```

**Appendix B77.** Mascot search result of peptide 1788.875 m/z of spot #104 and the protein sequence of glyceraldehyde-3 phosphate dehydrogenase (gi|5219) in the NCBInr database. Highlighted region is the matched sequence tag.

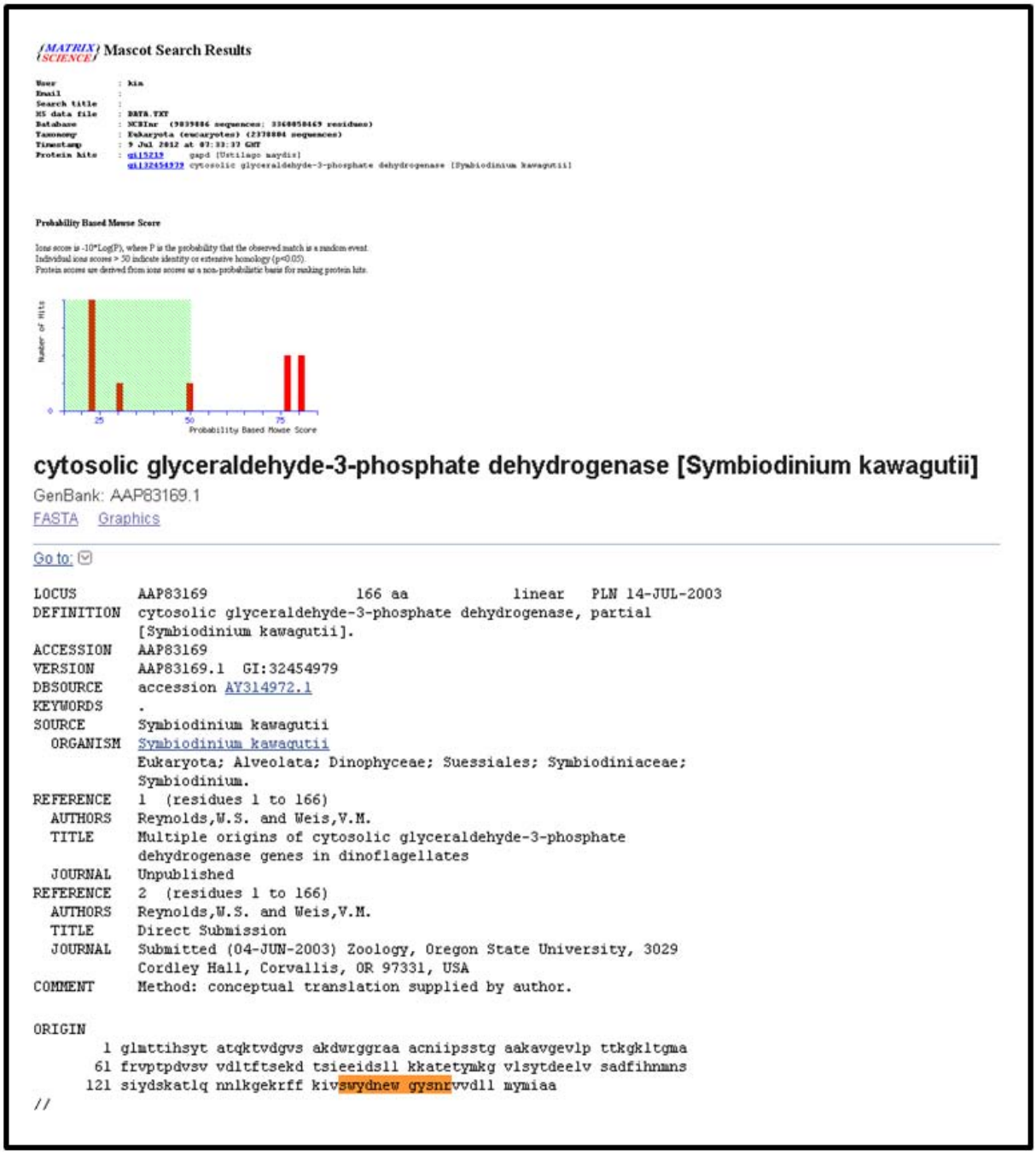

MATRIX SCIENCE Mascot Search Results

User : kia
Email :
Search title :
MS data file : DATA.TXT
Database : NCBInr (9839886 sequences; 3360858469 residues)
Taxonomy : Eukaryota (eucaryotes) (2370884 sequences)
Timestamp : 9 Jul 2012 at 07:33:37 GMT
Protein hits : gi|5219 gapd [Ustilago maydis]
gi|32454979 cytosolic glyceraldehyde-3-phosphate dehydrogenase [Symbiodinium kawagutii]

Probability Based Mowse Score

Ions score is -10*Log(P), where P is the probability that the observed match is a random event.
Individual ions scores > 30 indicate identity or extensive homology (p<0.05).
Protein scores are derived from ions scores as a non-probabilistic basis for ranking protein hits.




## cytosolic glyceraldehyde-3-phosphate dehydrogenase [Symbiodinium kawagutii]

GenBank: AAP83169.1

FASTA Graphics

Go to:

```
LOCUS       AAP83169                166 aa            linear   PLN 14-JUL-2003
DEFINITION  cytosolic glyceraldehyde-3-phosphate dehydrogenase, partial
            [Symbiodinium kawagutii].
ACCESSION   AAP83169
VERSION     AAP83169.1  GI:32454979
DBSOURCE    accession AY314972.1
KEYWORDS    .
SOURCE      Symbiodinium kawagutii
  ORGANISM  Symbiodinium kawagutii
            Eukaryota; Alveolata; Dinophyceae; Suessiales; Symbiodiniaceae;
            Symbiodinium.
REFERENCE   1  (residues 1 to 166)
  AUTHORS   Reynolds,W.S. and Weis,V.M.
  TITLE     Multiple origins of cytosolic glyceraldehyde-3-phosphate
            dehydrogenase genes in dinoflagellates
  JOURNAL   Unpublished
REFERENCE   2  (residues 1 to 166)
  AUTHORS   Reynolds,W.S. and Weis,V.M.
  TITLE     Direct Submission
  JOURNAL   Submitted (04-JUN-2003) Zoology, Oregon State University, 3029
            Cordley Hall, Corvallis, OR 97331, USA
COMMENT     Method: conceptual translation supplied by author.

ORIGIN
        1 glmttihsyt atqktvdgvs akdwrggraa acniipsstg aakavgevlp ttkgkltgma
       61 frvptpdvsv vdltftsekd tsieeidsll kkatetymkg vlsytdeelv sadfihnmns
      121 siydskatlq nnlkgekrff kivswydnew gysnrvvdll mymiaa
//
```

**Appendix B78.** Mascot search result of peptide 1172.464 m/z of spot #257 and the protein sequence of transcriptional regulator (gi|111223593) in the NCBInr database. Highlighted region is the matched sequence tag.

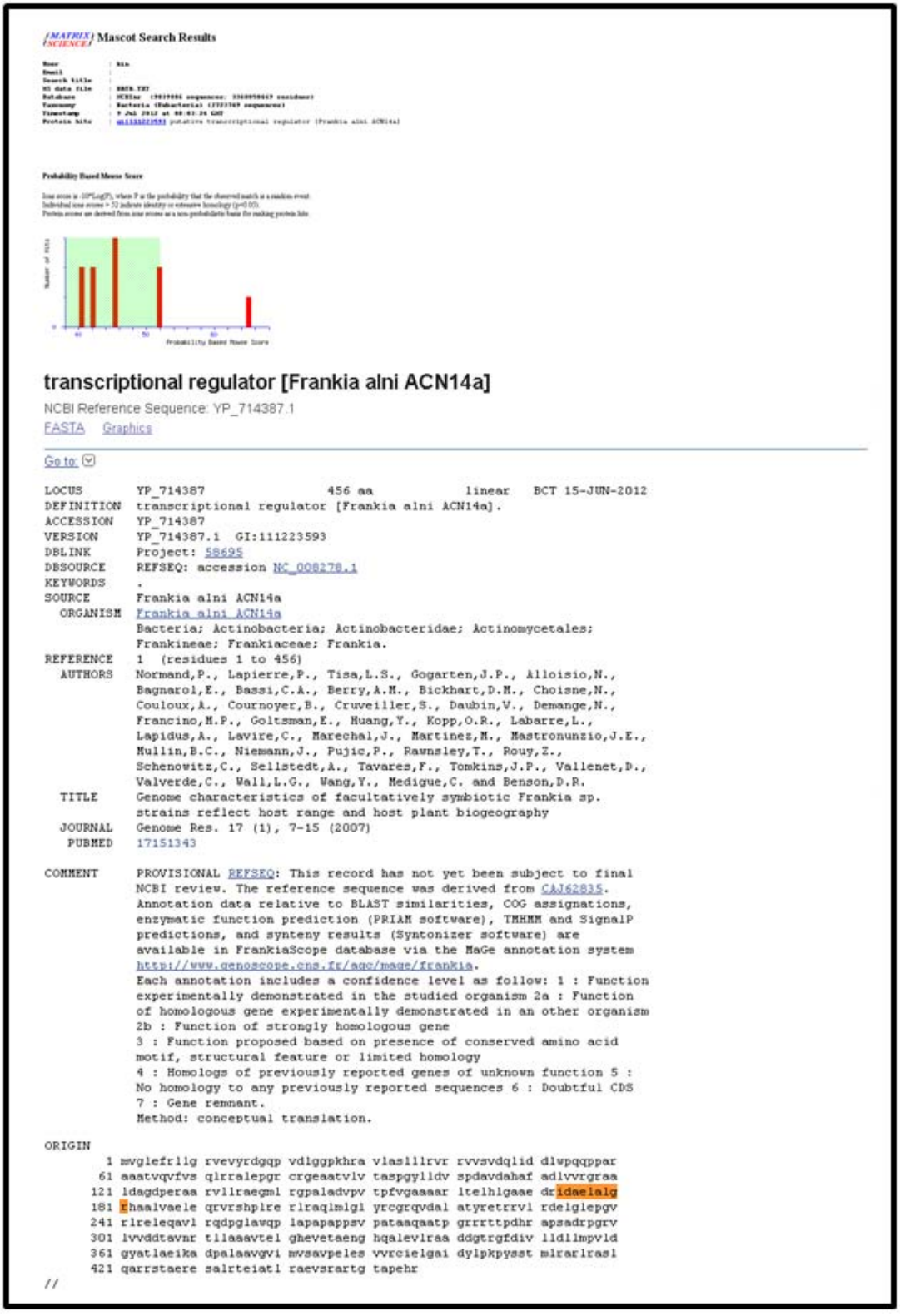

(MATRIX SCIENCE) Mascot Search Results

Probability Based Mowse Score

## transcriptional regulator [Frankia alni ACN14a]

NCBI Reference Sequence: YP_714387.1

FASTA Graphics

Go to:

```
LOCUS       YP_714387               456 aa            linear   BCT 15-JUN-2012
DEFINITION  transcriptional regulator [Frankia alni ACN14a].
ACCESSION   YP_714387
VERSION     YP_714387.1  GI:111223593
DBLINK      Project: 58695
DBSOURCE    REFSEQ: accession NC_008278.1
KEYWORDS    .
SOURCE      Frankia alni ACN14a
  ORGANISM  Frankia alni ACN14a
            Bacteria; Actinobacteria; Actinobacteridae; Actinomycetales;
            Frankineae; Frankiaceae; Frankia.
REFERENCE   1  (residues 1 to 456)
  AUTHORS   Normand,P., Lapierre,P., Tisa,L.S., Gogarten,J.P., Alloisio,N.,
            Bagnarol,E., Bassi,C.A., Berry,A.M., Bickhart,D.M., Choisne,N.,
            Couloux,A., Cournoyer,B., Cruveiller,S., Daubin,V., Demange,N.,
            Francino,M.P., Goltsman,E., Huang,Y., Kopp,O.R., Labarre,L.,
            Lapidus,A., Lavire,C., Marechal,J., Martinez,M., Mastronunzio,J.E.,
            Mullin,B.C., Niemann,J., Pujic,P., Rawnsley,T., Rouy,Z.,
            Schenowitz,C., Sellstedt,A., Tavares,F., Tomkins,J.P., Vallenet,D.,
            Valverde,C., Wall,L.G., Wang,Y., Medigue,C. and Benson,D.R.
  TITLE     Genome characteristics of facultatively symbiotic Frankia sp.
            strains reflect host range and host plant biogeography
  JOURNAL   Genome Res. 17 (1), 7-15 (2007)
   PUBMED   17151343

COMMENT     PROVISIONAL REFSEQ: This record has not yet been subject to final
            NCBI review. The reference sequence was derived from CAJ62835.
            Annotation data relative to BLAST similarities, COG assignations,
            enzymatic function prediction (PRIAM software), TMHMM and SignalP
            predictions, and synteny results (Syntonizer software) are
            available in FrankiaScope database via the MaGe annotation system
            http://www.genoscope.cns.fr/agc/mage/frankia.
            Each annotation includes a confidence level as follow: 1 : Function
            experimentally demonstrated in the studied organism 2a : Function
            of homologous gene experimentally demonstrated in an other organism
            2b : Function of strongly homologous gene
            3 : Function proposed based on presence of conserved amino acid
            motif, structural feature or limited homology
            4 : Homologs of previously reported genes of unknown function 5 :
            No homology to any previously reported sequences 6 : Doubtful CDS
            7 : Gene remnant.
            Method: conceptual translation.

ORIGIN
        1 mvglefrllg rvevyrdgqp vdlggpkhra vlaslllrvr rvvsvdqlid dlwpqqppar
       61 aaatvqvfvs qlrralepgr crgeaatvlv taspgylldv spdavdahaf adlvvrgraa
      121 ldagdperaa rvllraegml rgpaladvpv tpfvgaaaar ltelhlgaae dridaelalg
      181 rhaalvaele qrvrshplre rlraqlmlgl yrcgrqvdal atyretrrvl rdelglepgv
      241 rlreleqavl rqdpglawqp lapapappsv pataaqaatp grrrttpdhr apsadrpgrv
      301 lvvddtavnr tllaaavtel ghevetaeng hqalevlraa ddgtrgfdiv lldllmpvld
      361 gyatlaeika dpalaavgvi mvsavpeles vvrcielgai dylpkpysst mlrarlrasl
      421 qarrstaere salrteiatl raevsrartg tapehr
//
```

**Appendix B79.** Matched protein hits (E value < 0.05) of NCBI BLAST search result of 1215.692 m/z and 1254.805 m/z of spot #27 and the protein sequence of Rubisco II (AAO13045.1) in the NCBInr database. Highlighted region is the matched sequence tag.

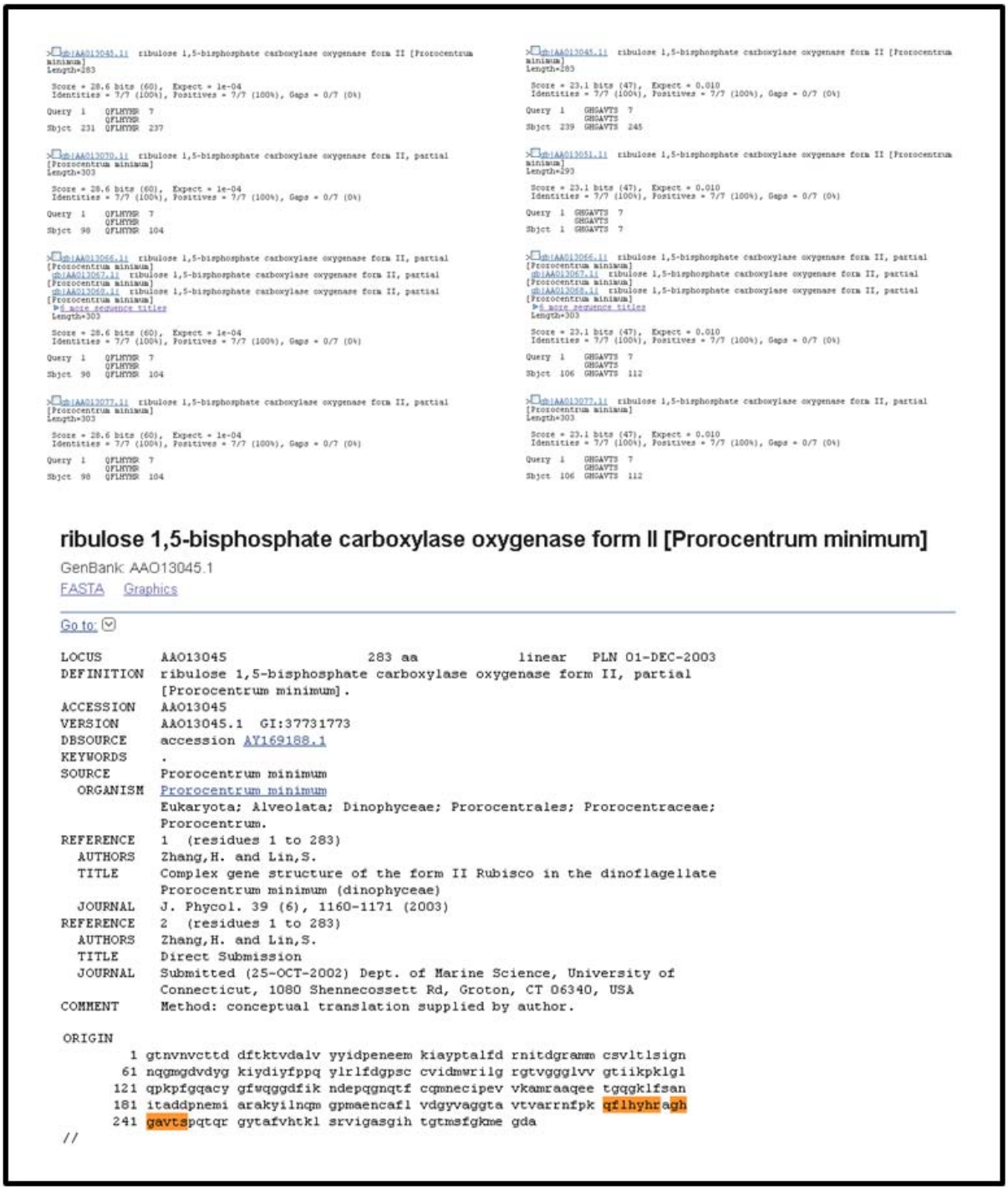

>gb|AAO13045.1| ribulose 1,5-bisphosphate carboxylase oxygenase form II [Prorocentrum minimum]
Length=283

Score = 28.6 bits (60), Expect = 1e-04
Identities = 7/7 (100%), Positives = 7/7 (100%), Gaps = 0/7 (0%)

Query 1 QFLHYHR 7
QFLHYHR
Sbjct 231 QFLHYHR 237

>gb|AAO13070.1| ribulose 1,5-bisphosphate carboxylase oxygenase form II, partial [Prorocentrum minimum]
Length=303

Score = 28.6 bits (60), Expect = 1e-04
Identities = 7/7 (100%), Positives = 7/7 (100%), Gaps = 0/7 (0%)

Query 1 QFLHYHR 7
QFLHYHR
Sbjct 98 QFLHYHR 104

>gb|AAO13066.1| ribulose 1,5-bisphosphate carboxylase oxygenase form II, partial [Prorocentrum minimum]
gb|AAO13067.1| ribulose 1,5-bisphosphate carboxylase oxygenase form II, partial [Prorocentrum minimum]
gb|AAO13069.1| ribulose 1,5-bisphosphate carboxylase oxygenase form II, partial [Prorocentrum minimum]
▶6 more sequence titles
Length=303

Score = 28.6 bits (60), Expect = 1e-04
Identities = 7/7 (100%), Positives = 7/7 (100%), Gaps = 0/7 (0%)

Query 1 QFLHYHR 7
QFLHYHR
Sbjct 98 QFLHYHR 104

>gb|AAO13077.1| ribulose 1,5-bisphosphate carboxylase oxygenase form II, partial [Prorocentrum minimum]
Length=303

Score = 28.6 bits (60), Expect = 1e-04
Identities = 7/7 (100%), Positives = 7/7 (100%), Gaps = 0/7 (0%)

Query 1 QFLHYHR 7
QFLHYHR
Sbjct 98 QFLHYHR 104

>gb|AAO13045.1| ribulose 1,5-bisphosphate carboxylase oxygenase form II [Prorocentrum minimum]
Length=283

Score = 23.1 bits (47), Expect = 0.010
Identities = 7/7 (100%), Positives = 7/7 (100%), Gaps = 0/7 (0%)

Query 1 GHGAVTS 7
GHGAVTS
Sbjct 239 GHGAVTS 245

>gb|AAO13051.1| ribulose 1,5-bisphosphate carboxylase oxygenase form II [Prorocentrum minimum]
Length=293

Score = 23.1 bits (47), Expect = 0.010
Identities = 7/7 (100%), Positives = 7/7 (100%), Gaps = 0/7 (0%)

Query 1 GHGAVTS 7
GHGAVTS
Sbjct 1 GHGAVTS 7

>gb|AAO13066.1| ribulose 1,5-bisphosphate carboxylase oxygenase form II, partial [Prorocentrum minimum]
gb|AAO13067.1| ribulose 1,5-bisphosphate carboxylase oxygenase form II, partial [Prorocentrum minimum]
gb|AAO13068.1| ribulose 1,5-bisphosphate carboxylase oxygenase form II, partial [Prorocentrum minimum]
▶6 more sequence titles
Length=303

Score = 23.1 bits (47), Expect = 0.010
Identities = 7/7 (100%), Positives = 7/7 (100%), Gaps = 0/7 (0%)

Query 1 GHGAVTS 7
GHGAVTS
Sbjct 106 GHGAVTS 112

>gb|AAO13077.1| ribulose 1,5-bisphosphate carboxylase oxygenase form II, partial [Prorocentrum minimum]
Length=303

Score = 23.1 bits (47), Expect = 0.010
Identities = 7/7 (100%), Positives = 7/7 (100%), Gaps = 0/7 (0%)

Query 1 GHGAVTS 7
GHGAVTS
Sbjct 106 GHGAVTS 112

## ribulose 1,5-bisphosphate carboxylase oxygenase form II [Prorocentrum minimum]

GenBank: AAO13045.1
FASTA Graphics

Go to:

```
LOCUS       AAO13045                283 aa            linear   PLN 01-DEC-2003
DEFINITION  ribulose 1,5-bisphosphate carboxylase oxygenase form II, partial
            [Prorocentrum minimum].
ACCESSION   AAO13045
VERSION     AAO13045.1  GI:37731773
DBSOURCE    accession AY169188.1
KEYWORDS    .
SOURCE      Prorocentrum minimum
  ORGANISM  Prorocentrum minimum
            Eukaryota; Alveolata; Dinophyceae; Prorocentrales; Prorocentraceae;
            Prorocentrum.
REFERENCE   1  (residues 1 to 283)
  AUTHORS   Zhang,H. and Lin,S.
  TITLE     Complex gene structure of the form II Rubisco in the dinoflagellate
            Prorocentrum minimum (dinophyceae)
  JOURNAL   J. Phycol. 39 (6), 1160-1171 (2003)
REFERENCE   2  (residues 1 to 283)
  AUTHORS   Zhang,H. and Lin,S.
  TITLE     Direct Submission
  JOURNAL   Submitted (25-OCT-2002) Dept. of Marine Science, University of
            Connecticut, 1080 Shennecossett Rd, Groton, CT 06340, USA
COMMENT     Method: conceptual translation supplied by author.

ORIGIN
        1 gtnvnvcttd dftktvdalv yyidpeneem kiayptalfd rnitdgramm csvltlsign
       61 nqgmgdvdyg kiydiyfppq ylrlfdgpsc cvidmwrilg rgtvggglvv gtiikpklgl
      121 qpkpfgqacy gfwqggdfik ndepqgnqtf cqmnecipev vkamraaqee tgqgklfsan
      181 itaddpnemi arakyilnqm gpmaencafl vdgyvaggta vtvarrnfpk qflhyhragh
      241 gavtspqtqr gytafvhtkl srvigasgih tgtmsfgkme gda
//
```

**Appendix B80.** Matched protein hits (E value < 0.05) of NCBI BLAST search result of 1813.884 m/z of spot #196 and the protein sequence of plastid oxygen-evolving enhancer 1-2 precursor (ABO47876.1) in the NCBInr database. Highlighted region is the matched sequence tag.

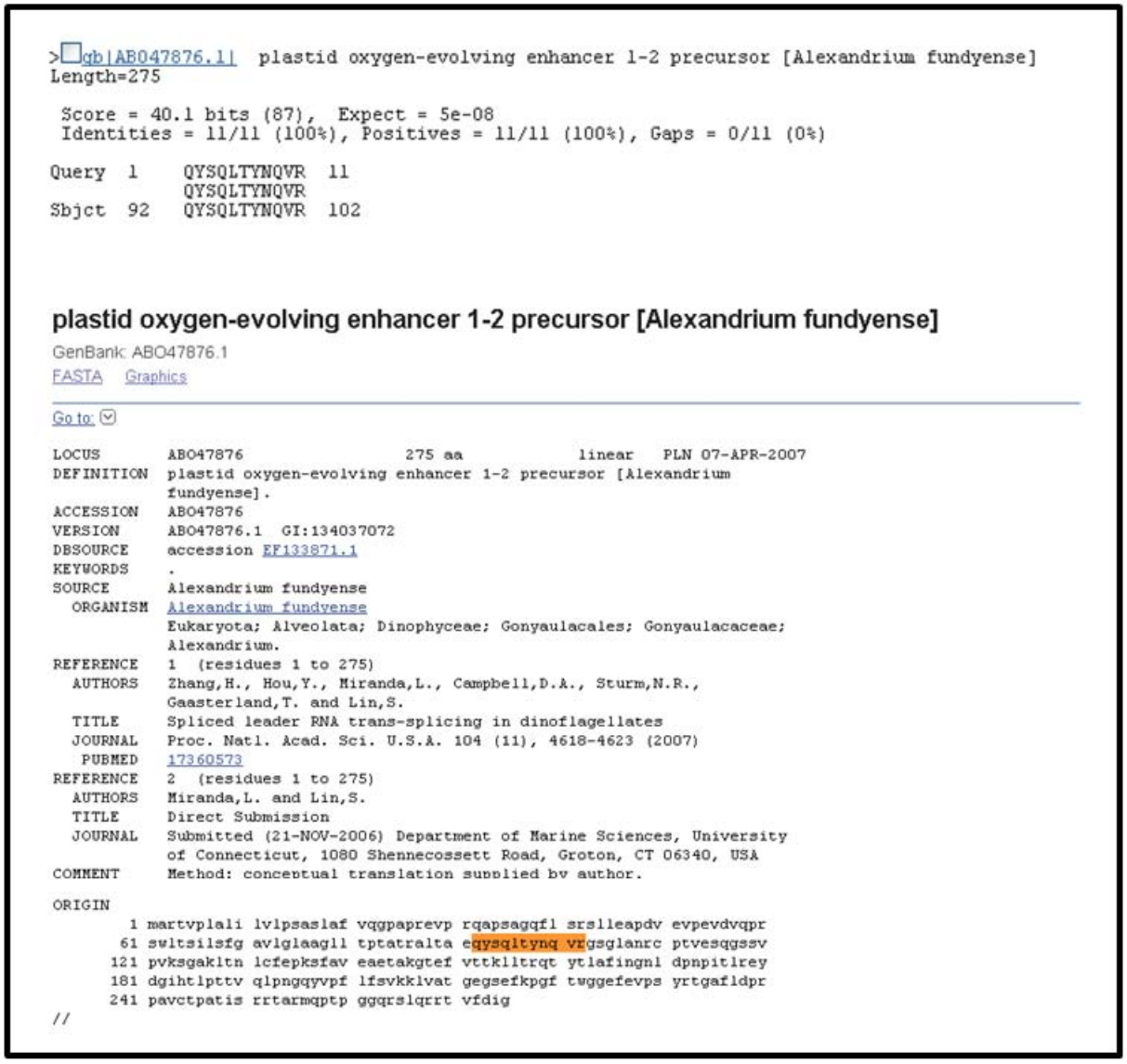

>gb|ABO47876.1| plastid oxygen-evolving enhancer 1-2 precursor [Alexandrium fundyense]
Length=275

Score = 40.1 bits (87), Expect = 5e-08
Identities = 11/11 (100%), Positives = 11/11 (100%), Gaps = 0/11 (0%)

```
Query  1    QYSQLTYNQVR  11
            QYSQLTYNQVR
Sbjct  92   QYSQLTYNQVR  102
```

## plastid oxygen-evolving enhancer 1-2 precursor [Alexandrium fundyense]

GenBank: ABO47876.1

FASTA Graphics

Go to:

```
LOCUS       ABO47876                275 aa            linear   PLN 07-APR-2007
DEFINITION  plastid oxygen-evolving enhancer 1-2 precursor [Alexandrium
            fundyense].
ACCESSION   ABO47876
VERSION     ABO47876.1  GI:134037072
DBSOURCE    accession EF133871.1
KEYWORDS    .
SOURCE      Alexandrium fundyense
  ORGANISM  Alexandrium fundyense
            Eukaryota; Alveolata; Dinophyceae; Gonyaulacales; Gonyaulacaceae;
            Alexandrium.
REFERENCE   1  (residues 1 to 275)
  AUTHORS   Zhang,H., Hou,Y., Miranda,L., Campbell,D.A., Sturm,N.R.,
            Gaasterland,T. and Lin,S.
  TITLE     Spliced leader RNA trans-splicing in dinoflagellates
  JOURNAL   Proc. Natl. Acad. Sci. U.S.A. 104 (11), 4618-4623 (2007)
   PUBMED   17360573
REFERENCE   2  (residues 1 to 275)
  AUTHORS   Miranda,L. and Lin,S.
  TITLE     Direct Submission
  JOURNAL   Submitted (21-NOV-2006) Department of Marine Sciences, University
            of Connecticut, 1080 Shennecossett Road, Groton, CT 06340, USA
COMMENT     Method: conceptual translation supplied by author.

ORIGIN
        1 martvplali lvlpsaslaf vqgpaprevp rqapsagqfl srslleapdv evpevdvqpr
       61 swltsilsfg avlglaagll tptatralta eqysqltynq vrgsglanrc ptvesqgssv
      121 pvksgakltn lcfepksfav eaetakgtef vttklltrqt ytlafingnl dpnpitlrey
      181 dgihtlpttv qlpngqyvpf lfsvkklvat gegsefkpgf twggefevps yrtgafldpr
      241 pavctpatis rrtarmqptp ggqrslqrrt vfdig
//
```

**Appendix B81.** Matched protein hits (E value < 0.05) of NCBI BLAST search result of 1317.951 m/z of spot #118 and the protein sequence of glyceraldehyde-3 phosphate dehydrogenase (ABI14256.1) in the NCBInr database. Highlighted region is the matched sequence tag.

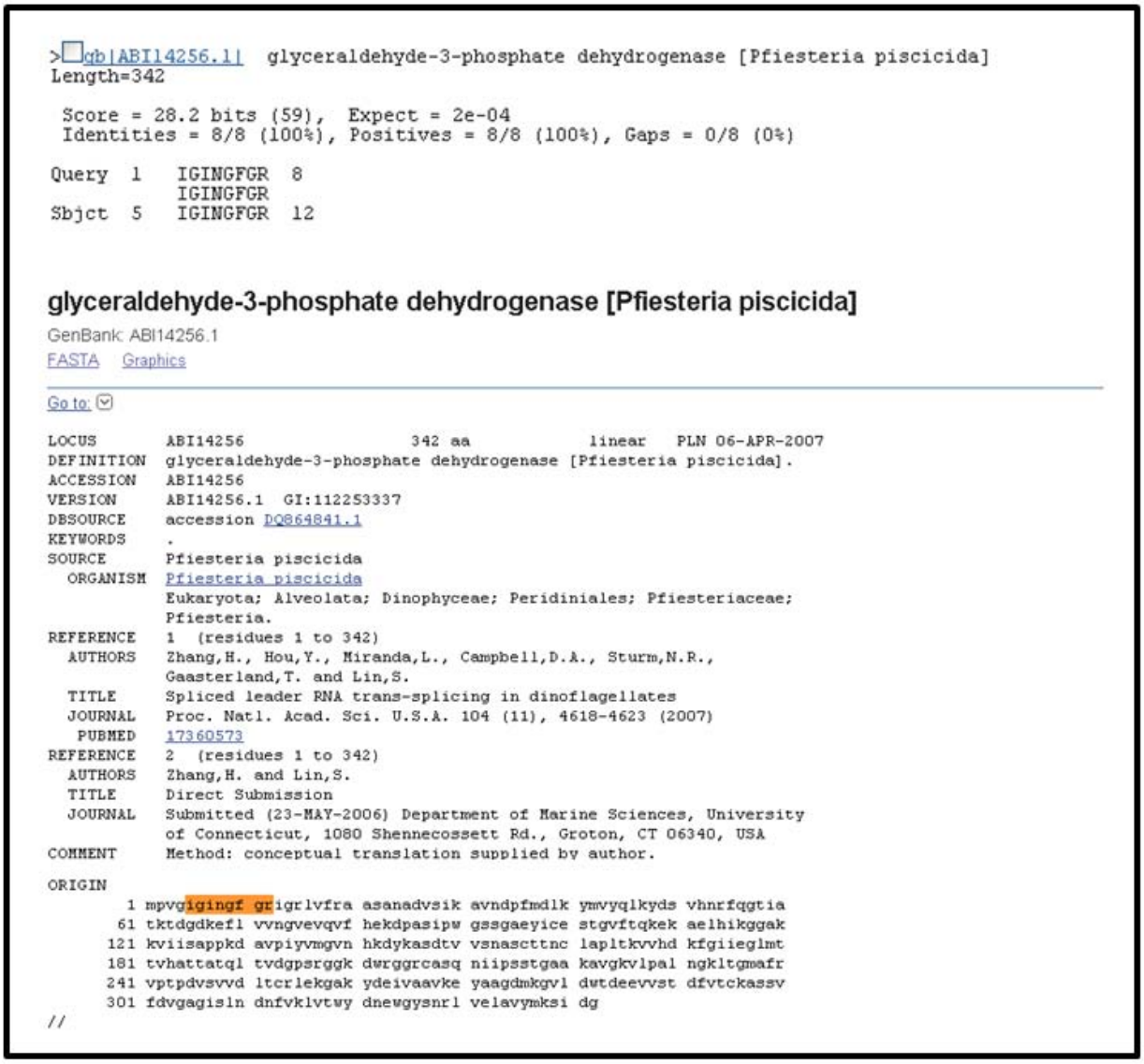

>gb|ABI14256.1| glyceraldehyde-3-phosphate dehydrogenase [Pfiesteria piscicida]
Length=342

Score = 28.2 bits (59), Expect = 2e-04
Identities = 8/8 (100%), Positives = 8/8 (100%), Gaps = 0/8 (0%)

Query 1 IGINGFGR 8
IGINGFGR
Sbjct 5 IGINGFGR 12

## glyceraldehyde-3-phosphate dehydrogenase [Pfiesteria piscicida]

GenBank: ABI14256.1
FASTA Graphics

Go to:

LOCUS ABI14256 342 aa linear PLN 06-APR-2007
DEFINITION glyceraldehyde-3-phosphate dehydrogenase [Pfiesteria piscicida].
ACCESSION ABI14256
VERSION ABI14256.1 GI:112253337
DBSOURCE accession DQ864841.1
KEYWORDS .
SOURCE Pfiesteria piscicida
ORGANISM Pfiesteria piscicida
Eukaryota; Alveolata; Dinophyceae; Peridiniales; Pfiesteriaceae;
Pfiesteria.
REFERENCE 1 (residues 1 to 342)
AUTHORS Zhang,H., Hou,Y., Miranda,L., Campbell,D.A., Sturm,N.R.,
Gaasterland,T. and Lin,S.
TITLE Spliced leader RNA trans-splicing in dinoflagellates
JOURNAL Proc. Natl. Acad. Sci. U.S.A. 104 (11), 4618-4623 (2007)
PUBMED 17360573
REFERENCE 2 (residues 1 to 342)
AUTHORS Zhang,H. and Lin,S.
TITLE Direct Submission
JOURNAL Submitted (23-MAY-2006) Department of Marine Sciences, University
of Connecticut, 1080 Shennecossett Rd., Groton, CT 06340, USA
COMMENT Method: conceptual translation supplied by author.

ORIGIN
1 mpvgigingf grigrlvfra asanadvsik avndpfmdlk ymvyqlkyds vhnrfqgtia
61 tktdgdkefl vvngvevqvf hekdpasipw gssgaeyice stgvftqkek aelhikggak
121 kviisappkd avpiyvmgvn hkdykasdtv vsnascttnc lapltkvvhd kfgiieglmt
181 tvhattatql tvdgpsrggk dwrggrcasq niipsstgaa kavgkvlpal ngkltgmafr
241 vptpdvsvvd ltcrlekgak ydeivaavke yaagdmkgvl dwtdeevvst dfvtckassv
301 fdvgagisln dnfvklvtwy dnewgysnrl velavymksi dg
//

**Appendix B82.** Mascot search result of ESI-iontrap-MS/MS analysis of spot #96 and the protein sequence of glyceraldehyde-3 phosphate dehydrogenase (gi|4103871) in the NCBInr database. Highlighted region is the matched sequence tags.

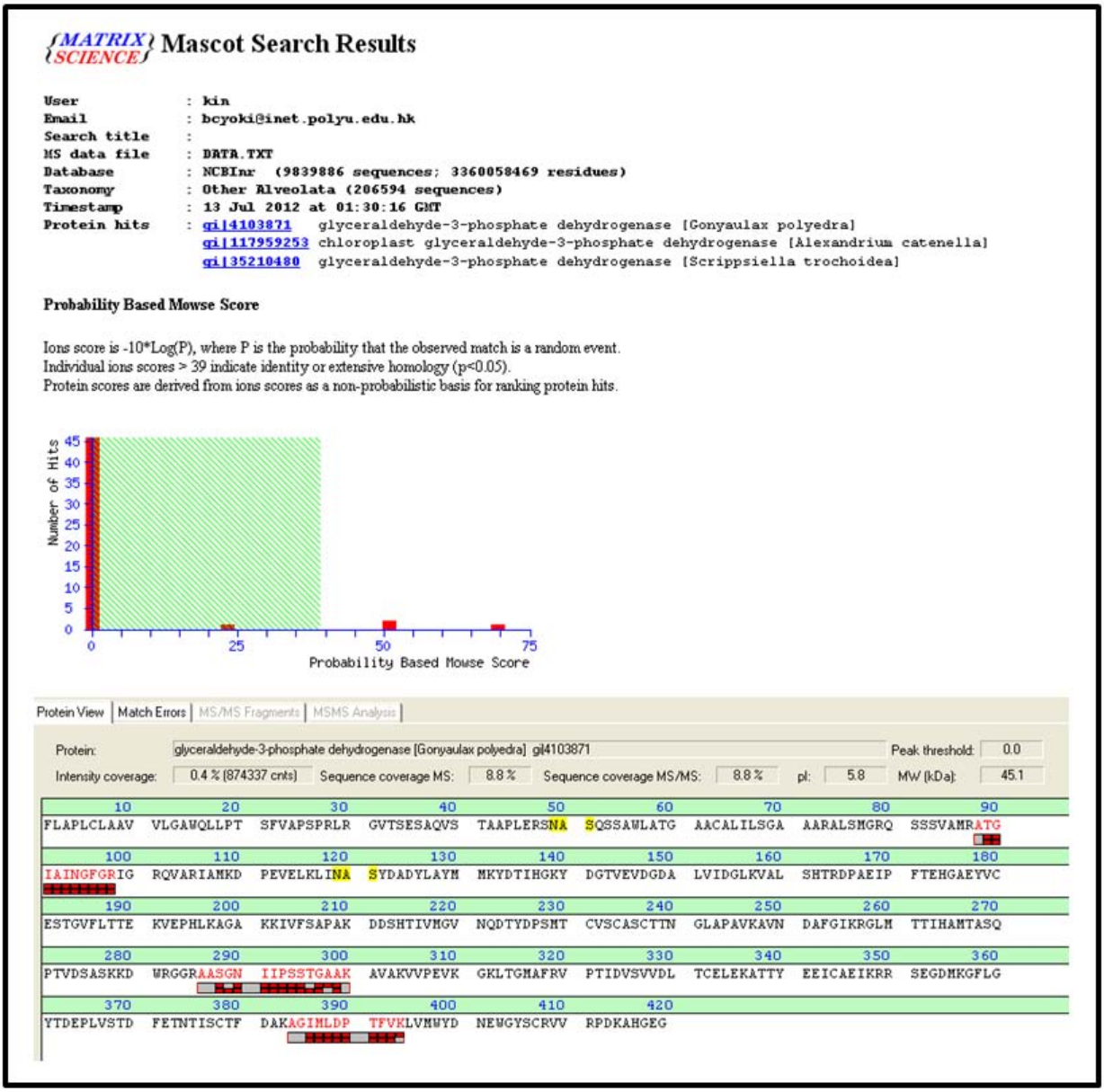

MATRIX SCIENCE Mascot Search Results

User : kin
Email : bcyoki@inet.polyu.edu.hk
Search title :
MS data file : DATA.TXT
Database : NCBInr (9839886 sequences; 3360058469 residues)
Taxonomy : Other Alveolata (206594 sequences)
Timestamp : 13 Jul 2012 at 01:30:16 GMT
Protein hits : gi|4103871 glyceraldehyde-3-phosphate dehydrogenase [Gonyaulax polyedra]
gi|117959253 chloroplast glyceraldehyde-3-phosphate dehydrogenase [Alexandrium catenella]
gi|35210480 glyceraldehyde-3-phosphate dehydrogenase [Scrippsiella trochoidea]

**Probability Based Mowse Score**

Ions score is -10*Log(P), where P is the probability that the observed match is a random event.
Individual ions scores > 39 indicate identity or extensive homology (p<0.05).
Protein scores are derived from ions scores as a non-probabilistic basis for ranking protein hits.



Protein View | Match Errors | MS/MS Fragments | MSMS Analysis

Protein: glyceraldehyde-3-phosphate dehydrogenase [Gonyaulax polyedra] gi|4103871 Peak threshold: 0.0
Intensity coverage: 0.4 % (874337 cnts) Sequence coverage MS: 8.8 % Sequence coverage MS/MS: 8.8 % pI: 5.8 MW (kDa): 45.1

```
10         20         30         40         50         60         70         80         90
FLAPLCLAAV VLGAWQLLPT SFVAPSPRLR GVTSESAQVS TAAPLERSNA SQSSAWLATG AACALILSGA AARALSMGRQ SSSVAMRATG
100        110        120        130        140        150        160        170        180
IAINGFGRIG RQVARIAMKD PEVELKLINA SYDADYLAYM MKYDTIHGKY DGTVEVDGDA LVIDGLKVAL SHTRDPAEIP FTEHGAEYVC
190        200        210        220        230        240        250        260        270
ESTGVFLTTE KVEPHLKAGA KKIVFSAPAK DDSHTIVMGV NQDTYDPSMT CVSCASCTTN GLAPAVKAVN DAFGIKRGLM TTIHAMTASQ
280        290        300        310        320        330        340        350        360
PTVDSASKKD WRGGRAASGN IIPSSTGAAK AVAKVVPEVK GKLTGMAFRV PTIDVSVVDL TCELEKATTY EEICAEIKRR SEGDMKGFLG
370        380        390        400        410        420
YTDEPLVSTD FETNTISCTF DAKAGIMLDP TFVKLVMWYD NEWGYSCRVV RPDKAHGEG
```

**Appendix B83.** Mascot search result of ESI-iontrap-MS/MS analysis of spot #175 and the protein sequence of heat shock protein 70 (gi|61969374) in the NCBInr database. Highlighted region is the matched sequence tags.

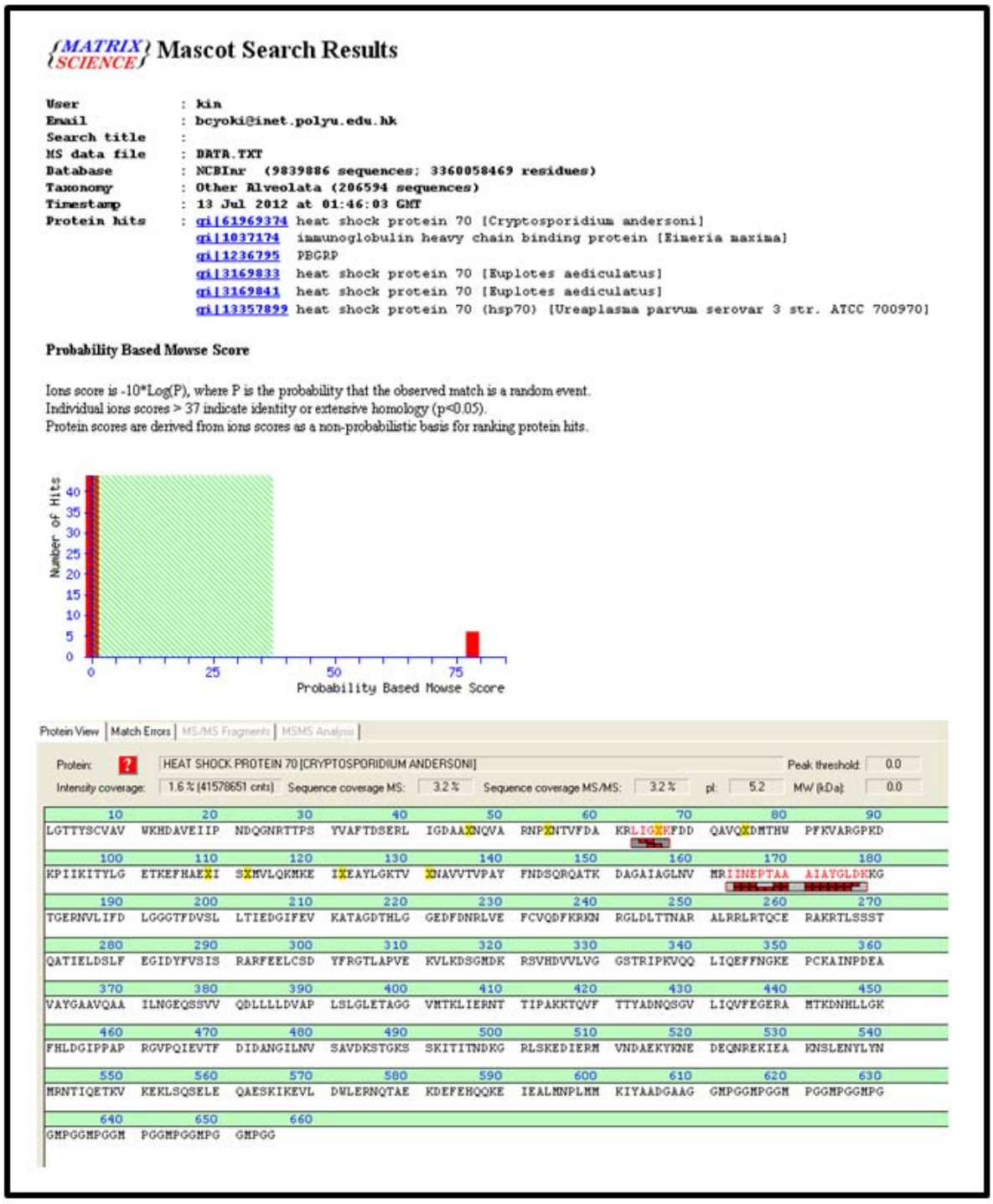

MATRIX SCIENCE **Mascot Search Results**

```
User           : kin
Email          : bcyoki@inet.polyu.edu.hk
Search title   :
MS data file   : DATA.TXT
Database       : NCBInr  (9839886 sequences; 3360058469 residues)
Taxonomy       : Other Alveolata (206594 sequences)
Timestamp      : 13 Jul 2012 at 01:46:03 GMT
Protein hits   : gi|61969374 heat shock protein 70 [Cryptosporidium andersoni]
                 gi|1037174  immunoglobulin heavy chain binding protein [Eimeria maxima]
                 gi|1236795  PBGRP
                 gi|3169833  heat shock protein 70 [Euplotes aediculatus]
                 gi|3169841  heat shock protein 70 [Euplotes aediculatus]
                 gi|13357899 heat shock protein 70 (hsp70) [Ureaplasma parvum serovar 3 str. ATCC 700970]
```

**Probability Based Mowse Score**

Ions score is -10*Log(P), where P is the probability that the observed match is a random event.
Individual ions scores > 37 indicate identity or extensive homology (p<0.05).
Protein scores are derived from ions scores as a non-probabilistic basis for ranking protein hits.




Protein View | Match Errors | MS/MS Fragments | MSMS Analysis

Protein: HEAT SHOCK PROTEIN 70 [CRYPTOSPORIDIUM ANDERSONI] Peak threshold: 0.0

Intensity coverage: 1.6 % (41578651 cnts) Sequence coverage MS: 3.2 % Sequence coverage MS/MS: 3.2 % pI: 5.2 MW (kDa): 0.0

```
       10         20         30         40         50         60         70         80         90
LGTTYSCVAV WKHDAVEIIP NDQGNRTTPS YVAFTDSERL IGDAAXNQVA RNPXNTVFDA KRLIGXKFDD QAVQXDMTHW PFKVARGPKD

      100        110        120        130        140        150        160        170        180
KPIIKITYLG ETKEFHAEXI SXMVLQKMKE IXEAYLGKTV XNAVVTVPAY FNDSQRQATK DAGAIAGLNV MRIINEPTAA AIAYGLDKKG

      190        200        210        220        230        240        250        260        270
TGERNVLIFD LGGGTFDVSL LTIEDGIFEV KATAGDTHLG GEDFDNRLVE FCVQDFKRKN RGLDLTTNAR ALRRLRTQCE RAKRTLSSST

      280        290        300        310        320        330        340        350        360
QATIELDSLF EGIDYFVSIS RARFEELCSD YFRGTLAPVE KVLKDSGMDK RSVHDVVLVG GSTRIPKVQQ LIQEFFNGKE PCKAINPDEA

      370        380        390        400        410        420        430        440        450
VAYGAAVQAA ILNGEQSSVV QDLLLLDVAP LSLGLETAGG VMTKLIERNT TIPAKKTQVF TTYADNQSGV LIQVFEGERA MTKDNHLLGK

      460        470        480        490        500        510        520        530        540
FHLDGIPPAP RGVPQIEVTF DIDANGILNV SAVDKSTGKS SKITITNDKG RLSKEDIERM VNDAEKYKNE DEQNREKIEA KNSLENYLYN

      550        560        570        580        590        600        610        620        630
MRNTIQETKV KEKLSQSELE QAESKIKEVL DWLERNQTAE KDEFEHQQKE IEALMNPLMM KIYAADGAAG GMPGGMPGGM PGGMPGGMPG

      640        650        660
GMPGGMPGGM PGGMPGGMPG GMPGG
```

**Appendix B84.** Information of immunoglobulin heavy chain binding protein and PBGRP in UniProtKB. Sequence similaritiries shows that they belong to heat shock protein 70 family.

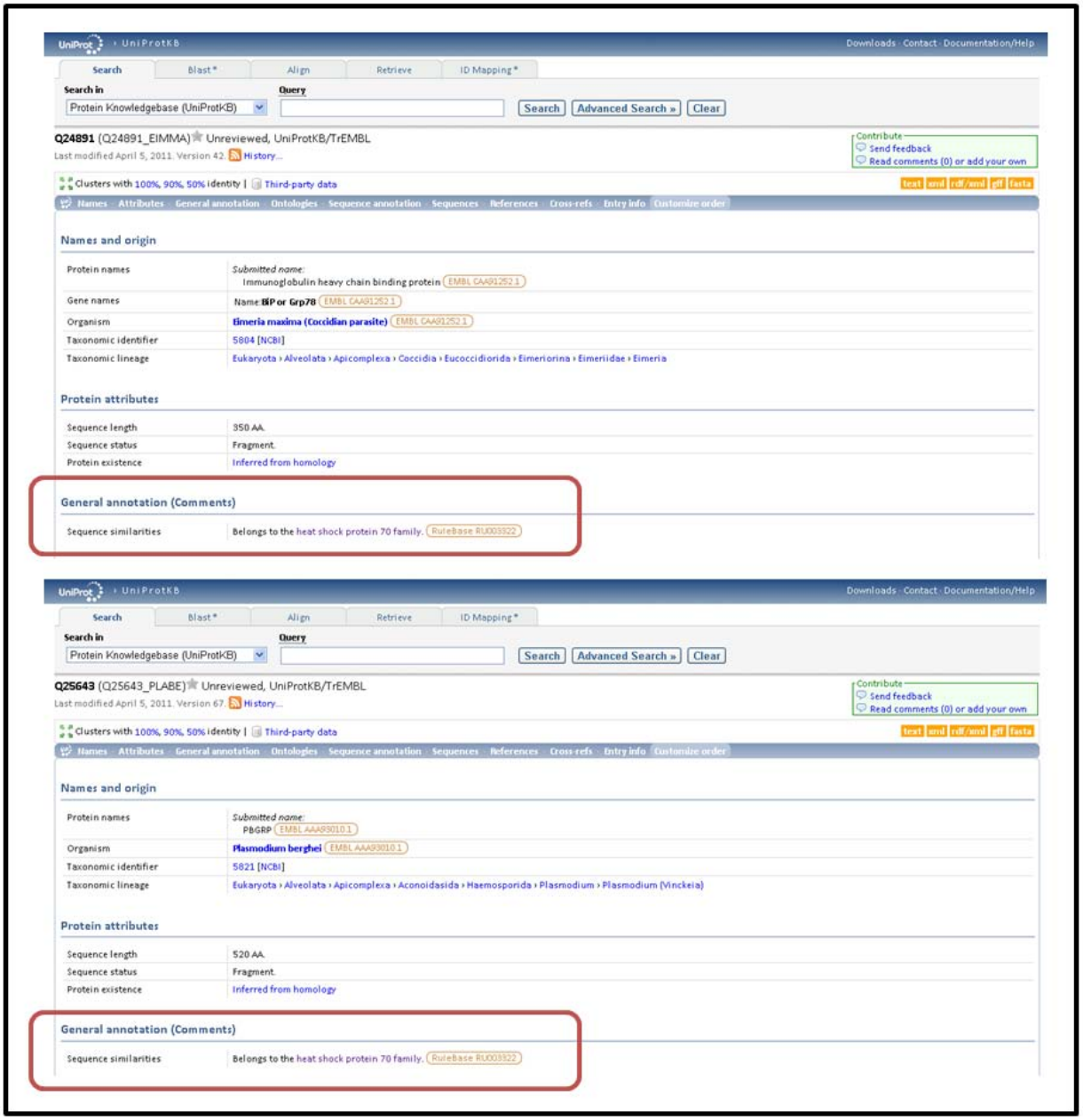

**Appendix B85.** Mascot search result of ESI-iontrap-MS/MS analysis of spot #192 and the protein sequence of heat plastid oxygen-evolving enhancer 1-2 precursor (gi|134037072) in the NCBInr database. Highlighted region is the matched sequence tags.

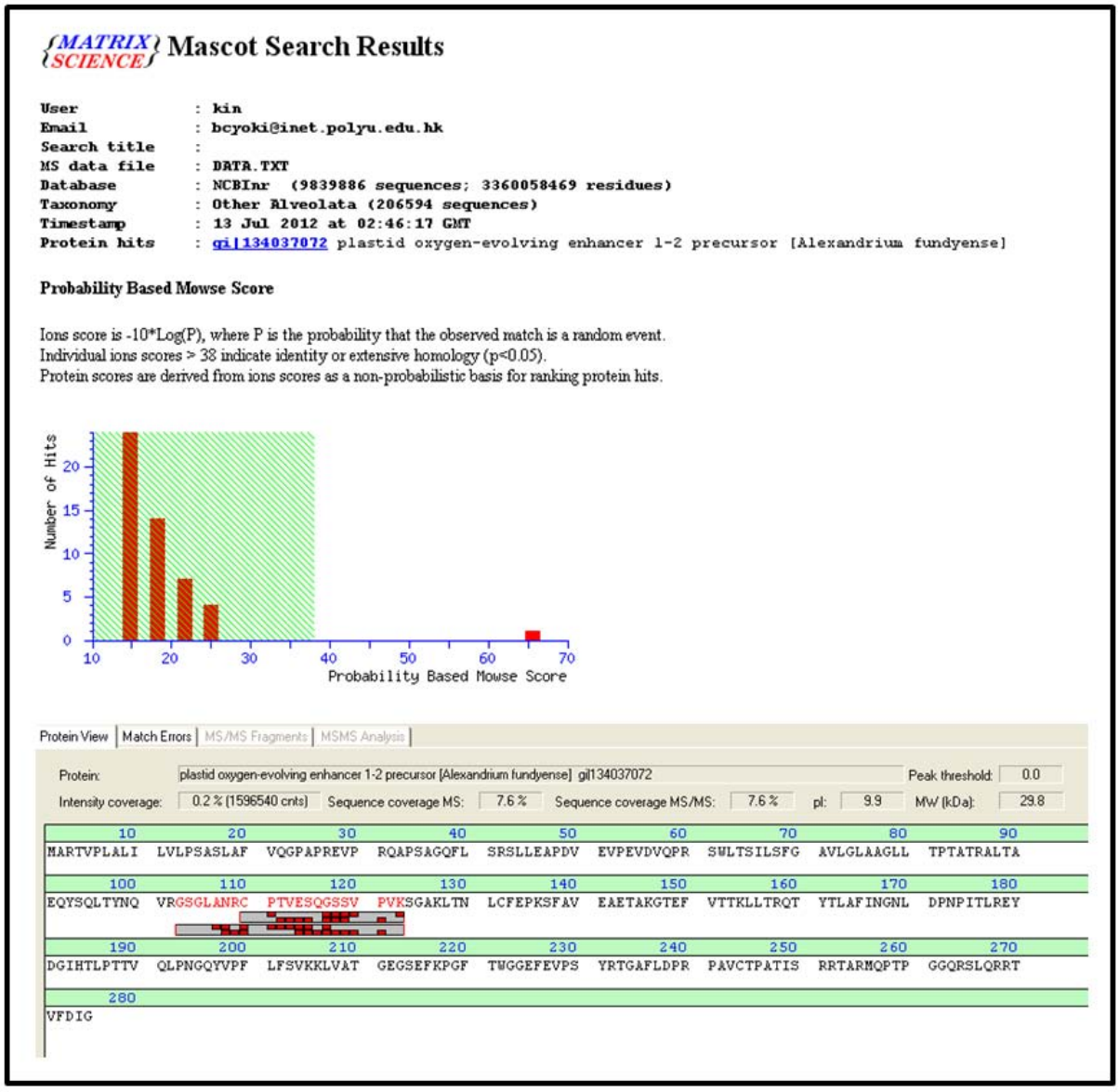

MATRIX SCIENCE **Mascot Search Results**

```
User            : kin
Email           : bcyoki@inet.polyu.edu.hk
Search title    :
MS data file    : DATA.TXT
Database        : NCBInr  (9839886 sequences; 3360058469 residues)
Taxonomy        : Other Alveolata (206594 sequences)
Timestamp       : 13 Jul 2012 at 02:46:17 GMT
Protein hits    : gi|134037072 plastid oxygen-evolving enhancer 1-2 precursor [Alexandrium fundyense]
```

**Probability Based Mowse Score**

Ions score is -10*Log(P), where P is the probability that the observed match is a random event.
Individual ions scores > 38 indicate identity or extensive homology (p<0.05).
Protein scores are derived from ions scores as a non-probabilistic basis for ranking protein hits.



Protein View | Match Errors | MS/MS Fragments | MSMS Analysis

Protein: plastid oxygen-evolving enhancer 1-2 precursor [Alexandrium fundyense] gi|134037072 Peak threshold: 0.0

Intensity coverage: 0.2 % (1596540 cnts) Sequence coverage MS: 7.6 % Sequence coverage MS/MS: 7.6 % pI: 9.9 MW (kDa): 29.8

```
          10         20         30         40         50         60         70         80         90
MARTVPLALI LVLPSASLAF VQGPAPREVP RQAPSAGQFL SRSLLEAPDV EVPEVDVQPR SWLTSILSFG AVLGLAAGLL TPTATRALTA

         100        110        120        130        140        150        160        170        180
EQYSQLTYNQ VRGSGLANRC PTVESQGSSV PVKSGAKLTN LCFEPKSFAV EAETAKGTEF VTTKLLTRQT YTLAFINGNL DPNPITLREY

         190        200        210        220        230        240        250        260        270
DGIHTLPTTV QLPNGQYVPF LFSVKKLVAT GEGSEFKPGF TWGGEFEVPS YRTGAFLDPR PAVCTPATIS RRTARMQPTP GGQRSLQRRT

         280
VFDIG
```

**Appendix B86.** Mascot search result of ESI-iontrap-MS/MS analysis of spot #266 and the protein sequence of light-harvesting chlorophyll a-c binding protein (gi|757520), light-harvesting polyprotein precursor (gi|3355306) and chloroplast light harvesting complex protein (gi|58613557) in the NCBInr database. Highlighted region is the matched sequence tags.

**Appendix B87.** Mascot search result of ESI-iontrap-MS/MS analysis of spot #73 and the protein sequence of ATP synthase subunit beta (gi|15966787) and beta-tubulin (gi|168830539) in the NCBInr database. Highlighted region is the matched sequence tags.

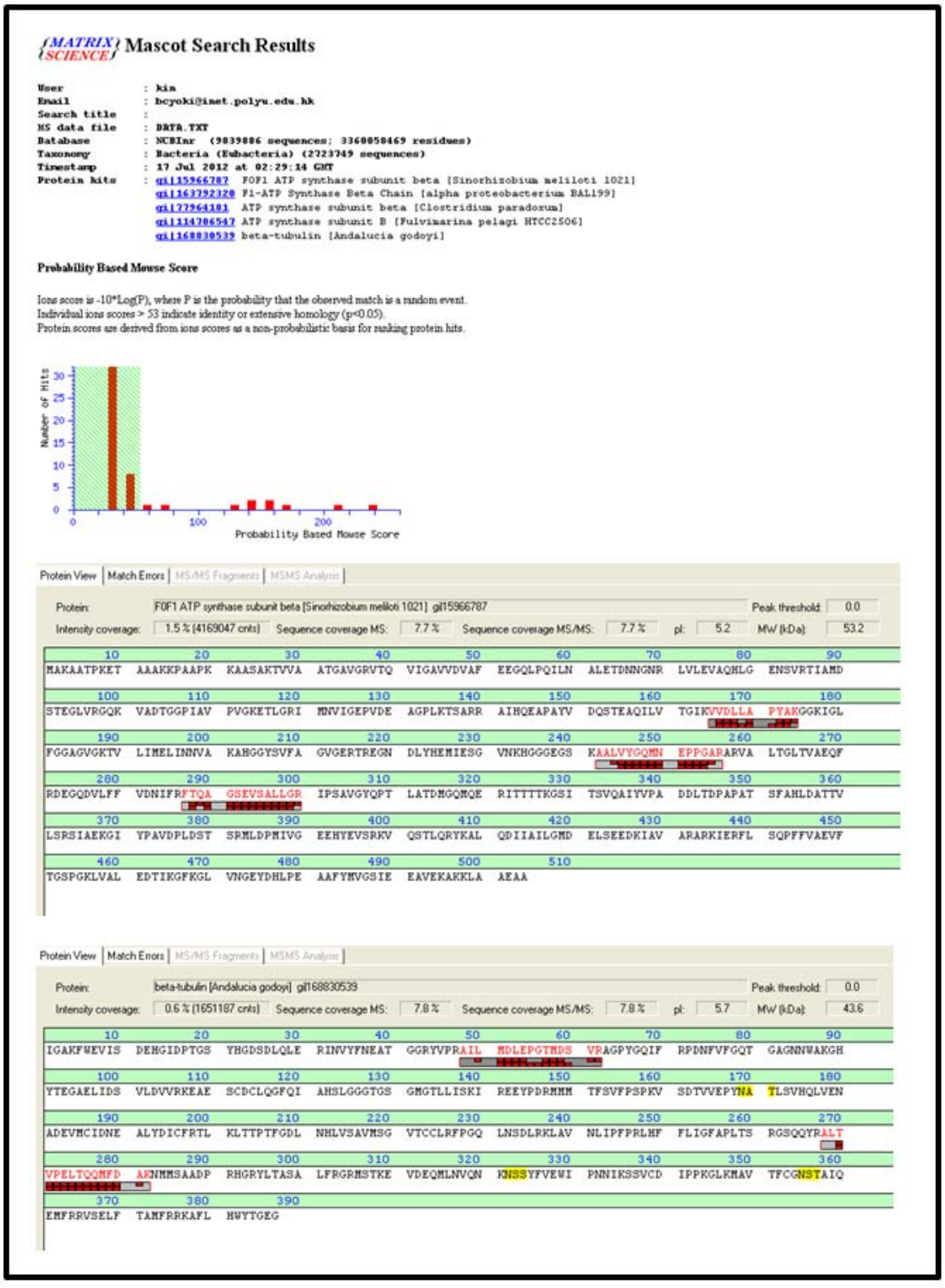

MATRIX SCIENCE **Mascot Search Results**

User : kin
Email : bcyoki@inet.polyu.edu.hk
Search title :
MS data file : DATA.TXT
Database : NCBInr (9839886 sequences; 3360858469 residues)
Taxonomy : Bacteria (Eubacteria) (2723749 sequences)
Timestamp : 17 Jul 2012 at 02:29:14 GMT
Protein hits : gi|15966787 F0F1 ATP synthase subunit beta [Sinorhizobium meliloti 1021]
gi|163792320 F1-ATP Synthase Beta Chain [alpha proteobacterium BAL199]
gi|77964181 ATP synthase subunit beta [Clostridium paradoxum]
gi|114706547 ATP synthase subunit B [Fulvimarina pelagi HTCC2506]
gi|168830539 beta-tubulin [Andalucia godoyi]

**Probability Based Mouse Score**

Ions score is -10*Log(P), where P is the probability that the observed match is a random event.
Individual ions scores > 53 indicate identity or extensive homology (p<0.05).
Protein scores are derived from ions scores as a non-probabilistic basis for ranking protein hits.




Protein View | Match Errors | MS/MS Fragments | MSMS Analysis

Protein: F0F1 ATP synthase subunit beta [Sinorhizobium meliloti 1021] gi|15966787 Peak threshold: 0.0
Intensity coverage: 1.5 % (4169047 cnts) Sequence coverage MS: 7.7 % Sequence coverage MS/MS: 7.7 % pI: 5.2 MW (kDa): 53.2

```
10        20        30        40        50        60        70        80        90
MAKAATPKET AAAKKPAAPK KAASAKTVVA ATGAVGRVTQ VIGAVVDVAF EEGQLPQILN ALETDNNGNR LVLEVAQHLG ENSVRTIAMD

100       110       120       130       140       150       160       170       180
STEGLVRGQK VADTGGPIAV PVGKETLGRI MNVIGEPVDE AGPLKTSARR AIHQEAPAYV DQSTEAQILV TGIKVVDLLA PYAKGGKIGL

190       200       210       220       230       240       250       260       270
FGGAGVGKTV LIMELINNVA KAHGGYSVFA GVGERTREGN DLYHEMIESG VNKHGGGEGS KAALVYGQMN EPPGARARVA LTGLTVAEQF

280       290       300       310       320       330       340       350       360
RDEGQDVLFF VDNIFRFTQA GSEVSALLGR IPSAVGYQPT LATDMGQMQE RITTTTKGSI TSVQAIYVPA DDLTDPAPAT SFAHLDATTV

370       380       390       400       410       420       430       440       450
LSRSIAEKGI YPAVDPLDST SRMLDPNIVG EEHYEVSRKV QSTLQRYKAL QDIIAILGMD ELSEEDKIAV ARARKIERFL SQPFFVAEVF

460       470       480       490       500       510
TGSPGKLVAL EDTIKGFKGL VNGEYDHLPE AAFYMVGSIE EAVEKAKKLA AEAA
```

Protein View | Match Errors | MS/MS Fragments | MSMS Analysis

Protein: beta-tubulin [Andalucia godoyi] gi|168830539 Peak threshold: 0.0
Intensity coverage: 0.6 % (1651187 cnts) Sequence coverage MS: 7.8 % Sequence coverage MS/MS: 7.8 % pI: 5.7 MW (kDa): 43.6

```
10        20        30        40        50        60        70        80        90
IGAKFWEVIS DEHGIDPTGS YHGDSDLQLE RINVYFNEAT GGRYVPRAIL MDLEPGTMDS VRAGPYGQIF RPDNFVFGQT GAGNNWAKGH

100       110       120       130       140       150       160       170       180
YTEGAELIDS VLDVVRKEAE SCDCLQGFQI AHSLGGGTGS GMGTLLISKI REEYPDRMMM TFSVFPSPKV SDTVVEPYNA TLSVHQLVEN

190       200       210       220       230       240       250       260       270
ADEVMCIDNE ALYDICFRTL KLTTPTFGDL NHLVSAVMSG VTCCLRFPGQ LNSDLRKLAV NLIPFPRLHF FLIGFAPLTS RGSQQYRALT

280       290       300       310       320       330       340       350       360
VPELTQQMFD AKNMMSAADP RHGRYLTASA LFRGRMSTKE VDEQMLNVQN KNSSYFVEWI PNNIKSSVCD IPPKGLKMAV TFCGNSTAIQ

370       380       390
EMFRRVSELF TAMFRRKAFL HWYTGEG
```

**Appendix B88.** Mascot search result of ESI-iontrap-MS/MS analysis of spot #66 and the protein sequence of heat shock protein 90 (gi|161875) and glyceraldehyde-3 phosphate dehydrogenase (gi|58618206) in the NCBInr database. Highlighted region is the matched sequence tags.

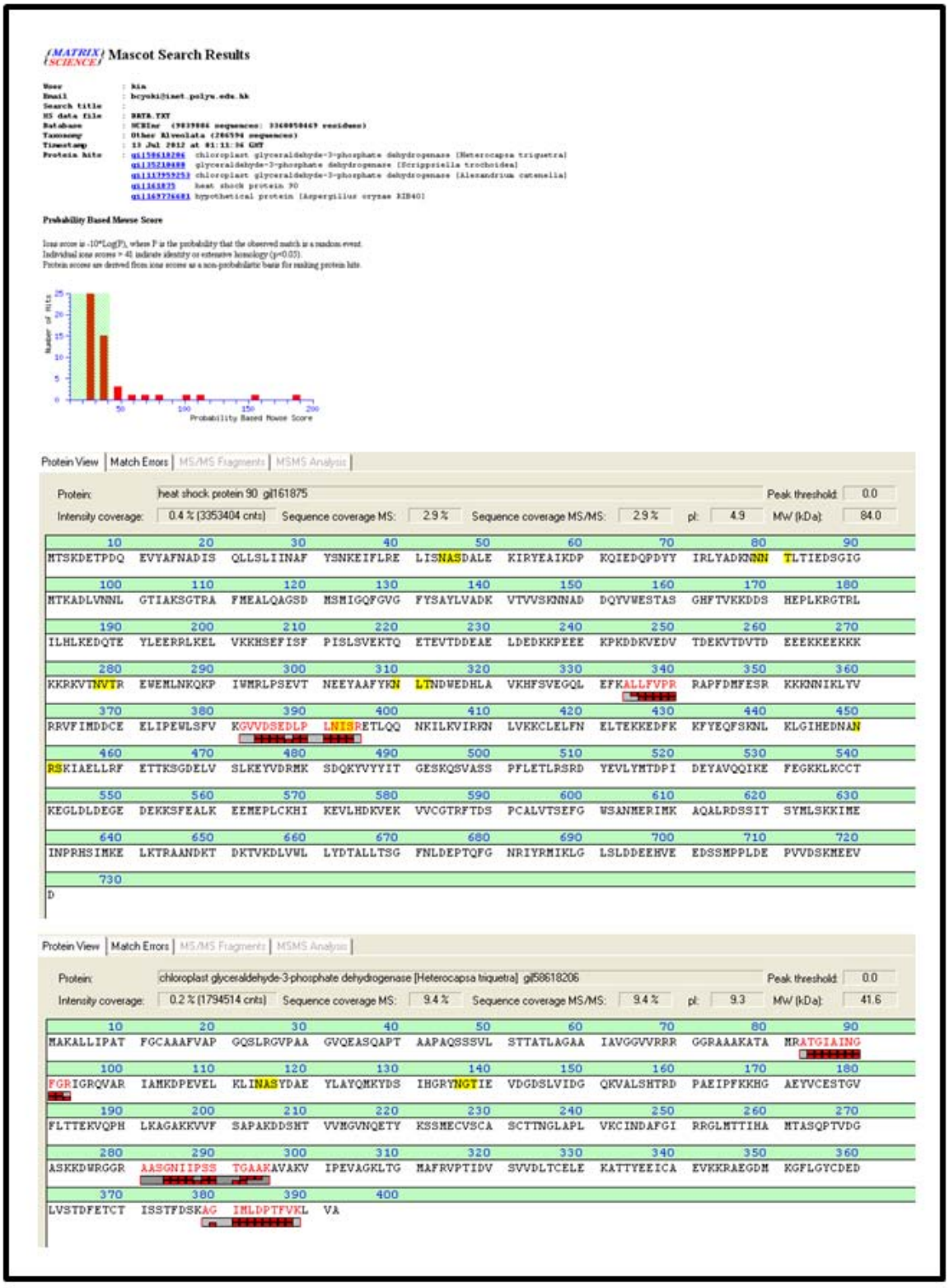

Mascot Search Results

User : kin
Email : bcyoki@inet.polyu.edu.hk
Search title :
MS data file : DATA.TXT
Database : NCBInr (7819986 sequences; 3160858469 residues)
Taxonomy : Other Alveolata (286594 sequences)
Timestamp : 13 Jul 2012 at 01:11:36 GMT
Protein hits : gi|158618206 chloroplast glyceraldehyde-3-phosphate dehydrogenase [Heterocapsa triquetra]
gi|195218488 glyceraldehyde-3-phosphate dehydrogenase [Scrippsiella trochoidea]
gi|113759253 chloroplast glyceraldehyde-3-phosphate dehydrogenase [Alexandrium catenella]
gi|161875 heat shock protein 90
gi|169776681 hypothetical protein [Aspergillus oryzae RIB40]

Probability Based Mowse Score

Ions score is -10*Log(P), where P is the probability that the observed match is a random event.
Individual ions scores > 42 indicate identity or extensive homology (p<0.05).
Protein scores are derived from ions scores as a non-probabilistic basis for ranking protein hits.

Number of Hits
Probability Based Mowse Score

Protein View | Match Errors | MS/MS Fragments | MSMS Analysis

Protein: heat shock protein 90 gi|161875 Peak threshold: 0.0
Intensity coverage: 0.4 % (3353404 cnts) Sequence coverage MS: 2.9 % Sequence coverage MS/MS: 2.9 % pI: 4.9 MW (kDa): 84.0

10 20 30 40 50 60 70 80 90
MTSKDETPDQ EVYAFNADIS QLLSLIINAF YSNKEIFLRE LISNASDALE KIRYEAIKDP KQIEDQPDYY IRLYADKNNN TLTIEDSGIG

100 110 120 130 140 150 160 170 180
MTKADLVNNL GTIAKSGTRA FMEALQAGSD MSMIGQFGVG FYSAYLVADK VTVVSKNNAD DQYVWESTAS GHFTVKKDDS HEPLKRGTRL

190 200 210 220 230 240 250 260 270
ILHLKEDQTE YLEERRLKEL VKKHSEFISF PISLSVEKTQ ETEVTDDEAE LDEDKKPEEE KPKDDKVEDV TDEKVTDVTD EEEKKEEKKK

280 290 300 310 320 330 340 350 360
KKRKVTNVTR EWEMLNKQKP IWMRLPSEVT NEEYAAFYKN LTNDWEDHLA VKHFSVEGQL EFKALLFVPR RAPFDMFESR KKKNNIKLYV

370 380 390 400 410 420 430 440 450
RRVFIMDDCE ELIPEWLSFV KGVVDSEDLP LNISRETLQQ NKILKVIRKN LVKKCLELFN ELTEKKEDFK KFYEQFSKNL KLGIHEDNAN

460 470 480 490 500 510 520 530 540
RSKIAELLRF ETTKSGDELV SLKEYVDRMK SDQKYVYYIT GESKQSVASS PFLETLRSRD YEVLYMTDPI DEYAVQQIKE FEGKKLKCCT

550 560 570 580 590 600 610 620 630
KEGLDLDEGE DEKKSFEALK EEMEPLCKHI KEVLHDKVEK VVCGTRFTDS PCALVTSEFG WSANMERIMK AQALRDSSIT SYMLSKKIME

640 650 660 670 680 690 700 710 720
INPRHSIMKE LKTRAANDKT DKTVKDLVWL LYDTALLTSG FNLDEPTQFG NRIYRMIKLG LSLDDEEHVE EDSSMPPLDE PVVDSKMEEV

730
D

Protein View | Match Errors | MS/MS Fragments | MSMS Analysis

Protein: chloroplast glyceraldehyde-3-phosphate dehydrogenase [Heterocapsa triquetra] gi|58618206 Peak threshold: 0.0
Intensity coverage: 0.2 % (1794514 cnts) Sequence coverage MS: 9.4 % Sequence coverage MS/MS: 9.4 % pI: 9.3 MW (kDa): 41.6

10 20 30 40 50 60 70 80 90
MAKALLIPAT FGCAAAFVAP GQSLRGVPAA GVQEASQAPT AAPAQSSSVL STTATLAGAA IAVGGVVRRR GGRAAAKATA MRATGIAING

100 110 120 130 140 150 160 170 180
FGRIGRQVAR IAMKDPEVEL KLINASYDAE YLAYQMKYDS IHGRYNGTIE VDGDSLVIDG QKVALSHTRD PAEIPFKKHG AEYVCESTGV

190 200 210 220 230 240 250 260 270
FLTTEKVQPH LKAGAKKVVF SAPAKDDSMT VVMGVNQETY KSSMECVSCA SCTTNGLAPL VKCINDAFGI RRGLMTTIHA MTASQPTVDG

280 290 300 310 320 330 340 350 360
ASKKDWRGGR AASGNIIPSS TGAAKAVAKV IPEVAGKLTG MAFRVPTIDV SVVDLTCELE KATTYEEICA EVKKRAEGDM KGFLGYCDED

370 380 390 400
LVSTDFETCT ISSTFDSKAG IMLDPTFVKL VA

**Appendix C: Publications**

Harmful Algae 12 (2011) 1–10

Contents lists available at SciVerse ScienceDirect

Harmful Algae

journal homepage: www.elsevier.com/locate/hal

# Authentication of the proteins expression profiles (PEPs) identification methodology in a bloom of *Karenia digitata*, the most damaging harmful algal bloom causative agent in the history of Hong Kong

Fred Wang-Fat Lee [a,b], Kin-Chung Ho [b], Yun-Lam Mak [a], Samuel Chun-Lap Lo [a,*]

[a] The Proteomic Task Force, Department of Applied Biology and Chemical Technology, The Hong Kong Polytechnic University, Kowloon, Hong Kong
[b] School of Science and Technology, The Open University of Hong Kong, Hong Kong SAR, China

ARTICLE INFO

*Article history:*
Received 16 May 2011
Received in revised form 11 August 2011
Accepted 11 August 2011
Available online 19 August 2011

*Keywords:*
Harmful algal bloom (HAB)
Identification
*Karenia digitata*
MALDI-TOF
Protein expression profiles (PEPs)

ABSTRACT

Identification of harmful algal bloom (HAB) causative agents makes use either of morphology-based techniques or genetic tools. These techniques are often time-consuming, labor intensive, and/or based on subjective judgment. Recently, matching with protein/peptide expression profiles (PEPs) obtained with matrix-assisted laser desorption ionization time-of-flight mass spectrometry (MALDI–TOF–MS) has emerged as a new technique for species identification of various microorganisms. We were the first group to adopt this rapid and simple methodology for the identification of dinoflagellates (Lee et al., 2008). In the present study, we evaluated the use of PEPs from MALDI–TOF–MS for species identification of field samples obtained from a local red-tide caused by *Karenia digitata*. PEPs obtained from direct MALDI–TOF–MS analysis of field samples were compared to that of established monospecific reference culture. Several species-specific peaks of *K. digitata* were found in the reference monoculture and most of these observed peaks could be matched to the PEPs of the field samples. Matched species-specific peaks observed from the PEPs of field samples would allow rapid identification of the causative agents in corresponding and future HABs. Furthermore, as *K. digitata* is the most damaging dinoflagellate in Hong Kong's history, we were interested in obtaining its SSU, partial LSU rDNA and ITS sequences for future studies. In the present study, besides reporting on the ITS and rDNA sequences of *K. digitata*, phylogenetic tree analysis was also performed. The results showed that *K. digitata* fell within the *Karlodinium* clade and had a closer relationship with the *Karlodinium species* than the *Karenia species*.



## 1. Introduction

A harmful algal bloom (HAB) caused by *Karenia digitata* was reported in Silver Mine Bay of Hong Kong in mid-March 2009. This is the second bloom of this species in Hong Kong. The first bloom caused by this species occurred in Hong Kong in 1998 with serious fish kills (Yang and Hodgkiss, 2004; Yang et al., 2000). It is the most serious HAB that had ever occurred in these waters (Lee and Qu, 2004; Yang and Hodgkiss, 2004). This unprecedented HAB had invaded nearly all corners of the coastal waters of Hong Kong, including 22 of the 26 fish farms and 5 swimming beaches. In Hong Kong alone, 1260 fishery households were affected and 2500 tones of fishes were killed. A direct economic loss of HK$ 250 million (about US$ 32 million) was estimated by the fish farmers (Yang and Hodgkiss, 2004). The scale of this recent bloom was much smaller with no associated fish-kill reported. Nevertheless, officials of the Hong Kong Special Administrative Region Government in charge of aquaculture, beaches as well as food safety were on high alert during that second bloom. Various strategies were formulated to address a second bloom as big as the first one. The need for a forewarning system has repeatedly been raised. Given that there is no effective prevention for the occurrence of HABs, accurate identification, early detection and warning will provide aquaculturists some much needed time to take necessary measures and minimize their loss. Protein/peptide expression profiles (PEPs) as obtained with matrix-assisted laser desorption ionization time-of-flight mass spectrometry (MALDI–TOF–MS) has emerged as a new method for species identification for various microorganisms (Fenselau and Demirev, 2001; Dworzanski and Snyder, 2005). Our group had previously successfully used PEP-based identification technique to identify different dinoflagellates species (Lee et al., 2008). The basic concept is to match the PEPs of the unknown species to PEPs of various reference species in a database. In the present study, we intended to extend our previous application of MALDI–MS-based identification technique on the culture samples to real-life field samples of HAB. Field samples were collected on four consecutive days from an algal bloom caused by *K. digitata* in Silver Mine Bay during the period from March 23rd 2009 to March

* Corresponding author. Tel.: +852 34008669; fax: +852 23649932.
*E-mail address:* bcsamlo@ (S.-L. Lo).

1568-9883/$ – see front matter © 2011 Elsevier B.V. All rights reserved.
doi:10.1016/j.hal.2011.08.007

26th 2009. We evaluated MALDI–TOF–MS-based technique for the identification of the HAB samples by comparing the PEPs obtained from direct MALDI–TOF–MS analysis of the field samples to that of an established reference of *K. digitata* monoculture (KD01). Further, since *K. digitata* is the most damaging dinoflagellate in the history of Hong Kong, we were interested in obtaining its ribosomal DNA (rDNA) and internal transcribed spacer (ITS) sequences for future studies. For the past few years, phylogenetic and species identification studies based on rDNA (Scholin et al., 1993, 1994a) and ITS (Adachi et al., 1996; Litaker et al., 2007) sequence data have begun to appear more frequently in the literature. In the molecular analysis of *K. digitata*, we have chosen three sequence regions for analysis (including the ITS1-5.8S-ITS2 (ITS), small (18S) and large (26S) subunit ribosomal DNA sequences) because these regions had been sequenced in many marine dinoflagellates and these data we obtained could be used for phylogenetic comparison.

## 2. Materials and methods

### 2.1. Phytoplankton sampling

Phytoplankton samples were collected daily for four consecutive days from the algal bloomed area in Silver Mine Bay during the period of March 23–26, 2009 (Table 1). Identities of the causative agents were confirmed morphologically by officials of the Agricultural, Fisheries and Conservation Department of the Hong Kong SAR Government.

### 2.2. Cell counts

One milliliter of either monoculture or field samples was fixed with 10 μL Lugol's solution and counted under a light microscope with a Sedgwick-Rafter cell counter.

### 2.3. Culture condition

Single cells of *K. digitata* collected from the field were capillary isolated and transferred to L1 seawater based medium. A monoculture called KD01 was successfully established using the L1 medium and was used as the reference culture in this study. Cells in the culture were kept at the exponential growth phase by transferring to new medium every two week in a ratio of 1:10 (v/v). Vegetative cells from the cultures in mid- or late-exponential phases of growth were inoculated into freshly prepared culture medium. Possible contamination of the culture was checked by regular microscopic examination. The cell cultures were maintained at 20 °C under a 12-h light:12-h dark cycle at a light intensity of 120 mol photons $m^{-1}$ $s^{-1}$ provided by cool white fluorescent tubes in a Conviron growth chamber (Model EF7, USA).

### 2.4. Sample preparation to obtain PEPs using MALDI–TOF–MS

Samples were prepared as described previously (Lee et al., 2008). Briefly, around 1500 mL of cultures in exponential growth phase or field samples were collected by centrifugation (1500 × g for 15 min at room temperature). Cell pellets were re-suspended in 0.1% trifluoroacetic acid (TFA) (Aldrich, USA). These cells were lysed by sonication. Cells debris were removed by centrifugation at 13,000 × g at room temperature for 5 min. Inorganic salts in the samples were cleaned up by absorbing the proteins/peptides onto either C-18 or C-4 zip tips (Millipore, USA) according to instructions from the manufacturer. Proteins/peptides were eluted from the zip-tips with 1–2 μL of 0.1% TFA in 70% acetonitrile. Eluted proteins/peptides solutions were mixed with matrix solution in a ratio of 1:1 (v/v). Matrix solution was made up of saturated sinapinic acid (SA) in a 1:1 (v/v) ratio with 0.1% TFA/acetonitrile. Subsequently, 1 μL lots of the resulting mixtures were spotted onto a mass spectrometer target plate (MTP AnchorChip™ 600/384TF, Bruker, Germany) for subsequent MALDI–TOF–MS analysis.

### 2.5. MALDI-TOF MS analysis

Proteins/peptides expression profiles (PEPs) of all samples tested were obtained with a MALDI–TOF–TOF mass spectrometer (Autoflex III Smartbeam, Bruker, Germany) in linear mode at an accelerating voltage of 20 kV with a 300 ns delay time and over a mass range of 2000–16,000 Da. For each sample, spectra from 500 laser shots at several different positions of the protein spot on the anchor chip were combined to generate a mass spectrum. The mass spectra were calibrated using the Protein Calibration Standard I (Bruker, Germany) and were used to provide a mass accuracy of 1 part in 3000. The calibrants mixture contained insulin (5734.51 Da), ubiquitin (8565.76 Da), cytochrome C (12,360.97 Da) and myoglobin (16,952.3 Da). Fresh calibration was performed for different samples and for different individual experiments.

### 2.6. ITS and ribosomal DNA gene sequencing

DNA extraction was performed according to the procedures reported previously (Lee et al., 2008). Three regions, including ITS1-5.8S-ITS2, SSU (18S) and partial LSU (26S) rDNA were amplified. ITS regions were amplified from the extracted DNA using primers described previously (D'Onofrio et al., 1999), ITS1 (forward): 5′TCCGTAGGTGAACCTGCGG3′ and ITS4 (reverse): 5′TCCTCCGCTTATTGATATGC3′. 18S SSU region was amplified using primer described in Logares et al. (2007), 4616 (forward): 5′AACCTGGTTGATCCTGCCAG3′ and 4618 (reverse): 5′TGATCCTTCTGCAGGTTCACCTAC3′. 26S LSU region was amplified using primers described previously (Daugbjerg et al., 2000; Scholin et al., 1994b). PCR was performed according to the following scheme: 95 °C 5 min; 35 cycles of 94 °C 45 s, 55 °C 45 s and 72 °C 2 min; 72 °C 10 min. PCR products were cloned into pGEM-T easy vectors (Promega, USA) prior to DNA sequencing. DNA sequencing of all cloned plasmids were performed by commercial facilities using traditional dideoxy-methodology.

### 2.7. Phylogenetic analysis

Using the Clustal X program (Thompson et al., 1997), ITS DNA sequence of *K. digitata* was aligned and compared with the ITS DNA

**Table 1**
Red-tide samples from the Silver Mine Bay of Hong Kong.

| Day | Date | Cell concentration (cells/mL) | Sampling volume | Total number of cells[a] | Observation of cells under microscope |
|---|---|---|---|---|---|
| 1 | 23rd March 2009 | 7000 | ~0.1 L | $7 \times 10^5$ | Active and healthy |
| 2 | 24th March 2009 | 800 | ~0.5 L | $4 \times 10^5$ | Active and healthy |
| 3 | 25th March 2009 | 500 | ~1.5 L | $7.5 \times 10^5$ | Moving slowly |
| 4 | 26th March 2009 | 216 | ~3 L | $6.5 \times 10^5$ | Stop moving, most cells started to disintegrate, cell lysis occurred |

[a] $10^5$ of *Karenia digitata* cells in the bloom samples were used for MALDI–TOF–MSPEP analysis.

sequence of 10 different *Karenia/Karlodinium* species retrieved from PubMed. Phylogenetic analysis was carried out using PHYLIP, version 3.69 (Joe Felsenstein, Department of Genetics, University of Washington) with ITS DNA sequence of *Gymnodinium* species (AM184203) as an outgroup. Distance matrices were produced using the DNADIST module and a Neighbor-Join tree was built with the NEIGHBOR module. One thousand bootstrap replicates were generated and performed using the SEQBOOT module and the consensus tree was generated using CONSENSE. Tree was viewed with the Treeview software (Page, 1996).

## 3. Results and discussion

### 3.1. MALDI–TOF–MS analysis of real time harmful algal bloom samples

Rapid and accurate identification of the causative agent of a HAB is important during a HAB crisis. Our group has shown the great potential of using PEPSs obtained with MALDI–TOF–MS for species identification of dinoflagellates (Lee et al., 2008). However, is this technique applicable readily in the field to harmful algal bloom samples? In the present study, we present results of MALDI–TOF–MS analysis on four field-HAB samples collected daily from the bloomed area in Silver Mine Bay, Hong Kong (Table 1). The algal bloom was believed to be caused by *K. digitata* (Fig. 1) and the identity of the causative agent was confirmed morphologically by officials of the Agricultural, Fisheries and Conservation Department, HKSAR Government. As shown in Table 1, from the 4 real life HAB samples, we were able to obtain $4 \times 10^5$ to $7 \times 10^5$ cells. According to our previous experience, samples with cell number in the order of $10^5$ were adequate for generating a comparable PEP for HAB species identification purposes (Lee et al., 2008).

Previous studies by others e.g. that of Fenselau and Demirev (2001), reported that dinoflagellates and other microorganisms generally exhibited about ten discrete mass peaks ranging from 2000 to 20,000 *m/z* (Lee et al., 2008). However, in our initial experiments with *K. digitata*, we found that most of the peak mass ions observed from the PEPs of both reference culture and field samples of *K. digitata* were in the range from 500 to 2000 *m/z*

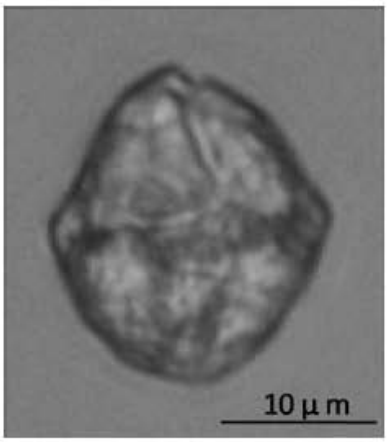


**Fig. 1.** Light microscopic photo of *Karenia digitata* obtained from the bloom area (Silver Mine Bay) of Hong Kong (400× magnifications) in March 2009.

(Fig. 2). The lowered number of mass ions observed could be due to the fact that the major and structural proteins/peptides presented in this species are really in the lower mass range. However, it may not be the case as most of the spectra ions observed in other dinoflagellates are in the range of 2000–20,000 *m/z* as well (Lee et al., 2008). Therefore, we speculated that there might be significant protein loss during the C-18 ziptip sample cleaning step. Proteins with MW > 2000 *m/z* might have weaker binding to the C-18 resin and hence washed away during the washing steps. To test our hypothesis, we replaced the C-18 ziptips with C4 ziptips in the sample cleaning step. C-4 and C-18 refers to the alkyl chain length of a reversed-phase adsorbent immobilized in the ziptips and C4 has a shorter chain length. Interestingly, more peak mass ions (specially ranged from 2000 to 6000 *m/z*) were observed with the use of C-4 ziptips (Fig. 3). Although, C-18 ziptips are commonly chosen for the sample clean-up as most proteins would bind,

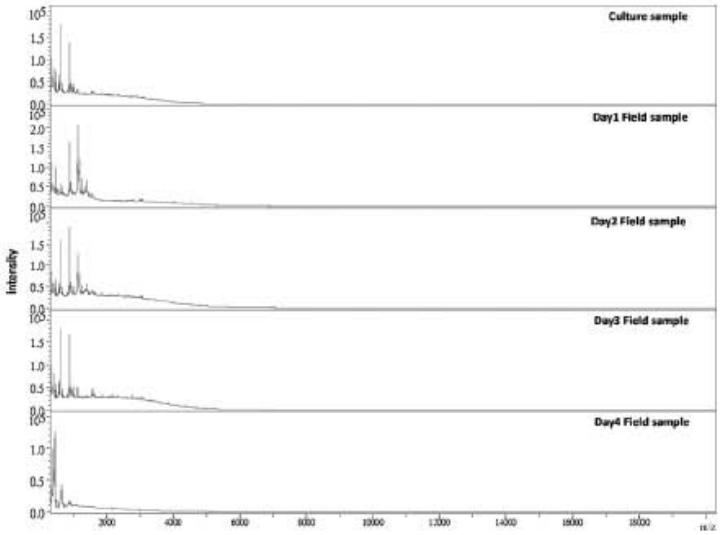


**Fig. 2.** MALDI–TOF–MS protein expression profiles (PEPs) of both culture and field samples of *Karenia digitata*. The samples were cleaned with C-18 ziptips. The mass range depicted was from *m/z* 1000 to 20,000.

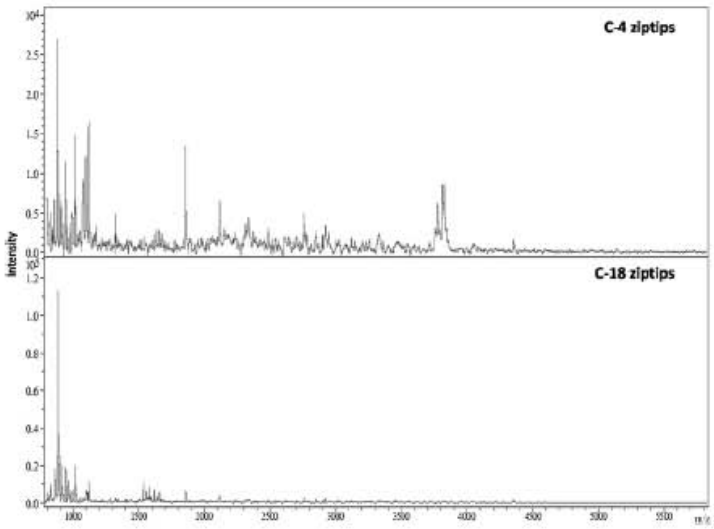


**Fig. 3.** MALDI–TOF–MS PEPs of culture sample of *Karenia digitata* which was cleaned with either C-4 ziptips (upper panel) or C-18 ziptips (lower panel). The mass range depicted is from *m/z* 1000 to 6000.

binding of the proteins also depends greatly on their amino acid compositions and their hydrophobicities. In the case of *K. digitata*, C-4 resin allows better protein binding, especially in the higher molecular mass range. Interestingly, similar results are not unique to *K. digitata*. Currently our team has generated PEPs for more than 40 HAB causative species with the MALDI–TOF–MS-based methodology and we found that some species would give better PEPs with more distinct peaks when C-4 ziptips, rather than C-18, were used (data not shown).

PEPs of the reference monoculture KD01were compared to that of *Karenia brevis*, another *Karenia* species in our procession (Fig. 4). In our earlier report, we found that PEPs of different dinoflagellate species within the same genus are distinct (Lee et al., 2008). In this study, we also confirmed that PEPs of the two *Karenia* species obtained are distinct. Some characteristic signature peak mass ions of each *Karenia* species can also be easily identified by visual inspection. On the other hand, as in the case of *K. brevis*, PEP generated from samples that were cleaned through C-18 ziptips was highly similar to the one produced with C-4 ziptips (Fig. 4). Expressed proteins of *K. brevis* exhibited similar binding capacities to both C-18 and C-4 resins. This further indicated that the pattern of the PEP obtained (i.e. the binding capacities of the proteins to the

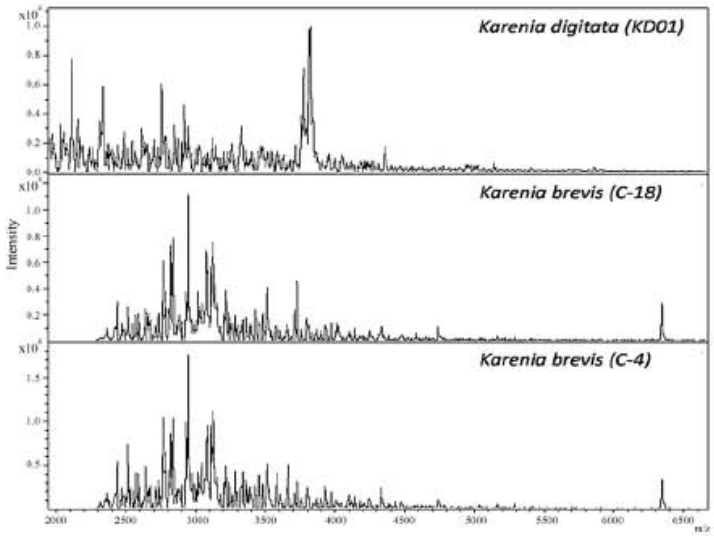


**Fig. 4.** MALDI–TOF–MS PEPs of culture samples of *Karenia digitata* (HK01) and *Karenia brevis*. The mass range depicted is from *m/z* 2000 to 6500.

C-18/C-4 resins) of a specific species is greatly attributable to a specific set of expressed proteins with particular sizes and varies degree of hydrophobicities. Therefore, in order to obtain as many peak-masses as possible for identification purposes, 2 sets of clean-up procedures (i.e. with C-18 and C-4 ziptips) were used to treat the reference culture and the field samples before subsequent MALDI–TOF–MS analysis.

We compared PEPs of the field samples to the one of the reference monoculture KD01 (culture sample) obtained under identical conditions (Figs. 5 and 6). Beside the unique sets of PEPs observed, several unique and consistently expressing species-specific peak masses could be annotated from the spectra of the culture sample. There were 10–15 peaks in the PEPs of both C-18 cleaned-up (Fig. 5) and C-4 cleaned up samples (Fig. 6). Typically, 5–10 peak mass ions were sufficient to discriminate microorganisms at the species level (Dieckmann et al., 2008). Most of the peaks observed from PEPs of the culture sample could easily be identified and matched to PEP of the field samples by visual inspection. Since the peaks mass ions shown in PEP of the culture samples were derived from the mono-reference culture of *K. digitata* and only highly abundant expressed proteins would be shown in the MS spectra, we believe that the peaks mass ions shown in PEP of the culture samples were most likely derived from *K. digitata* cells only. It should be stressed that the MALDI–TOF–MS technology is very different from PCR technology in terms of species identification. Height of peak masses in a PEP is semi-quantitatively related to its abundance. Hence, minute amounts of specific proteins in a complex protein mixture may not show up easily. Consequently, simply because of the minute amounts of proteins presented, even some microorganisms such as bacteria that may have co-existed with the dinoflagellates but in low abundance, their major proteins may not be seen clearly in the MALDI–TOF–MS-PEP spectra. The

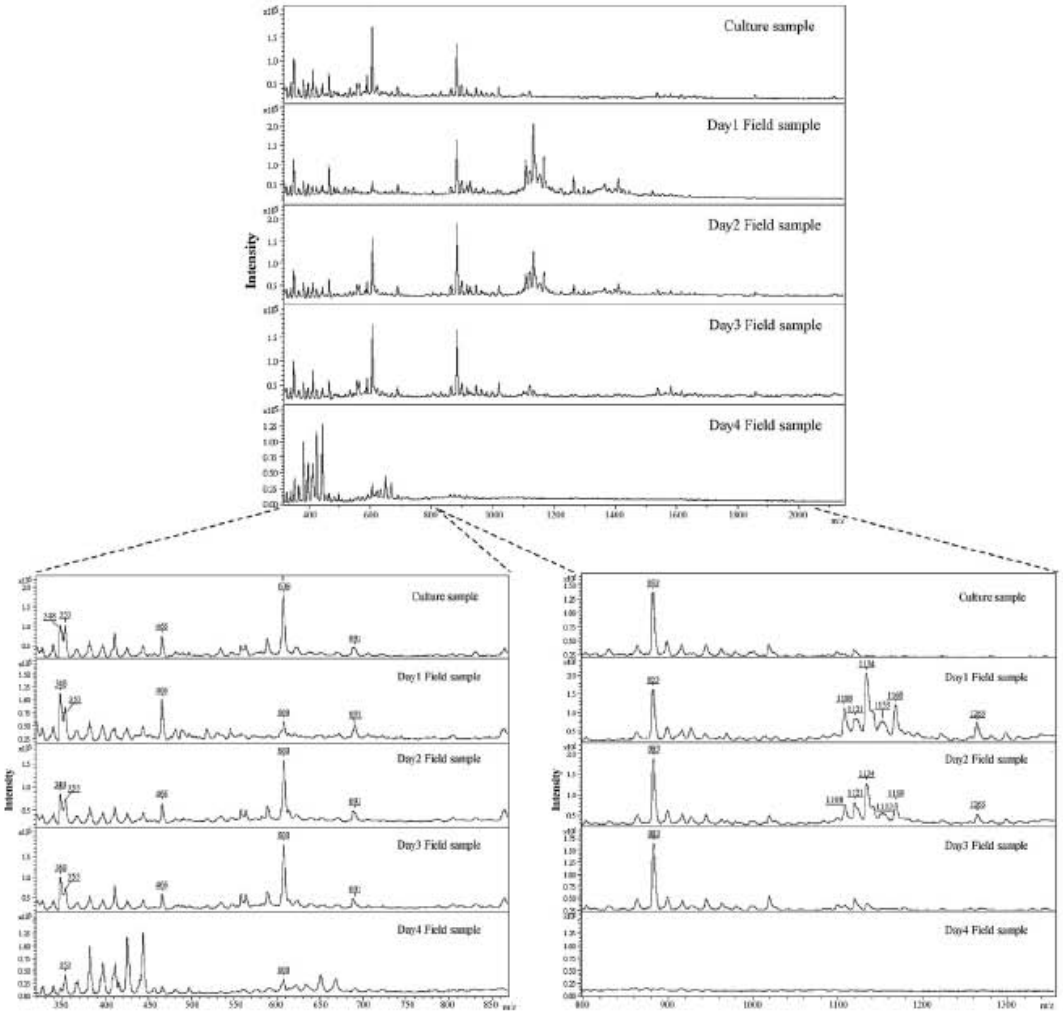


**Fig. 5.** MALDI–TOF–MS PEPs of both culture and field samples of *Karenia digitata* after being cleaned up with C-18 ziptips. The mass range depicted is from *m/z* 350 to 2500. Diagrams in the lower panel are the enlarged images from the corresponding mass range.

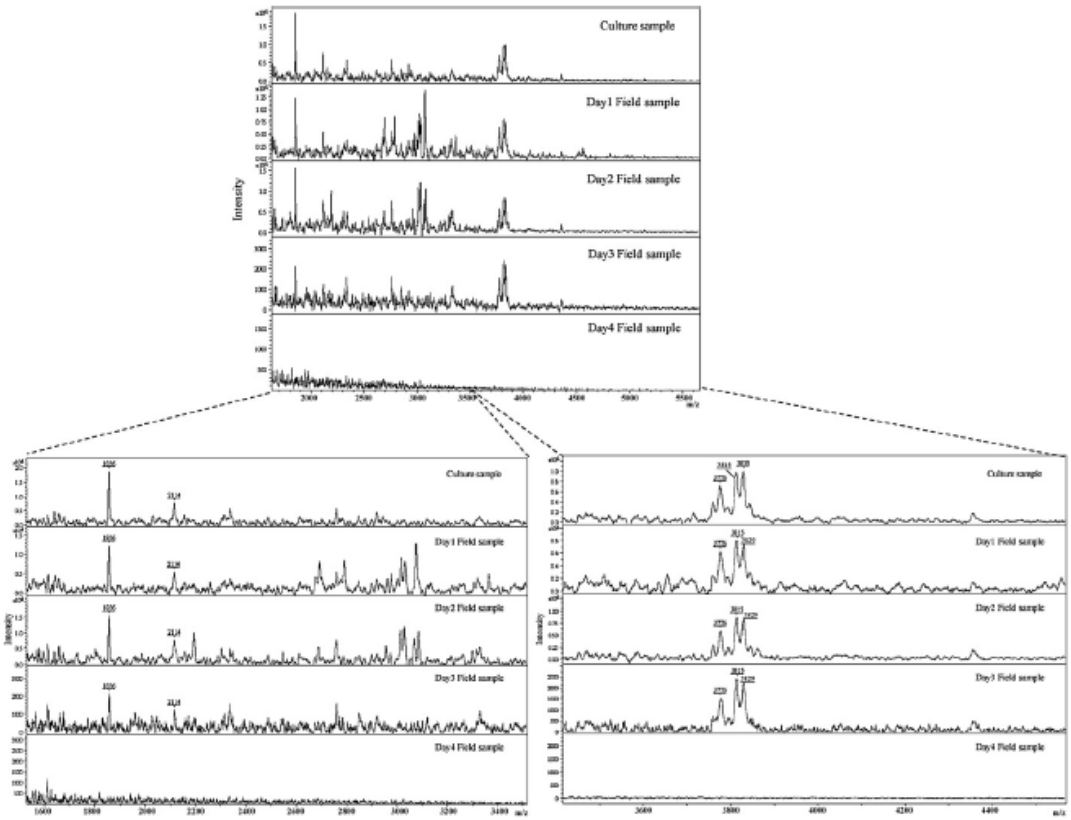


**Fig. 6.** MALDI–TOF–MS PEPs of both culture and field samples of *Karenia digitata* after being cleaned up with C-4 ziptips. The mass range depicted is from *m/z* 1500 to 5500. Diagrams in the lower panel are the enlarged images from the corresponding mass range.

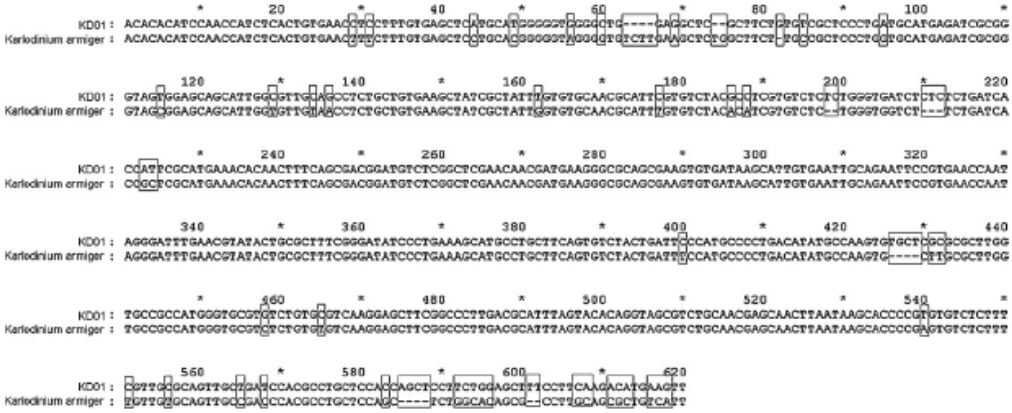


**Fig. 7.** ITS1-5.8S-ITS2 DNA sequences of the established monoculture of *Karenia digitata* KD01. The most similar sequence obtained from bioinformatic search against the NCBInr database was the ITS sequence from *Karlodinium armiger* (AM184205). The alignment of both sequences and their differences are shown (nucleotides highlighted with dotted lines). There are 64 mismatches/gaps between these two sequences.

**Table 2**
Peak mass ions from PEPs of the field samples matched/unmatched to that of culture sample.

| | |
|---|---|
| Matched peak mass ions ($m/z$)[a] | 348, 353, 466, 608, 691, 883, 1856, 2114, 3776, 3815, 3829 |
| Unmatched peak mass ions ($m/z$)[b] | 1108, 1121, 1134, 1153, 1168/1169, 1265 |

Since cells from day 4 samples were disintegrated, the peak mass ions were not counted in the table.

[a] The "matched" peak mass ions represented the peak mass ions that could be identified from the PEPs of both culture sample and field samples from days 1 to 3.

[b] The "unmatched" peak mass ions represented the peak mass ions that could only be found from the field samples but not from the culture sample.

PEP patterns of days 1–3 field samples were highly similar. However, there were some peak mass ions (e.g. $m/z$ 1108, 1121, 1134, 1153, and 1168 in Fig. 5) that could only be found in PEPs of the field samples. It should be noted that in day 4, the bloom was already in its dissipation phase and the cell numbers of *K. digitata* were much lowered. Although the total number of *K. digitata* cells used for the MS analysis were similar to the samples from days 1 to 3 (i.e. $10^5$ cells), the relative abundance of proteins contributed by the several unidentified species of micro-phytoplankton/zooplankton (with size ~1–3 μm) found in the field samples became significant when compared to proteins contributed by *K. digitata*. This observation could also explain why some of the peak mass

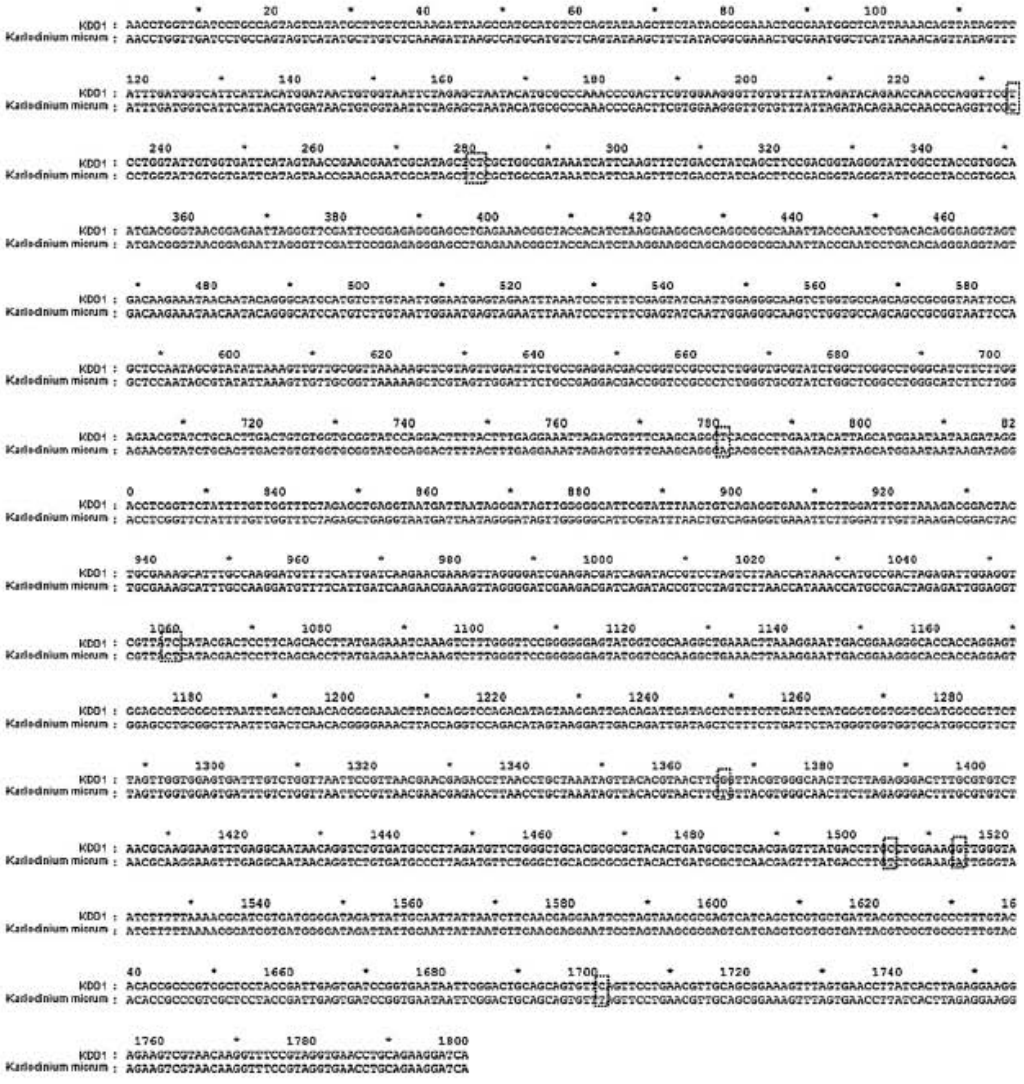


**Fig. 8.** SSU 18S rDNA sequences of the established monoculture of *Karenia digitata* KD01. The most similar sequence resulted from bioinformatic search against the NCBInr database was the 18S sequence from *Karlodinium micrum* (AY245692). The alignment of both sequences and their differences are shown (nucleotides highlighted with dotted lines). There are 10 mismatches/gaps between these two sequences.

ions in PEP of the field samples could not be found in PEP of the monoculture. However, as *K. digitata* cells were the dominant species in the HAB phytoplankton populations, most of the species-specific peaks of *K. digitata* could still be detected easily in the PEP. Representative matched and unmatched peak mass ions of PEPs of the field samples and the culture sample are summarized in Table 2.

### 3.2. ITS/rDNA sequence and phylogenetic analysis of *K. digitata*

*K. digitata* was assigned to the *Karenia* genus because of the presence of a straight apical groove (Daugbjerg et al., 2000). It is named *digitata* because of its finger-like protrusions of sulcus on the ventral epicone surface (Yang et al., 2000). Unfortunately, in the laboratories of these researchers and others, there are no live cultures of *K. digitata* from the 1998 bloom that survived to conduct studies at the molecular level. Hence, there is no DNA sequence of this species available in any public database. Fortunately, the present algal bloom allowed us to collect real-time field samples and we have successfully established a monoculture of *K. digitata* (KD01). The ITS as well as both SSU and LSU rDNA sequences of *K. digitata* were established and analyzed.

The sequences obtained in our study were searched against the NCBInr database. Interestingly, the species with the most similar sequences for ITS (Fig. 7), 18S (Fig. 8) and 26S (Fig. 9) regions of *K.*

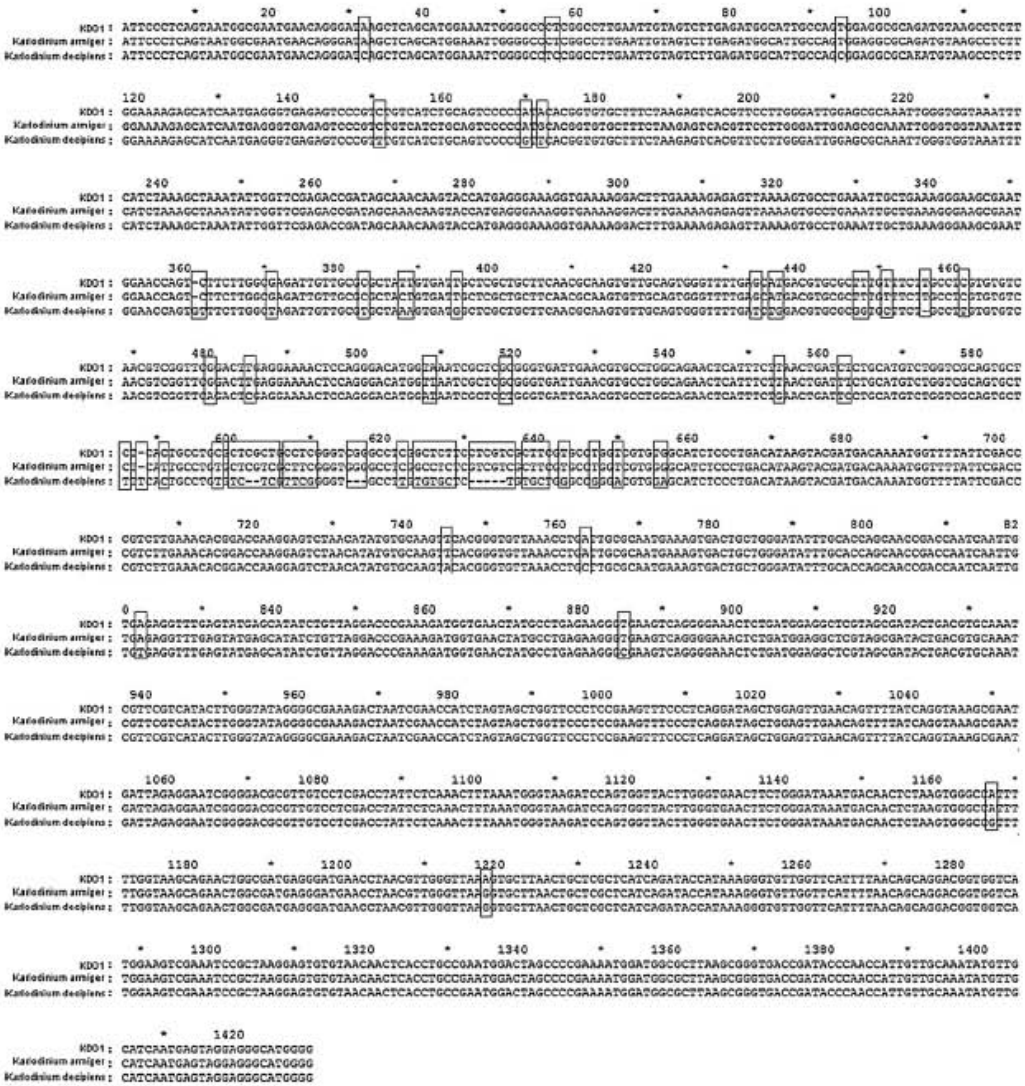


**Fig. 9.** LSU 26S rDNA sequences of the established monoculture of *Karenia digitata* KD01. The most similar sequence resulted from bioinformatic search against the NCBInr database was the 26S sequence from *Karlodinium armiger* (DQ114467). The alignment of the sequences together with *Karlodinium decipiens* (EF469236) and their differences are shown (nucleotides highlighted with dotted lines). There are 75 mismatches/gaps between the two sequences.

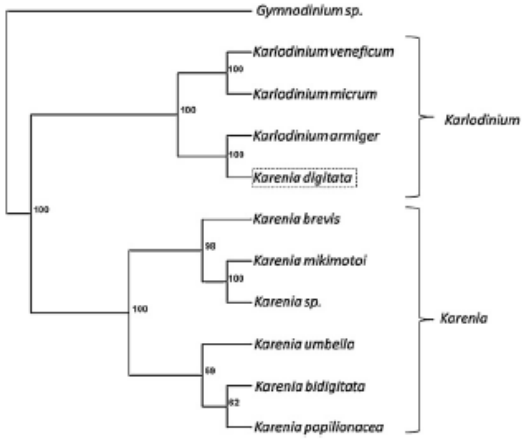


**Fig. 10.** Neighbor-joining tree showing the phylogenetic relationship of *Karenia digitata* (highlighted with dotted line) with other *Karenia* and *Karlodinium* species based on the ITS (ITS1-5.8S-ITS2) DNA sequences. The numbers represent the percentage of 1000 replications (bootstrap support) for which the same branching patterns were obtained. *Gymnodinium* species was used as an outgroup. NCBI accession numbers of the ITS sequences used for are AM184203 (*Gymnodinium* sp.), AJ557028 (*Karlodinium veneficum*), AJ557025 (*Karlodinium micrum*), AM184205 (*Karlodinium armiger*), FJ823563 (*Karenia brevis*), FJ823564 (*Karenia mikimotoi*), AM184206 (*Karenia* sp.), FJ823566 (*Karenia umbella*), FJ823561 (*Karenia bidigitata*), and FJ823565 (*Karenia papilionacea*).

*digitata* are either *Karlodinium armiger* (accession no. AM184205 for ITS, DQ114467 for 26S) or *Karlodinium micrum* (accession no. AY245692 for 18S). When aligned with the corresponding sequences, there are around 5–10% of mismatched nucleotides or gaps in each region of the sequences. The *Karlodinium* species, especially *K. decipiens*, was reported to bear striking morphological similarity to *K. digitata* (de Salas et al., 2008). Although Haifeng Gu of the Third Institute of Oceanography, Xiamen, claimed that the two species share almost identical LSU (26S) rDNA sequences (de Salas et al., 2008), the authors have excluded the possibility that *K. decipiens* is a junior synonym of *K. digitata* by defining the significant morphological differences between the two species. Indeed, based on the alignment results of the 26S sequences of *K. digitata* to those of *K. decipiens* (Fig. 9), 75 mismatches/gaps out of the entire 26S sequence (1429 bp) were found. Followed by the sequence analysis, we conducted phylogenetic analysis based on the ITS DNA sequences obtained (Fig. 10). The tree shows a clear distinction between the *Karenia* and *Karlodinium* clades. However, *K. digitata* is located in the *Karlodinium* clade at 100% bootstrap values, with a close relationship to the *K. armiger*. This may be due to the lack of other *Karlodinium* ITS sequences (e.g. *K. decipiens*) available for the phylogenetic analysis. Hence, more in-depth studies with additional molecular sequences of *Karenia* and *Karlodinium* species are required before any conclusion can be drawn. However, based on our consolidated sequence alignment data of the ITS, 18S, 26S as well as from the phylogenetic analysis of the species, we suggest that *K. digitata* (KD01) is closely related, but not identical to, the *Karlodinium* species. These results are in line with those reported previously (de Salas et al., 2008). To the best of our knowledge, this is the first report on DNA sequences of *K. digitata*.

### 3.3. PCR-based vs MALDI–TOF–MS-based identification methodology

PCR-based identification technique remains one of the best methods for species identification. However, an incomplete description of the algal genome has hampered this approach. In the case of *K. digitata*, the lack of DNA sequence data posed additional time requirements and difficulties in the primer design during the identification process. Contrasting with PCR-based identification technique, the MALDI–TOF–MS-based identification method requires no prior knowledge of the unknown HAB sample. It saves much preparation time for rapid reporting and response. In addition, it was very difficult to obtain the correct ITS and rDNA sequences from PCR of the DNA extracted from the field samples. Even with the same PCR condition used for the DNA extracted from the monoculture, there were numerous bands (PCR products) that appeared on the gels when PCR was conducted on the field samples (data not shown). Since PCR is a very sensitive method and the primer binding regions of the rDNA sequences are usually much conserved, templates from other phytoplankton in the field sample (not that of *K. digitata*) can be amplified in parallel with those from *K. digitata* during the PCR process. In contrast, only the most abundantly expressed proteins show up in the MS spectrum and usually only one (at most two) algal species predominate in a bloom area of a HAB (Hallegraeff, 1993), therefore, peak mass ions of a PEP obtained from the MALDI–TOF–MS analysis would most likely be derived from the blooming species involved. Hence, the much more rapid MALDI–TOF–MS-based methodology seems to be the better choice for species identification in real-life HAB field samples.

## 4. Conclusion

MALDI–TOF–MS has been widely used for identification of various microorganisms. In the present study, we demonstrated that it is possible to identify the causative agent in a real-life HAB field sample based on the presence of species-specific ions in the PEPs. The sample preparation protocol that we developed is simple and fast. We strongly believe that this new technology, assisted by bioinformatics, will become an attractive and powerful tool for identification of HAB causative species in various HAB field samples. In the near future, this technique may even be adopted by the Government/Monitoring Agencies/large industrial fish-farming and aquaculture companies for rapid identification or monitoring of field samples. In addition, we have successfully established and maintained the monoculture of *K. digitata* (KD01) and reported their novo ITS/rDNA sequences. Although DNA sequence data of *K. digitata* in the database are limited, the results from the molecular sequences and phylogenetic analysis suggests that *K. digitata* is closely related, but not identical to the *Karlodinium* species.

## Acknowledgements

We thank The Agriculture, Fisheries and Conservation Department of the Hong Kong SAR Government for its contribution in the identification and sampling of the red-tide samples. We also thank Prof. Georges M. Halpern for editing the manuscript for us. Our work was partially supported by the Environmental and Conservation Fund (ECF) from Hong Kong SAR Government (PolyU K–ZK69). [SS]

## References

Adachi, M., Sako, Y., Ishida, Y., 1996. Analysis of *Alexandrium* (dinophyceae) species using sequences of the 5.8S ribosomal DNA and internal transcribed spacer regions. J. Phycol. 32 (3), 424–432.

D'Onofrio, G., Marino, D., Bianco, L., Busico, E., Montresor, M., 1999. Toward an assessment on the taxonomy of dinoflagellates that produce calcareous cysts (Calciodinelloideae, Dinophyceae): a morphological and molecular approach. J. Phycol. 35 (5), 1063–1078.

Daugbjerg, N., Hansen, G., Larsen, J., Moestrup, O., 2000. Phylogeny of some of the major genera of dinoflagellates based on ultrastructure and partial LSU rDNA

sequence data, including the erection of three new genera of unarmoured dinoflagellates. Phycologia 39 (4), 302–317.
de Salas, M.F., Laza-Martinez, A., Hallegraeff, G.M., 2008. Novel unarmored dinoflagellates from the toxigenic family Kareniaceae (gymnodiniales): five new species of *Karlodinium* and one new Takayama from the Australian sector of the Southern Ocean. J. Phycol. 44 (1), 241–257.
Dieckmann, R., Helmuth, R., Erhard, M., Malorny, B., 2008. Rapid classification and identification of salmonellae at the species and subspecies levels by whole-cell matrix-assisted laser desorption ionization-time of flight mass spectrometry. Appl. Environ. Microbiol. 74 (24), 7767–7778.
Dworzanski, J.P., Snyder, A.P., 2005. Classification and identification of bacteria using mass spectrometry-based proteomics. Expert Rev. Proteomics 2 (6), 863–878.
Fenselau, C., Demirev, P.A., 2001. Characterization of intact microorganisms by MALDI mass spectrometry. Mass Spectrom. Rev. 20 (4), 157–171.
Hallegraeff, G.M., 1993. A Review of harmful algal blooms and their apparent global increase. Phycologia 32 (2), 79–99.
Lee, F.W.F., Ho, K.C., Lo, S.C.L., 2008. Rapid identification of dinoflagellates using protein profiling with matrix-assisted laser desorption/ionization mass spectrometry. Harmful Algae 7 (4), 551–559.
Lee, J.H.W., Qu, B., 2004. Hydrodynamic tracking of the massive spring 1998 red tide in Hong Kong. J. Environ. Eng.: ASCE 130 (5), 535–550.
Litaker, R.W., Vandersea, M.W., Kibler, S.R., Reece, K.S., Stokes, N.A., Lutzoni, F.M., Yonish, B.A., West, M.A., Black, M.N.D., Tester, P.A., 2007. Recognizing dinoflagellate species using ITS rDNA sequences. J. Phycol. 43 (2), 344–355.
Logares, R., Shalchian-Tabrizi, K., Boltovskoy, A., Rengefors, K., 2007. Extensive dinoflagellate phylogenies indicate infrequent marine-freshwater transitions. Mol. Phylogenet. Evol. 45 (3), 887–903.
Page, R.D., 1996. TreeView: an application to display phylogenetic trees on personal computers. Comput. Appl. Biosci. 12 (4), 357–358.
Scholin, C.A., Anderson, D.M., Sogin, M.L., 1993. 2 distinct small-subunit ribosomal-RNA genes in the North-American toxic dinoflagellate *Alexandrium fundyense* (Dinophyceae). J. Phycol. 29 (2), 209–216.
Scholin, C.A., Herzog, M., Sogin, M., Anderson, D.M., 1994a. Identification of group-specific and strain-specific genetic-markers for globally distributed *Alexandrium* (Dinophyceae). 2. Sequence-analysis of a fragment of the LSU ribosomal RNA gene. J. Phycol. 30 (6), 999–1011.
Scholin, C.A., Villac, M.C., Buck, K.R., Krupp, J.M., Powers, D.A., Fryxell, G.A., Chavez, F.P., 1994b. Ribosomal DNA sequences discriminate among toxic and non-toxic *Pseudonitzschia* species. Nat. Toxins 2 (4), 152–165.
Thompson, J.D., Gibson, T.J., Plewniak, F., Jeanmougin, F., Higgins, D.G., 1997. The CLUSTAL_X windows interface: flexible strategies for multiple sequence alignment aided by quality analysis tools. Nucleic Acids Res. 25 (24), 4876–4882.
Yang, Z.B., Hodgkiss, I.J., 2004. Hong Kong's worst "red tide" – causative factors reflected in a phytoplankton study at Port Shelter station in 1998. Harmful Algae 3 (2), 149–161.
Yang, Z.B., Takayama, H., Matsuoka, K., Hodgkiss, I.J., 2000. *Karenia digitata* sp nov (Gymnodiniales, Dinophyceae), a new harmful algal bloom species from the coastal waters of west Japan and Hong Kong. Phycologia 39 (6), 463–470.

# Comparative study between a toxic and non-toxic strain of *Alexandrium catenella*

Daniel Yun-Lam Mak[1], Fred Wang-Fat Lee[2], Kin-Chung Ho[2], Samuel Chun-Lap Lo[1*]
[1] The Proteomic Task Force, Department of Applied Biology and Chemical Technology, The Hong Kong Polytechnic University, Hong Kong
[2] School of Science and Technology, The Open University of Hong Kong, Hong Kong
* Corresponding author

**Abstract**
Some species of dinoflagellates are major producers of paralytic shellfish toxins (PSTs). The study of the biosynthesis of PSTs in dinoflagellates at genomic level is difficult because of their large genome sizes. Comparing the protein expression of two different strains of the same species which differ in toxigenicity could aid the study of PSTs production. In the present study, one toxic (AC-T) and one non-toxic (AC-N) strain of *Alexandrium catenella* were compared. Their ribosomal DNA internal transcribed spacer (ITS) sequences, cell sizes, growth curves, toxin contents, effects by phosphate limitation were compared befre analysis with 2-dimensional gel electrophoresis. AC-T and AC-N shared very similar ITS DNA sequences and exponential growth rates. AC-T always produced PSTs while no toxin was detected from AC-N at any stage of growth and also under phosphate limitation. Upon 2D-gel electrophoretic analysis, 64 proteins were found to be differently expressed between the two strains; 75% were up-regulated in AC-T while the other 25% were up-regulated in AC-N. Identification of these differentially expressed proteins is currently in process.
**Keywords**
Paralytic Shellfish Toxins (PSTs); *Alexandrium catenella*

## Introduction

Paralytic shellfish poisoning (PSP) could be caused by ingestion of different types of paralytic shellfish toxins (PSTs), in which saxitoxin (STX) is the parent compound. Consumption of PST through ingestion of contaminated shellfish and filter feeders are common. The mortality rate of PSP could be as high as 14% (Rodrigue et al. 1990). The major PSTs producer is dinoflagellates. Genera *Alexandrium*, *Gymnodinium* and *Pyrodinium* were found to be PSTs producing dinoflagellates. The study of PSTs production in these marine photosynthetic microorganisms started for decades. However, the complete biosynthetic pathway of STX is still inconclusive. Partial mechanism such as the use of arginine as a precursor and the formation of imidazole ring were proposed after labeling experiments (Shimizu et al. 1984). The studies focusing on STX biosynthesis were hindered by the lack of genomic information of dinoflagellates due to its large genome size (Lin 2006). Furthermore, methods to disable its toxin synthesis or trigger PST-producing ability in non-toxic species are currently lacking. On the other hand, proteomic comparison between a PSTs producing and a non-PSTs producing dinoflagellates is a viable alternative. Such comparison will be of more significance if the candidates pair is genetically close to each other and has very similar physiological and behavioral characteristics. *Alexandrium catenella* is one of the common PSTs producing

dinoflagellates (Proctor et al. 1975). Among the several strains of *A. catenella* in the culture library of our group, the toxin content of one of them was always undetectable with HPLC-post-column derivatization methodology. Together with a toxic strain of *A. catenella*, an ideal comparative model was established. The present study aims to investigate the difference in protein expression in these 2 strains of *A. catenella*.

**Materials and Methods**

*Culturing condition*

The experimental culture of toxic (AC-T) and non-toxic (AC-N) *A. catenella* were kept in L1 seawater based medium, at 22°C, 5000 lux, under 12:12 hours light:dark cycle in a Versatile Environmental Test Chamber (SANYO, Japan). All experimental cultures were started with 1000 cells $mL^{-1}$ by cell density and 500 mL by volume on Day 0.

*Cell size measurement*

Cell volumes of exponential culture were performed by a calculation method adopted from H. Hillebrand ((Hillebrand et al. 1999) after measuring the dimensions of the algae under light microscope. The formula for cell volume ($V$) assessment is: $V = (\pi/6) \times d^2 \times h$, where $d$ and $h$ are the diameter and height respectively.

*PCR-based identification*

Internal Transcribed Spacer (ITS) region and the 5.8s ribosomal DNA of the dinoflagellates were sequenced and compared to each other. DNA contents were extracted by the High Pure PCR Template Preparation Kit (Roche, Switzerland). The target sequences were first amplified by PCR with standard *Alexandrium* primers, ITSA and ITSB (Adachi et al. 1996). 35 cycles of PCR were performed with denaturing at 94°C for 40s, annealing at 50°C for 40s, elongation at 72°C for 60s and ended with 72°C for further 10 minutes. PCR product were purified and cloned with pGEM-T vectors (Promega, USA). Followed with QIAprep® Spin Miniprep Kit (QIAGEN, USA), the sequencing process was completed by commercial facilities with Sanger Method.

*Protein expression profiling*

Our group previously demonstrated the use of MALDI-TOF mass spectrometry for fast identification of dinoflagellates (Lee et al. 2008). Protein samples of centrifuged (13000 x g; 5 minutes) exponential cultures were extracted with 0.1% trifluoroacetic acid (TFA) through 3 minutes sonication and cleaned up with C-18 zip tip. Followed with elution from the zip tip with 0.1% TFA with 50% acetonitrile, the samples were then mixed with matrix solution prepared by saturated sinapinic acid (SA) in elution buffer in the ratio 1:1. The mixtures were then spotted onto the target plate, MTP AnchorChip™ (Bruker, Germany). Mass spectrometry by Autoflex III (Bruker, Germany) was performed with linear mode at an accelerating voltage of 20kV by using a 300ns delay time. Spectrum of a sample ranged from 0.2 to 2kDa was generated by summation of spectra from 2000 to 3000 laser shots of each sample. Calibration was performed simultaneously with Protein Calibration Standard I (Bruker, Germany).

*Growth curve study*

Growth curves were constructed by computing cell densities during the period of investigation. Determination of algal density in the cultures was conducted using the Sedgewick-Rafter counting chamber. 1 mL of algal culture, fixed with 10 μL of Lugol's solution, was filled into the chamber before counting the number of cells under light microscope.

*Toxin analysis*

Toxin levels in the algal samples were analyzed by a UPLC system (Waters, USA), with pre-column oxidation method adopted by Lawrence (Lawrence et al. 1996). After extracted with 0.05M acetic acid, toxin samples were oxidized either by 10% hydrogen peroxide solution for 2 minutes (for STX, dcSTX, GTX2+3, GTX5 & C1+2) or periodate oxidant prepared with 0.1M periodic acid, 0.1M ammonium formate and 0.1M sodium phosphate dibasic for 1 minute (for NEO & GTX1+4). After the reaction has stopped with 5% acetic acid, samples were filtered (0.2μm) allowed entering the UPLC system for analysis, using 2.1 X 100 mm HSS T3 column (Waters, USA). Two mobile phases were used for the LC analyses: 0.1M ammonium formate (pH 6.0, buffer A) and 0.1M ammonium formate with 5% acetonitrile (pH 6.0, buffer B). Flow rate was kept at 0.5 mL/minute and the column temperature was kept at 35°C. The gradient program was divided into 3 categories with different ratio of buffer A to buffer B: 95:5 from the 0 to 2.5 minute, 70:30 from the 2.5 to 5 minute and 100:0 from the 5 to 6 minute. Separated toxins were detected by fluorometer with λex 340nm and λem 395nm. Amount of the cellular toxins were quantified with the standard curves and according to the peak areas.

*Phosphate limitation study*

The effects on exponential growth and toxin content by phosphate limitation were examined. The two strains were cultured under one-tenth amount of normal phosphate supply, with no changes to the others nutrients. Amount of growth were examined and toxin analyses were performed at the time-point of mid-exponential phase of normal growth, i.e. Day 18.

*2-dimensional gel electrophoresis*

Protein expressions of the 2 *Alexandrium catenella* were examined by two-dimensional gel electrophoresis (2-DE). Trizol-extracted proteins were first rehydrated into an IPG strip (Bio-Rad, USA) with pH range 4-7 for 16-20 hours at room temperature. Isoelectric focusing was then performed with following protocol: 500V for 3 hours, 1000V for 6 hours, 8000V for 3 hours and finally with 120000 voltage hours. After reduction and alkylation with 1% dithiothreitol and 2.3% iodoacetamine respectively, the second dimension was performed in 12% polyacrylamide gel and ran with 35 mA/gel. After the second dimension, the gel was fixed in 10% v/v acetic acid, 40% v/v methanol. Visualization of the proteins was subsequently performed with several steps of silver staining: Sensitization (8mM sodium thiosulphate and 30% v/v methanol; 30 minutes); silver staining (14.7mM silver nitrate; 20 minutes); Developing (0.24M sodium carbonate (usb, USA) in 0.004‰ v/v formaldehyde; until image clear) and Stopping (35mM EDTA). Images of gels were scanned and analyzed by software Melanie 3 (GeneBio, Switzerland).

## Results and Discussion

There has been some arguments that it is easy to confuse the identity between *A. catenella* and *A. tamarense* as the latter one could be non-toxic. Several works have been done for confirming its identity before the toxicological experiments. DNA sequences of the internal transcribed spacer (ITS) region are used as the "DNA barcode" for identification (Litaker et al. 2007). Sequencing results (Figure 1) showed there was 97% similarity existed between the ITS sequences of the toxic (AC-T) and the non-toxic (AC-N) strain in this study. Aligning the ITS sequences of AC-N to the a strain of *Alexandrium tamarense* showed that the similarity between the two species was 80% only. Results of the ITS sequences supported that AC-N is more like *A. catenella* than *A. tamarense*.

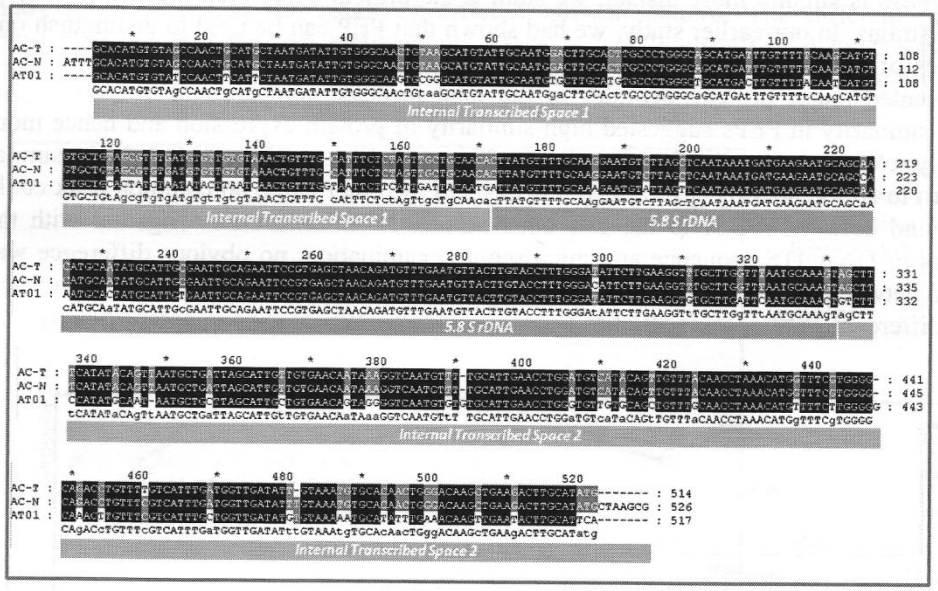


**Figure 1.** Alignment of the complete sequences of the ITS1-5.8S-ITS2 regions of toxic (AC-T) and non-toxic (AC-N) *A. catenella* and one strain of *A. tamarense* (AT01). Similarity between AC-T and AC-N is 97%. However, similarity calculation between AC-T and AC-N to AT01 is 82% and 80% respectively.

Microscopic examination (Figure 2) and cell volume computation showed that AC-T and AC-N have very similar shapes and sizes. Both the strains were around 8 X $10^3$ $\mu m^3$ in size and is only about 50% of that of *A. tamarense*.

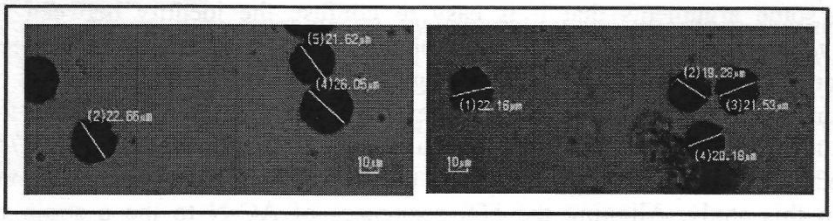


**Figure 2.** Cell dimension measurements of AC-N (left panel) and AC-T (right panel) under microscopic examination.

To provide additional set of proof that the 2 *A. catenella* are more closely related while *A. tamarense* is slightly more distant, we studied the protein expression profiles (PEPs) of these strains. In our earlier study, we had shown that PEP can be used to distinguish one species of dinoflagellates from another (Lee et al. 2008). The major peaks in the PEP represented major proteins/peptides in the total proteins compartment of these algae. High similarity in PEPs suggested high similarity of protein expression and hence more closely related genetically. Result in Figure 3 showed that the PEP of AC-N had a similar pattern to AC-T, sharing several major peaks. On the other hand, no common peak could be found between AC-N to the two other strains of *A. tamarense*. Together with the results of DNA ITS sequence and microscopic examination, no obvious difference was found between AC-T and AC-N to differentiate either one of them as a different species. The difference in their toxigenicities becomes more prominent for comparative study.

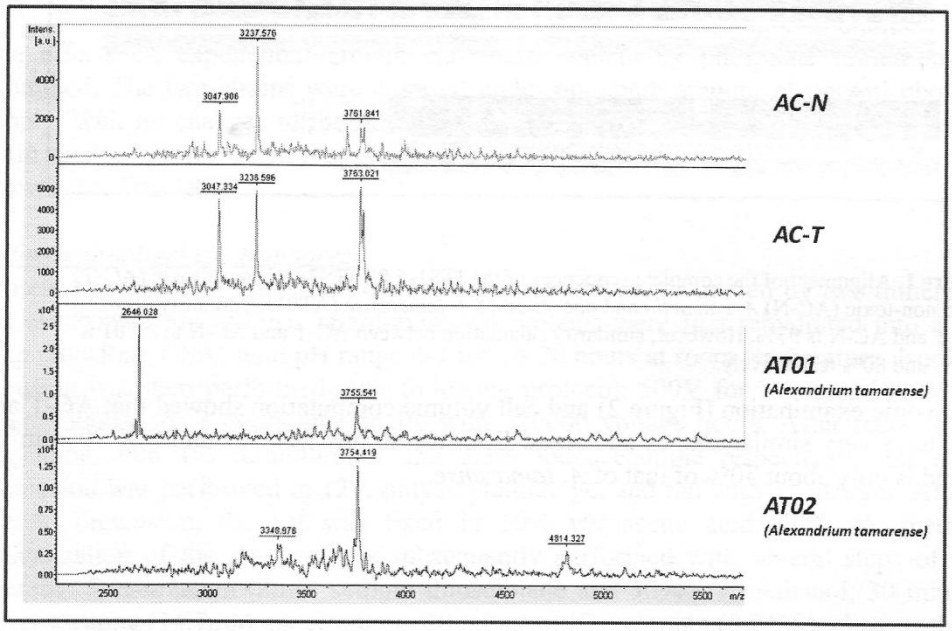


**Figure 3.** Protein expression profiles of AC-N, AC-T and two strains of *A. tamarense* (AT01 & AT02).

Growth rates of dinoflagellates have a close relation with their toxicity. Non-toxic dinoflagellates were reported to have slower growth rates when compared to toxic ones

(Martins et al. 2004).On the other hand, *Alexandrium catenella* is a fast growing dinoflagellate. The results of their growth curves (Figure 4) in the present study showed that the growths of the two strains of *A. catenella* are similar during the first part (up to Day 2-25) of the exponential phase, in which the specific growth rates were 0.13 $day^{-1}$ (AC-T) and 0.12 $day^{-1}$ (AC-N) respectively. Duration of exponential growth of AC-T was longer than that of AC-N, the former also had a higher maximum cell density. However, the difference in toxicity is always seen for the strains. Illustrated in Figure 5, from early exponential phase to the decline phase, PSTs were detected with a trend of decreasing toxin content, dominant with C toxins (Figure 6). In contrast, AC-N showed no toxins in every growth phases. Inability to produce PSTs was not accompanied with slower exponential growth rate in the case of AC-N. This may imply that the difference in protein expression during the exponential growth between the two strains in the present study is probably not the result of different growth pattern. The different protein expression between the two strain at this stage is less likely affected by the growth physiology and is expected to be the more reflected by the difference in toxigenicity.

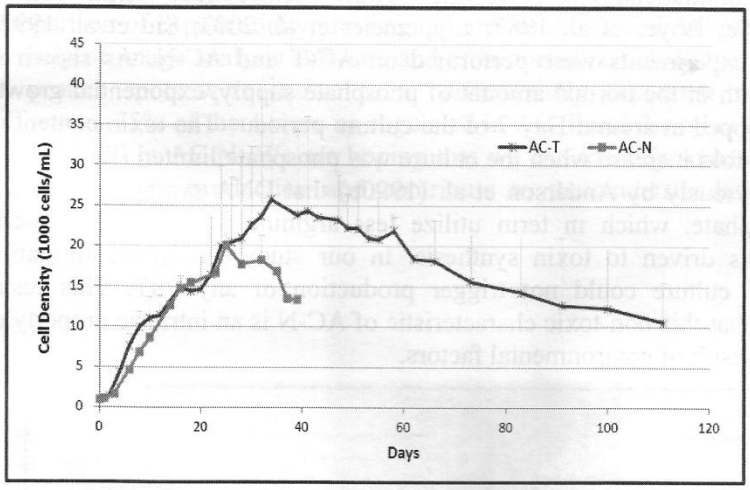


**Figure 4.** Growth curves of AC-T and AC-N. Vertical lines indicate SD of triplicate samples.

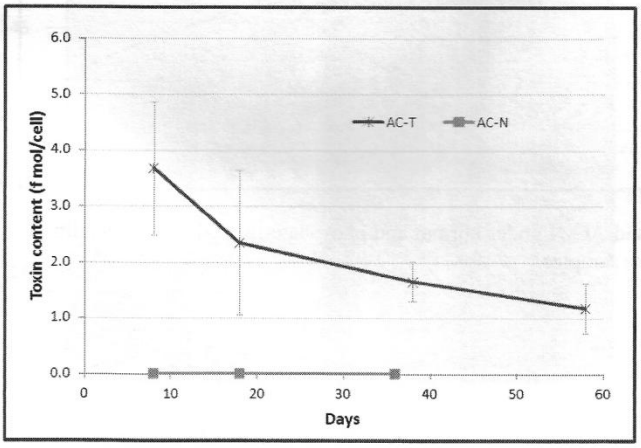


**Figure 5.** Cellular toxin content (fmol/cell) of AC-T and AC-N against different growth phases. Vertical lines indicate SD of triplicate samples.

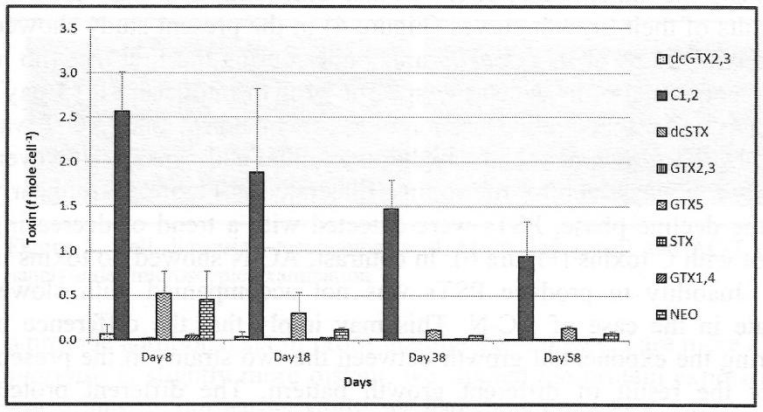


**Figure 6.** PSTs composition (fmol/cell) of AC-T at different growth phases. Vertical lines indicate SD of triplicate samples.

Availability of phosphates in the culture medium is known to be one of the factors affecting PSTs toxigenicity of dinoflagellates. It was reported that phosphate-limiting environment would dramatically increase the cellular endogenous toxin content (Anderson et al. 1990a; Boyer et al. 1987; Lippemeier et al. 2003; Siu et al. 1997). Phosphate limitation experiments were performed on AC-T and AC-N. As shown in Figure 7, with one-tenth of the normal amount of phosphate supply, exponential growth of the both strains stopped at around Day 7 of the culture period. The toxin content of AC-T had a around 4-fold increase when the culture was phosphate limited (Figure 8). It was hypothesized previously by Anderson et al. (1990b) that DNA synthesis ceased in the absence of phosphate, which in term utilize less arginine. The resultant overly abundant arginine was driven to toxin synthesis. In our study, phosphate limitation studies in the AC-N culture could not trigger production of any PST. This result reinforced the notion that this non-toxic characteristic of AC-N is an intrinsic property of the strain and not the result of environmental factors.

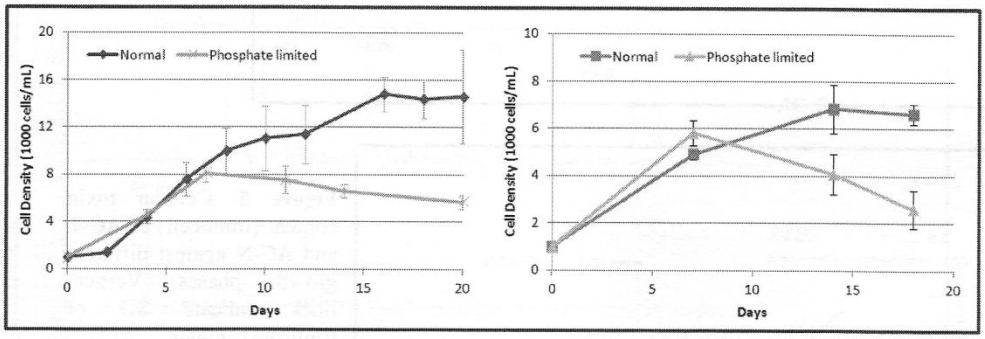


**Figure 7.** Growth curves of AC-T and AC-N under normal and phosphate-limited culture condition. Vertical lines indicate SD of triplicate samples.

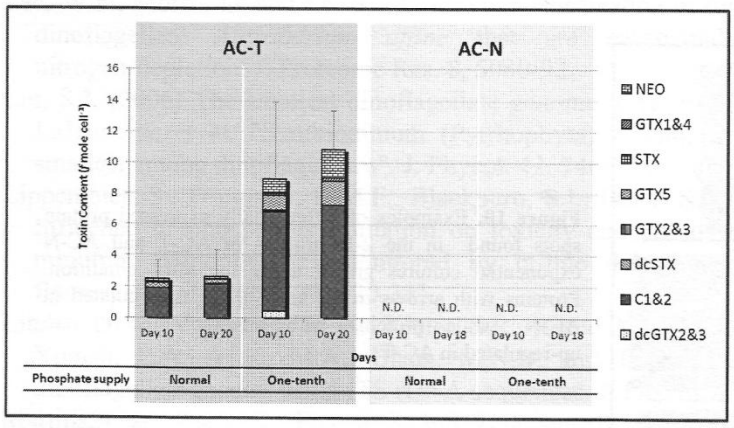


**Figure 8.** Toxin content (fmol/cell) at Day 10 & 20 of AC-T and at Day 10 & 18 of AC-N under normal and phosphate-limited culture. Vertical lines indicate SD of triplicate samples.

As mentioned previously, study on the biosynthesis pathway of PSTs at the genomic level is difficult due to the lack of genomic information. On the other hand, study on the protein expression may provide more information about the mechanism. 2-D gel comparison of exponentially growing cultures of AC-T and AC-N were performed. With the help of image analysis software and after normalization of the intensities of staining, 64 protein spots were shown to be differentially expressed with at least a 2-fold difference. 75% of them were up-regulated in AC-T and the other 25% were found to be up-regulated in AC-N. We are hoping that we can identify some proteins that could be related to PSTs production and contribute to the understanding of the biosynthetic pathway of PSTs.

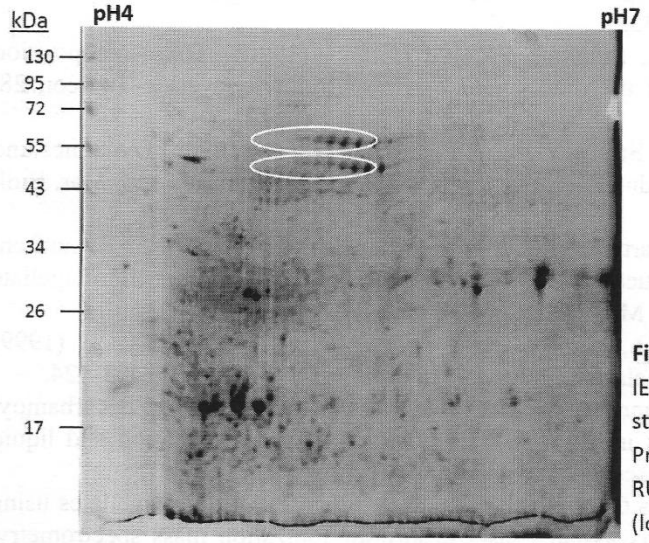


**Figure 9.** 2D gel image of AC-T. IEF was performed with an IPG strip with a pH range 4-7. Proteins in circles are isoforms of RUBIOSCO II (upper) and NAP50 (lower) (Lee et al. 2009).

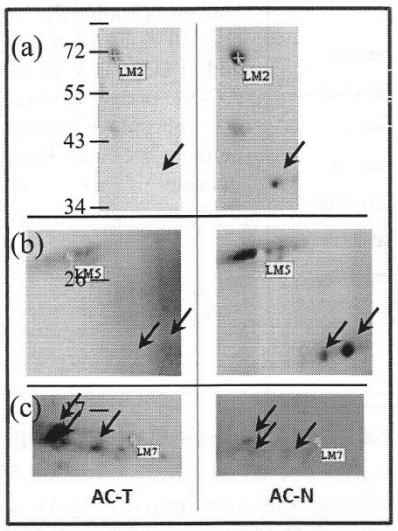


**Figure 10.** Examples of differentially expressed protein spots found in the 2-D profiles of AC-T and AC-N exponential cultures grown under the same condition. Proteins with arrows in (a) and (b) are up-regulated in AC-N, while proteins with arrows in (c) are up-regulated in AC-T.

**Acknowledgement**

This project is supported partly by a grant from the NSFC-RGC jointed research scheme (RGC Ref.:N_PolyU502/08) and partly by a grant from the Research Committee of the Hong Kong Polytechnic University (PolyU Ref.: G-U735).

**Reference**

Adachi, M., Sako, Y. and Ishida, Y. (1996) Analysis of Alexandrium (dinophyceae) species using sequences of the 5.8S ribosomal DNA and internal transcribed spacer regions. J. Phycol. 32, 424-432.

Anderson, D.M., Kulis, D.M., Sullivan, J.J. and Hall, S. (1990a) Toxin composition variations in one isolate of the dinoflagellate Alexandrium fundyense. Toxicon 28, 885-893.

Anderson, D.M., Kulis, D.M., Sullivan, J.J. and Hall, S.a.L., C.,. (1990b) Dynamics and physiology of saxitoxin production by the dinoflagellates Alexandrium spp. Mar. Biol. 104, 511-524.

Boyer, G.L., Sullivan, J.J., Harrison, P.J. and Taylor, F.J.R. (1987) Effects of nutrient limitation on toxin production and composition in the marine dinoflagellate *Protogonyaulax tamarensis* Mar. Biol. 96, 123-128.

Hillebrand, H., Durselen, C.D., Kirschtel, D., Pollingher, U. and Zohary, T. (1999) Biovolume calculation for pelagic and benthic microalgae. J. Phycol. 35, 403-424.

Lawrence, J.F., Wong, B. and Menard, C. (1996) Determination of decarbamoyl saxitoxin and its analogues in shellfish by prechromatographic oxidation and liquid chromatography with fluorescence detection. J. AOAC Int. 79, 1111-1115.

Lee, W.F., Ho, K.C. and Lo, S.C.L. (2008) Rapid identification of dinoflagellates using protein profiling with matrix-assiated laser desorption/ionization mass spectrometry. Harmful Algae 7, 551-559.

Lee, W.F., Morse, D. and Lo, S.C.L. (2009) Identification of two plastid proteins in the dinoflagellate *Alexandrium affine* that are substantially down-regulated by nitrogen-depletion. J. Proteome Res. 8, 5080-92.

Lin, S.J. (2006) The smallest dinoflagellate genome is yet to be found: A comment on LaJeunesse et al. "Symbiodinium (Pyrrhophyta) genome sizes (DNA content) are smallest among dinoflagellates". J. Phycol. 42, 746-748.

Lippemeier, S., Frampton, D.M.F., Blackburn, S.I., Geier, S.C. and Negri, A.P. (2003) Influence of phosphorus limitation on toxicity and photosynthesis of Alexandrium minutum (DInophyceae) monitored by in-line detection of variable chlorophyll fluorescence. J Phycol. 38, 320-331.

Litaker, R.W., Vandersea, M.W., Kibler, S.R., Reece, K.S., Stokes, N.A., Lutzoni, F.M., Yonish, B.A., West, M.A., Black, M.N.D. and Tester, P.A. (2007) Recognizing dinoflagellate species using ITS rDNA sequences. J. Phycol. 43, 344-355.

Martins, C.A., Kulis, D., Franca, S. and Anderson, D.M. (2004) The loss of PSP toxin production in a formerly toxic Alexandrium lusitanicum clone. Toxicon 43, 195-205.

Proctor, N.H., Chan, S.L. and Trevor, A.J. (1975) Production of saxitoxin by cultures of Gonyaulax-catenella. Toxicon 13, 1-9.

Rodrigue, D.C., Etzel, R.A., Hall, S., Deporras, E., Velasquez, O.H., Tauxe, R.V., Kilbourne, E.M. and Blake, P.A. (1990) Lethal Paralytic Shellfish Poisoning In Guatemala. Am. J. Trop. Med. Hyg. 42, 267-271.

Shimizu, Y., Norte, M.A., Hori, A., Genenah, A. and Kobayashi, M. (1984) Biosynthesis of saxitoxin analogues: the unexpected pathway. J Am. chem. Soc. 106, 6433-6434.

Siu, G.K.Y., Young, M.L.C. and Chan, D.K.O. (1997) Environmental and nutritional factors which regulate population dynamics and toxin production in the dinoflagellate Alexandrium catenella. Hydrobiologia 352, 117-140.

**Appendix D: Conference Presentation – Talk**

## 第 5 届南中国海红潮预防和管理国际研讨会- HABSCS-2012

| Day 2 | 31 March 2012 | 地點: 澳門威尼斯人酒店會議廳<br>Convention Centre, Venetian Hotel Macao |
|---|---|---|
| 09:00-09:30 | 大會開幕式、貴賓剪綵、頒授紀念品及大合照<br>● Grand Opening Ceremony, address by VIPs of Macau<br>● Group Photos | 主禮 Officiating VIPs:<br>● 澳門政府各主責長官<br>➢劉藝良 人大代表<br>➢梁維特副主席，澳門環境咨詢委員會<br>➢劉關華執行委員，澳門貿易投資促進局<br>➢澳張紹基局長，澳門環境保護局<br>➢澳曾澤瑤主任，澳門生產力暨科技轉移中心<br>➢梁冠峰委員，澳門民政總署<br>其他嘉賓 (other Guests):<br>● 錢宏林(钱宏林教授，國家海洋局,南海分局副局长)<br>● 文 斌教授 (广东省海洋与渔业局副局长)<br>● 齊雨藻教授 (AoHABSCS 會長)<br>● 周名江教授 (中国科学院海洋研究所，國家973項目-有害藻華與生態安全首席科學家) |
| 10:00-12:30 | 主題演講 (二):<br>Keynote speeches (2): | Chairman: Prof. Kin-Chung HO<br>Dean of Science, University of St. Joseph, Macao & Dean of the School of Science & Technology, The Open University of Hong Kong<br>主席: 何建宗教授(聖若瑟大學科學總監、香港公開大學科技學院院長) |
| 10:00-10:25 | Prof. Ming-Jiang ZHOU,<br>Institute of Oceanology, Chinese Academy of Sciences, China<br>(周名江教授，中國科學院海洋研究所) | Modeling Harmful Algal Blooms (HABs) in the Chinese Coastal Waters |
| 10:25-10:50 | Dr. Pat TESTER, National Ocean Service, National Oceanography and Atmosphere Administration (NOAA), USA (美國國家海洋及大氣管理局) | The Accidental Taxonomist" and review our *Gambeirdiscus* work through the discovery of new species, development of qPCR assays for all the Caribbean species and the physiology and biogeography of the genus. |
| 10:50-11:15 | Dr. Beatriz Reguera (Chairlady, ISSHA, from Spain; Instituto Espanol de Oceanografia (IEO), Spain) (國際有害藻華學會會長) | Harmful Algal Blooms Prevention and Management: A Northeast Atlantic European Perspective |
| 11:15-11:40 | Prof. David MORSE, *Institut de Recherche en Biologie*, Canada (加拿大生物研究所) | RNA-Seq derived insights into genes and gene expression in Lingulodinium |
| 11:40-12:05 | Prof. Jaw-Kai WANG, (王兆凱教授，美國國家工程院院士), Academician, National Academy of Engineering, USA; CEO, Shenzhen Jawkai Bioengineering R&D Center, Ltd. | Beneficial use of Harmful Algae - Micro-algae as biofuel |

| | | |
|---|---|---|
| 12:05-12:30 | Dr. Hakgyoon KIM,<br>National Fisheries Research<br>& Development Institute, Republic of Korea;<br>Chair, Local Organizing Committee, 15th International Conference on Harmful Algae;<br>(大韓民國國家漁業研究及發展所; 第 15 屆有害藻華國際學術研討會本地籌委會主席) | Korea early-warning system and contingency plan for HAB mitigation |
| **12:30 – 14:30** | **Lunch 午餐** | |
| **14:30-16:00** | **主題演講 (三):**<br>**Keynote speeches (3):** | Chairman: Prof. Mingyuan Zhu<br>First Institute of Oceanography, China<br>主席: 朱名遠教授<br>中國海洋局海洋研究所 |
| 14:30-14:55 | Prof. Tianling ZHENG, Xiamen University, China<br>(鄭天凌教授, 廈門大學) | (1) Study on an uncultured algicidal microorganism directly against Phaeodactylum tricornutum;<br>(2) Phycosphere Bacterial Community of Alexandrium tamarense and Lysis of A. tamarense Caused by Bacteria from its Phycosphere |
| 14:55-15:20 | Prof. Liang-Min HUANG and Ms Pengpeng SHEN, South China Sea Institute of Oceanology, Chinese Academy of Sciences, China<br>(黃良民教授、沈萍萍博士: 中國科學院南海海洋研究所) | Identification and Blooms of *Cochlodinium geminatum* (Schütt) Schütt (*Gymnodiniales, Pyrrophyta*) in the Pearl River Estuary |
| 15:20-15:45 | Dr. Tao JIN, BGI-Shenzhen<br>(金桃博士, 深圳華大基因研究院) | The transcriptome of a Dinoflagellate *Alexandrium sp.* using next-generation sequencing |
| **15:45-17:30** | **論文報告:**<br>**Scientific Session:** | Chairman: Prof. Yahui GAO<br>Xiamen University; Vice Chairman, AoHABSCS<br>主席: 高亞輝教授<br>廈門大學、南中國海赤潮學會副主席 |
| 15:45-16:00 | Daniel Yun-Lam MAK, Hong Kong Polytechnic University | Comparative study between a toxic and non-toxic strain of *Alexandrium catenella* |
| 16:00-16:15 | Xin CHEN, Xiamen University, China | Protein expression profiles between toxic and non-toxic strains of *Pseudo-nitzschia* |
| 16:15-16:30 | Deo Florence L. ONDA, The Marine Science Institute,<br>University of the Philippines, Diliman<br>Republic of the Philippines | Bacteria-Algal association: insights from a (meta)genome data generated from Pyrodinium bahamense var. compressum using a high throughput (next generation) sequencing approach |
| 16:30-16:45 | Kamille Joshua V. MANSET, The Marine Science Institute,University of the Philippines. | Marine Bacteria isolated from Bolinao, Pangasinan, Philippines with Algicidal and Antagonistic Activities |
| 16:45-17:00 | Xiao-Li XING, Shanghai Ocean University, China | The morphology of two cryptomonads red tide species by scanning microscopy |

## Appendix E: Conference Presentation – Poster

# Toxin production and endogenous arginine level of *Gymnodinium catenatum*, a marine dinoflagellate

Daniel Yun Lam MAK[1], Fred Wang Fat LEE[1,2], Samuel Chun Lap LO[1]

1. The Proteomic Task Force, The Department of Applied Biology and Chemical Technology, The Hong Kong Polytechnic University
2. School of Science and Technology, The Open University of Hong Kong

### Introduction

Harmful algal blooming (HAB) in coastal areas (usually called red tides) are usually related to the loading of nutrients from human activities. Eutrophication caused by agricultural run-off and also deposition of untreated aquatic residues enormously increases the availabilities of nitrates and phosphates for the growth of planktonic microorganism. Blooming of *Gymnodinium catenatum*, a marine dinoflagellate, is an example of HAB. *G. catenatum* is a toxic microalgae which could cause paralytic shellfish poisoning (PSP). Around 100 death cases [1] related to this species have been reported. Besides being a direct treat to swimmers, shellfish farm businesses were also affected because the shellfish are not appropriate for harvest as toxin would accumulated and concentrated once they fed on those algae. These harmful effects collectively hindered the progress of sustainable development of our water resources. *G. catenatum* widely spread in difficult regions including Argentina, Australia, Mexico, Spain, Pacific Ocean, Japan and also Hong Kong [2]. They produce saxitoxin as secondary metabolites and it was found that arginine is the major precursor for the biosynthesis of saxitoxin and its derivatives. This study is to evaluate the toxin content and also the endogenous arginine level throughout the growth of *G. catenatum*.

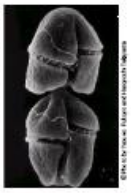

### Methods

Growth monitored with cell density

Toxicity evaluated with neuroblastoma assay

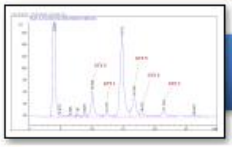

Toxin profiles accessed with HPLC system

Arginine profiles accessed with amino acid analyzer

### Results

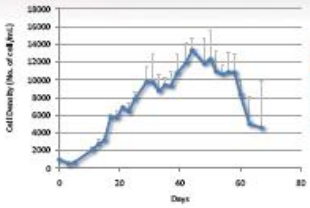

| Species | Toxicity (pg STXeq cell$^{-1}$) |
|---|---|
| *G. catenatum* | 57.1 ±17.71 |
| *A. catenella* | 1.64 ±0.58 |

Maximum cell density of *G. catenatum was found at* Day 44, around 13300 cell mL$^{-1}$. The growth rate of exponential growth was 0.77 day$^{-1}$. Cellular toxicity at mid-exponential phase was 57 *p*g STXeq cell$^{-1}$. Toxin content was ranged from 22-35 *f* mol cell$^{-1}$. 70-90 % of the toxins produced were C1 and GTX5, with small amount of GTX4 & C2 and

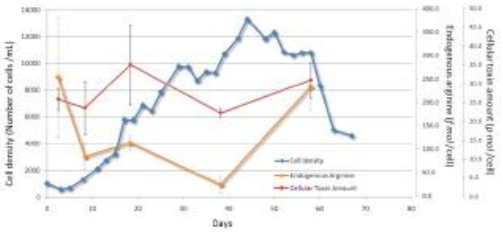

minute amount of GTX1-3. Endogenous arginine levels were 3.8 *m*M in the lag phase, and then dropped to 0.4-1.7 *m*M in exponential phase and rebound to 3.4 *m*M in stationary phase.

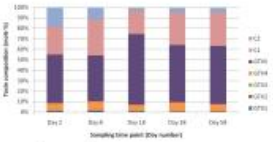

### Discussion

Compared to *Alexandrium catenella*, one of the common PSP producing dinoflagellates, *G. catenatum* is a slow growing species. Larger portion of the nutrients was dedicated to growth in bio-volume. Due to its larger size, cellular toxicity were 35 times higher than the *Alexandrium sp.* Toxin content was highest during mid-exponential phases (35 *f* mol cell$^{-1}$) and in the presence of abundant nutrients. Toxin composition was kept consistent throughout the growth. During exponential growth, biosynthesized arginine were used to make structural and functional proteins and also for toxin production. There are similarity as well as difference in the trends of the toxin curve and arginine curve, indicating toxin production are not solely depends on the availability of intracellular arginine. The association is much more complicated that other factors should be involved.

**Acknowledgement**

This project is supported partly by a grant from the NSFC-RGC jointed research scheme (RGC ref.: N_PolyU 502/08). Daniel is a M.Phil. Student supported by a grant from the Research Committee of the Hong Kong Polytechnic University.

**Reference**

[1] Negri AP, Bolch C, Geier S, Green DH, Park TG and Blackburn SI. Widespread presence of hydrophobic paralytic shellfish toxins in *Gymnodinium catenatum*. *Harmful Algae* 2004; 6: 774–782

[2] Lu SH, Hodgkiss IJ. Harmful algal bloom causative collected from Hong Kong waters. *Hydrobiologia* 2004; 512: 231-238

**Reference**


Adachi, M., Sako, Y., Ishida, Y., 1996. Analysis of Alexandrium (dinophyceae) species using sequences of the 5.8S ribosomal DNA and internal transcribed spacer regions. J. Phycol. 32(3), 424-432.

Agriculture Fisheries and Conservative Department, 2008. Harmful Marine Microalgae in Hong Kong., Hong Kong, p. 2.

Anderson, D.M., Kulis, D.M., Doucette, G.J., Gallagher, J.C., Balech, E., 1994. Biogeography of toxic dinoflagellates in the genus Alexandrium from the northeastern United States and Canada. Mar. Biol. 120(3), 467-468.

Anderson, D.M., Kulis, D.M., Sullivan, J.J., Hall, S., 1990a. Toxin composition variations in one isolate of the dinoflagellate Alexandrium fundyense. Toxicon 28(8), 885-893.

Anderson, D.M., Kulis, D.M., Sullivan, J.J., Hall, S.a.L., C.,, 1990b. Dynamics and physiology of saxitoxin production by the dinoflagellates Alexandrium spp. Mar. Biol. 104, 511-524.

Azanza, R.V., MaxTaylor, F.J.R., 2001. Are *Pyrodinium* Blooms in the Southeast Asian Region Recurring and Spreading? A View at the End of the Millennium. AMBIO 30(6), 356-364.

Badylak, S., Kelley, K., Phlips, E.J., 2004. A description of Pyrodinium bahamense (Dinophyceae) from the Indian river lagoon, florida, USA. Phycologia 43(6), 653-657.

Balech, E., 1985a. The genus Alexandrium or Gonyaulax of the tamarensis group, In: Anderson, D.M., White, A.W., Baden, D.G. (Eds.), Toxic Dinoflagellates. Elsevier, New York, pp. 33-38.

Balech, E., ,, 1985b. A redescription of Pyrodinium bahamense Plate (Dinoflagellata). Rev. Paleobot. Palyn. 45, 17-34.

Band-Schmidt, C., Bustillos-Guzman, J., Morquecho, L., Garate-Lizarraga, I., Alonso-Rodriguez, R., Reyes-Salinas, A., Erler, K., Luckas, B., 2006. Variations of PSP toxin profiles during different growth phases in Gymnodinium catenatum (Dinophyceae) strains isolated from three locations in the Gulf of California, Mexico. J. Phycol. 42(4), 757-768.

Band-Schmidt, C.J., Lechuga-Deveze, C.H., Kulis, D.M., Anderson, D.M., 2003. Culture studies of Alexandrium affine (Dinophyceae), a non-toxic cyst forming dinoflagellate from Bahia Concepcion, Gulf of California. Bot. Mar. 46, 44-54.

Barbrook, A.C., Howe, C.J., 2000. Minicircular plastid DNA in the dinoflagellate Amphidinium operculatum. Mol. Gen. Genet. 263, 152-158.

Blackburn, S.I., Hallegraeff, G.M., Bolch, C.J., 1989. Vegetative reproduction and sexual life cycle of the toxic dinoflagellate *Gymnodinium catenatum* from Tasmania, Australia. J Phycol. 25, 577-590.

Boczar, B.A., Beitler, M.K., Liston, J., Sullivan, J.J., Cattolico, R.A., 1988. Prarlytic shellfish toxins in Protogonyaulax tamarensis and Protogonyaulax catenella in axenic culture. Plant Physiol 88, 1285-1290.

Bold, J.C., Wynn, M.J., 1978. Introduction to the Algae: Structure and Reproduction. Prentice Hall, Inc., New Jersey, p. 706.

Boyer, G.L., Sullivan, J.J., Harrison, P.J., Taylor, F.J.R., 1987. Effects of nutrient limitation on toxin production and composition in the marine dinoflagellate *Protogonyaulax tamarensis* Mar. Biol. 96(1), 123-128.

Camacho, F.G., Rodríguez, J.G., Mirón, A.S., García, M.C., Belarbi, E.H., Chisti, Y., Grima, E.M., 2007. Biotechnological significance of toxic marine dinoflagellates. Biotechnol Adv. 25(2), 176-194.

Cembella, A.D., 1998. Ecophysiology and metabolism of paralytic shellfish toxins in marine microalgae, Physiological Ecology of Harmful Blooms. Springer-Verlag, Berlin, pp. 381-404.

Cembella, A.D., Sullivan, J.J., Boyer, G.L., Taylor, F.J.R., Anderson, R.J., 1987. Variation in paralytic shellfish toxin composition within the Protogonyaulax tamarensis I catenella species complex: red tide dinoflagellates. Biochem. Syst. Ecol. 15, 171-186.

Chan, E.Y., 2005. Advances in sequencing technology. Mutation Research 573, 13-40.

Chan, L.L., Hodgkiss, I.J., Lam, P.K.S., Wan, J.M.F., Chou, H.N., Lum, J.H.K., Lo, M.G.E., Mak, A.S.C., Sit, W.H.a.L., S.C.L.,, 2005. Use of two-dimensional gel electrophoresis to differentiate morphospecies of Alexandrium minutum, a paralytic shellfish poisoning toxin-producing dinoflagellate of harmful algal blooms. Proteomics 5, 1580-1593.

Chan, L.L., Hodgkiss, I.J., Lu, S., Lo, S.C.L., 2004. Use of two-dimensional gel electrophoresis proteome reference maps of dinoflagellates for species recognition of causative agents of harmful algal blooms. Proteomics 4(1), 180-192.

Chan, L.L., Sit, W.H., Lam, P.K.S., Hsieh, D.P.H., Hodgkiss, I.J., Wan, J.M.F., Ho, A.Y.T., Choi, N.M.C., Wang, D.Z.a.D., 2006. Identification and characterization of a “biomarker of toxicity” from the proteome of the paralytic shellfish toxin-producing dinoflagellate Alexandrium tamarense (Dinophyceae). Proteomics 6, 654-666.

Cho, Y., Hiramatsu, K., Ogawa, M., Omura, T., Ishimaru, T., Oshima, Y., 2008. Non-toxic and toxic subclones obtained from a toxic clonal culture of Alexandrium tamarense (Dinophyceae): Toxicity and molecular biological feature. Harmful Algae 7, 740-751.

Clark, R.F., Williams, S.R., Nordt, S.P., Manoguerra, A.S., 1999. A review of selected seafood poisoning. Undersea Hyperb Med. 26(3), 175-184.

Claudia, A.M., Kulis, D.M., Franca, S., Anderson, D.M., 2004. The loss of PSP toxin production in a formerly toxic *Alexandrium lusitanicum* Clone. Toxicon 43, 195-205.

Davio, S.R., 1985. Neutralization of saxitoxin by anti-saxitoxin rabbit serum. Toxicon 23(4), 669-675.

Dell’Aversano, C., Walter, J.A., Burton, I.W., Stirling, D.J., Fattorusso, E., Quilliam, M.A., 2008. Isolation and Structure Elucidation of New and Unusual Saxitoxin Analogues from Mussels. J. Nat. Prod. 71(9), 1518-1523.

DOE Joint Genome Institute, 2009. Genome projects. US Department of Energy, p. search results of "symbiodinium" genome projects.

Doucette, G.J., Kodama, M., Gallacher, S., 1998. Bacterial interaction with harmful algal bloom species: bloom ecology, toxigenesis and cytology, In: Anderson, D.M., Cembella, A.D., Hallegraeff, G.M. (Eds.), Physiological Ecology of Harmful Algal Bloom. Springer-verlag Heidelberg, Berlin, pp. 619-647.

Fagan, T., Morse, D., Hastings, J.W., 1999. Circadian synthesis of a nuclear-encoded chloroplast glyceraldehyde-3-phosphate dehydrogenase in the dinoflagellate Gonyaulax polyedra is translationally controlled. Biochemistry 38(24), 7689-7695.

Flynn, K., Franco, J.M., Fernandez, P., Reguera, B., Zapata, M., Wood, G., Flynn, K.J., 1994. Change in toxin content, biomass and pigments of the dinoflagellate Alexandrium minutum during nitrogen refeeding and growth into nitrogen or phosphate stressq. Mar. Ecol. Prog. Ser. 111, 99-109.

Flynn, K.J., Jones, K.J., Flynn, K.J., 1996. Comparisons among species of Alexandrium grown in nitrogen-or phosphate-limiting batch culture. Mar. Biol. 126, 9-18.

Fukuyo, Y., Takano, H., Chihara, M., Matsuoka, K., 1990. Red Tide Organisms in Japan, An Illustrated Taxonomic Guide. Uchida Rokakuho, Co., Ltd., Tokyo, p. 407.

Gallacher, S., Smith, E.A., 1999. Bacteria and paralytic shellfish toxins. Protist 150, 245-255.

Gárate-Lizárraga, I., Bustillos-Guzmán, J.J., Morquecho, L., Band-Schmidt, C.J., Alonso-Rodríguez, R., Erler, L., Luckas, B., Reyes-Salinas, A., Góngora-González, D.T., 2005. Comparative paralytic shellfish toxin profiles in the strains of Gymnodinium catenatum Graham from the Gulf of California, Mexico. Mar. Pollut. Bull. 50, 208-236.

García, C., del Carmen Bravo, M., Lagos, M., Lagos, N., 2004. Paralytic shellfish poisoning: post-mortem analysis of tissue and body fluid samples from human victims in the Patagonia fjords. Toxicon 43(2), 149-158.

Gedaria, A.I., Luckas, B., Reinhardt, K., Azanza, R.V., 2007. Growth response and toxin concentration of cultured Pyrodinium bahamense var. compressum to varying salinity and temperature conditions. Toxicon 50, 518-529.

Gessner, B.D., Middaugh, J.P., 1995. Paralytic shellfish poisoning in Alaska: a 20-year retrospective analysis. Am J Epidemiol 141(8), 766-770.

Gibbs, S.P., 1981. The chloroplasts of some algal groups may have evolved from endosymbiotic eukaryotic algae, Annuals of the New York Academy of Sciences361(FEB), pp. 193-208.

Gill, S., Murphy, M., Clausen, J., Richard, D., Quilliam, M., MacKinnon, S., LaBlanc, P., Mueller, R., Pulido, O., 2003. Neural Injury Biomarkers of Novel Shellfish Toxins, Spirolides: A Pilot Study Using Immunochemical and Transcriptional Analysis NeuroToxicology 24(4-5), 593-604.

Graham, H.W., 1943. Gymnodinium catenatum, a new dinoflagellate from the Gulf of California. Tans. Am. Micr. Soc. 62, 259-261.

Graham, L.E., Lee, W.W., 2000. Dinoflagellates. Upper Saddler River, NJ: Prentice Hall.

Hackett, J.D., Wisecaver, J.H., Brosnahan, M.L., Kulis, D.M., Anderson, D.M., Bhattacharya, D., Plumley, F.G., Erdner, D.L., 2012. Evolution of Saxitoxin Synthesis in Cyanobacteria and Dinoflagellates. Molecular Biology and Evolution 0(0), 1-9.

Hallegraeff, G.M., 1993. A review of harmful algal blooms and their apparent global increase. Phycologia 32, 79-99.

Hallegraeff, G.M., 1998. Transporrt of toxic dinoflagellates via ships' ballast water: bioeconomic risk assessment and efficacy of possible ballast water management strategies. Mar. Ecol. Prog. Ser. 168, 279-309.

Hallegraeff, G.M., Bolch, C.J., Blackburn, S.I., Oshima, Y., 1991. Species of the toxigenic dinoflagellate genus *Alexandrium* in southeastern Australian waters. Bot. Mar. 34(6), 575-587.

Halstead, B.W., Schantz, E.J., 1984. Paralytic Shellfish Poisoning, WHO Offset Publ. World Health Organization, Geneva, pp. 9-10.

Hamasaki, K., Horie, M., Tokimuitsu, A., Toda, A., Taguchi, S., 2001. Varibility in toxicity of the dinoflagellate Alexandrium tamarense isolated from Hiroshima Bay, Western Japan, as a reflection of changing environmental conditions. J Plank. Res. 23, 271-278.

Helbling, E.W., Buma, A.G.J., van de Poll, W., Zenoff, M.V.F., Villafane, V.E., 2008. UVR-induced photosynthetic inhibition dominates over DNA damage in marine dinoflagellates exposed to fluctuating solar radiation regimes. J. Exp. Mar. Biol. Ecol. 365(2), 96-102.

Hernández-Becerril, D.U., Alonso-Rodríguez, R., Alvarez-Góngora, C., Barón-Campis, S.A., Ceballos-Corona, G., Herrera-Silveira, J., Meave Del Castillo, M.E., Juárez-Ruíz, N., Merino-Virgilio, F., Morales-Blake, A., Ochoa, J.L., Orellana-Cepeda, E., Ramírez-Camarena, C., Rodríguez-Salvador, R., 2007. Toxic and harmful marine phytoplankton and microalgae (HABs) in Mexican Coasts. J Environ Sci Health A 42(10), 1349-1363.

Hillebrand, H., Durselen, C.D., Kirschtel, D., Pollingher, U., Zohary, T., 1999. Biovolume calculation for pelagic and benthic microalgae. J. Phycol. 35(2), 403-424.

Hold, G.L., Smith, E.A., Birkbeck, T.H., Gallacher, S., 2001a. Comparison of paralytic shellfish toxin (PST) production by the dinoflagellates Alexandrium lusitanicum NEPCC 253 and Alexandrium tamarense EPCC 407 in the presence and absence of bacteria. FEMS Microbiol. Ecol. 36, 223-234.

Hold, G.L., Smith, E.A., Rappe, M.S., Maas, E.W., Moore, E.R.B., Stroempl, C., 2001b. Characterisation of bacterial communities associated with toxic and non-toxic dinoflagellates: Alexandrium spp. and Scrippsiella trochoidea. FEMS Microbiol. Ecol. 37, 161-173.

Horwitz, W., 1980. Official methods of analysis of the Association of official Analytical Chemists, 13 ed. Association of Official Analytical Chemists, Washington, DC, pp. 298-299.

Hughes, J.M., Merson, M.H., 1976. Current Concepts - Fish and Shellfish Poisoning. N Engl J Med 295(20), 1117-1120.

Hwang DF, Lu YH, 2000. Infuence of environmental and nutritional factors on growth, toxicity, and toxin profile of dinofagellate Alexandrium minutum. Toxicon 38, 1491-1503.

Hwang, D.F., Lu, Y.H., 2001. Infuence of environmental and nutritional factors on growth, toxicity, and toxin profile of dinofagellate Alexandrium minutum. Toxicon 38, 1491-1503.

Ichimi, K., Suzuki, T., Ito, A., 2002. Variety of PSP toxin profiles in various culture strains of Alexandrium tamarense and change of toxin profile in natural A. tamarense population. J Exp. Mar. Biol. Ecol. 273, 51-60.

Ishida, K., Green, B.R., 2002. Second- and third-hand chloroplasts in dinoflagellates: Phylogeny of oxygen-evolving enhancer 1 (PsbO) protein reveals replacement of a nuclear-encoded plastid gene by that of a haptophyte tertiary endosymbiont. Proc. Natl. Acad. Sci. U. S. A. 99(14), 9294-9299.

John, E.H., Flynn, K.J., 1999. Amino acid uptake by the toxic dinoflagellate Alexandrium fundyense. Mar. Biol. 133, 11-19.

John, E.H., Flynn, K.J., 2000. Growth dynamics and toxicity of Alexandrium fundyense (Dinophyceae): the effect if changing N:P supply ratios on internal toxin and nutrient levels. Eur. J. Phycol. 35, 11-23.

John, E.H., Flynn, K.J., 2002. Modelling changes in paralytic shellfish toxin content of dinoflagellates in response to nitrogen and phosphorus supply. Mar. Ecol.-Prog. Ser. 225, 147-160.

Kim, C.H., Sako, Y., Ishida, Y., 1993. COMPARISON OF TOXIN COMPOSITION BETWEEN POPULATIONS OF ALEXANDRIUM SPP FROM GEOGRAPHICALLY DISTANT AREAS. Nippon Suisan Gakkaishi 59(4), 641-646.

Kodama, M., Ogata, T., Sakamota, S., Sato, S., Honda, T., Miwatani, T., 1990. Production of paralytic shellfish toxins by a bacterium Moraxella sp. isolated from Protogonyaulax. Toxicon 28, 707-714.

Kofoid, C.A., Swezy, O., 1921. The free-living unarmored dinoflagellata. Mem. Univ. Calif. 5, 1-562.

Lagos, N., Onodera, H., Zagatto, P.A., Andrinolo, D., Azevedo, S.M., Oshima, Y., 1999. The first evidence of paralytic shellfish toxins in the fresh water cyanobacterium Cylindrospermopsis raciborskii, isolated from Brazil. Toxicon 37(10), 1359-1373.

Landsberg, J.H., Sherwood, H., Johannessen, J.N., White, K.D., Conrad, S.M., Abbott, J.P., Flewelling, L.J., Richardson, R.W., Dickey, R.W., Jester, E.L.E., Etheridge, S.M., Deeds, J.R., Van Dolah, F.M., Leighfield, T.A., Zou, Y., Beaudry, C.G., Benner, R.A., Rogers, P.L., Scott, P.S., Kawabata, K., Wolny, J.L., Steidinger, K.A., 2006. Saxitoxin puffer fish poisoning in the United States, with the first report of Pyrodinium bahamense as the putative toxin source. Environ. Health Persp. 114, 1502-1507.

Larsen, J., Moestrup, O., 1989. Guide to Toxic and Potentially Toxic Marine Algae, The Fish Inspection Service, Ministry of Fisheries, Copenhagen, p. 61.

Lawrence, J.F., Wong, B., Menard, C., 1996. Determination of decarbamoyl saxitoxin and its analogues in shellfish by prechromatographic oxidation and liquid chromatography with fluorescence detection. J. AOAC Int. 79(5), 1111-1115.

Lee, F.W., Ho, K.C., Lo, S.C.L., 2008. Rapid identification of dinoflagellates using protein profiling with matrix-assiated laser desorption/ionization mass spectrometry. Harmful Algae 7, 551-559.

Lee, F.W., Morse, D., Lo, S.C., 2009. Identification of two plastid proteins in the dinoflagellate Alexandrium affine that are substantially down-regulated by nitrogen-depletion. J Proteome Res. 11, 5080-5092.

Lee, W.F., 2007. Proteomic Study of Harmfulalgal Blooming Causative Agents: Nitrogen-induced Growth and Identification of Dinoflagellates, Department of applied biology with chemical technology. The Hong Kong Polytechnic University, Hong Kong, p. 325.

Lefebvre, K.A., Bill, B.D., Erickson, A., Baugh, K.A., O'Rourke, L., Costa, P.R., Nance, S., Trainer, V.L., 2008. Characterization of intracellular and extracellular saxitoxin levels in both field and cultured Alexandrium spp. samples from Sequim Bay, Washington. Mar. Drugs 6(2), 103-116.

Leong, S.C.Y., Murata, A., Nagashima, Y., Taguchi, S., 2004. Variability in toxicity of the dinoflagellate Alexandrium tamarense in response to different nitrogen sources and concentrations. Toxicon 43, 407-415.

Li, T.S., Yu, R.C., Zhou, M.J., 2011. Short-term effects of different nitrogen substrates on growth and toxin production of dinoflagellate Alexandrium catenella Balech (strain ACDH). Harmful Algae 12, 46-54.

Lim, P.T., Leaw, C.P., Kobiyama, A., 2009. Growth and toxin production of tropical Alexandrium minutum Halim (Dinophyceae) under various nitrogen to phosphorus ratios. J Appl. Phycol.

Lim, P.T., Leaw, C.P., Usup, G., Kobiyama, A., Koike, K., Ogata, T., 2006. Effects of light and temperature on growth, nitrate uptake, and toxin production of two tropical dinoflagellates: Alexandrium tamiyavanchii and Alexandrium minutum (Dinophyceae). J Phycol. 42, 786-799.

Lim, P.T., Ogata, T., 2005. Salinity effect on growth and toxin production of four tropical Alexandrium species (Dinophyceae). Toxicon 45, 699-710.

Lin, S., 2006. The Smallest Dinoflagellate Genome Is Yet To Be Found: A Comment On Lajeunesse st al. ‘‘Symbiodinium (Pyrrhophyta) Genome Sizes (DNA Content) Are Smallest Among Dinoflagellates. J Phycol. 42, 746748.

Lippemeier, S., Frampton, D.M.F., Blackburn, S.I., Geier, S.C., Negri, A.P., 2003. Influence of phosphorus limitation on toxicity and photosynthesis of Alexandrium minutum (DInophyceae) monitored by in-line detection of variable chlorophyll fluorescence. J Phycol. 38, 320-331.

Litaker, R.W., Vandersea, M.W., Kibler, S.R., Reece, K.S., Stokes, N.A., Lutzoni, F.M., Yonish, B.A., West, M.A., 2007. Recognizing dinoflagellate species using ITS rDNA sequences. J Phycol. 43(2), 344-355.

Llewellyn, L.E., 2006. Saxitoxin, a toxic marine natural product that targets a multitude of receptors. Nat Prod Rep. 23(2), 200-222.

Loeblich, A.R.I., 1984. Dinoflagellate physiology and biochemistry, In: DL, S. (Ed.), Dinolagellates. Academic Press, Orlando, pp. 299-342.

Maas, E.W., Brooks, H.J.L., 2010. Is photosynthesis a requirement for paralytic shellfish toxin production in the dinoflagellate Alexandrium minutum algal-bacterial consortium? J. Appl. Phycol. 22(3), 293-296.

MacLean, J.L., 1977. Observation on Pyrodinium-bahamense Plate, a toxic Dinoflagellate, in Papua-New-Guinea. Limnol. Oceanogr. 22(2), 234-254.

Martins, C.A., Kulis, D., Franca, S., Anderson, D.M., 2004. The loss of PSP toxin production in a formerly toxic Alexandrium lusitanicum clone. Toxicon 43(2), 195-205.

McBarron, E.J., Walker, R.I., Gardner, I., Walker, K.H., 1975. Toxicity to livestock of the blue-green algae Anabaena circinalis. Aust Vet J. 51(12), 587-588.

McIntyre, J.G., Cullen, J.J., Cembella, A.D., 1997. Vertical migration, nutrition and toxicity of Alexandrium tamarense. Mar. Ecol. Prog. Ser. 148, 201-216.

Morquecho, L., 2008. Morphology of *Pyrodinium bahamense* Plate (Dinoflagellata) near Isla San José, Gulf of California, Mexico. Harmful Algae 7(5), 664-670.

Morse, D., Milos, P.M., Roux, E., Hastings, J.W., 1989. Circadian regulation of bioluminescence in *Gonyaulax* involves translational control. Proc. Natl. Acad. Sci. 86, 172-176.

Moustafa, A., Loram, J.E., Hackett, J.D., Anderson, D.M., Plumley, F.G., Bhattacharya, D., 2009. Origin of saxitoxin biosynthetic genes in cyanobacteria. PLoS One 4, e5758.

Nagai, K., Thøgersen, H.C., 1987. Sythesis and sequence-specific proteolysis of hybrid proteins produced in Escherichia coli. Meth. Enzymo. 153, 461-481.

Nagai, S., Sekino, M., Matsuyama, Y., Itakura, S., 2006. Development of microsatellite markers in the toxic dinoflagellate Alexandrium catenella (Dinophyceae). Molecular Ecology Notes 6(1), 120-122.

Navarro, J.M., Muñoz, M.G., Contreras, A.M., 2006. Temperature as a factor regulating growth and toxin content in the dinoflagellate Alexandrium catenella. Harmful Algae 5, 762-769.

Ogata, T., Ishimaru, T., Kodama, M., 1987. Effect of water temperature and light intensity on growth rate and toxicity change in Protogonyaulax tamarensis. Mar. Biol. 95, 217-220.

Ogata, T., Kodama, M., Ishimaru, T., 1989. Effect of water temperature and light intensity on growth rate and toxin production in toxic dinoflagellates, In: Okaichi T, Anderson DM, Nemoto T (Eds.), Red tides: Biology, Environmental Science and Toxicology. Elsevier, New York, pp. 423-426.

Oh, S.J., Yamamoto, T., Kataoka, Y., Matsuda, O., Matsuyama, Y., Kotani, Y., 2002. Utilization of dissolved organic phosphorus by the two toxic dinoflagellates, Alexandrium tamarense and Gymnodinium catenatum (Dinophyceae). Fisheries Science 68(2), 416-424.

Omura, T., Onodera, H., Ishimaru, T., Oshima, Y., 2003. Non-toxic mutational subclones in the paralytic shellfish poisoning caustive dinoflagellates, *Alexandrium spp.* La. Mer. 41, 86-93.

Ordas, M.C., Fraga, S., Franco, J.M., Ordas, A., Figueras, A., 2004. Toxin and molecular analysis of Gymnodinium catenatum (Dinophyceae) strains from Galicia (NW Spain) and Andalucía (S Spain). J Plank. Res. 26(3), 341-349.

Oshima, Y., 1995a. Chemical and enzymatic transformation of paralytic shellfish toxins in marine organisms, Harmful algal blooms. Proc. 6th Int. Conf. on Toxic Marine Phytoplankton, Lavoisier, pp. 475-480.

Oshima, Y., 1995b. Postcolumn Derivation Liquid-Chromatographic Method for Paralytic Shellfish Toxins. J AOAC Int. 78(2), 528-532.

Oshima, Y., Blackburn, S.I., Hallegraeff, G.M., 1993. Comparative study on paralytic shellfish toxin profiles of the dinoflagellate Gymnodinium catenatum from three different countries. Mar. Biol. 116, 471-476.

Oshima, Y., Bolch, C.J., Hallegraeff, G.M., 1992. Toxin composition of resting cysts of Alexandrium tamarense (Dinophyceae). Toxicon 30(12), 1539-1544.

Oshima, Y., Sugino, K., Itakura, H., Hirota, M., Yasumoto, T., 1990. Comparative studies on paralytic shellfish toxin profile of dinoflagellates and bivalves, Toxic Marine Phytoplankton. Elsevier Press, New York, pp. 391-396.

Oshima, Y., Yasumoto, T., 1979. Analysis of toxins in cultured Gonyaulax excavata cells originating in Ofunato Bay, Japan, In: Taylor, D.L., Seliger, H.H. (Eds.), Toxic Dinoflagellate Blooms. Elsevier North Holland, New York, pp. 377-380.

Oshima, Y., Yasumoto, T., Hallegraeff, G.M., Blackburn, S.I., 1987. Paralytic shellfish toxins and causative organisms in the tropical Pacific and Tasmanian waters, Progress in Venom and Toxin Research. University of Singapore, Singapore, pp. 423-428.

Parkhill, J.P., Cembella, A.D., 1999. Effects of salinity, light and inorganic nitrogenon the growth and toxigenicity of the marine dinoflagellate Alexandrium tamarense. J Plank. Res. 21, 939-955.

Plate, L., 1906. *Pyrodinium bahamense* n.g., n. sp. die Leucht-Peridinee des "Feuersees" von Nassau, Bahamas. Arch. Protistenk 7, 411-429.

Pomati, F., Kellmann, R., Cavalieri, R., Burns, B.P., Neilan, B.A., 2006. Comparative gene expression of PSP-toxin producing and non-toxic Anabaena circinalis strains. Environ. Int. 32(6), 743-748.

Prezelin, B.B., Alberte, R.S., 1978. PHOTOSYNTHETIC CHARACTERISTICS AND ORGANIZATION OF CHLOROPHYLL IN MARINE DINOFLAGELLATES. Proc. Natl. Acad. Sci. U. S. A. 75(4), 1801-1804.

RaLonde, R., 1996. Paralytic Shellfish Poisoning: The Alaska Problem, Alaska's Marine Resources, pp. 14-15.

Ramagli, L.S., Rodriguez, L.V., 1985. QUANTITATION OF MICROGRAM AMOUNTS OF PROTEIN IN TWO-DIMENSIONAL POLYACRYLAMIDE-GEL ELECTROPHORESIS SAMPLE BUFFER. Electrophoresis 6(11), 559-563.

Reguera, B., Oshima, Y., 1990. Response of Gymnodinium catenatum to increasing levels of nitrate: Growth patterns and toxicity. Elsevier, New York.

Rodrigue, D.C., Etzel, R.A., Hall, S., Deporras, E., Velasquez, O.H., Tauxe, R.V., Kilbourne, E.M., Blake, P.A., 1990. Lethal Paralytic Shellfish Poisoning In Guatemala. Am. J. Trop. Med. Hyg. 42(3), 267-271.

Rosales-Loessener, F., Porras, E.D., Dix, M.W., 1989. Toxic shellfish poisoning in Guatemala, In: Okaichi, T., Anderson, D.M., Nemoto, T. (Eds.), Red Tides, Biology, Environmental Science and Toxicology. Elsevier, New York, pp. 113-116.

Rowan, R., Whitney, S.M., Fowler, A., Yellowlees, D., 1996a. Rubisco in marine symbiotic dinoflagellates: Form II enzymes in eukaryotic oxygenic phototrophs encoded by a nuclear multigene family. Plant Cell 8(3), 539-553.

Rowan, R., Whitney, S.M., Fowler, A., Yellowless, D., 1996b. Rubisco in marine symbiotic dinoflagellates: Form II enzymes in eukaryotic oxygenic phototrophs encoded by a nuclear multigene family. Plant Cell 8, 539-553.

Sako, Y., Kim, C., Ishida, Y., 1992. Mendelian inheritance of paralytic shellfish poisoning toxin in the marine dinoflagellate *Alexandrium catenella*. Biosci. Biotechnol. Biochem. 56, 692-694.

Saroja, G., Bose, S., 1983. CORRELATION BETWEEN INHIBITION OF PHOTOSYNTHESIS AND GROWTH OF CHLORELLA TREATED WITH METHYL PARATHION. J. Biosci. 5(1), 71-78.

Sharma, S.K., 1986. On the recovery of genetically engineered proteins from Escherichia coli. Sep. Sci. Technol. 21, 701-726.

Shilo M., Aschner, M., 1953. Factors governing the Toxicity of Cultures containing the Phytoflagellate *Prymnesium parvum* Carter. J Gen Microbiol. 8, 333-343.

Shimizu, Y., 1993. Microalgal metabolites. Chem. Rev. 93(5), 1685-1698.

Shimizu, Y., Gupta, S., Prasad, A.V.K., 1990. Biosynthesis of dinoflagellate toxins. Elsevier, New York.

Shimizu, Y., Norte, M.A., Hori, A., Genenah, A., Kobayashi, M., 1984. Biosynthesis of saxitoxin analogues: the unexpected pathway. J Am. chem. Soc. 106, 6433-6434.

Shumway, S.E., Hurst, J.W., Sherman-Caswell, S.S., 1988. Paralytic shellfish poisoning in Maine: Monitoring a monster. Journal of Shellfish Research 7(1), 175.

Silva, E.S., Sousa, I., 1981. Experimental work on the dinoflagellate toxin production. Arq. Inst. Nac. Saúde 6, 381-387.

Siu, G.K.Y., Young, M.L.C., Chan, D.K.O., 1997. Environmental and nutritional factors which regulate population dynamics and toxin production in the dinoflagellate Alexandrium catenella. Hydrobiologia 352, 117-140.

Sobel, J., Painter, J., 2005. Illnesses Caused by Marine Toxins. Food Safety 41(9), 1290-1296.

Sommer, H., Whedon, W.F., Kofoid, C.A., Stohler, R., 1937. Relation of paralytic shellfish poison to certain plankton organisms of the genus *Gonyaulax*. A.M.A. Arch. Pathol. 24, 537-559.

Song, Z., Chen, L.N., Ganapathy, A., Wan, X.F., Brechenmacher, L., Tao, N.B., Emerich, D., Stacey, G., Xu, D., 2007. Development and assessment of scoring functions for protein identification using PMF data. Electrophoresis 28(5), 864-870.

Staats, N., Stal, L.J., de Winder, B., Mur, L.R., 2000. Oxygenic photosynthesis as driving process in exopolysaccharide production of benthic diatoms. Mar. Ecol.-Prog. Ser. 193, 261-269.

Steidinger, K.A., Tangen, K., 1996. Dinoflagellates, In: CR, T. (Ed.), Identifying Marine Diatoms and Dinoflagellates. Academic Press, New York, pp. 387-598.

Steidinger, K.A., Tester, L.S., 1980. A redescription of Pyrodinium bahamense var. compressa (Bohm) stat. nov. from Pacific red tides. Phycologia 19, 329-337.

Strausberg, R.L., Levy, S., Rogers, Y.H., 2008. Emerging DNA sequencing technologies for human genomic medicine. Drug Discovery Today 13, 569-577.

Strichartz, G., 1984. Structural determinants of the affinity of saxitoxin for neuronal sodium channels. Electrophysiological studies on frog peripheral nerve. . J Gen Physiol 84(2), 281-305.

Stuken, A., Orr, R.J.S., Kellmann, R., Murray, S.A., Neilan, B.A., Jakobsen, K.S., 2011. Discovery of Nuclear-Encoded Genes for the Neurotoxin Saxitoxin in Dinoflagellates. PLoS One 6(5), 12.

Su, Z., Sheets, M., Ishida, H., Li, F., Barry, W.H., 2004. Saxitoxin blocks L-type ICa. J Pharmacol Exp Ther. 308(1), 3324-3329.

Sukenik, A., Eshkol, R., Livne, A., Hadas, O., Rom, M., Tchernov, D., Vardi, A., Kaplan, A., 2002. Inhibition of growth and photosynthesis of the dinoflagellate Peridinium gatunense by Microcystis sp (cyanobacteria): A novel allelopathic mechanism. Limnol. Oceanogr. 47(6), 1656-1663.

Sze, P., 1998. Haptophytes, Dinoflagellates, Crytomonads, and Euglenophytes, A biology of the algae. WCB/McGraw-Hill, Boston, pp. 129-150.

Tabita, F.R., Satagopan, S., Hanson, T.E., Kreel, N.E., Scott, S.S., 2008. Distinct form I, II, III, and IV Rubisco proteins from the three kingdoms of life provide clues about Rubisco evolution and structure/function relationships. J. Exp. Bot. 59(7), 1515-1524.

Takishita, K., Patron, N.J., Ishida, K.I., Maruyama, T., Keeling, P.J., 2005. A transcriptional fusion of genes encoding glyceraldehyde-3-phosphate dehydrogenase (GAPDH) and enolase in dinollagellates. J. Eukaryot. Microbiol. 52(4), 343-348.

Taroncher-Oldenburg, G., Anderson, D.M., 2000. Identification and Characterization of Three Differentially Expressed Genes, Encoding S-Adenosylhomocysteine Hydrolase, Methionine Aminopeptidase, and a Histone-Like Protein, in the Toxic Dinoflagellate Alexandrium fundyense. Appl. Environ. Microbiol. 66, 2105-2112.

Taroncher-Oldenburg, G., Kulis, D.M., Anderson, D.M., 1997. Toxin varibility during the cell cycle of the dinoflagellate Alexandrium fundyense. Limnol. Oceanogr. 42, 1178-1188.

Taylor, F.J.R., Fukuyo, Y., Larsen, J., Hallegraeff, G.M., 2003. Taxonomy of harmful dinoflagellates, In: Hallegraeff, G.M., Anderson, D.M., Cembella, A.D. (Eds.), Manual on Harmful Marine Microalgae. UNESCO, Paris, pp. 389-432.

Touzet, N., Franco, J.M., Raine, R., 2007a. Characterization of Nontoxic and Toxin-Producing Strains of Alexandrium minutum (Dinophyceae) in Irish Coastal Waters. Appl. Environ. Microbiol. 73, 3333-3342.

Touzet, N., Franco, J.M., Raine, R., 2007b. Influence of inorganic nutrition on growth and PSP toxin production of Alexandrium minutum (Dinophyceae) from Cork Harbour, Ireland. Toxicon 50, 106-119.

Uribe, P., Espejo, R.T., 2003. Effect of associated bacteria on the growth and toxicity of *Alexandrium catenella*. Appl. Environ. Microbiol. 69, 659-662.

Uribe, P., Fuentes, D., Valdes, J., Shmaryahu, A., Zuniga, A., Holmes, D., Valenzuela, P.D.T., 2008. Preparation and Analysis of an Expressed Sequence Tag Library from the Toxic Dinoflagellate Alexandrium catenella. Mar. Biotechnol. 10(6), 692-700.

Usup, G., Kulis, D.M., Anderson, D.M., 1994. Growth and toxin production of the toxic dinoflagellate Pyrodinium bahamense var. compressum in laboratory cultures. Nat. Toxins 2, 254-262.

Wang, C.H., Hsieh, D.D.P., 2002a. Nutritional supplementation to increase growth and paralytic shellfish toxin productivity by the marine dinoflagellate *Alexandrium tamarense*. Biochem. Eng. J. 11, 131-135.

Wang, D.Z., 2008. Neurotoxins from Marine Dinoflagellates: A Brief Review. Mar. Drugs 6(2), 349-371.

Wang, D.Z., Hesieh, D.P.H., 2005. Growth and toxin production in batch cultures of a marine dinoflagellate Alexandrium tamarense HK9301 isolated from the South China Sea. Harmful Algae 4, 401-410.

Wang, D.Z., Hsieh, D.P.H., 2002b. Effects of nitrate and phosphate on growth and C2 toxin productivity of Alexandrium tamarense CI01 in culture. Mar. Pollut. Bull. 45, 286-289.

Wang, D.Z., Zhang, S.G., Gu, H.F., Chan, L.L., Hong, H.S., 2006. Paralytic shellfish toxin profiles and toxin variability of the genus Alexandrium (Dinophyceae) isolated from the Southeast China Sea. Toxicon 48, 138-151.

Wang, J., Salata, J.J., Bennett, P.B., 2003. Saxitoxin is a gating modifier of HERG K+ channels. J Gen Physiol 121(6), 583-598.

Weising, K., Schell, J., Kahl, G., 1988. Foreign genes in plants; transfer; structure, expression, and applications. Annu. Rev. Genet. 22, 421-477.

White, A.W., 1978. Salinity effects on growth and toxin content of Gonyaulax excavata, a marine dinoflagellate causing paralytic shellfish poison. J Phycol. 14, 475-479.

Wiberg, G.S., Stephenson, N.R., 1960. Toxicologic studies on paralytic shellfish poison. Toxicol Appl Pharmacol. 2, 607-615.

Wood, G., Flynn, K.J., 1995. Growth of Heterosigma carterae (Raphidophyceae) on nitrate and ammonium at three photon flux densities: evidence for N-stress in nitrate-growing cells. J Phycol. 31, 859-867.

Yang, I., John, U., Beszteri, S., Glockner, G., Krock, B., Goesmann, A., Cembella, A.D., 2010. Comparative gene expression in toxic versus non-toxic strains of the marine dinoflagellate Alexandrium minutum. BMC Genomics 11, 18.

Zhang, Z., Green, B.R., Cavalier-Smith, T., 1999. Single gene circles in dinoflagellate chloroplast genomes. Nature 400, 155-159.